CHARACTERIZATION OF SHORT PINEAPPLE LEAF FIBER REINFORCED TAPIOCA BIOPOLYMER COMPOSITES

JAMILUDDIN BIN JAAFAR

Doctor of Philosophy

UNIVERSITI MALAYSIA PAHANG

UNIVERSITI MALAYSIA PAHANG

DECLARATION OF THESIS AND COPYRIGHT

Author's Full Name : JAMILUDDIN BIN JAAFAR

Date of Birth : 01 JANUARY 1982

Title : CHARACTERIZATION OF SHORT PINEAPPLE LEAF FIBER REINFORCED TAPIOCA BIOPOLYMER COMPOSITES

Academic Session : 2018/2019

I declare that this thesis is classified as:

☐	CONFIDENTIAL	(Contains confidential information under the Official Secret Act 1997)*
☐	RESTRICTED	(Contains restricted information as specified by the organization where research was done)*
☑	OPEN ACCESS	I agree that my thesis to be published as online open access (Full Text)

I acknowledge that Universiti Malaysia Pahang reserves the following rights:

1. The Thesis is the Property of Universiti Malaysia Pahang
2. The Library of Universiti Malaysia Pahang has the right to make copies of the thesis for the purpose of research only.
3. The Library has the right to make copies of the thesis for academic exchange.

Certified by:

(Student's Signature)	(Supervisor's Signature)
820101-11-6891	JANUAR PARLAUNGAN SIREGAR
New IC/Passport Number	Name of Supervisor
Date:	Date:

NOTE : * If the thesis is CONFIDENTIAL or RESTRICTED, please attach a thesis declaration letter.

Universiti
Malaysia
PAHANG
Engineering • Technology • Creativity

SUPERVISOR’S DECLARATION

We hereby declare that We have checked this thesis and in our opinion, this thesis is adequate in terms of scope and quality for the award of the degree of Doctor of Philosophy.

(Supervisor’s Signature)

Full Name : DR. JANUAR PARLAUNGAN SIREGAR
Position : SENIOR LECTURER
Date :

(Co-supervisor’s Signature)

Full Name : DR. SALWANI BINTI MOHD. SALLEH
Position : SENIOR LECTURER
Date :

STUDENT'S DECLARATION

I hereby declare that the work in this thesis is based on my original work except for quotations and citations which have been duly acknowledged. I also declare that it has not been previously or concurrently submitted for any other degree at Universiti Malaysia Pahang or any other institutions.

____

(Student's Signature)

Full Name : JAMILUDDIN BIN JAAFAR

ID Number : PMM14013

Date :

CHARACTERIZATION OF SHORT PINEAPPLE LEAF FIBER REINFORCED TAPIOCA BIOPOLYMER COMPOSITES

JAMILUDDIN BIN JAAFAR

Thesis submitted in fulfillment of the requirements
for the award of the degree of
Doctor of Philosophy

Faculty of Mechanical Engineering

UNIVERSITI MALAYSIA PAHANG

FEBRUARY 2019

ACKNOWLEDGEMENTS

Alhamdulillah, thanks to Almighty Allah S.W.T, Lord of heaven and earth, for giving me sustenance, opportunities and convenience to complete my research. First and foremost, I would like to express my gratitude to my respected supervisor Dr. Januar Parlaungan Siregar for his encouragement, help, support, wonderful ideas, and continuous guidance in making this research possible. I am also thankful to my co-supervisor Dr. Salwani Mohd Salleh for a lot of help and suggestions during my study. My sincere thanks go to my beloved parents, Jaafar bin Mamat and my late mother, Jara binti Embong, lovely wife, Suziyati Abd. Majid and my dear daughters, Sofea Qalishah, Syifa Qistina and Syaza Qaireena for their love support, understanding and patience.

Thank you very much to all of my research colleagues and technical members especially Mr. Mahadhir Mohd Yusof, Mr. Khairul Azha A Jalal and Mr. Rozikin Kamaluddin from Center for Technology and Management Services. Also my gratitude to Ir. Dr. Mohd. Bijarimi Mat Piah from Faculty of Chemical Engineering and Natural Resources, Dr. Noryanti Mohammad from Faculty of Industrial Science and Technology, Dr. Ahmed Nurye Oumer, Dr. Yuli Panca Asmara, Dr. Ahmad Syahrizan Sulaiman and Dr. Nasrul Azuan Alang from Faculty of Mechanical Engineering, Universiti Malaysia Pahang.

I would also like to express my thanks to Assco. Prof. Dr. Cionita Tezara from INTI University, Dr.Sharmiza Adnan from Forest Research Institute Malaysia (FRIM) and Prof. Ir. Dr. Sapuan Mohd Salit from Institute of Tropical Forestry and Forest Product (INTROP), Universiti Putra Malaysia for many help and suggestions during my research. Last but not least, extraordinary thanks to all members of the Faculty of Mechanical Engineering, University Malaysia Pahang.

ABSTRAK

Pembangunan bahan mesra alam seperti komposit serat semulajadi semakin mendapat perhatian dalam beberapa tahun kebelakangan ini disebabkan oleh peningkatan kesedaran terhadap alam sekitar berhubung dengan pelbagai kesan buruk yang telah dihasilkan oleh polimer berasaskan petroleum. Di antara kesemua serat semulajadi, serat daun nanas (PALF) mempunyai potensi besar sebagai agen pengukuhan komposit kerana kosnya yang rendah, ketersediaan yang tinggi, kandungan selulosa yang tinggi dan sifat mekanik yang relatifnya lebih tinggi berbanding dengan serat semulajadi yang lain. Dalam kebanyakan penyelidikan terdahulu, PALF digunakan sebagai penguat dalam polimer berasaskan petroleum yang tidak terbiodegradasi bagi menghasilkan komposit serat semulajadi. Walau bagaimanapun, inovasi polimer berasaskan kanji yang dipanggil biopolimer ubi kayu (TBP) menyediakan alternatif sebagai matriks biodegradasi untuk pembangunan komposit mesra alam. Oleh itu, gabungan PALF dan TBP dalam pembangunan komposit bio kelihatan seimbang antara perspektif ekologi dan ekonomi. Sebagai gabungan baru, penyelidikan ini dijalankan untuk menentukan parameter gabungan optimum komposit PALF-TBP dalam menghasilkan sifat mekanik yang kompetitif. Terdapat empat pertimbangan penting dalam pembuatan komposit dalam menghasilkan sifat mekanik yang tinggi seperti suhu pemprosesan yang digunakan dalam proses pembuatan, panjang serat, peratusan kandungan serat dan rawatan yang terlibat. Kerja eksperimen bermula dengan proses pencirian bahan TBP dan PALF. Selepas itu, penyediaan sampel yang dijalankan terdiri daripada proses menghancurkan serat dan pengasingan, proses pencampuran dalaman, pengacuan mampatan dan proses pemesinan. Sampel TBP dengan suhu pemprosesan yang berbeza (160°C, 165°C, 170°C, 175°C, 180°C dan 185°C) disediakan untuk menentukan suhu pemprosesan optimum TBP. Selain itu, sampel komposit dengan panjang serat yang berbeza (≤ 0.50 mm, 0.51-1.00 mm dan 1.01-2.00 mm) dan kandungan serat yang berbeza (10%, 20%, 30% dan 40%) disediakan untuk menilai kesan variasi panjang serat dan peratusan serat pada sifat mekanikal komposit PALF-TBP. Selain itu, tiga rawatan yang berbeza telah dipilih iaitu compatibilizer maleic anhydride polypropylene (MAPP), compatibilizer maleic anhidride polietilena (MAPE) dan rawatan alkali untuk penyiasatan kesan rawatan terhadap sifat tegangan komposit PALF-TBP. Analisis untuk menentukan keseluruhan objektif penyelidikan terdiri daripada analisis sifat terma, dan analisis sifat mekanik. Di samping itu, pemeriksaan mikroskop elektron (SEM) telah dijalankan sebagai pengesahan keputusan. Hasil kajian mendapati bahawa suhu pemprosesan optimum untuk TBP adalah 165°C hingga 170°C dan kombinasi terbaik untuk pembangunan komposit TBP yang diperkuatkan oleh PALF pendek adalah yang dihasilkan oleh pengacuan mampatan yang terdiri daripada 30% kandungan serat dan 7% kandungan agen gandingan MAPP. Walau bagaimanapun, pengaruh pelbagai panjang serat sehingga 2.00 mm tidak memberikan pengaruh yang signifikan ke atas menghasilkan sifat tegangan maksimum. Penemuan ini menunjukkan bahawa gabungan PALF dan TBP yang pendek mempunyai potensi besar sebagai komposit mesra alam untuk menjadi alternatif kepada polimer konvensional dalam aplikasi kejuruteraan terutamanya dalam sektor automotif. Peningkatan pembangunan komposit PALF-TBP pada masa akan datang seperti penggunaan PALF dengan kekuatan tegangan yang lebih tinggi yang diharapkan mampu meningkatkan dan memperbaiki hasil yang ada sekarang.

ABSTRACT

The development of environmental friendly material, such as natural fiber composites, has been getting more attention in recent years due to increase in environmental awareness of various adverse petroleum-based polymer effects. Among all natural fibers, pineapple leaf fiber (PALF) has great potential as a reinforcement agent because it is low cost, highly available with high cellulose content, and has relatively higher mechanical properties as compared to other natural fibers. Most previous research works had used PALF as reinforcement in non-biodegradable petroleum-based polymers to produce natural fiber composites. However, the starch-based polymer innovation, called tapioca biopolymer (TBP), provides an alternative for biodegradable matrix for the development of environmental friendly composites. Therefore, the combination of PALF and TBP in bio-composites development appears to be a perfect balance between the ecology and economic perspectives. As a new combination, this research was conducted to determine the optimum PALF-TBP composites combination parameters to produce competitive mechanical properties. To produce high mechanical properties, there are four essential considerations in the preparation of composites, such as the manufacturing process temperature, fiber length, fiber composition and treatment involved. The experimental work began with material characterization of TBP and PALF. Then, sample preparation was conducted, which consisted of fiber crushing and sieving, internal mixing, hot press and machining. TBP samples at different processing temperatures (160°C, 165°C, 170°C, 175°C, 180°C and 185°C) were prepared to determine the optimum processing temperature. Also, composite samples with different fiber lengths (0.10-0.50 mm, 0.51-1.00 mm and 1.01-2.00 mm) and different fiber loadings (10%, 20%, 30% and 40%) were prepared to evaluate the effect of varying fiber lengths and fiber loadings on mechanical properties of PALF-TBP composites. On the other hand, three different treatments were selected, which were maleic anhydride polypropylene (MAPP) compatibilizer, maleic anhydride polyethylene (MAPE) compatibilizer and alkali treatment for investigating the treatment effect on tensile properties of PALF-TBP composites. The analyses to determine the entire research objective consisted of thermal properties analysis and mechanical properties analysis. In addition, the scanning electron microscopy (SEM) analysis was carried out for result validation. Test results established that the optimum processing temperatures for TBP are 165°C to 170°C with the best combination for the development of short PALF reinforced TBP composite was produced by a hot press process, comprising 30% fiber loading and 7% MAPP coupling agent. However, the influence of various fiber lengths of up to 2.00 mm provided no significant influence on the production of maximum tensile properties. The finding demonstrated that the combination of short PALF and TBP had great potential as environmental friendly composites to be an alternative for the conventional polymers in engineering applications, especially in the automotive sector. Improvement of future PALF-TBP composites development, such as the utilization of PALF with higher tensile strength, is expected to be capable of enhancing and improving the present result.

TABLE OF CONTENT

LIST OF TABLES

LIST OF FIGURES

LIST OF SYMBOLS

α	Alpha
β	Beta
cm	Centimeter
°C	Degree Celsius
E	Margin of error for statistical application
E	Chord modulus
ε	Strain value
GPa	Giga Pascal
g	Gram
h	Hour
J	Joule
kJ	Kilo Joule
kN	Kilo Newton
m	Meter
min	Minutes
ml	Mililiter
MPa	Mega Pascal
M_a	Weight of air-dried sample
M_c	Weight of crucible
M_{cl}	Weight of crucible containing lignin content
M_o	Weight of oven-dried sample
N	Newton
n	Sample size
n_1	Sample size for group 1
n_2	Sample size for group 2
°	Degree
σ	Stress value
σ_f	Tensile strength of natural fiber
σ_m	Tensile strength of matrix
S	Standard deviation
S_1	Standard deviation for group 1
S_2	Standard deviation for group 2
υ	Degree of freedom for statistical application
υ_f	Composition of fiber
υ_m	Composition of matrix

w/v	Weigt per volume
$\bar{x}$	Mean
$\bar{x}_1$	Mean for population group 1
$\bar{x}_2$	Mean for population group 2
γ	Gamma
%	Percent

LIST OF ABBREVIATIONS

ANOVA	Analysis of Variance
ASTM	American Society for Testing and Materials
ATR	Attenuated Total Reflectance
CMC	Ceramic Matrix Composites
CNC	Computer Numerical Control
DSC	Differential Scanning Calorimetry
FL	Fiber Length
FTIR	Fourier Transform Infrared Spectroscopy
HDPE	High-Density Polyethylene
ICBP	Indochine Bio Plastiques
IUPAC	International Union of Pure and Applied Chemistry
LDPE	Low-Density Polyethylene
MAPE	Maleic Anhydride Polyethylene
MAPP	Maleic Anhydride Polypropylene
MMC	Metal Matrix Composite
NaOH	Sodium Hydroxide
PALF	Pineapple Leaf Fiber
PBS	Poly (Butylene Succinate)
PC	Polycarbonate
PE	Polyethylene
PET	Polyethylene Terephthalate
PLA	Polylactic Acid
PMC	Polymer Matrix Composites
PP	Polypropylene
PU	Polyurethane
PVC	Polyvinylchloride
SEM	Scanning Electron Microscopy
TAPPI	Technical Association of the Pulp and Paper Industry
TBP	Tapioca Biopolymer
TGA	Thermogravimetric Analysis
UNFCC	United Nations Framework Convention on Climate Change

CHAPTER 1

INTRODUCTION

1.1 Introduction

The development of natural fiber composites started during ancient Egypt approximately 3,000 years ago, when clay was reinforced by straw to build building walls (Sapuan & Maleque, 2005). However, the advancement in material technology has caused natural fiber composites to lose their attractiveness, especially with the introduction of the world's first revolutionary carbon-based product that came from petroleum, which is Nylon 6. It was introduced on February 28, 1935 by a former Harvard professor who was working at DuPont Corporation research laboratory (Matthies & Seydl, 1986; Otsuki & Funahashi, 1959; Seavey et al., 2003; Xu & Wu, 2007). After a long abandonment, biodegradable and renewable material like natural fiber composites regained its attractiveness since the1990s (Balan et al., 2017; Palumbo et al., 2015; Rajesh & Pitchaimani, 2017). It was due to the increase in environmental awareness on various adverse effects generated by the accumulation of non-biodegradable waste from petroleum-based polymer (Kim et al., 2015; Loh et al., 2013; Palumbo et al., 2015). Moreover, signing of the Kyoto Protocol, which is an international agreement that was linked to the 1992 United Nations Framework Convention on Climate Change (UNFCCC), had urged the commitment of state party to reduce greenhouse gas emissions to an average of 5% lower from the 1990 level. The Kyoto Protocol was adopted in Kyoto, Japan, on December 11, 1997 and entered into force on February 16, 2005 (Mohanty et al., 2002; Pervaiz & Sain, 2003).

Therefore, environmental friendly materials like natural fiber composites have great potential as an alternative to petroleum-based polymers, and thus to overcome the environmental issue. It is because bio-based composites offer many advantages over the environment, such as biodegradable, renewable, recyclable, non-abrasive to equipment, reduced energy consumption, non-irritating to the skin and less health risk (Edhirej et al., 2017a, 2017b; Fairuz et al., 2015; Lee et al., 2016; Xia et al., 2017).

Natural fiber reinforced polymer composites are mostly used as an alternative for conventional polymers in the automotive and construction industries. In the automotive industry, natural fiber composites are primarily used for interior car components , such as door panels, seat backs, dashboards, truck liners, headliners, decking, railing, window, and frames (Valášek et al., 2018; Valášek et al., 2017). Holbery J.et al. (Holbery & Houston, 2006) revealed that many automobile companies, such as Mercedes Benz, Toyota and Daimler Chrysler, have already established this usage and are looking to expand the application of natural fiber composites for their automotive industry. Daimler AG achieved improvement in door panels of Mercedes-Benz E-class by replacing its material with flax/sisal fiber mat embedded with epoxy resin. Other examples are by replacing side panels for Audi A3 car, which was made from acryloni-trile–butadiene–styrene (ABS) copolymer, with hemp fiber/epoxy resin composites (Shalwan & Yousif, 2013). Remarkably, the utilization of natural fiber composites is able to contribute a 20% weight reduction and 20% cost reduction during the manufacturing of vehicles. Moreover, yearly demands for natural fiber composites are forecasted to grow at 15% - 20% in automobile applications and 50% or more in selected building applications (Ahmad et al., 2015).

The bio-based composites are a combination of natural fiber for reinforcement and polymer as a matrix (Väisänen et al., 2017). Research has typically utilized agriculture residue from pineapple leaves, sugar palm, oil palm and coconut waste as a source of composite fillers. The pineapple leaf fiber (PALF), which is obtained from pineapple leaves, is an attractive reinforcement agent because it is low cost and highly available. There are approximately 2.1 million acres of pineapple cultivations worldwide, including some of the world's major pineapple producers, such as Malaysia, Thailand, Indonesia, the Philippines, Brazil, Costa Rica and Hawaii. The primary problem of pineapple plantation to producer countries is the pineapple leaf waste, which is approximately 20,000 - 25,000 tons per acre after harvesting (Nanthaya & Taweechai, 2014). Traditionally, pineapple leaves are dumped or burned, causing serious environmental problems. The utilization of PALF provides a solution to the unused pineapple leave problems after harvesting. On the other hand, PALF relatively has good potential as a filler or reinforcement material due to its high crystalline cellulose but lower hemicellulose and lignin contents. Consequently, it has higher mechanical properties as compared to other natural fibers like coir and bamboo (Liu et al., 2005; Neto et al., 2015; Neto et al., 2013).

In most previous research works, PALF was used for reinforcement in either thermoset or thermoplastic polymers, such as polypropylene (PP) (Arib et al., 2006; Nanthaya & Taweechai, 2014), polyurethane (PU) (Cherian et al., 2011), high impact polystyrene (HIPS) (Siregar et al., 2011), low-density polyethylene (LDPE) (George et al., 1996b), high-density polyethylene (HDPE) (Aji et al., 2011), nylon (Nopparut & Amornsakchai, 2016; Panyasart et al., 2014), polycarbonate (PC) (Threepopnatkul et al., 2009) and elastomer (Kalapakdee & Amornsakchai, 2014; Shih et al., 2014). However, literature on PALF reinforced biodegradable polymer, such as tapioca biopolymer (TBP), is limited to date.

TBP is a biodegradable and compostable starch-based polymer derived from tapioca which is 100% annually renewable resource (Jamiluddin et al., 2016; Liu et al., 2009a). The innovation of TBP becomes an alternative to petroleum-based polymer in the manufacture of natural fiber composites. TBP, as a starch-based polymer, is expected to have better compatibility with natural fibers during the manufacture of composites. Referring to the aforementioned factors, the combination of PALF and TBP in bio-composites development appears to be a perfect balance between ecology and economic perspectives. Therefore, this research was conducted to determine the optimum design of PALF-TBP composites development to produce maximum mechanical properties.

1.2 Problem Statements

A significant difficulty in the development of natural fiber composites is the manufacturing process or sample preparation of the composites, which produces low mechanical properties. The phenomenon occurs due to the incompatibility and weak interfacial adhesion between hydrophilic natural fiber and hydrophobic petroleum-based polymer as a matrix. Therefore, the combination between PALF and starch-based polymer like TBP, as a new biodegradation and renewable bio-composite, requires determination of optimum combination parameters to produce bio-composites with competitive mechanical properties.

The first primary factor that influences the outcome of bio-composites is the processing temperature used in composite manufacturing process. Previous research found that different range of operating temperatures between petroleum-based polymer as a matrix and fiber degradation temperature is a barrier in natural fiber composites development (Fairuz et al., 2015; Ku et al., 2011; Rashid et al., 2016). As a starch-based polymer, TBP is expected to have better compatibility with natural fiber in the processing temperature. Therefore, the analysis of thermal properties and processing behavior of TBP are required. Moreover, the determination of optimum TBP processing temperature is essential to produce high mechanical properties.

As a new combination in bio-based composites development, fiber length and fiber loading are other essential factors that influence the interfacial adhesion between fiber and matrix, which will affect the mechanical properties of the composites. George et al. (1996) in his study of PALF reinforced HDPE composites presented that PALF with fiber length of 2.00 mm in length is better in distribution, dispersion and align along the direction of flow as compared to a longer fiber length. On the other hand, theoretically, the increase in high strength fiber percentage leads to an increase in the mechanical properties of bio-composites. However, from an experimental perspective, the increase of over optimum value always deteriorate the mechanical properties.Therefore, the investigation of different fiber lengths and fiber loadings effect on composite mechanical properties is required.

Excluding that, the application of additional treatments, such as alkali treatment and coupling agent, like maleic anhydride polyethylene (MAPE) and maleic anhydride polypropylene (MAPP), can provide significant enhancement in interfacial adhesion; thus, producing composites with better mechanical properties. However, previous findings found that the effectiveness of coupling agent utilization was associated with compatibility between the coupling agent and composites matrix. Yang et al. suggested that MAPP appeared to be less effective when PE matrix polymer was used in the composites and vice versa (Yang et al., 2007). Moreover, the concentration of used coupling agent also played an essential role in producing the maximum result. Increase in coupling agent concentration over optimum value always deteriorates the mechanical properties; thus, the selection of effective treatment between alkali treatment, MAPP and MAPE is required in the development of PALF-TBP composites to generate maximum mechanical properties.

Natural fiber reinforced polymer composites are mostly used as an alternative or replacement for conventional polymers in engineering applications, especially in the automotive and construction industries. The most common conventional polymers that have been used in the automotive sectors are polyethylene terephthalate (PET), polypropylene (PP), low density polyethylene (LDPE), high density polyethylene (HDPE), high impact polystyrene (HIPS), polycarbonate (PC), acryloni-trile–butadiene–styrene (ABS) and Nylon 6.6 (Holbery & Houston, 2006; Štrumberger et al., 2005; Szeteiová, 2010). Therefore, the findings of this research are expected to produce environmental friendly composites that have competitive mechanical properties with the existing conventional polymers in the automotive sector.

1.3 Objective of Study

The primary objective of this study is to determine the optimum combination parameters of pineapple leaf fiber (PALF) and tapioca biopolymer (TBP) in producing an environmentally friendly composite with competitive mechanical properties. The specific objectives of this study are classified into the following four categories:

i. To determine the optimum processing temperature for tapioca biopolymer (TBP).

ii. To assess the influence of different fiber length on tensile properties of short PALF reinforced TBP composites.

iii. To investigate the effect of fiber loading on mechanical properties of short PALF - TBP composites.

iv. To evaluate the effect of chemical treatment and coupling agent on tensile properties of PALF - TBP composites.

1.4 Scope of Study

The accomplishment of the present research objective requires the following highlighted working features to elucidate the following scope of study:

i. The material used in the present study is short pineapple leaf fiber (PALF) as a reinforcement agent and tapioca biopolymer (TBP) as the composites matrix. The selected treatments used in this research are sodium hydroxide (NaOH) and the coupling agents, which are maleic anhydride polypropylene (MAPP) and maleic anhydride polyethylene (MAPE).

ii. The characterization of TBP is conducted through Fourier transform infrared spectroscopy (FTIR). Meanwhile, the characterization of PALF consists of chemical composition analysis, diameter measurement, thermogravimetric analysis (TGA) and tensile properties analysis for PALF.

iii. The determination of optimum processing temperature for TBP is conducted through thermal and tensile properties analysis. The thermal analysis consists of TGA and differential scanning calorimetry (DSC). Meanwhile, tensile properties analysis is held on six types of manufacture sample with different processing temperatures (160°C, 165°C, 170°C, 175°C, 180°C and 185°C).

iv. The evaluation on the effect of different fiber lengths on tensile properties of PALF-TBP composite is carried out on samples of 10% PALF with different fiber lengths, which are at most 0.50 mm, 0.51 mm to 1.00 mm and 1.01 mm to 2.00 mm. Meanwhile, the effect of varying fiber loadings is evaluated on samples of 10%, 20%, 30% and 40% of fiber percentage with 1.01 mm to 2.00 mm fiber length. All composite samples are prepared through internal mixing, compression molding and machining process. In addition, the mechanical properties analysis involved tensile, flexural and impact properties analyses.

v. Assessment on the effect of selected treatments on tensile properties of PALF-TBP composites involved alkali treatment with 5% of sodium hydroxide (NaOH) concentration, maleic anhydride polypropylene (MAPP) and maleic anhydride polyethylene (MAPE) with 1%, 3%, 5% and 7% concentration.

vi. All results and findings for the entire research objective are supported by quantitative analysis, which is analysis of variance (ANOVA), and are validated through qualitative analysis by using a scanning electron microscope (SEM).

1.5 Significance of Study

The tapioca biopolymer (TBP) innovation is expected to provide an alternative for petroleum-based polymer. However, the mechanical properties of TBP are low and noncompetitive to the petroleum-based polymer and restrict its application, primarily in automotive engineering. Therefore, the combination of TBP as a starch-based polymer with natural fiber like pineapple leaf fiber (PALF) by development of environmental friendly composites appears to be a perfect balance between ecology and economic perspectives. It is because PALF, which is obtained from pineapple leaves, is one of the natural fibers that have high tensile properties and high cellulose content, relatively inexpensive and grown in abundance in many countries.

On the other hand, pineapple leaves are presently a waste product of pineapple cultivation, which is approximately 20,000 - 25,000 tons per acre after harvesting process (Nanthaya & Taweechai, 2014). Pineapple leaves are dumped or burned, causing serious environmental problems. Therefore, the development of PALF reinforced TBP composites represents a huge opportunity for the development of low cost biodegradable and renewable composites for engineering applications, especially in the automotive industry.

1.6 Thesis Outline

The arrangement of this thesis is dedicated to fulfill its objectives in detail. Chapter 1 reviews on the introduction of natural fiber composites, pineapple leaf fiber, tapioca biopolymer, the current applications and requirements for bio-composites to be used in the engineering sector, especially in automotive industry. In addition, the research gap, objective, scope and significance of study are also explained in Chapter 1.

On the other hand, a brief review of the basic definitions, concepts and essential factor in composites manufacturing which affect the mechanical properties of bio-based composites is presented in Chapter 2. In addition, previous research findings in regard to the manufacturing method and outcomes of natural fiber reinforced polymer composites are also reviewed in detail.

Chapter 3 is devoted to present the adopted methodology, which includes a brief description of material preparations, testing procedure, testing equipment and data collection, which are utilized to achieve the objectives.

Chapter 4 illustrates the experimental results and discussion. The analysis includes material characterizations, determination of TBP optimum processing temperature, evaluation on the effect of different fiber lengths on short PALF-TBP composites, and selection of optimum fiber loading to produce maximum mechanical properties. Moreover, the investigation on the effect of selected treatments on tensile properties of PALF-TBP composites is also analyzed.

Finally, the significant findings and future recommendations are summarized in Chapter 5.

CHAPTER 2

LITERATURE REVIEW

2.1 Introduction

This chapter aims to establish the significance of the general field of natural fiber composites research reviewed from various relevant studies, and identify the contributions through the research gap. In this chapter, the importance of obtaining renewable and biodegradable materials through the development of natural fiber composites is discussed. There are specific requirements for the development of environmental friendly materials, which will become the benchmark for the research methodology for the experimental works in Chapter 3. The definition and concept of composite materials are briefly described. Moreover, the essential considerations in the development of competitive and high mechanical properties of natural fiber composites are critically reviewed. The characteristic of the individual component involved in bio-composites, type and parameter used in composites manufacturing, effect of different fiber physical properties and fiber percentages are highlighted. Furthermore, the selected treatment related to natural fiber modification is also reviewed. Finally, the results from previous research on the development of natural fiber composites are thoroughly studied for surveys to gain information for the selection of the best methodology application for the experimental works of the present study.

2.2 Composites Materials

Composite materials are a system of materials comprising a combination of two or more components with an interface that separates them. (Shah et al., 2017; Smith & Hashemi, 2011). Another definition of composites materials is fibers of high strength and modulus embedded in or bonded to a matrix with distinct interfaces between them (Mallick, 2007). Generally, fibers are the load-carrying members, while the surrounding matrix keeps them in the desired location and orientation acts as a load transfer medium between them and protects them from environmental damages due to elevated temperatures and humidity. Many authors have expressed the composite materials in different ways. Moreover, Gay, Hoa and Tsai (2007) also specified that the term composite materials represent materials with strong fibers surrounded by weaker matrix, which distribute the load equally (Gay et al., 2007). Therefore, a composite material can be summarized as a material that consists of two or more components with different interfaces between matrix and filler.

The composites materials can be classified according to matrix type or fiber type, as shown in Figure 2.1. According to the type of matrix, composites can be classified into three primary groups which are metal matrix composites (MMC), ceramic matrix composites (CMC) and polymer matrix composites (PMC). The subdivisions of polymer matrix composites are synthetic fiber composites and natural fiber composites. The synthetic fiber composites consist of synthetic fiber as reinforcement agents, such as glass, carbon and aramid fibers.

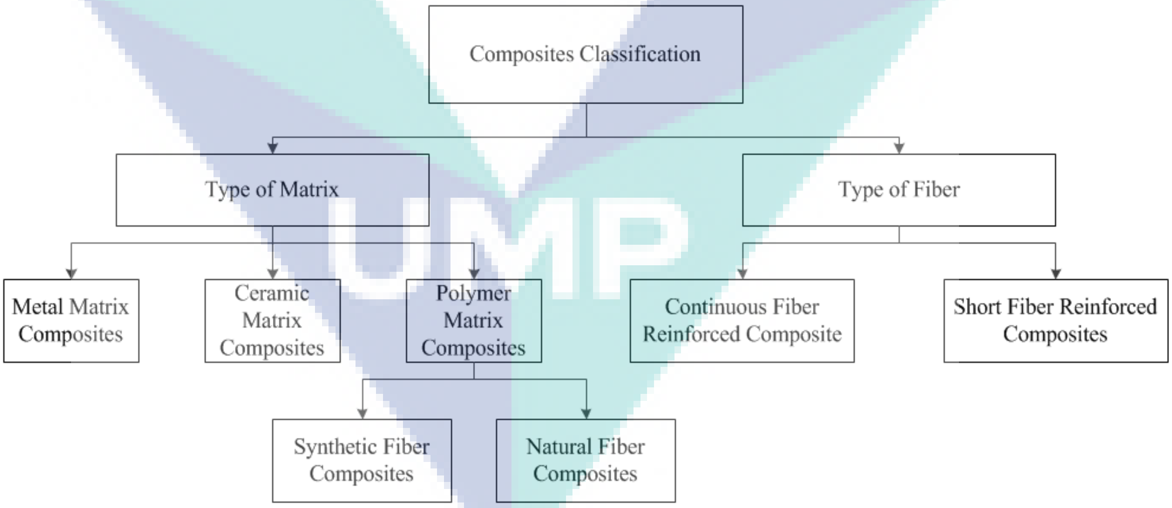

Figure 2.1 Classification of composites

Source: John & Anandjiwala (2008)

However, natural fiber composites are composed of natural fiber, such as kenaf, jute and pineapple leaf fiber (PALF) as a reinforcement agent. The renewable and biodegradable natural fiber composites regained attractiveness since the 1990s due to increase in environmental awareness on various adverse effects which were generated by the accumulation of non-biodegradable waste (Kim et al., 2015; Loh et al., 2013; Palumbo et al., 2015).

On the other hand, composite materials can also be classified according to the type of fiber, which is either continuous or short fiber reinforced composite. However, short fiber composites have gained considerable attention because of their processing advantages, anisotropy in properties and low cost (Liu et al., 2009b; Ranganathan et al., 2016). George et al. (1996) in his study of PALF reinforced HDPE composites presented that short fiber is better in distribution, dispersion and aligned along the direction of flow as compared to a longer fiber length (George et al., 1996b).

2.3 Natural Fiber Reinforced Polymer Composites

The natural fiber reinforced polymer composites are a combination of natural fiber as a reinforcement and polymer as the matrix. The utilization of natural fiber for polymer reinforcing began in 1908 with cellulose material reinforced phenolic (Jawaid & Khalil, 2011). The first reported application of natural fiber reinforced plastics was cotton–polymer composites which were used as radar aircraft by the military (Chiao et al., 1982; Piggott, 2002). Natural fibers can be sourced from two major groups, which are plants and animals (Sanyang et al., 2016). Figure 2.2 illustrates a classification of various natural fibers. The primary categories of natural fiber from animal are silk, wool and hair. Meanwhile, plant fibers or lignocellulose fibers have seven main types, depending on the plant extraction part.

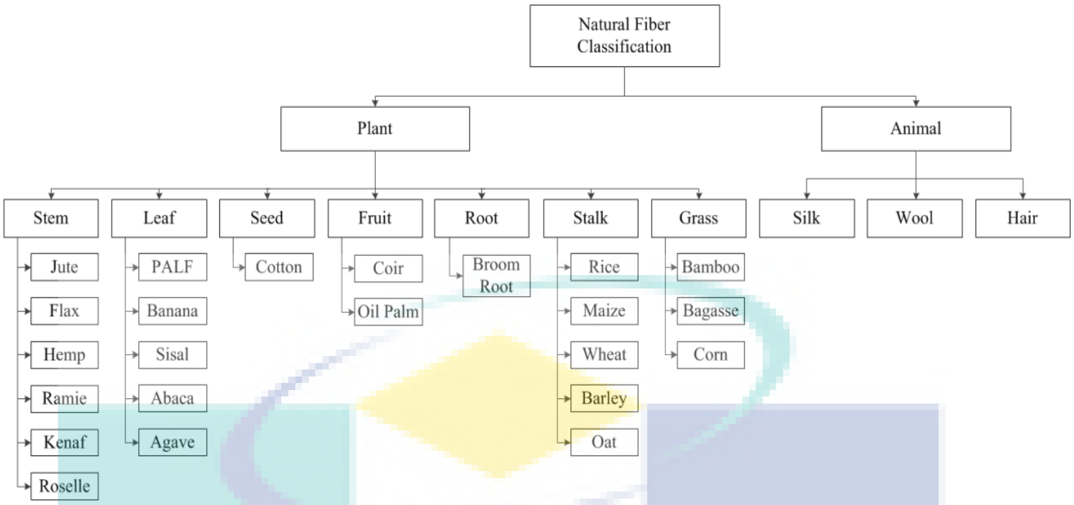

Figure 2.2 Classification of natural fibers

Source: Azwa et al. (2013)

It is worth to note that plant fiber structures are quite complicated. Each fiber is a combination of rigid cellulose microfibrils embedded in soft lignin and hemicellulose matrix, as shown in Figure 2.3 (Rong et al., 2001). Cellulose is the primary structural component of lignocellulose fibers, as it provides strength and stability to the cell walls, and the fiber as a whole. Hemicellulose contributes to fiber stiffness and lignin is a highly cross-linked molecular complex with amorphous structure and acts as a binder agent between individual fiber cells and between fibrils, forming the cell wall (Mohanty et al., 2000a).

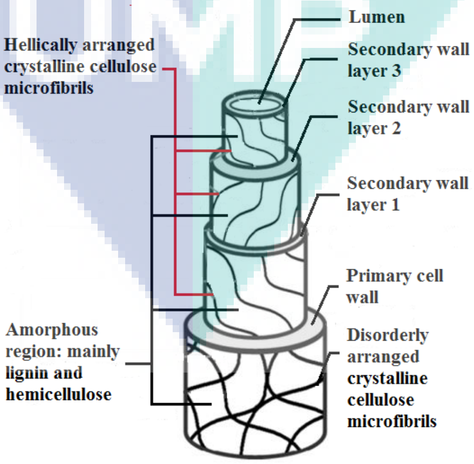

Figure 2.3 Structure of natural fibers

Source: Azwa et al. (2013)

However, many plant fibers, or lignocellulose fibers such as PALF, are natural waste products, and hence available at minimal cost. Moreover, lignocellulose fibers offer many advantages and have a marketing potential. Table 2.1 presents the advantages and disadvantages of lignocellulose fiber (Al-Oqla et al., 2016; Ali et al., 2015; Binoj et al., 2016; Chaudhuri et al., 2013; Sun et al., 2018).

Table 2.1 Advantages and disadvantages of natural fibers

Advantages	**Disadvantages**
Biodegradable and renewable.	Poor moisture resistant which causes swelling of the fibers
Low cost and lightweight	Incompatibility with hydrophobic thermoplastic
High specific properties and low density	Thermal and mechanical degradation during processing
Non-hazardous and no skin irritation	Variable quality, influence by weather, location and plant species
Non-abrasive, friendly processing and no wear of tools.	

2.4 Short Pineapple Leaf Fiber (PALF) Reinforced Polymer Composites

PALF is attractive as a reinforcement agent due to its low commercial value and high availability. On the other hand, PALF relatively has higher mechanical properties as compared to other natural fibers (Liu et al., 2005; Nanthaya & Taweechai, 2014; Neto et al., 2015; Neto et al., 2013). In most previous research works, short PALF was used as reinforcement agent in either thermoset or thermoplastic polymers, such as polypropelene (PP), high density polyethylene (HDPE), low density polyethylene (LDPE), high impact polystyrene (HIPS), nylon, polycarbonate (PC), elastomer and polylactic acid (PLA), as presented in Figure 2.4 (Aji et al., 2011; Arib et al., 2006; Cherian et al., 2011; Kalapakdee & Amornsakchai, 2014; Nanthaya & Taweechai, 2014; Nopparut & Amornsakchai, 2016; Shih et al., 2014; Siregar, 2011; Threepopnatkul et al., 2009). However, a particular previous finding showed that the weak mechanical properties were produced by the combination of PALF and petroleum-based polymer, such as PALF-HIPS and PALF-HDPE composites. The primary factor of this occurrence was the weak interfacial adhesion between hydrophilic PALF and hydrophobic petroleum-based matrix (Sapuan et al., 2011; Siregar et al., 2010). This weakness can be improved by understanding the requirement in the manufacturing process of natural fiber composites.

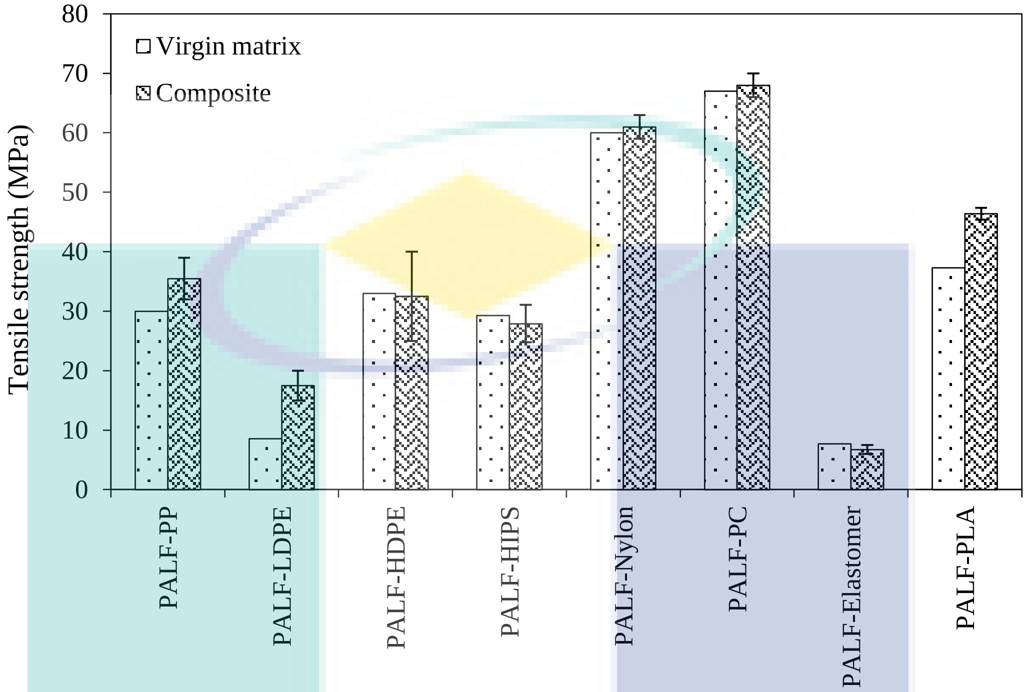

Figure 2.4 The comparison of tensile strength result between virgin polymer and PALF reinforced polymer composites

The essential considerations in the manufacturing of bio-composites can be classified into several elements, as shown in Figure 2.5. The first factor is the characteristic or properties of individual components formed by polymer as matrix and natural fiber as reinforcement agent. Then, the second crucial consideration is the manufacturing process or techniques used. Moreover, the parameter involved in composites manufacturing is another important consideration which involves fiber composition and additional treatment.

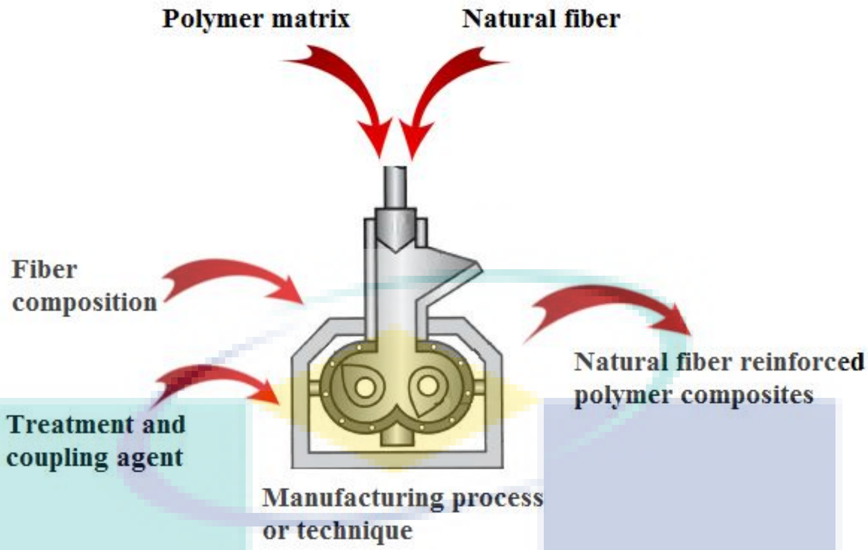

Figure 2.5 Essential considerations in manufacturing of bio-based composites

2.4.1 Polymer Matrix

The common petroleum-based polymer as matrix in the development of natural fiber composites can be broadly classified into two types which are thermoplastics and thermosetting as shown in Figure 2.6. A thermoplastic is a material that becomes moldable or pliable above a specific temperature and solidifies upon cooling. The most commonly used thermoplastics for matrix application in composites development are PP, PE and PVC. On the other hand, thermosetting is plastic that is irreversibly cured of a soft solid or viscous liquid pre-polymer or resin. Curing converts the resin into an infusible, insoluble polymer network, and is driven by an appropriate heat or radiation action often under high pressure, or by mixing with a catalyst. The most common thermosets are epoxy, polyester and phenolic (Callister Jr & Rethwisch, 2012; Ku et al., 2011; Ned J. Chou, 2010; Siregar et al., 2011; Smith & Hashemi, 2011). These two polymers can be easily distinguished through thermal application, where thermoplastics can be repeatedly melt without causing any chemical changes or bonding between the polymer chains. On the other hand, a thermoset does not melt when it is heated, but its components decompose and do not reform upon cooling. Although these two types of matrices are the backbone of natural fiber composites development, thermoplastic materials have the advantage for the plastic recycling industry (Ku et al., 2011).

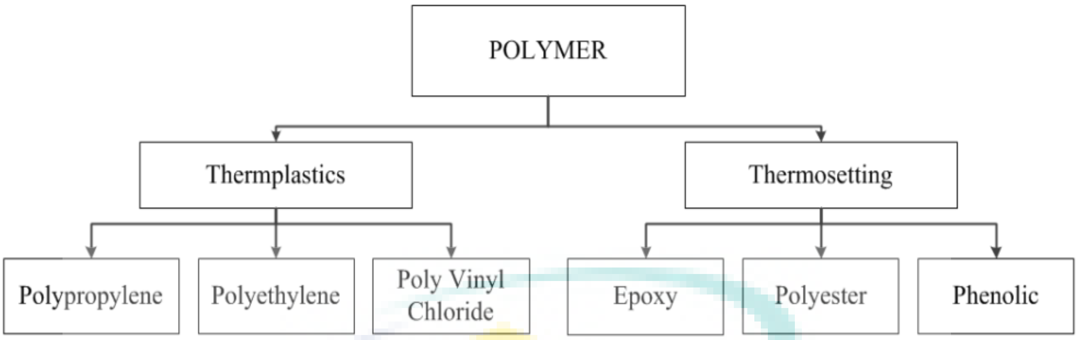

Figure 2.6 Types of the polymers

However, bio-polymer such as starch-based polymer has currently become very popular and attractive as an alternative for the petroleum-based matrix in natural fiber composites development. According to the European Bioplastics, bio-polymers must have two main features made from renewable sources and also must be biodegradable and compostable (Bioplastics, 2017; Siracusa et al., 2008). However, plastic based on renewable sources is not necessarily biodegradable or compostable because biodegradability is directly related to the chemical structure of the substance rather than the polymer origin. According to ASTM D5488-94d, the terminology of degradation is the ability of a polymer to undergo decomposition processes into carbon dioxide, methane, water, organic compounds or biomass, where the primary mechanism is the enzymatic action of microorganisms that can be measured by standard testing over specific time periods, reflecting the existing disposal conditions (ASTM, 1994; Avérous, 2004). Several synthetic polymers are biodegradable and compostable, such as polybutylene adipate terephthalate (PBAT). Meanwhile, some of the bioplastics based on natural monomer, can lose their biodegradability property through chemical modification like polymerization, for example, Nylon 9 polymers which was obtained from the polymerization of oleic acid monomer or Polyamide 11 derived from the polymerization of castor oil monomer (Bioplastics, 2017). Figure 2.7 presents the details on the classification of the polymer according to its resource and biodegradable capability.

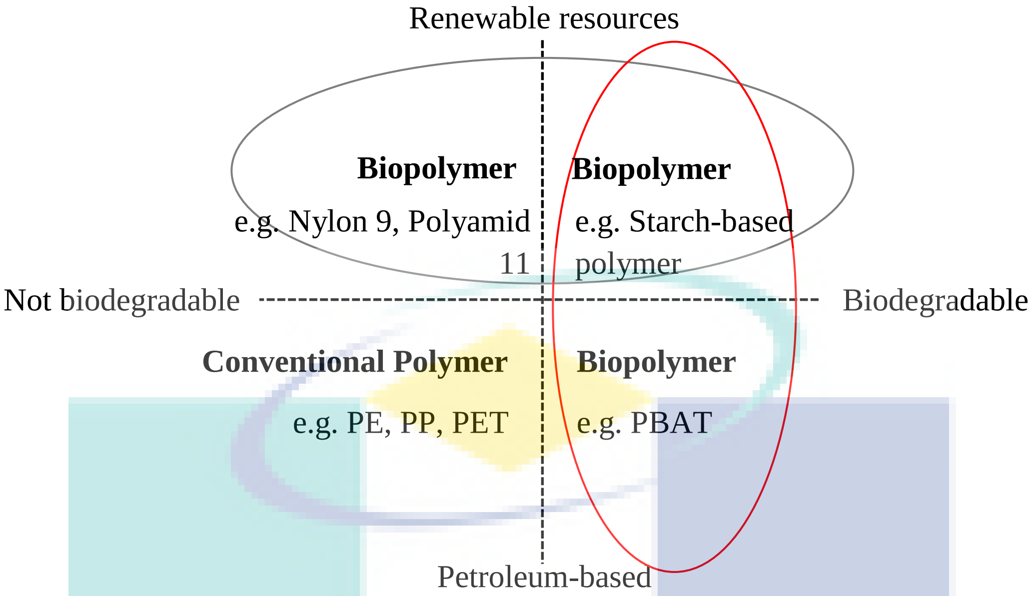

Figure 2.7 Classification of the polymer

Owing to its complete biodegradability and renewability, the starch-based polymer is considered as a promising matrix to develop sustainable environmental friendly composites (Lu et al., 2009; Marques et al., 2002). Previous findings showed that there were three primary methods in the development of starch-based polymers which were blending, deviation and graft copolymerization (Lu et al., 2009). Deviation process of starch is generally carried out via the reaction of hydroxyl groups in the starch molecule to develop thermoplastic starch. The derivatives have physicochemical properties that differ significantly from the parent starch, but the biodegradability is still maintained. On the other hand, another promising bio-polymer is poly lactic acid (PLA), which is obtained from the complex controlled ring-opening graft copolymerization of ε-caprolactone or L-lactide technique (Garlotta, 2001; Lu et al., 2009). Although PLA is no longer classified as starch-based polymer after the copolymerization process, it is still biodegradable and compostable. However, the commercially available PLA in the current market is still limited without a competitive price as compared to the petroleum-based polymer. Therefore, the blending method is the most attractive process in the development of cost-effective bio-polymer with acceptable mechanical properties of starch-based polymer.

2.4.1.1 Tapioca Biopolymer (TBP)

In the United States and Canada, corn starch is a common renewable resource for the development of starch-based polymer (Garlotta, 2001; Gruber & O'Brien, 2005; Martin & Averous, 2001; Vink et al., 2003). However, tapioca starch is one of the most widely available renewable resources in the Asian regions. Therefore, the innovation of starch-based polymer derived from tapioca, called tapioca biopolymer (TBP), was developed. The TBP was produced by using a blending method with the composition of 60% of tapioca starch, 30% of PLA and 10% of additive.

The tapioca is a chemically complex polymeric carbohydrate material, comprising two significant microstructures, which are amylose and amylopectin. Amylose is mostly a linear structure of α-1 with four linked glucose units, and amylopectin is a highly branched structure of short α -1 with four chains linked by α -1 and six bonds (George et al., 1996a). The structures of amylose and amylopectin are shown in Figure 2.8.

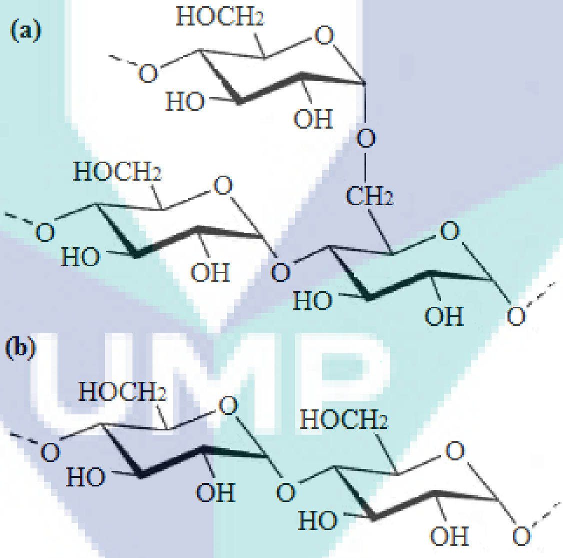

Figure 2.8 Structure of (a) amylopectin, (b) amylose
Source: Avérous (2004)

2.4.1.2 Polymer Processing Temperature

Most of the petroleum-based polymers, such as polycarbonate and PVC, have processing temperatures higher than 200°C. Previous research found that these range of operating temperatures become a significant barrier in manufacturing natural fiber reinforced polymer composites. It is because most natural fibers have degradation temperature at approximately 200°C. However, starch-based polymer like TBP has a lower range of processing temperature as compared to most petroleum-based polymers. Figure 2.9 shows the comparison of processing temperature range between starch-based polymer and selected thermoplastic matrix, such as PC, PP, PVC, HDPE, LDPE, HIPS and Nylon 6.6 (Callister Jr & Rethwisch, 2012; Gong et al., 2004; Levchik et al., 1999; Luyt et al., 2006; Siregar et al., 2011; Smith & Hashemi, 2011; Threepopnatkul et al., 2009; Vink et al., 2003). Figure 2.9 also indicates that the degradation temperature for most natural fiber which is approximately 200°C (Ku et al., 2011; Shalwan & Yousif, 2013; Yousif et al., 2012).

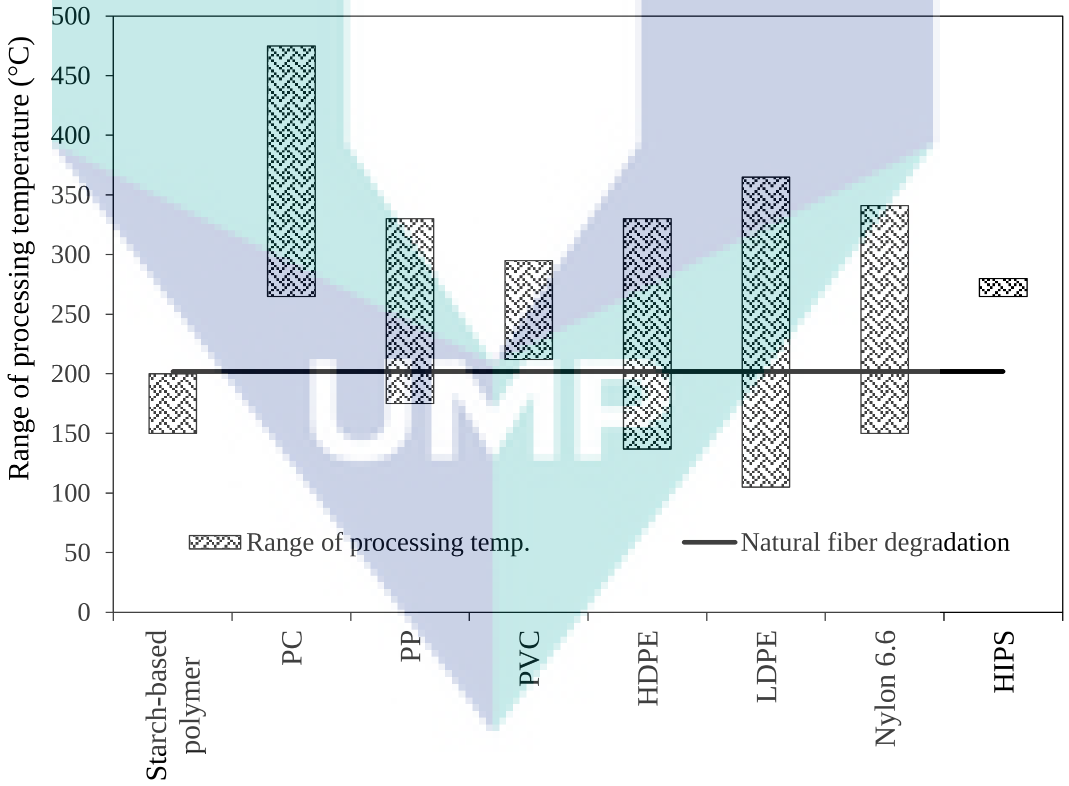

Figure 2.9 Comparison of selected composites matrix processing temperature

According to Figure 2.9, the range of processing temperature technically makes starch-based polymer like TBP compatible with almost all types of natural fibers, especially with PALF. The manufacturing of natural fiber composites by using TBP as a matrix can be performed before natural fiber degradation. However, the thermal processing for starch-based polymer like TBP is more complex than petroleum-based polymer resin because of numerous chemicals and the physical reactions that occurred during processing, such as water evaporation, granular expansion, glass transition, melting, and decomposition (George et al., 1996a). Previous findings present that starch-based polymer has the glass-transition and melt temperature of about 55°C and 175°C, respectively. Moreover, the drying process must be carried out on starch-based polymer before it is used in the manufacturing process as water evaporation occurs in this material at a temperature of 80°C. Moreover, the starch-based polymer undergoes thermal degradation at temperature above 200°C (Jamiluddin et al., 2016).

On the other hand, temperature is one of the crucial processing parameters which can establish the phase morphology and crystalline structure of polymer. Crystalline structure was controllable by designing a suitable temperature during processing. It is because the processing temperature has a significant effect on the co-continuous structure. The co-continuous structure is a structure formation in melt-mixed immiscible polymers blends which can be formed over certain interval of volume fractions (Pötschke & Paul, 2003). Thus, previous finding indicate that the modification of continuity degree and stability has significantly affects the mechanical properties results (Khondker et al., 2005; Su et al., 2010). Therefore, the determination of optimum processing temperature for TBP is vital for the best development of PALF-TBP composites.

2.4.2 Natural Fiber

The properties of natural fiber are other essential considerations in the manufacture of natural fiber composites. The chemical composition and physical properties of natural fiber were proven to affect the performance of bio-based composites. Therefore, proper investigation, screening and selection of natural fiber before the manufacture of composite are required to produce high mechanical properties of composite materials

2.4.2.1 Influence of Chemical Composition of Natural Fiber

Theoretically, the combination of polymer matrix and natural fiber is directly related to the mechanical properties of bio-composite enhancement. However, not all natural fibers have excellent mechanical properties. The mechanical properties of natural fiber are varied between natural fibers. One of the significant factors that influence the mechanical properties of natural fiber is cellulose content (Neto et al., 2015; Neto et al., 2013). Cellulose is the main structural component of the lignocellulose fibers, as it provides strength and stability to the cell walls and the fiber as a whole. Previous findings established that natural fiber with high cellulose content presents high tensile strength results (Azwa et al., 2013; John & Thomas, 2008; Methacanon et al., 2010). The other two major components in natural fiber are hemicellulose and lignin. Hemicellulose contributes to fiber stiffness and lignin is a highly cross-linked molecular complex with amorphous structure and acts as a binder agent between individual fiber cells and fibrils, which form the cell wall (Mohanty et al., 2000a; Tian et al., 2017). However, high content of hemicellulose and lignin possesses several disadvantages which cause high moisture absorption and biodegradation. This phenomenon results in reduced interfacial adhesion between the fiber and matrix.

The process of water absorption by hemicellulose and lignin is presented in Figure 2.10. When a natural fiber composite is exposed to moisture or water, the moisture or water will penetrate and attach to the hemicellulose and lignin components. This phenomenon will establish intermolecular hydrogen bonding in fiber and reduce interfacial adhesion between natural fiber and matrix, as shown in Figure 2.10a. Degradation process occurred when swelling of cellulose fiber develops stress at the fiber-matrix interface and produces a micro-cracking condition in the matrix around the fiber and produces capillarity. The transport through microcracks is presented in Figure 2.10b. At this stage, bound water increases because water is absorbed excessively and water-soluble substance in natural fiber starts to leach from fiber and produce debonding phenomenon between the fiber and matrix, as illustrated in Figure 2.10c.

This phenomenon was reported by Dhakal et al. in hemp fiber reinforced unsaturated polyester composites (Dhakal et al., 2007). Figure 2.10d presents the development of osmotic pressure pockets at the surface of the fibers due to the leaching of water-soluble substances from the fiber surface, which produces ultimate debonding situation between the fiber and matrix.

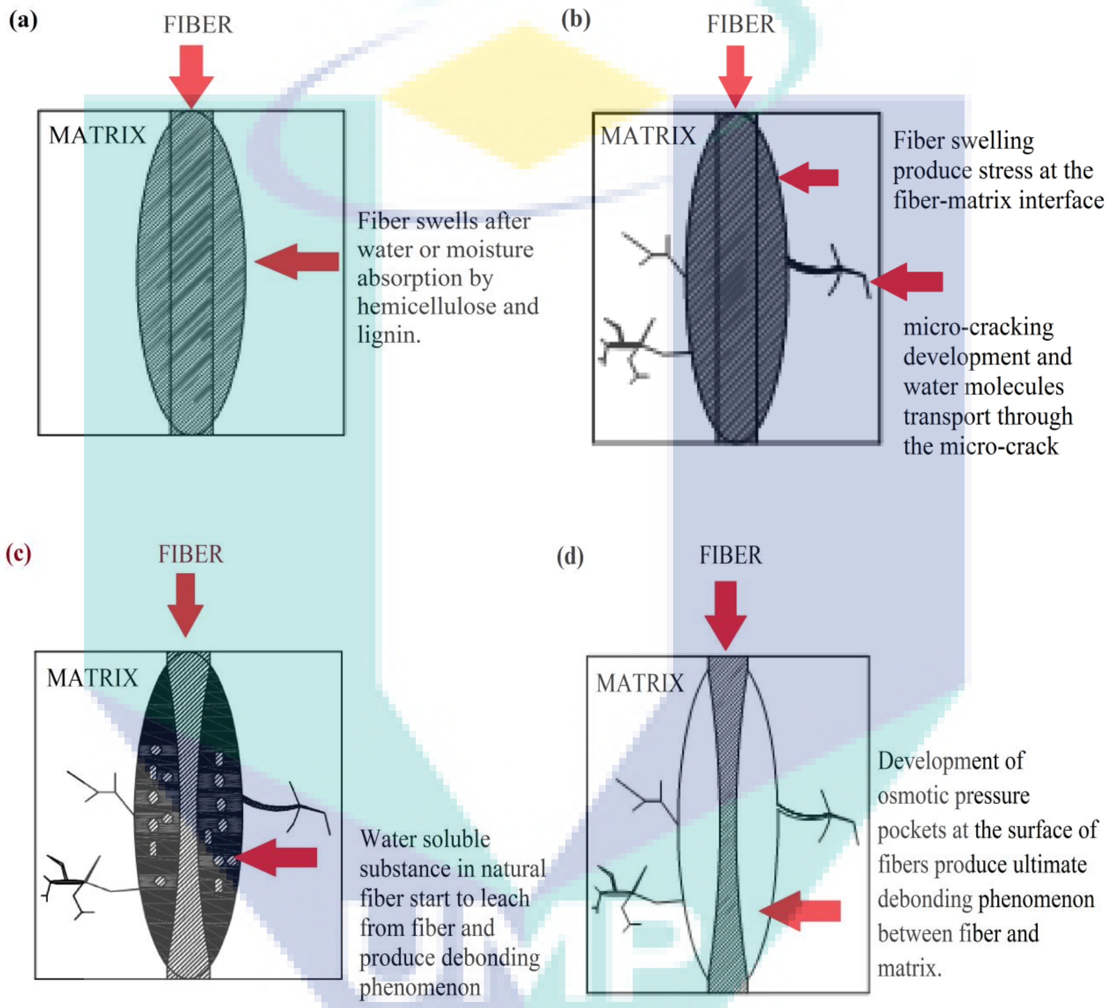

Figure 2.10 Moisture absorption by hemicellulose and lignin components
Source: Azwa et al. (2013)

Figure 2.11 presents the comparison of chemical composition among selected natural fibers. Moreover, the tensile strength value of each fiber is also presented. According to Figure 2.11, PALF presents the highest content of cellulose and lowest content of hemicellulose and lignin (Haque et al., 2009; Hu & Lim, 2007; Manaila et al., 2015; Mohanty & Nayak, 2006; Prasad et al., 2016; Shah et al., 2017; Xia et al., 2017). Majority of the natural fiber with high cellulose content present high tensile strength results and PALF is among the highest in tensile strength as compared to other natural fibers. As a comparison, three natural fibers with the lowest cellulose content (coir, bamboo and cotton) present low tensile strength result (Azwa et al., 2013; John & Thomas, 2008; Methacanon et al., 2010). The finding showed that PALF has extraordinary potential as reinforcement agent in the development of bio-composite materials.

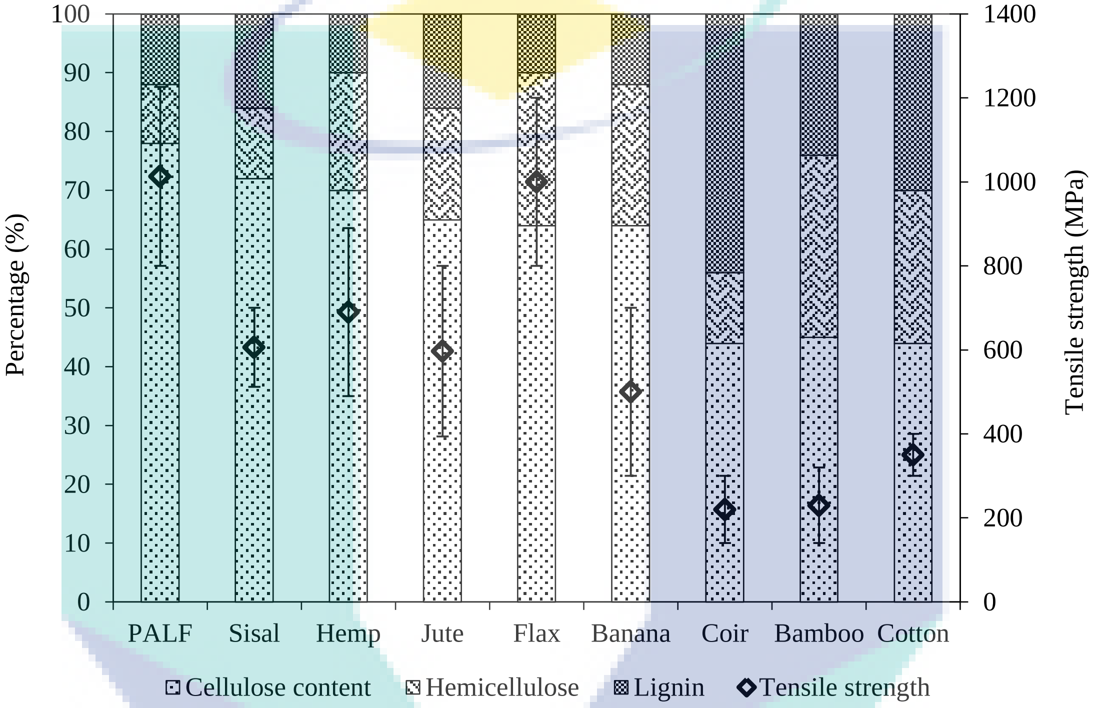

Figure 2.11 Comparison of cellulose content and tensile strength

However, the chemical composition and tensile strength of PALF still differ from one sample to another. Table 2.2 shows the chemical composition of PALF obtained from several published articles. The results indicated that the chemical composition of fiber varied, depending on species, age of fibers, extraction used and location of the pineapple plant, as reported by Neto et al. (Nanthaya & Taweechai, 2014; Neto et al., 2015; Pickering et al., 2016).

Table 2.2 Comparison of chemical composition of PALF

Chemical composition (%)	**(Devi et al., 1997)**	**(Mohanty et al., 2000b)**	**(Khalil et al., 2007)**	**(Hidayat, 2008)**	**(Sapuan et al., 2011)**	**(Nanthaya & Taweechai, 2014)**
Cellulose	53.4 ± 0.3	81.5	70 - 82	73.4	79.36	67.12 - 69.34
Hemicellulose	31.9 ± 0.3	-	-	7.1	13.07	12.96 - 18.38
Lignin	23.0 ± 1.9	12.7	5 - 12.7	10.5	4.25	14.5 - 15.4
Ash	1.8 ± 0.1	-	-	2	2.29	1.21
Extractive	-	-	-	5.5	5.73	0.97 - 3.83

In addition, Figure 2.12 presents the influence of chemical composition on PALF single fiber tensile strength studied by Sena Neto et. al. (Sena Neto et al., 2013). According to the graph, the PALF sample with cellulose index more than 50% produce higher single fiber tensile strength result which is between 500 to 700 MPa. In contrast, PALF sample with less than 50% of the cellulose index produces lower tensile strength result which is between 200 to 400 MPa only.

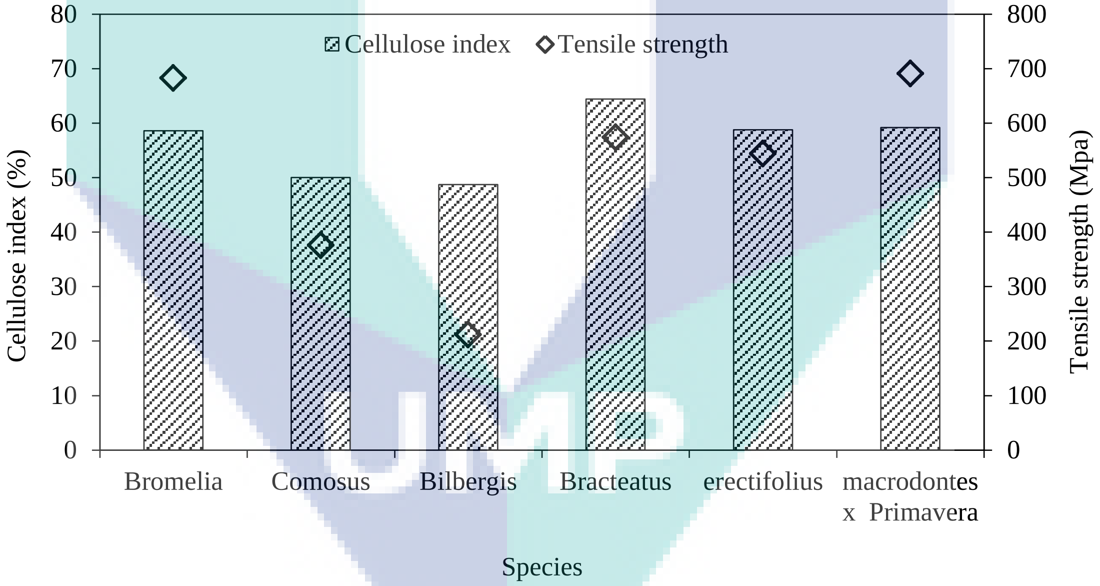

Figure 2.12 Comparison of PALF cellulose index and single fiber tensile strength

Therefore, the PALF chemical composition analysis and single fiber testing are required as an initial screening in the selection of fiber for bio-composites development. Moreover, the outcomes from PALF characterization have become essential in understanding and interpretation of PALF performance as reinforcement agent in composite materials.

2.4.2.2 Effect of Physical Properties of Natural Fiber

The physical property of natural fiber is one of the crucial considerations that affect mechanical properties of composites. The diameter and length of natural fiber play a significant factor in affecting the mechanical properties of composites (Beg & Pickering, 2008; Duval et al., 2011; Liu et al., 2007; Park et al., 2006; Shibata et al., 2005). For natural fiber individual diameter, a small fiber diameter has better effect in enhancing the mechanical properties of bio-composites as compared to a big diameter. For instance, increasing the cross-sectional area of natural fibers increases the occurrence of stress concentration defects (Sena Neto et al., 2013). On the other hand, micrograph analysis by Liu et al. discovered that small diameter fiber has better fiber dispersion in the matrix as compared to the bigger diameter fiber (Liu et al., 2005).

The present study also reviews the influences of various fiber extraction methods on individual fiber diameter. Figure 2.13 illustrates the different fiber diameters produced by various methods, such as retting, scrapping, ball milling, disc milling and disc milling of dried leaf (Kengkhetkit & Amornsakchai, 2012). Retting and scrapping techniques are the traditional methods of natural fiber extraction. Water retting is a process by micro-organism to separate or decompose the sticky substances around the natural fiber. Retting process is done by inserting raw fiber materials into water within a particular time. Water conditions, water pH, temperature, macro-nutrients, bacteria, and process duration are among the factors that influence the production of extraction. Whereas, the scraping method is the process of separating fibers and substances that are attached to the fibers by using non-sharp plates or knives. In addition, ball-milling or discs milling methods are other alternatives of extraction for mass production purposes. In general, retting and scrapping techniques produce low fiber content, low cycle time and labor intensive, also they are problematic to the environment. In ball milling, chopped fiber and specific quantity of water are placed inside a cylinder with the steel balls, and the barrel is capped at both ends. Then, the cylinder is driven to rotate at specified rpm and duration. Meanwhile disc milling process requires mixing of fiber and water and to go through a grinding process by using disc mill machine at certain speed and duration.

However, disc milling of the dried leaf is the same method with disc milling but without water mixing. According to Figure 2.13, ball milling process is capable of producing the smallest diameter of single fiber as compared to other extraction processes. However, ball milling techniques are still new and not commercialized in the fiber extraction industry. Moreover, retting and scrapping techniques are common methods applied in fiber extraction industry, primarily in Indonesia and Thailand. It is due to lower production cost and high availability as compared to other methods. Therefore, extracted fibers through scrapping are prioritized to be used as reinforcement in this study since PALF and TBP combinations are new as bio-composites.

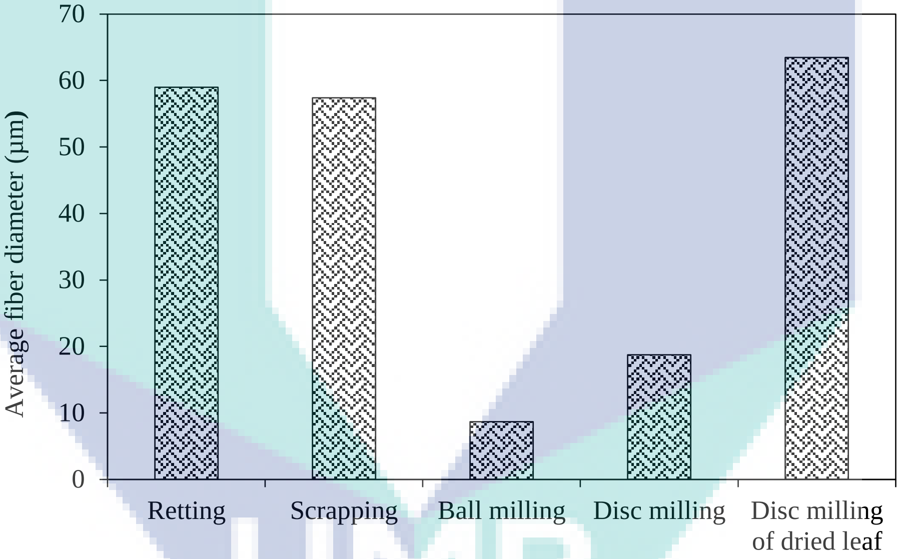

Figure 2.13 Comparison of fiber diameter against different extraction method

Individual fiber length is another important consideration in bio-composites development (Aji et al., 2011; Amuthakkannan et al., 2013; Takagi & Ichihara, 2004). Decreasing the fiber length more than the critical length will reduce stress transfer efficiency between the matrix and fiber. This phenomenon is due to the fiber pull-out process requires less energy, and it decreases with the mean fiber length (Ranganathan et al., 2016); thus, producing a low mechanical properties result.

However, long and continuous natural fiber reinforced polymer composites manufacturing is limited to particular manufacturing processes, such as manual mixing process, hand lay-up process and thermoset matrix utilization. According to industrial mass production requirement and material recycling needs, thermoplastic matrix enhanced with short fibers, is more preferable. The industrial mass production requires recycling capability and compatibility with large-scale production process, which require automatic mixing processes, such as extrusion, internal mixing before sample manufacturing by using the hot press and injection molding method. It is due to short fiber composites offer advantages in processing, anisotropy in properties, better dispersion and low cost (Lee et al., 2009; Liu et al., 2009b; Ranganathan et al., 2016).

It can be noticed from a study by George et al. (George et al., 1996b) on PALF reinforced HDPE composites that the viscosity marginally increases upon an increase in fiber length from 2.00 mm 10.00 mm. At higher fiber length, the fiber dispersion is not so good and at the same time difficult to orient in the direction of flow. However, fiber with 2.00 mm length is better in distribution, dispersion and is aligned along the direction of flow as compared to 4.00 mm, 6.00 mm, 8.00 mm and 10.00 mm fiber lengths. Moreover, a tensile strength with fibers parallel with the tension direction, showed a maximum value while fibers with perpendicular direction tended to decrease in tensile strength (Hargitai et al., 2008; Ku et al., 2011).

2.4.3 Manufacturing Process of Composites

Manufacturing process or technique used in bio-composites development is a primary consideration that significantly affects the properties and interfacial characteristics of composites (Ku et al., 2011; Liu et al., 2007; Westman et al., 2010; Zampaloni et al., 2007). Fiber processing techniques can be classified into three steps, which are raw material moisture removal, mixing process between fiber and matrix and sample or part fabrication. The results of the previous studies agreed that 80°C is the optimum temperature for natural fiber moisture removal (Nanthaya & Taweechai, 2014; Sapuan et al., 2011; Siregar, 2011; Siregar et al., 2011).

Then, the subsequent process is the mixing of fiber and matrix. The two typical processes are extrusion by using an extruder and melt mixing by using an internal mixing machine. The findings by Joseph et al. (Joseph et al., 1999) on the influence of processing variables on the mechanical properties of sisal-fiber reinforced polypropylene composites, indicated that melt mixing process is capable of producing higher tensile properties than extrusion method, as shown in Figure 2.14. The finding is associated with melt-mixed process which produces more efficient mixing and orientation, possibly at the fiber-matrix interface region, and thus presents higher tensile properties. In their research, samples with different fiber loading were prepared with two different mixing processes, namely extrusion and melt mixing process. Meanwhile, sample fabrication used compression molding.

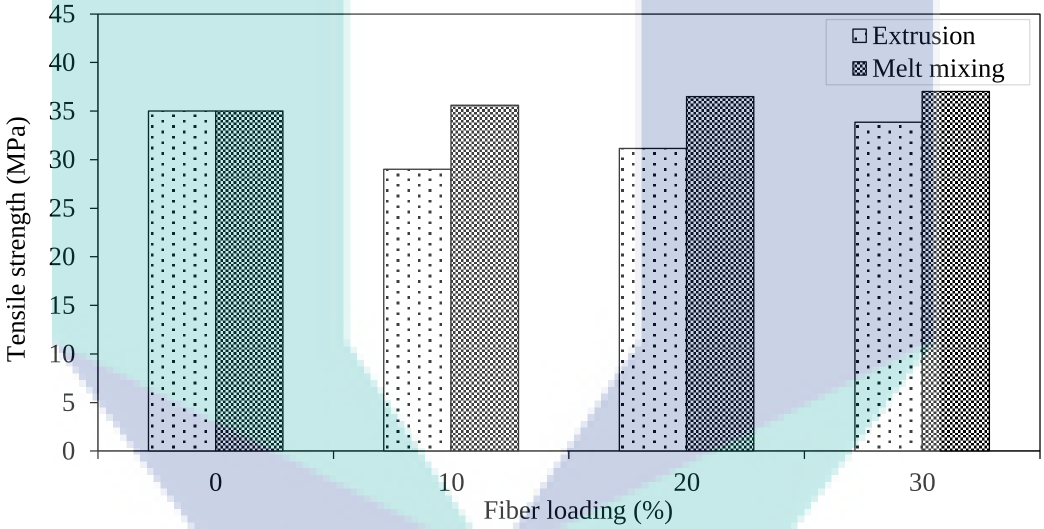

Figure 2.14	Effect of different mixing process

Meanwhile, techniques used in composite manufacturing have great influence on the mechanical properties of composites. Injection molding and compression molding are the standard techniques in bio-composites manufacturing (Westman et al., 2010). Injection molding is one of the most common types of manufacturing processes in use today. Injection molding has several advantages over other methods, such as high production rate, shorter production cycle, allows close tolerances in small intricate parts and requires little post-production work because parts have a finished look upon ejection (Callister Jr & Rethwisch, 2012; Kalpakjian & Schmid, 2014; Smith &

Hashemi, 2011). Compression molding also offers several advantages like low cost and little waste due to little material loss during processing as compared to injection molding, which requires gates, sprues and runners. Moreover, compression molding is ideal for large and intricate parts (Callister Jr & Rethwisch, 2012; Kalpakjian & Schmid, 2014; Smith & Hashemi, 2011).

Previous finding by Liu et al. (Liu et al., 2007) presented that compression molding produces higher mechanical properties' result than those produced by using injection molding. Impact strength and tensile modulus results of compression molding samples presented 80% and 10%, respectively, which were higher than the injection molding samples, as shown in Figure 2.15. Tungjitpornkull and Sombatsompop (Tungjitpornkull & Sombatsompop, 2009) also presented a similar argument to this finding, whereby their experimental results suggested that compression molding process gave better tensile modulus than the sample produced by injection molding. Moreover, previous review by Ku et al. (Ku et al., 2011) also presented consistent results, whereby the composites manufactured by compression molding had higher specific density, which resulted in less void and air; hence, stronger than injection molding samples. Zampaloni et al. deduced in their article that the optimal fabrication method for natural fiber composites was determined by compression molding (Zampaloni et al., 2007)

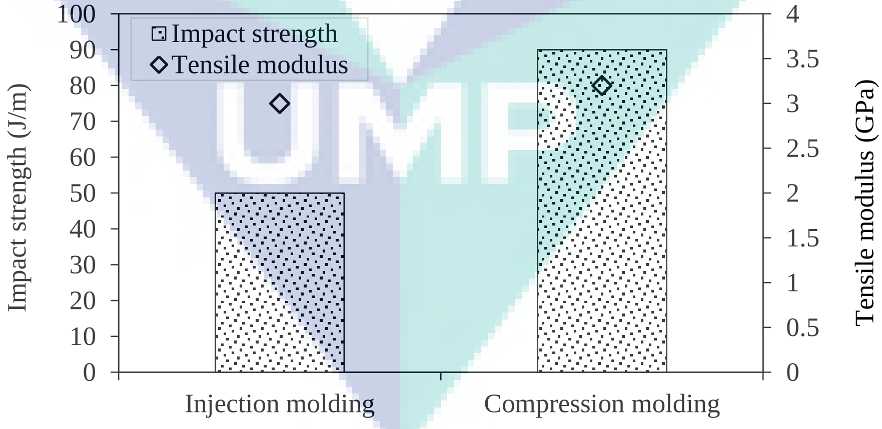

Figure 2.15 Effect of different manufacturing process

However, the determination of appropriate parameter used in compression molding process is vital to produce complete melted-matrix and thoroughly penetrate into the fiber bundles. Tables 2.3 presents various parameters used in compression molding from previous research on bio-composites manufacturing.

Table 2.3 Comparison of parameters used in compression molding process for bio-composites manufacturing

Natural fiber	**Matrix**	**Processing temperature (°C)**	**Heating duration (min)**	**Pressure used (MPa)**	**Reference**
Agar	Sugar palm starch	140	10	2.5	(Jumaidin et al., 2016)
Bagasse	Corn starch	160	10	10	(Shibata et al., 2005)
Banana fiber	LDPE	180	10	20	(Prasad et al., 2016)
Hemp	PLA	170	10	1.3	(Hu & Lim, 2007)
Jute	Polyester	135	5	0.2	(Mohanty et al., 2000a)
Jute	PP	160	15	2	(Khondker et al., 2005)
Kenaf	Corn starch	160	10	10	(Shibata et al., 2005)
Kenaf	Polyester	140	5	2.5	(Ibrahim et al., 2010)
Kenaf	PP	190	10	69	(Zampaloni et al., 2007)
Kenaf	Soy flour	135	10	17	(Liu et al., 2007)
Kenaf	Vinyl ester	135	25	8	(Westman et al., 2010)
PALF	PLA	190	10	4	(Huda et al., 2008)
Poly (Butylene Succinate)	Corn starch	150	4	14	(Yun et al., 2016)
Ramie	PLA	170	4	20	(Yu et al., 2010)
Sisal	PP	170	-	8	(Joseph et al., 1999)
Sweet sorghum	PLA	180	10	5	(Zhong et al., 2011)
Wood	PP	190	5	20	(Bledzki & Faruk, 2004)

The processing temperature and duration set between 135°C to 190°C and 4 to 25 min, respectively, as shown in Table 2.3. Li et al. (Liu et al., 2009b) recommended that the processing temperature should be lower than 192ºC for better composite quality. However, the temperature should not be lower than 160ºC to ensure sufficient melting of the matrix. Moreover, Khondker et al. (Khondker et al., 2005) recommended that processing temperatures of higher than 175ºC should be heated in short duration to maintain the natural fiber ability as a reinforcement agent. Therefore, according to the previous study, the best processing temperature to be used for composite manufacturing is between 160°C to 190°C.

Another crucial parameter in compression molding process is the pressure used. Previous finding presented that pressure used in composites fabrication was between 0.2 MPa to 69 MPa. The use of high pressure in bio-composite manufacturing is good to produce better interfacial adhesion between fiber and matrix. Nevertheless, it must be considered that by increasing the press capacity, not only higher tensile values and flexural properties are recognized but also the structure of the hollow fibers could be damaged; and consequently, a negative effect on the mechanical properties can be found (Medina et al., 2009). Figure 2.16 illustrates the influence of pressure used on flexural strength of the hemp-epoxy composites. The result showed 6 MPa as the critical pressure for hemp-epoxy composites manufacturing. Further increase in pressure resulted in a decrease in impact strength of the composites due to damage in the fiber structure (Medina et al., 2009).

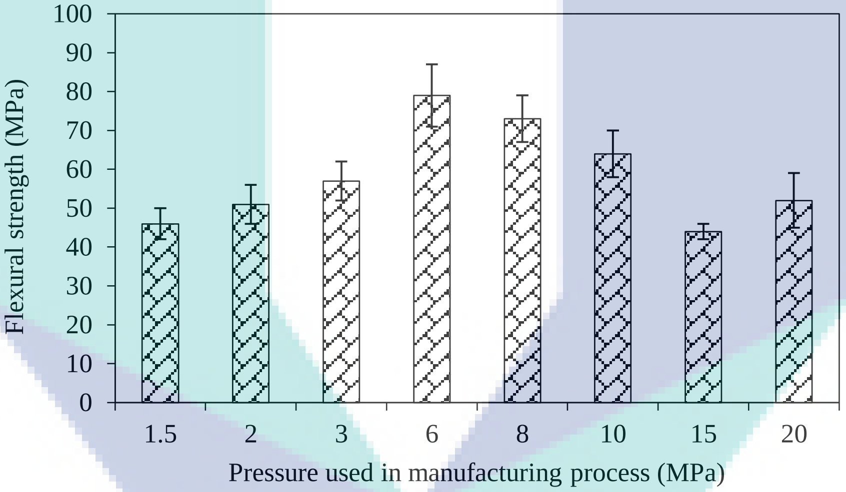

Figure 2.16 Influence of different pressure used in bio-composites manufacturing

2.4.4 Fiber Loading in Composites

Other crucial consideration in manufacturing of bio-composites is fiber loading or fiber percentage. According to the rules of mixture (see Equation 2.1), increase in fiber concentration of high strength fibers is directly related to increase in the mechanical properties of bio-composites.

$$\sigma_c = \upsilon_f \sigma_f + \upsilon_m \sigma_m \qquad 2.1$$

where, σ_f is natural fiber mechanical properties, σ_m is mechanical properties of virgin matrix, υ_f is fiber proportion, and υ_m is matrix proportion. However, from the experimental perspective, an increase of over optimum value always deteriorate the mechanical properties (El-Shekeil et al., 2012; Ku et al., 2011; Paglicawan et al., 2014; Sastra et al., 2006; Siregar et al., 2010). Several studies were conducted to determine the optimum value of fiber loading in composites to obtain the maximum mechanical properties, especially tensile properties. However, there is no universal value in which maximum tensile strength can be achieved. The optimum fiber loading in bio-composites development is summarized at 10% to 50% as presented in Table 2.4.

Table 2.4 Comparison of optimum fiber loading between various existing natural fiber reinforced polymer composites

Natural fiber	**Matrix**	**Fiber loading (%)**	**Optimum fiber loading (%)**	**Reference**
Coir	PP	0, 15, 20, 25, 30, 35	15	(Haque et al., 2009)
Flax	HDPE	0, 5, 10, 20, 30	30	(Li et al., 2006)
Hemp	PLA	30, 40, 50	40	(Hu & Lim, 2007)
Hemp	PP	0, 30, 40, 50,70	40	(Hargitai et al., 2008)
Jute	Poly butylene succinate (PBS)	0, 10, 20, 30	20	(Liu et al., 2009b)
Jute	PP	10, 20, 30, 40, 50, 60, 70	40	(Lee et al., 2009)
Kenaf	Corn-starch	0, 10, 30, 50, 60, 70	50	(Shibata et al., 2005)
Kenaf	Polyurethane	20, 30, 40, 50	30	(El-Shekeil et al., 2012)
Kenaf	PP	10, 20, 30, 40, 50, 60, 70	40	(Lee et al., 2009)
Micro winceyette	Corn-starch	0, 5, 10, 15, 20	20	(Ma et al., 2005)
PALF	HIPS	0, 10, 20, 30, 40, 50	10	(Sapuan et al., 2011; Siregar, 2011)
PALF	HDPE	10, 20, 30, 40, 50, 60, 70	30	(Aji et al., 2011)
PALF	PP	0, 10, 20, 30	30	(Nanthaya & Taweechai, 2014)
Palm	PP	0, 15, 20, 25, 30, 35	15	(Haque et al., 2009)
Rice husk	HDPE	0, 10, 20, 30, 40	30	(Tong et al., 2014)
Sisal- oil palm	Natural rubber	10, 20, 30, 40, 50	30	(Jacob et al., 2004)

The previous study reveals that the determination of optimum fiber loading was according to the tensile test output. Most of the previous study findings indicate that 30% of fiber loading is the optimum percentage in composite manufacturing. In natural fiber reinforced polymer composites, tensile failure depends on the fiber bonding on the fiber-matrix interface. The applied stress is transferred from the matrix to the fibers across the interface. Therefore, the interfacial adhesion between fiber and matrix plays an important role in crack propagation (Ku et al., 2011; Liu et al., 2005; Threepopnatkul et al., 2009). In higher fiber loading, a reduction in the matrices composition causes the interface adhesion between the fibers and matrix to become weak. Moreover, fibers with higher percentage, especially of greater than 50%, tend to aggregate in the composites and thereby deteriorate the interfacial adhesion between the fibers and matrix (Shalwan & Yousif, 2013). This phenomenon results in lower mechanical properties of the composites. Therefore, the selection of correct optimum fiber composition is essential to generate maximum mechanical properties of bio-composites.

2.4.5 Additional Treatments Engaged in Manufacturing of Composites

Additional treatments in bio-composites manufacturing, such as alkali treatment and coupling agent utilization, play a significant role in solving poor interfacial adhesion between fiber and matrix (Ku et al., 2011).

2.4.5.1 Alkali Treatment

The utilization of sodium hydroxide (NaOH), or also known as alkali treatment, was proven to increase interfacial adhesion between fiber and natural matrix in bio-composites manufacturing (Asim et al., 2016; Hamdan et al., 2017; Panyasart et al., 2014; Siregar et al., 2010). The alkali treatment is capable of increasing the fiber surface roughness. This phenomenon able to improve interfacial adhesion between fiber and matrix by provides physical interlocking between fiber and matrix, which affects the tensile properties of composites. Various extensive research was carried out with different alkali concentrations and soak durations to produce better interfacial adhesion as summarized in Table 2.5.

Table 2.5 Comparison of NaOH concentration and soak duration

Natural fiber	**Matrix**	**Concentration (% w/v)**	**Soak duration (hour)**	**Temperature (°C)**	**Reference**
Acacia	polyethylene terephthalate (PET)	10	4	Room temperature	(Ahmad et al., 2008)
Bagasse	Polyester	5	2	25 °C	(Cao et al., 2006)
Coir	Polyester	2	1	70 °C	(Rout et al., 2001)
Flax	PP	5, 10	1 to 24 hours	Room temperature	(El-Sabbagh, 2014)
Hemp	PP	5, 10	1 to 24 hours	Room temperature	(El-Sabbagh, 2014)
Jute	Polyester	5	0.5	30 °C	(Mohanty et al., 2000a)
Jute	Vinyl ester	5	4	25 °C	(Stocchi et al., 2007)
Kenaf	Polyester	2, 4, 6, 8	3	Room temperature	(Ibrahim et al., 2010)
Ramie	Epoxy	5	1	Room temperature	(Hamdan et al., 2017)
Ramie	PLA	5	3	Room temperature	(Yu et al., 2010)
Sisal	HDPE	10	1	-	(Paul et al., 1997)
Sisal	PP	5, 10	1 to 24 hours	Room temperature	(El-Sabbagh, 2014)
Sugar palm	Epoxy	1, 2	1, 4, 8	Room temperature	(Bachtiar et al., 2008)
PALF	Natural rubber	1, 3, 5, 7	18	Room temperature	(Lopattananon et al., 2006)
PALF	Phenolic resins	6	3	Room temperature	(Asim et al., 2016)
PALF	PLA	5	2	Room temperature	(Huda et al., 2008)
PALF	Polycarbonate	5	5	30 °C	(Threepopnatkul et al., 2009)
PALF	Polymide 6	5	5	Room temperature	(Panyasart et al., 2014)

According to Table 2.5, the optimum concentration for PALF treatment was summarized at 5% (w/v) of NaOH with 1 h immersion period at the room temperature. Findings from previous studies showed that alkali treatment was able to remove hemicellulose and lignin components from natural fiber to produce better purified cellulose (Panyasart et al., 2014). As lignin is removed, the middle lamella joining the ultimate cells is expected to be more plastic and homogeneous due to the gradual elimination of micro-voids. Moreover, alkali treatment increases the amount of crystalline cellulose and eliminates natural and artificial impurities, resulting in coarse surface topography. Increase in fiber surface roughness provides physical interlocking between fiber and matrix, which affects the tensile properties of composites. The reaction taking place in alkali treatment is shown in Figure 2.17.

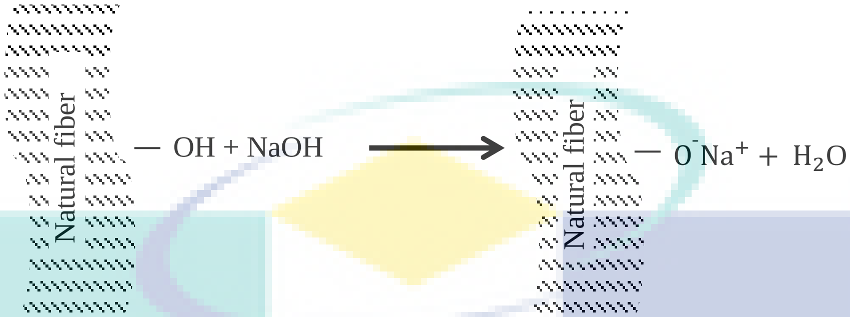

Figure 2.17 Reaction of alkali treatment
Source: Panyasart et al. (2014)

Despite all advantages offered by alkali treatment, it also produces a side effect which is considered insignificant in the enhancement of bio-composites mechanical properties. The primary disadvantage produced by alkali treatment is agglomeration due to fiber fibrillation process. The void can be seen clearly between fibril of fiber due to the matrix failure to fill the space. This void is thought to be a significant factor for crack propagation and stress concentration points in the composite sample (Ahmad et al., 2008; Panyasart et al., 2014). The finding is in good agreement with agglomeration issue is acacia sawdust reinforced recycled polyethylene terephthalate (PET), where the effect of alkali treatment has resulted in a negative improvement in tensile strength (Ahmad et al., 2008). Therefore, the precautionary measures on agglomeration issue during the alkali treatment process and bio-composite manufacturing process are expected to enhance the mechanical properties of bio-composites in the future.

2.4.5.2 Coupling Agent Utilization

In addition to the use of alkali treatment, the use of coupling agents also improves the interfacial adhesion between natural fibers and matrices. The chemical composition of coupling agents produces a reaction with the fiber surface by forming a chemical bond bridge between the fiber and matrix (Ku et al., 2011; Lee et al., 2009). The most common coupling agents that are widely used in dry blending process are maleic anhydride polypropylene (MAPP) and maleic anhydride polyethylene (MAPE) (Karmarkar et al., 2007; Kim et al., 2006). According to previous findings, the effectiveness of coupling agent is associated with the incorporation and incompatibility between the coupling agent and composites matrix. The maleic anhydride groups of MAPP or MAPE covalently link with the fiber hydroxyl groups, thereby increasing its wettability and dispersion within the matrix. Furthermore, the nonpolar part of MAPP or MAPE becomes compatible with the matrix, lowers the fiber surface energies , thereby increasing its wettability and dispersion within the composite matrix (Mohanty et al., 2006). However, Yang et al. (Yang et al., 2007) suggested that MAPP appeared to be less effective when PE matrix polymer was used in the composites and vice versa, as shown in Figure 2.18.

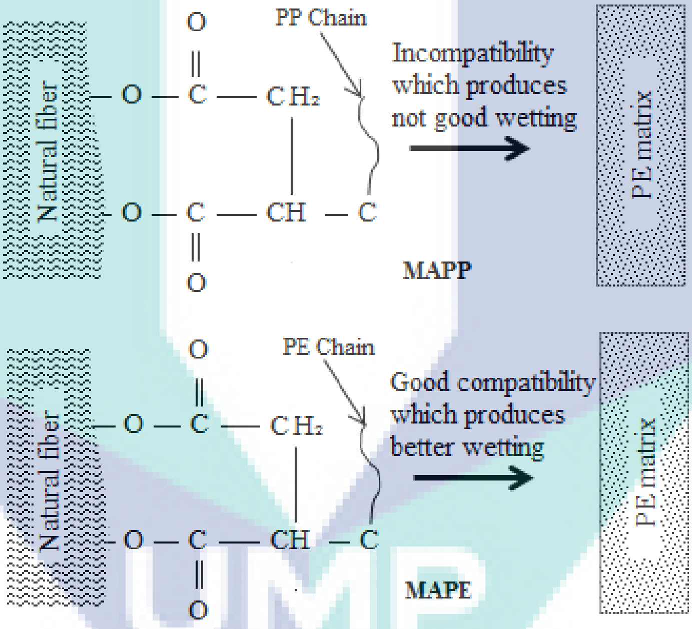

Figure 2.18 Wetting of MAPP and MAPE at the interface between fiber and matrix

Source: Yang et al. (2007)

In addition, Figure 2.19 presents the effect on the fracture surface of the sample that used the correct coupling agent in the fabrication of natural fiber composites. The fiber crack behavior and fiber breakage into smaller diameter fibrils on the fracture surface can be observed, which represented an effective stress transfer between the polymer matrix and natural fiber as filler.

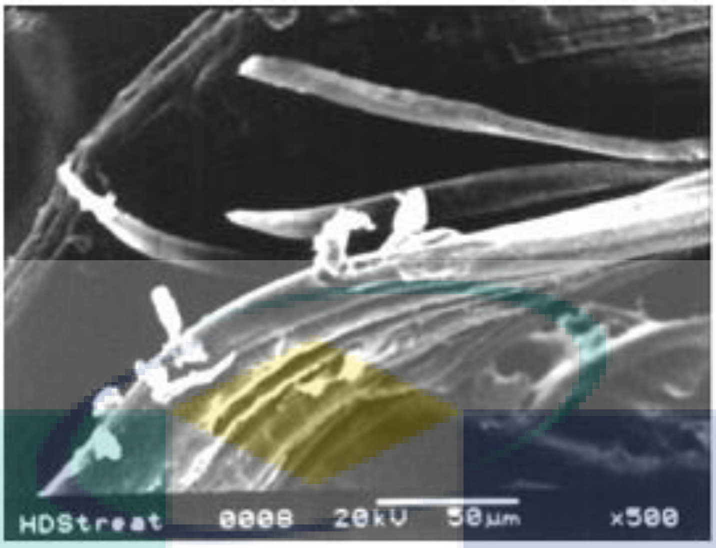

Figure 2.19 Wetting of MAPP and MAPE at the interface between fiber and matrix
Source: Mohanty & Nayak (2006)

Moreover, the concentration of coupling agent used also plays an essential role in bio-composites manufacturing. However, the increase in coupling agent concentration over optimum value always deteriorates the mechanical properties. A previous study of short jute fiber reinforced PP presented tensile strength and modulus increments by increasing the MAPP concentration up to 4%. However, a further increase in the compatibilizer concentration virtually had little effect (Rana et al., 1998). A similar finding was also observed in MAPE treated jute reinforced HDPE composites, whereby a decrease in tensile strength was observed when the MAPE concentration was increased from 1% to 2% (Mohanty et al., 2006). The reduction in tensile properties' result was due to the plasticizing effect from the MAPE, which has lower molecular weight as compared to TBP. The plasticizing effect eventually lowers the rigidity of composites; thus, decreasing the tensile strength and modulus (Khalid et al., 2006; Mohanty et al., 2004). Gassan and Bledzki (Gassan & Bledzki, 1997) also reported a similar finding for jute and flax fiber reinforced PP composites due to the migration of excess MAPE around the fibers, which caused self-entanglement among themselves rather than the polymer matrix, resulting in slippage of fibers within the matrix. The different coupling agents and their concentrations as well as the optimum concentration of the used coupling agent in bio-composite manufacturing by previous researchers are presented in Table 2.6.

Table 2.6 Comparison of coupling agent concentration

Natural fiber	Matrix	Coupling agent			Reference
		Type	Concentration used (% w/w)	Optimum concentration (% w/w)	
Corn chaff	PP	MAPP	5, 10	5	(Fuqua & Ulven, 2008)
Flax	PP	MAPP	2, 3, 4, 5	2	(El-Sabbagh, 2014)
Hemp	PP	MAPP	1, 2, 3, 4, 5	4	(Ku et al., 2011; Liu et al., 2009b)
Jute	HDPE	MAPP	0.3, 0.5, 1, 2	1	(Mohanty & Nayak, 2006)
Jute	HDPE	MAPE	0.3, 0.5, 1, 2	1	(Mohanty et al., 2006)
Jute	PP	MAPP	1, 2, 3, 4	3	(Rana et al., 2003)
Rice husk	PP	MAPP	1, 3, 5	5	(Malkapuram et al., 2009)
Rice husk	PP	MAPP	1, 3, 5	5	(Kim et al., 2006)
Rice husk	LDPE	MAPP	3	3	(Yang et al., 2007)
Sisal	PP	MAPP	2, 3, 4, 5	2	(El-Sabbagh, 2014)

According to the studies shown in Table 2.6, there seems to be no universal value for coupling agent concentration in which the maximum mechanical properties can be achieved. However, the majority of previous findings presented 5% of concentration as the optimum coupling agent concentration to generate the maximum strength result. Further increment of the compatibilizer concentration virtually had little effect or decreased the mechanical properties. In addition, the maximum suitable percentage for coupling agent is not more than 7% due to environmental friendly and cost issue (Rana et al., 1998). Therefore, the correct selection of coupling agent and suitable concentration is the vital factor in PALF-TBP composites manufacturing in order to produce high-performance materials.

2.5 Requirement for Natural Fiber Composites for Engineering Application

Natural fiber composites or bio-composites are mostly used as an alternative or replacement for conventional polymers in the automotive and construction industries. The use of natural fibers in the automotive industry is primarily for interior car components, such as door panels, seat backs, dashboards, truck liners, headliners, decking, railing, window and frames (Valášek et al., 2018; Valášek et al., 2017).

According to previous findings, the most common conventional polymers that are used in automotive sectors are polyethylene terephthalate (PET), PP, LDPE, HDPE, HIPS, PC, ABS and Nylon 6.6 (Holbery & Houston, 2006; Štrumberger et al., 2005; Szeteiová, 2010). Therefore, the primary requirement for natural fiber composites application in the automotive sector is to have the same or compete with the existing mechanical properties of these conventional polymers. Figure 2.20 shows the tensile and flexural properties of these common polymers used in the automotive sector. Also, Figure 2.21 presents the impact properties for these polymers.

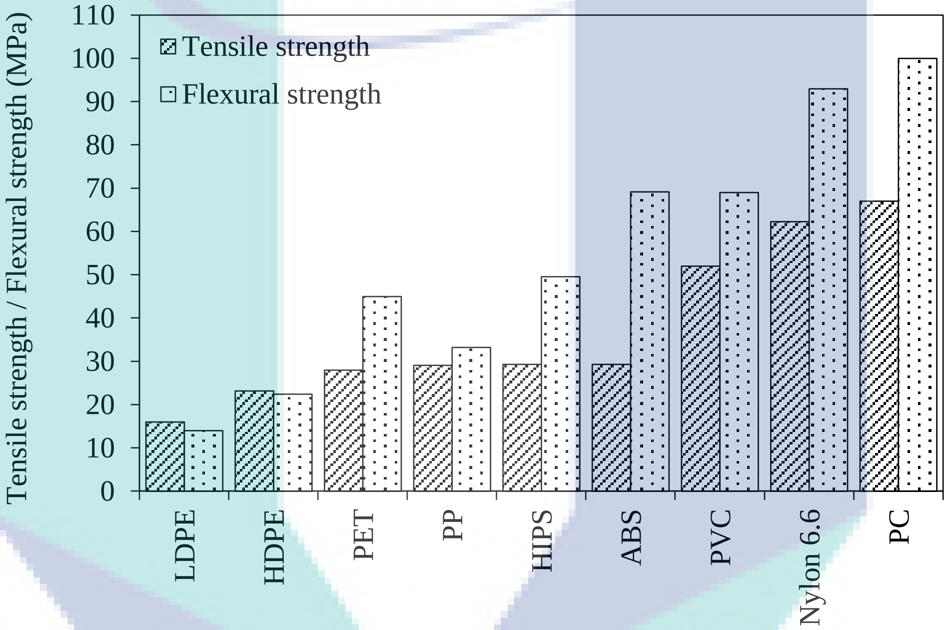

Figure 2.20 Tensile and flexural strength of the most common conventional polymer used in automotive sector

According to Figure 2.20, the requirement for tensile strength and flexural strength for polymer material in the automotive sector is varied between 16 MPa - 67 MPa and 14 MPa - 100 MPa, respectively. Moreover, the requirement for impact properties indicated between 8 J/m² 29 J/m² as shown in Figure 2.21. Therefore, the PALF reinforced TBF composite is required to achieve minimal mechanical properties to be an alternative for conventional polymer in the automotive sector.

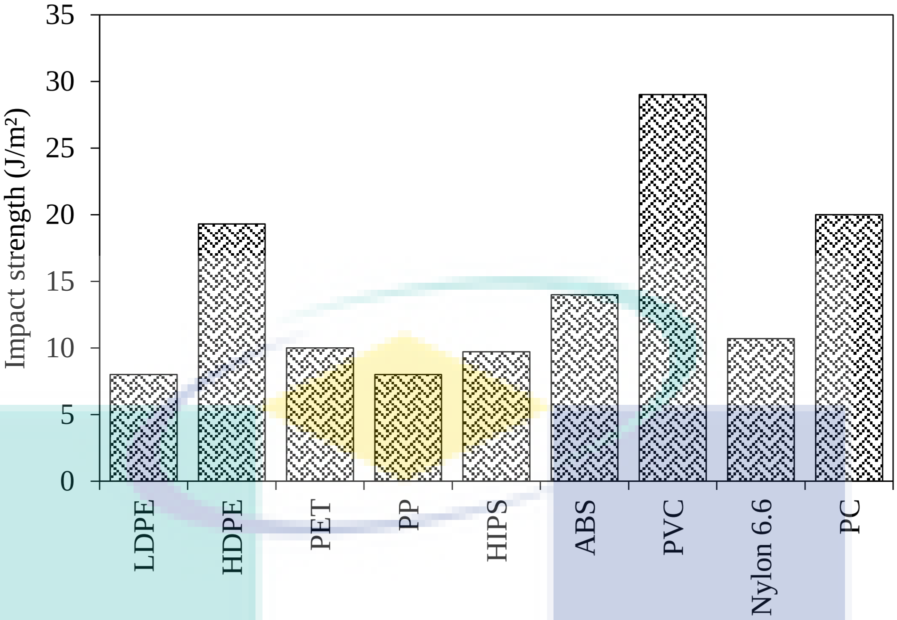

Figure 2.21 Impact strength of the most common conventional polymer used in automotive sector

2.6 Summary

The combination of PALF and TBP showed extraordinary potential as fully biodegradable materials. PALF is among the best option for reinforcement agent as compared to other natural fibers due to high cellulose content and high tensile strength value. Nevertheless, the characterization of PALF becomes essential to understand and interpretation of PALF performance as reinforcement agent in composite materials. A great number of studies on different manufacturing process of natural fiber composites are summarized in this chapter. The melt mixing process and compression molding with 10-min of 6 MPa full press was summarized as the ideal manufacturing process of bio-composites to produce high mechanical properties. The best processing temperature to be used in compression molding is the optimum TBP processing temperature. Therefore, the characterization of TBP and determination of optimum processing temperature are required in this study.

Investigation into the optimum PALF loading that is reinforced in TBP is needed to obtain the highest mechanical properties enhancement. This is due to the effect of weak interfacial adhesion between the fibers and matrix, which is caused by the reduction in the matrices composition. Also, the study on alkali treatment and coupling agent utilization need to be done to determine the best treatment for the best mechanical properties enhancement. There are specific requirements for alkali treatment and coupling agent to work well in improving the mechanical properties. The suitability of coupling agent with appropriate concentration depends on the matrix used in this study. The selection of appropriate treatment will be the benchmark for the development of environmental friendly PALF-TBP composites.

CHAPTER 3

METHODOLOGY

3.1 Introduction

The chapter mainly discusses the materials and methods used in this study. The detailed explanation of the materials used in this study is presented in the material section. Then, the characterization process of pineapple leaf fiber (PALF) and tapioca biopolymer (TBP) are described, which involves Fourier transform infrared spectroscopy (FTIR), chemical composition and analysis of physical and mechanical properties of the fiber. The preparation of a composite sample from the preparation of short fiber to the fabrication of test specimens is described in the method section. Experimental setup and facilities used for thermal properties analysis, mechanical testing and microstructure analysis are presented under thermal properties analysis, mechanical testing and morphological analysis, respectively. In addition, a detailed explanation is given in regard to the test condition and particulate matter analysis.

3.2 Research Flow Chart

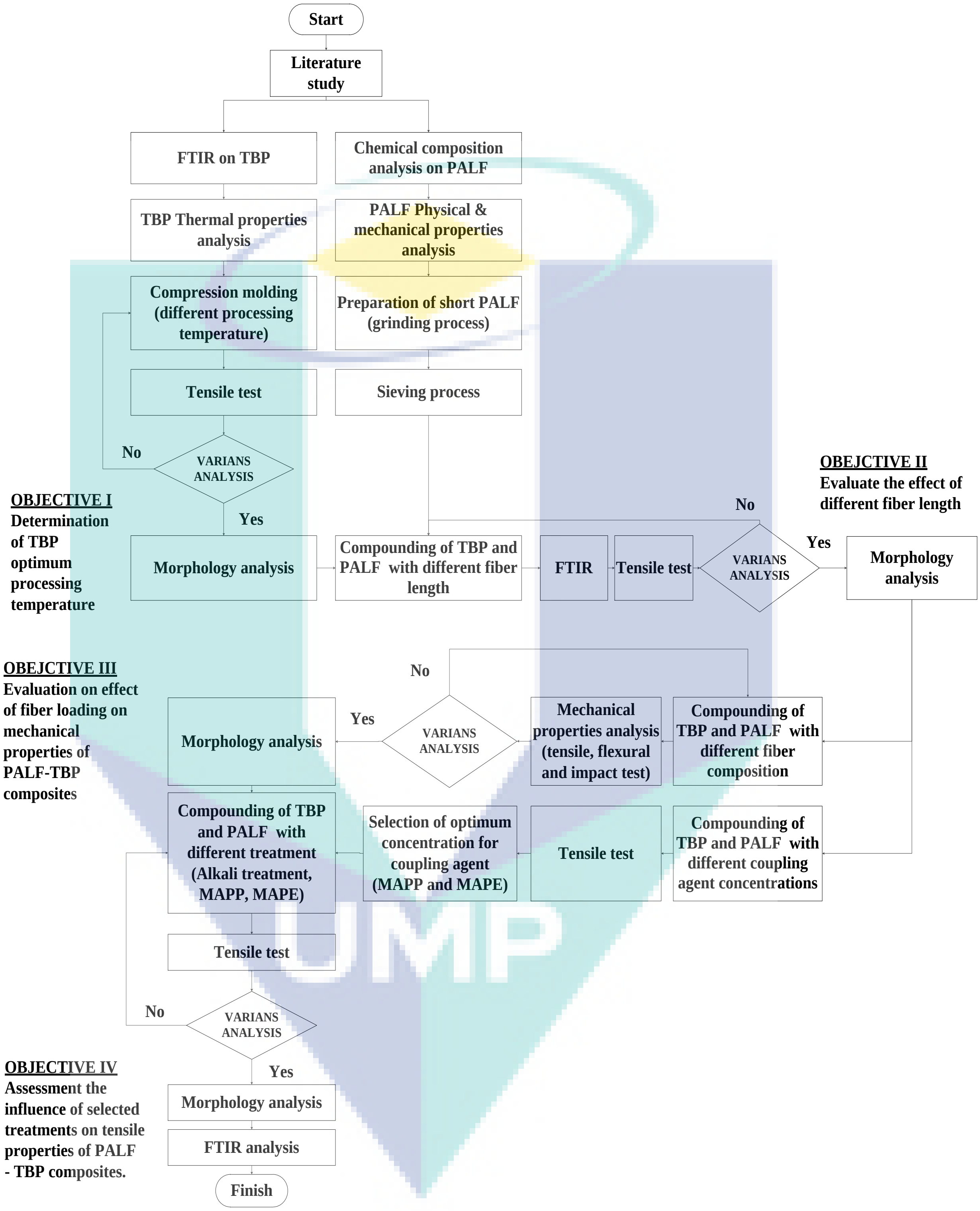

Figure 3.1 Process flow chart for research methodology

3.3 Materials

3.3.1 Pineapple Leaf Fiber (PALF)

The bundles of pineapple leaf fiber (PALF) were directly purchased from the PALF farmer at Permalang, in Central Java, Indonesia. That PALF were extracted from the leaf with a traditional hand scraping technique by using porcelain plate. Then, the fibers were washed with water and dried. Figure 3.2 shows the appearance of PALF after extraction. This manual extraction process is capable of extracting approximately 4% of fibers from the leaves (Paul, 1980; Siregar, 2011).

Figure 3.2 The PALF after scraping, washing and drying process

3.3.2 Tapioca Biopolymer (TBP)

Tapioca biopolymer (TBP) is a patterned product produced by Indochine Bio Plastiques (ICBP) Sdn. Bhd., Malaysia. This TBP was derived from industrial grade *Manihot esculenta* species. These tapioca species do not belong in the food grade due to bitterness in taste. In this study, TBP was purchased directly from ICBP Sdn Bhd to guarantee the authenticity of TBP. Figure 3.3 presents the TBP in pellet type and Table 3.1 shows the physical and mechanical properties of TBP provided by the manufacturer.

Figure 3.3 Tapioca biopolymer in pellet type

Table 3.1 Thermo-physical and mechanical properties of TBP

Properties	Unit	Value
Density	(g/cm³)	1.1
Melt index	(g/10min)	36
Tensile strength	(MPa)	14
Flexural strength	(MPa)	14
Hardness	(Shore D)	64

Source: ICBP (2017)

3.3.3 Sodium Hydroxide and Coupling Agent

In this research, the S/4920/AP1 Fisher Chemical sodium hydroxide (NaOH) for alkali treatment process was purchased from the Aldrich Chemical Company, Malaysia. The maleic anhydride polypropylene (MAPP) used in this research was POLYBOND ® 3200 manufactured by Addivant, United States. Meanwhile, maleic anhydride polyethylene (MAPE) used was OREVAC® 18302N and was manufactured by Arkema Coating Resins (M) Sdn. Bhd., in Malaysia. Figure 3.4 shows the NaOH, MAPE and MAPP in pellet type. Moreover, the properties of MAPP and MAPE used in this study are shown in Table 3.2.

Figure 3.4 The physical appearance of (a) NaOH, (b) MAPE, (c) MAPP in pellet type

Table 3.2 Properties of coupling agents used

Properties	MAPP	MAPE
Density	0.91 g/cm³	0.912 g/cm³
Melt point	157°C	123°C
Melt index	1.15 g/10 min	1.2 g/10 min
Molecular weight	120,000 g/mol	125,000 g/mol
Maleic anhydride content	1.0%	1.0%

Source: Addivant (2018); Arkema (2018)

3.4 Materials Characterization

Materials characterization process in the present study was consist of Fourier Transform Infrared Spectroscopy (FTIR), fiber chemical composition, single fiber thermal and mechanical properties analysis. All of these testing were conducted as a verification process for the raw material used in this research.

3.4.1 Fourier Transform Infrared Spectroscopy (FTIR)

Fourier Transform Infrared Spectroscopy (FTIR) is a method used to identify the substance in material by determining the presence of a functioning group in TBP. Moreover, findings from FTIR can also evaluate the possible interactions in the PALF-TBP composite sample. In this research, FTIR was conducted by using thermo fisher scientific, Nicolet iS50 FTIR machine, as shown in Figure 3.5. The diamond attenuated total reflectance (ATR) techniques were used in this FTIR analysis. Samples were analyzed for the wavenumber range of 500 cm^{-1} to 4000 cm^{-1}.

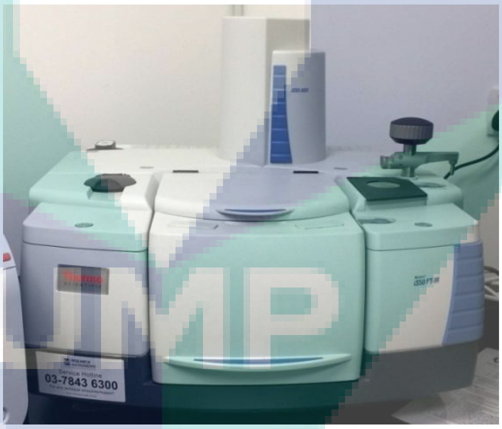

Figure 3.5 Thermo Fishcer Scientific, Nicolet iS50 FTIR machine

3.4.2 Fiber Chemical Composition

Analysis of the fiber chemical composition was crucial to understand and interpret PALF-TBP composite performance. The major components in PALF were moisture, lignin, cellulose and hemicellulose. The moisture content was measured according to TAPPI T264 cm-97 (TAPPI, 1997). Five samples of 2 g air-dried fiber were oven dried at 105°C for 3 h. The moisture content was calculated according to the following equation:

$$Moisture\ content\ (\%) = \frac{(M_a - M_o)}{M_a} \times 100 \qquad 3.1$$

where, M_a is the weight of air-dried sample and M_o is the weight of the oven-dried sample. Meanwhile, the composition of lignin content was determined according to TAPPI T 222 om-02 (TAPPI, 2002). The 10 ml of 72% sulphuric acid was carefully added by using a pipette into a 50 ml beaker that contained 1 g of air-dried PALF. Then, the mixture was stirred by using a glass rod at every 15 min for 2 h. Then the mixture was transferred into a 500 ml round-bottom flask and diluted with 300 ml distilled water. The mixture was boiled by using hot plate for 3 h.

The subsequent process was measurement of the crucible weight, which contained dried lignin (after drying at 110°C for 1 h and cooled in a desiccator for 15 min). After that, the crucible containing lignin was filtered and washed with distilled water. Then the crucible weight was measured after drying at 110°C for 1 h and cooled in a desiccator for 15 min. The percentage of lignin content calculated according to following equation:

$$Lignin\ content\ (\%) = \frac{(M_{cl} - M_c)}{M_a} \times 100 \qquad 3.2$$

where, M_{cl} is the weight of crucible containing lignin content, M_c is the weight of crucible and M_a is the weight of an air-dried sample. On the other hand, the cellulose and hemicellulose contents were measured according to TAPPI T203 om-93 and method of Wise, Murphy and D'Addie, respectively (TAPPI, 1999; Wise et al., 1946). Figure 3.6 shows the procedure for the determination of cellulose and hemicellulose content.

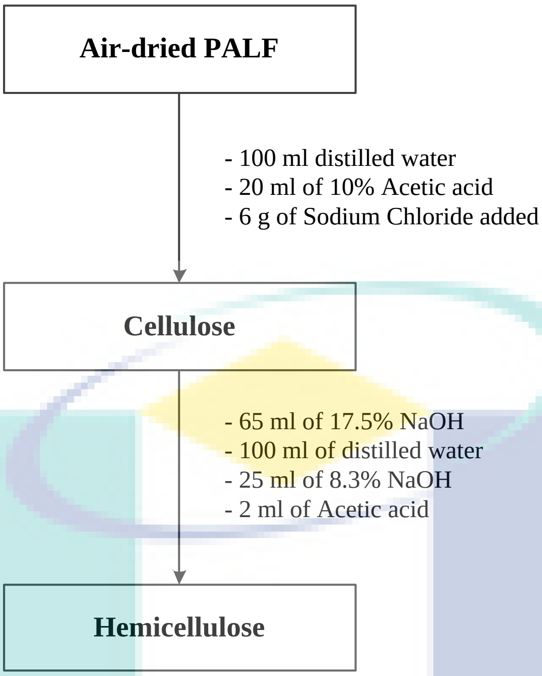

Figure 3.6 Procedure for the determination of cellulose and hemicellulose content

3.4.3 Single Fiber Thermo-Physical and Mechanical Properties

The single fiber physical measurement, thermal analysis and tensile test were performed as material characterization processes for PALF. The thermal properties of PALF were investigated through thermogravimetric analysis (TGA). The TGA is a method of thermal analysis that can measure changes in physical and chemical properties of materials, as a function of increasing temperature to determine the degradation temperature. In this research, TGA was performed in a Hitachi ST7000 thermogravimetric analyzer according to ASTM D6370-99. The sample was heated from 26°C to 700°C, under 75 cm^3/min nitrogen flow with a heating rate of 10°C/min (ASTM, 2003d).

The single fiber tensile test was performed as a fiber characterization for tensile property investigation. According to the statistical approaches at 95% confidence interval, a total of 100 fiber samples were selected as test samples (Chew Chong Bew, 1998; Siti Zanariah Satari, 2015). The number of samples for single fiber tensile test was selected according to the following equation:

$$\text{Sample size}, n = \left(\frac{Z_{\propto/2} S}{E}\right)^2 \tag{3.3}$$

where, $Z_{\propto/2}$ value is read from the standard normal table, S is standard deviation obtained from the pilot test, and E is the error of standard deviations which set as 0.2 due to varied fiber, depending on the species, age of fiber, and process used to obtain and location of the pineapple plant as reported by Neto et. al. (Allen, 2006; Neto et al., 2013; Siti Zanariah Satari, 2015; Yang & El-Haik, 2003). The $Z_{\propto/2}$ value read from the standard normal table was 1.96. Meanwhile, the standard deviation obtained from pilot test was 1.02. The tensile test samples were prepared according to ASTM C1557 with gauge length of 25.4 mm, as shown in Figure 3.7.

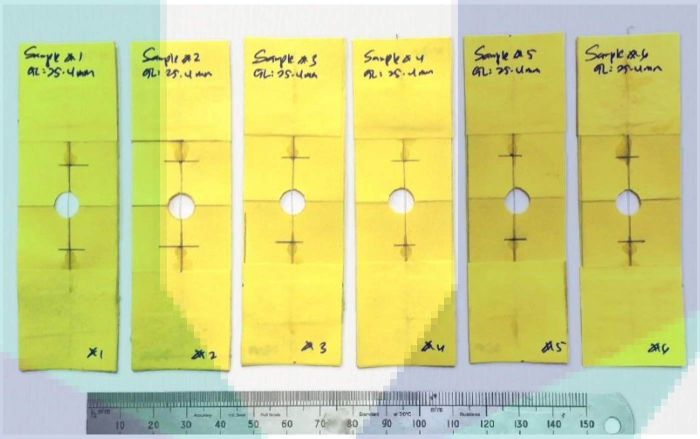

Figure 3.7 The single fiber tensile test samples

Prior to the tensile test, the fiber diameter was measured by using non-contact optical comparator, Mahr Quadra-Chek 300, as shown in Figure 3.8. In addition to being inputs for testing setup, fiber diameter measurement also served as characterization of fiber diameter produced through the scrapping technique used in present study.

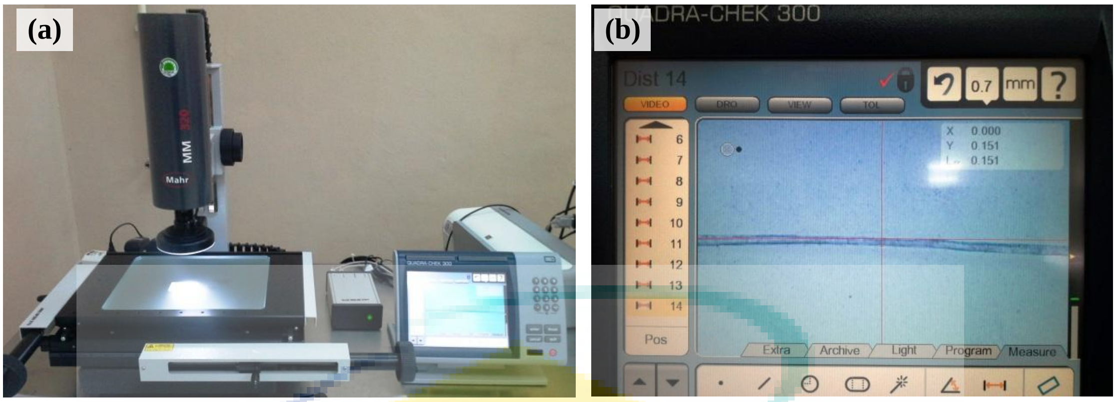

Figure 3.8 The fiber diameter measurement (a) optical comparator used, (b) single fiber under diameter measurement

The single fiber tensile test was conducted by using 5 kN Instron 5967 universal testing machine at a temperature of 23 ± 2°C and relative humidity of 50 ± 5%, according to ASTM C1557. The crosshead speed was set at 0.48 mm/min (ASTM, 2003a). The test experimental setup for the single fiber tensile test is presented in Figure 3.9.

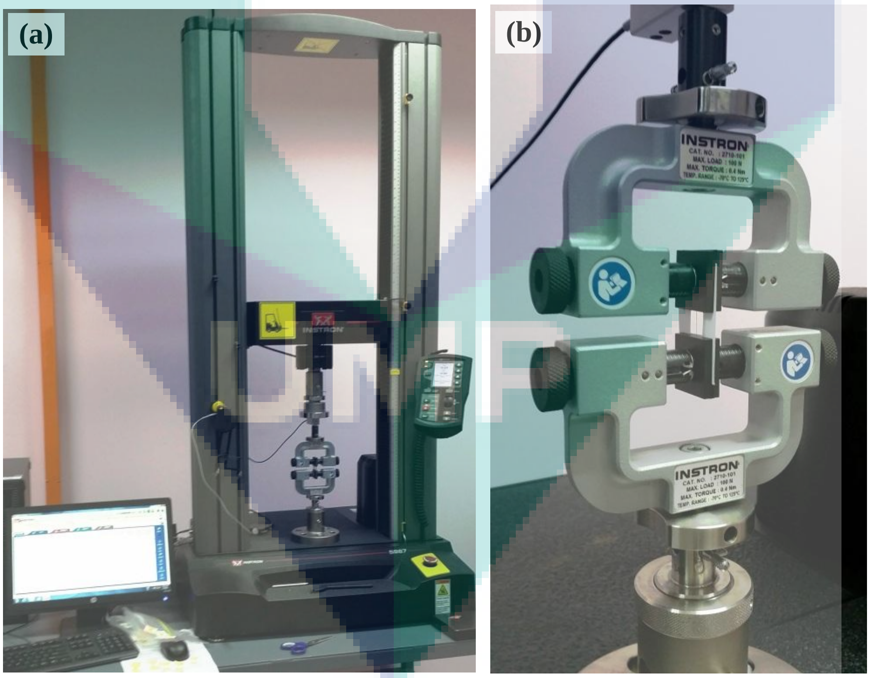

Figure 3.9 The experimental set-up for single fiber tensile test (a) 5 kN Instron 5967 universal testing machine, (b) single fiber sample under tensile test

3.5 Methods

3.5.1 Preparation of Short Pineapple Leaf Fiber (PALF)

The first process for short PALF preparation was crushing of the fibers by using the RL-L10 MPL crusher to reduce the fiber length. This was followed with subsequent sieving process by using SS304 GMP automatic sieving machine. The sieving process segregated the fibers into three fiber length groups as presented in Table 3.3. Figure 3.10 presents physical appearance of fiber samples respectively after crushing and sieving.

Table 3.3 The details of different fiber length

No.	Sample	Fiber length (mm)
1	FL0.5	≤ 0.50
2	FL1.0	0.51 – 1.00
3	FL2.0	1.01 – 2.00

Figure 3.10 The physical of short PALF

3.5.2 Alkali Treatment

Various extensive researches were carried out with different alkali concentrations and soak durations to produce better interfacial adhesion. Literature study found that the optimum concentration of NaOH for PALF treatment was 5% (w/v) with 1 h immersion duration (Asim et al., 2016; Panyasart et al., 2014; Siregar et al., 2010; Yu et al., 2010). In this work, the short PALF was soaked in 5% concentration of NaOH solution in a water bath for 1 h at room temperature. The ratio of fibers and solution was 1:20 (w/v). After treatment, the fibers were washed and rinsed for 10 times with distilled water. Then, they were spin-dried using the Neng Shin extractor to remove excess water. Later, the fibers were oven dried at 80°C for 24 h. Figure 3.11 presents the experimental setup for alkali treatment.

Figure 3.11 The experimental set-up for alkali treatment (a) short PALF was soak in NaOH solution in the water bath, (b) fiber was washed and rinsed, (c) the water was remove from fibers using spin-dried extractor

3.5.3 Preparation of Composite Mixture

In composite mixture preparation, the first process was where all raw materials, including treated and untreated fibers, TBP and coupling agent, were dried in a vacuum oven at 80°C for 24 h (Du et al., 2014; Liu et al., 2005). During the drying process, the weight value of TBP samples was measured at every hour for 8 h. This was because the TBP was a new matrix which was never used in the composite application. Therefore, the weight measurement was conducted to determine the minimum drying duration.

Composite mixture was prepared according to the research objectives. To assess the effect of different fiber lengths on tensile properties, PALF with fiber weight of 10% (≤ 0.50 mm, 0.51 mm -1.00 mm, 1.01 mm -2.00 mm) was mixed with 90% by weight of TBP. However, the objective to evaluate the effect of fiber loading requires the preparation of samples with different fiber percentages. According to the finding from evaluation on different fiber length, PALFs 20%, 30% and 40% with a length of 1.01mm to 2.00 mm were mixed with TBP.

The fourth objective required a sample to be provided for analysis on the effects of different treatments (alkali treatment, MAPP and MAPE) on the tensile properties of the composites. However, the selection of the correct concentration of the coupling agent was required before the three different treatments were compared. Therefore, samples at 10% PALF-TBP composites were mixed with MAPP and MAPE at different concentrations of 1%, 3%, 5% and 7% by weight. Then, the optimum concentration findings were used in the PALF-TBP composites preparation by utilizing MAPP and MAPE for comparing the three types of treatment. The samples were prepared with a variety of fiber loadings at 10%, 20%, 30% and 40% to determine the most effective treatment for PALF-TBP composites. Mixing in the composite mixtures' preparation was carried out according to the following equation:

$$1 = v_f + v_m + v_{ca} \qquad 3.4$$

where, v_f is the fiber composition, v_m is the TBP composition, and v_{ca} is the composition of coupling agents by weight. The detail mixing for sample preparation in this research is displayed in Table 3.4 and Table 3.5.

Table 3.4 The preparation of TBP samples for different processing temperature

Sample	**PALF (wt %)**	**TBP (wt %)**	**Processing temperature (°C)**	**Number of samples**
Sample 160	-	100	160	10
Sample 165	-	100	165	10
Sample 170	-	100	170	10
Sample 175	-	100	175	10
Sample 180	-	100	180	10
Sample 185	-	100	185	10
Total				**60**

Table 3.5 The preparation of composites mixture

Sample	**Fiber length (mm)**	**PALF (wt %)**	**TBP (wt %)**	**MAPP (wt %)**	**MAPE (wt %)**	**Number of samples**
Study of different fiber length						
PALF10 FL0.5	≤ 0.50	10	90	-	-	10
PALF10 FL1.0	0.51 - 1.00	10	90	-	-	10
PALF10	1.01 - 2.00	10	90	-	-	10
Study of different fiber loading						
PALF20	1.01 – 2.00	20	80	-	-	30
PALF30	1.01 – 2.00	30	70	-	-	30
PALF30	1.01 – 2.00	30	70	-	-	30
PALF40	1.01 – 2.00	40	60	-	-	30
Selection for coupling agent concentration						
PALF10 MAPP1	1.01 – 2.00	10	89	1	-	10
PALF10 MAPP3	1.01 – 2.00	10	87	3	-	10
PALF10 MAPP5	1.01 – 2.00	10	85	5	-	10
PALF10 MAPP7	1.01 – 2.00	10	83	7	-	10
PALF10 MAPE1	1.01 – 2.00	10	89	-	1	10
PALF10 MAPE3	1.01 – 2.00	10	87	-	3	10
PALF10 MAPE5	1.01 – 2.00	10	85	-	5	10
PALF10 MAPE7	1.01 – 2.00	10	83	-	7	10
Study the effect of different treatments						
PALF20 MAPP 7	1.01 – 2.00	20	73	7	-	10
PALF30 MAPP 7	1.01 – 2.00	30	63	7	-	10
PALF40 MAPP 7	1.01 – 2.00	40	53	7	-	10
PALF20 MAPE3	1.01 – 2.00	20	77	-	3	10
PALF30 MAPE3	1.01 – 2.00	30	67	-	3	10
PALF40 MAPE3	1.01 – 2.00	40	57	-	3	10
TreatedPALF10	1.01 – 2.00	10	90	-	-	10
TreatedPALF20	1.01 – 2.00	20	80	-	-	10
TreatedPALF30	1.01 – 2.00	30	70	-	-	10
TreatedPALF40	1.01 – 2.00	40	60	-	-	10
Total						**330**

3.5.4 Compounding

In the following process all the composite mixtures went through compounding by using the PL2000-6 Brabender Plasticorder internal mixing machine. Prior to compounding, the device was preheated and set at 165°C and 40 rpm processing speed. The TBP, in the form of pellets or composite mixing of TBP and coupling agent, was blended and allowed to stabilize before the fiber was introduced.

Figure 3.12 presents the changing of torque value and stock temperature during the compounding process. It is clear that the mixing torque initially increases rapidly when TBP is charged into the mixer chamber. As the mixing time increases, TBP undergoes melting, resulting in a torque reduction, and after a certain period, the value becomes stable. Then, the introduction of PALF into the chamber increases torque because of the increased viscosity of the system. In contrast, the stock temperature decreased rapidly with the introduction of PALF into the melt TBP. Then, both torque and stock temperature attains constant value at approximately 15 min of mixing duration. The mixing process was stopped after 5 min of the constant value for both torque and stock temperature. Therefore, the total time used for mixing the composites was 20 min.

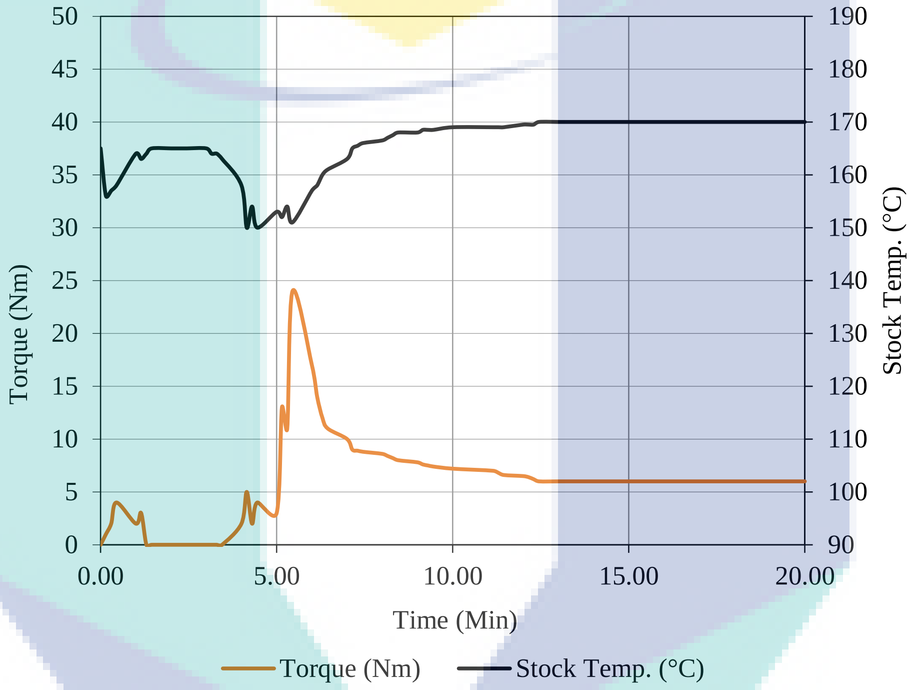

Figure 3.12 The change of torque value and stock temperature during the compounding process

Then, the mixed compounds obtained from the internal mixer were cut into pellets. Figure 3.13a and Figure 3.13b present the physical of mixed compounds and mixture after the crushing process, respectively. The fiber loading with 10%, 20%, 30% and 40% was selected in compounding process. It is due to literature study reveals that most of optimum fiber loading was 30% of fiber percentage with tensile performance as the primary considerations. Therefore, in this research, 40% was selected as an additional to 30% as optimum fiber loading.

Figure 3.13 The compounding of composite mixture (a) mixed compounds, (b) mixed compound after crushing process

3.5.5 Compression Molding

The subsequent process was the preparation of composite plate by using compression molding to form a plate with dimensions 200 mm × 200 mm × 3 mm. The mold temperature was set at 165°C, and a constant pressure of 6.0 MPa was applied for 5 min of preheating and 10 min of the full press. Then, this was followed by a cooling process under the same pressure for 5 min (Arib et al., 2006; Nanthaya & Taweechai, 2014; Siregar, 2011). However, the first research objective, which is to determine the optimum TBP processing temperature, required the preparation of samples with different sets of mold temperature. Therefore, six different temperatures, such as 160°C, 165°C, 170°C, 175°C, 180°C, and 185°C, were used in the compression molding to form a sheet of virgin TBP. Figure 3.14 shows the composite mixture before and after compounding.

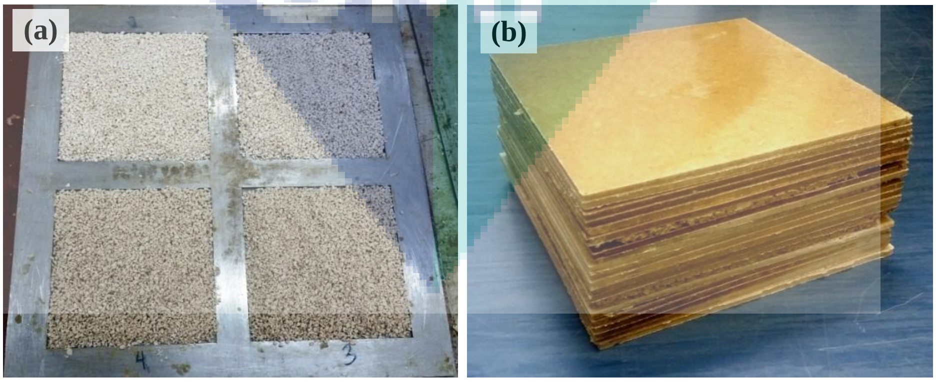

Figure 3.14 The composite mixture (a) during compounding preparation, (b) composite plates

3.5.6 Fabrication of Test Specimen

The flat tensile sample was fabricated through machining by using HASS VF 6 CNC milling machine according to ASTM D638-10 Type V, as shown in Figure 3.15 (ASTM, 2003b). In addition, the final tensile test samples after the fabrication process are presented in Figure 3.16.

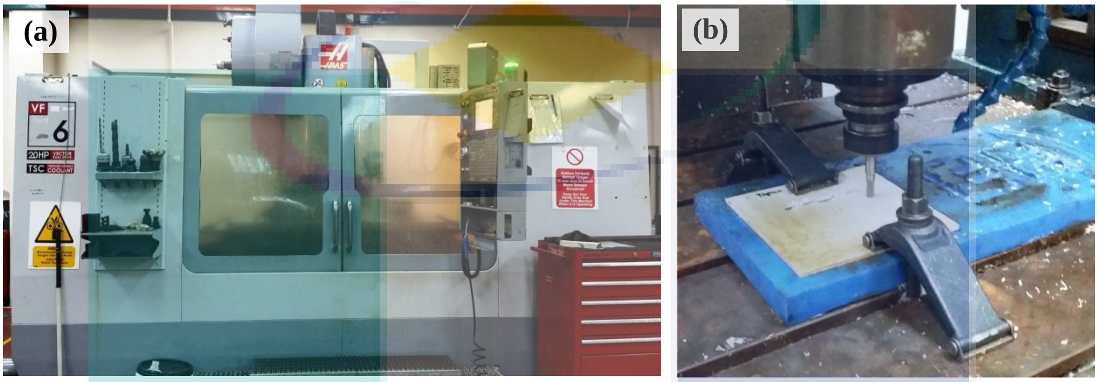

Figure 3.15 The tensile test sample fabrication (a) CNC milling machine used, (b) composite plates under machining process

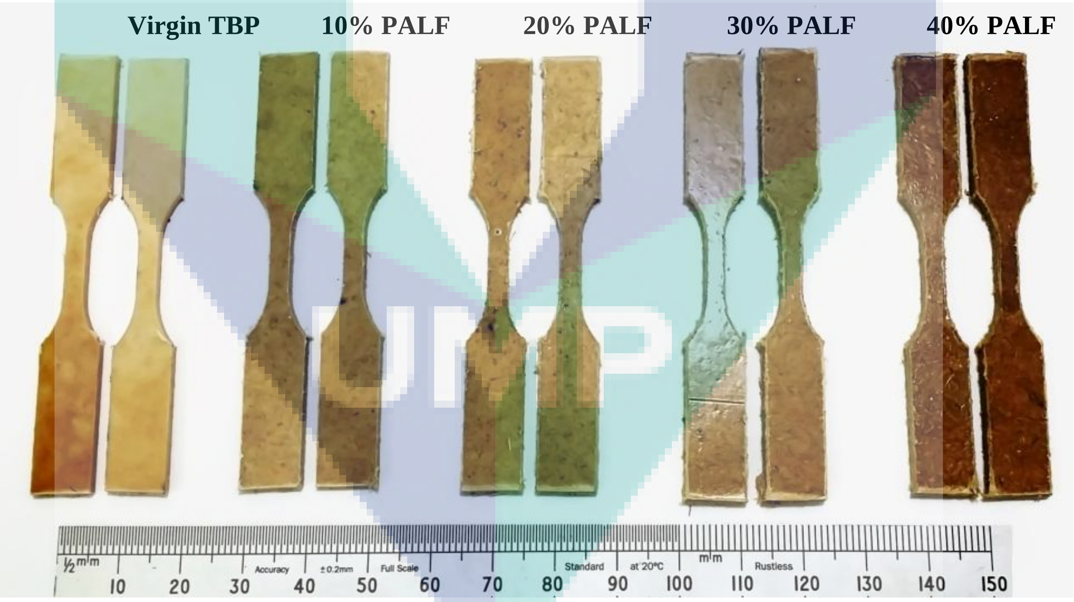

Figure 3.16 The final PALF-TBP tensile samples

The flexural samples were fabricated by using T-Jaw 400 vertical saw according to ASTM D790, and are presented in Figure 3.17 (ASTM, 2002). The flexural sample was prepared with dimension 150 mm × 12.7 mm × 3 mm.

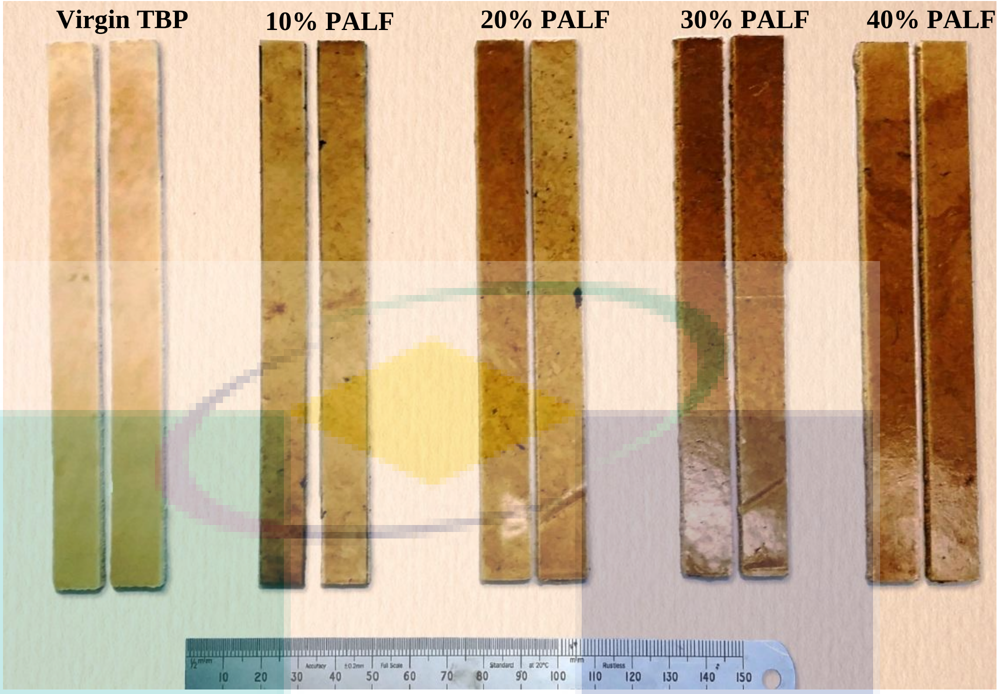

Figure 3.17 The flexural test sample of PALF-TBP composites

Meanwhile, the impact test samples were prepared according to ASTM D256 by using T-Jaw 400 vertical saw (ASTM, 2010). However, “V” notch for the impact test sample was fabricated by using EI 1705 manual notch cutter. Figure 3.18 presents the final impact test samples with dimensions of 65 mm × 12.7 mm × 3 mm.

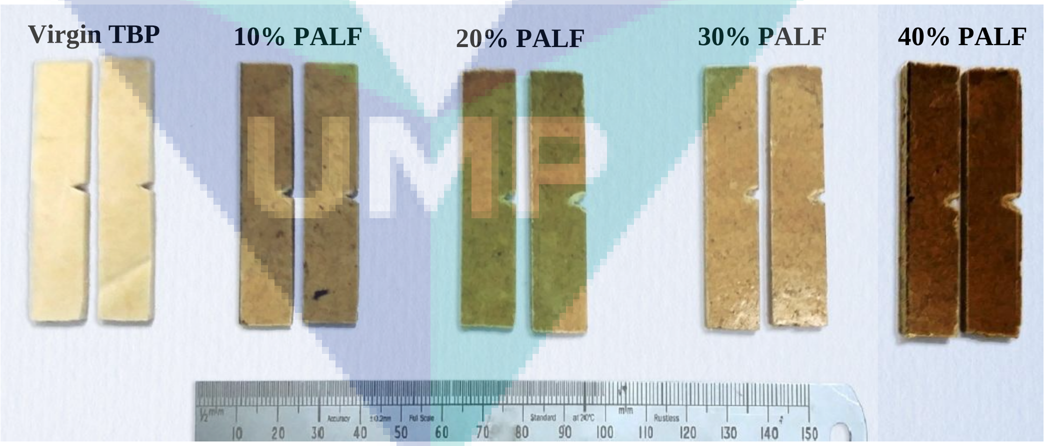

Figure 3.18 The impact test sample of PALF-TBP composites

3.6 Thermal Properties Analysis

3.6.1 Themogravimetric Analysis (TGA)

The TGA is a method of thermal analysis that measures the changes in physical and chemical properties of materials, as a function of increasing temperature to determine the degradation temperature. Same as the methodology for PALF's thermal properties characterization, TGA was performed by using Hitachi ST7000 thermogravimetric analyzer according to ASTM D6370-99. The sample was heated from 26°C to 700°C, under 75 cm³/min nitrogen flow with a heating rate of 10°C/min (ASTM, 2003d). Figure 3.19 shows the thermogravimetric analyzer used in this research.

Figure 3.19 The Hitachi ST7000 thermogravimetric analyzer

3.6.2 Differential Scanning Calorimetry (DSC) Analysis

The DSC analysis is essential in determining the melting point of TBP. In the present study, DSC was conducted by using Perkin Elmer DSC 8000 differential scanning calorimetry analyzer according to ASTM D3418, as shown in Figure 3.20. The sample was heated from -20°C to 200°C by using heat-cool-heat method with heating rate of 10°C/min and cooling rate of 5°C/min (ASTM, 2003c; Shah et al., 2017).

Figure 3.20 The DSC analyzer used in present study

3.7 Mechanical Testing

3.7.1 Tensile Test

The tensile test for virgin TBP sample and composite samples was conducted according to ASTM D638. The test was performed by using 5kN Instron 5967 universal testing machine at a temperature of 23 ± 2°C and relative humidity of 50 ± 5%. The crosshead speeds were set at 1 mm/min (ASTM, 2003b). For each type of sample, ten specimens were tested for failure. Tensile modulus calculation was set at the test machine according to the Chord modulus, *E*. The Chord modulus was calculated after the toe correction region, which was 0.1% strain value and ended at 0.5% strain value, which was the end of a straight line for the stress-strain curve. The detail of modulus calculation setting as follows:

$$E = \frac{(\sigma_{0.5\%\varepsilon} - \sigma_{0.1\%\varepsilon})}{(\varepsilon_{0.5\%} - \varepsilon_{0.1\%})} \qquad 3.5$$

where, σ is the stress value and ε is the strain value from stress-strain curve. Figure 3.21 illustrates the composite sample under tensile test.

Figure 3.21 The composite sample under tensile test

3.7.2 Flexural Test

The flexural test was performed by using the 5kN Instron 5967 universal test machine according to ASTM D790, as shown in Figure 3.22. The experimental room temperature was recorded at 23 ± 2°C and 50 ± 5% as the relative humidity. The test speed and span length were set at 1.28 mm/min and 48 mm, respectively. For each different type of fiber composition, ten specimens were tested for failure. The flexural modulus was also calculated according to the Chord modulus, *E*. The Chord modulus was calculated after the toe region, which was 0.1% strain value and ended at 0.5% strain value, which was the end of the straight line for the curved stress-strain curve.

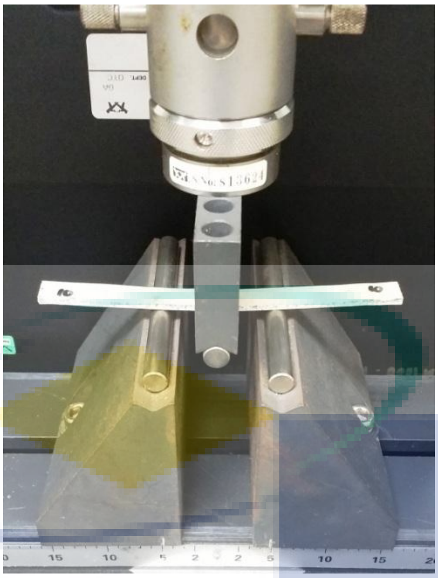

Figure 3.22 The composite sample under flexural test

3.7.3 Impact Test

The third test for mechanical properties analysis in the present study was the Izod impact test. The Izod impact tests was conducted by using the Zwick B 5113.300 impact test machine according to ASTM D256 at temperature of 23 ± 2°C and relative humidity of 50 ± 5% (ASTM, 2010). The impact load applied was a 1 J pendulum at a maximum pendulum height of 160°. Figure 3.23 shows the equipment used in the impact test and sample position during testing.

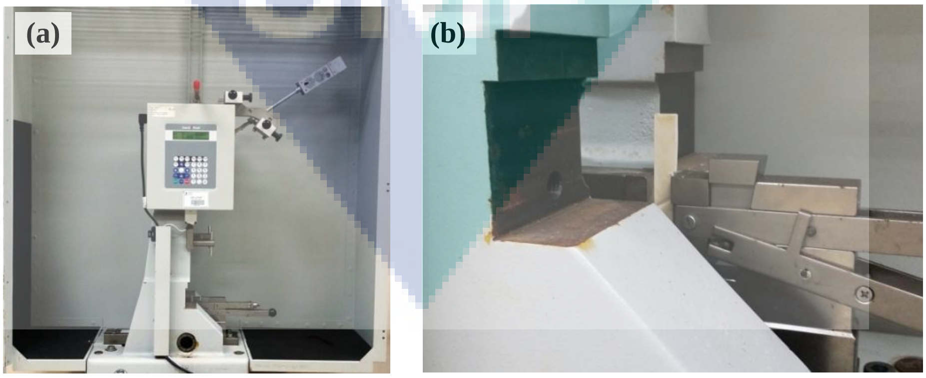

Figure 3.23 The experimental set-up for impact test (a) Zwick B 5113.300 impact test machine, (b) sample position during izod impact test

3.8 Variance Analysis

The analysis of variance (ANOVA) is a test hypothesis to identify the difference between two population means with unknown population variances. The test is concerned with two population means, $\bar{x}_1 - \bar{x}_2$ and represents a set of very important analytical tools for data analysis and widely used by scientists and engineers (Siti Zanariah Satari, 2015). In this research, one-way or single factor ANOVA that used Microsoft excel was selected as the analysis method. The fundamental of ANOVA analysis involved the t_{test} and υ calculations. For sample size, *n* of less than 30, the t_{test} calculation was as follows:

$$t_{test} = \frac{(\bar{x}_1 - \bar{x}_2) - \mu_0}{\sqrt{\frac{S_1^2}{n_1} + \frac{S_2^2}{n_2}}} \qquad 3.6$$

where, $\bar{x}_1$ is the mean for population group 1, $\bar{x}_2$ is the mean for population group 2, μ_0 is equal for 0 (claimn), S_1 is the standard deviation for group 1, S_2 is the standard deviation for group 2, n_1 is the sample size for group 1 and n_2 is the sample size for group 2. On the other hand, the degree of freedom calculation as follows:

$$\upsilon = \frac{\left(\frac{S_1^2}{n_1} + \frac{S_2^2}{n_2}\right)^2}{\frac{\left(\frac{S_1^2}{n_1}\right)^2}{n_1 - 1} + \frac{\left(\frac{S_2^2}{n_2}\right)^2}{n_2 - 1}} \qquad 3.7$$

The 5% of the significance level of variation between different groups of samples was determined according to the *p*-value. The result of *p*-value less than 0.05 indicated that there was a significant difference between two population means (Allen, 2006; Chew Chong Bew, 1998; Siti Zanariah Satari, 2015; Yang & El-Haik, 2003). Figure 3.24 illustrates the area of *p*-value from the t-distribution graph.

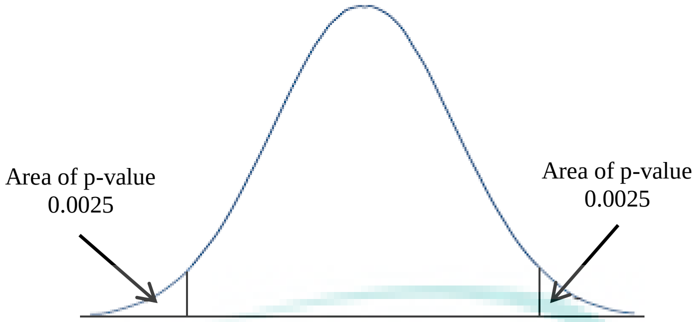

Figure 3.24 The location of P-value in t-distribution chart

3.9 Morphology Analysis

The fractured surfaces, after being subjected to tensile testing, were visually inspected by using a Carl Zeiss Evo 50 scanning electron microscopy (SEM), as shown in Figure 3.25. The samples were mounted onto SEM holder by using double-sided electrically conducted carbon adhesive tapes to prevent surface charge on the specimens when exposed to the electron beam. The test samples sputtered with titanium by using Bal-Tec SCD 005 sputter coater before their morphological observation.

Figure 3.25 Carl Zeiss Evo 50 scanning electron microscopy

3.10 Conclusions

As conclusions, the precise methodology of the research was explained in this chapter. The characterization of the individual component, which was PALF and TBP were conducted by FTIR, chemical composition and mechanical properties analysis. The preparation of short PALF reinforced in TBP was presented, and the samples were used in the mechanical properties evaluation of the fully bio-degradable composites development. The mechanical properties of the PALF-TBP composites with different fiber lengths and different fiber compositions will be measured. The result from mechanical properties measurement will be the primary factor for the effect analysis on different fiber lengths and selection of optimum fiber composition for the development of PALF-TBP bio-composites. The statistical analysis was used in making judgments as a quantitative analysis. The validation of the judgments was conducted through qualitative analysis by using the SEM visual observation on fiber-matrix interfacial adhesion. Investigation related to the selected treatment involved was also described, and the appropriate treatment with suitable concentration was determined to enhance the mechanical properties of composites material. In the next chapter, the research outcome from the present research methodology was presented accordingly for material characterization, determination of optimum TBP processing temperature, the effect of fiber length, justification of optimum fiber composition and the assessment of selected treatment on mechanical properties of PALF- TBP composites.

CHAPTER 4

RESULTS AND DISCUSSION

4.1 Introduction

In this chapter, the performance of the PALF reinforced TBP composites with different fiber lengths and various fiber compositions were analyzed and discussed. The properties of TBP thermal-mechanical were presented before the optimum processing temperature of TBP was selected to be utilized in composites manufacturing. The justification of optimum fiber composition for the development of PALF-TBP composites was conducted via investigation of fiber composition effect on mechanical properties. On the other hand, the experimental study of different concentrations of coupling agent was critically evaluated. Furthermore, the investigation of various treatments on tensile properties of the PALF reinforced TBP composites with different fiber compositions were also discussed.

4.2 Material Characterization

4.2.1 FTIR Analysis on Tapioca Biopolymer (TBP)

Figure 4.1 shows the FTIR result of TBP. As a comparison, Figure 4.1 also indicates the FTIR result of native tapioca starch and PLA. The peaks, at approximately 2900 cm^{-1} and 1740 cm^{-1}, represented the C-H stretching vibration from CH_2 or CH_3 and stretching vibration of the carbonyl groups (C=O), respectively (Lomelí-Ramírez et al., 2014a). On the other hand, the peak around 2900 cm^{-1} was also related to the hemicellulose and cellulose components in the natural material like cassava starch (Nadlene et al., 2016). The peaks at around 1460 cm^{-1} and 1376 cm^{-1} were assigned to

O-H bonding and methyl (CH_3) bonding, respectively (Jumaidin et al., 2017b). Meanwhile, the characteristics of the anhydrous-glucose ring C-O stretch were associated with the peaks at approximately 1078 cm^{-1}. This band was also associated with the C-O group stretching from the glucose of natural starch and the bands at 718 - 573 cm^{-1}, which were assigned to the tapioca skeletal (C–C–O) modes (Mutungi et al., 2012).

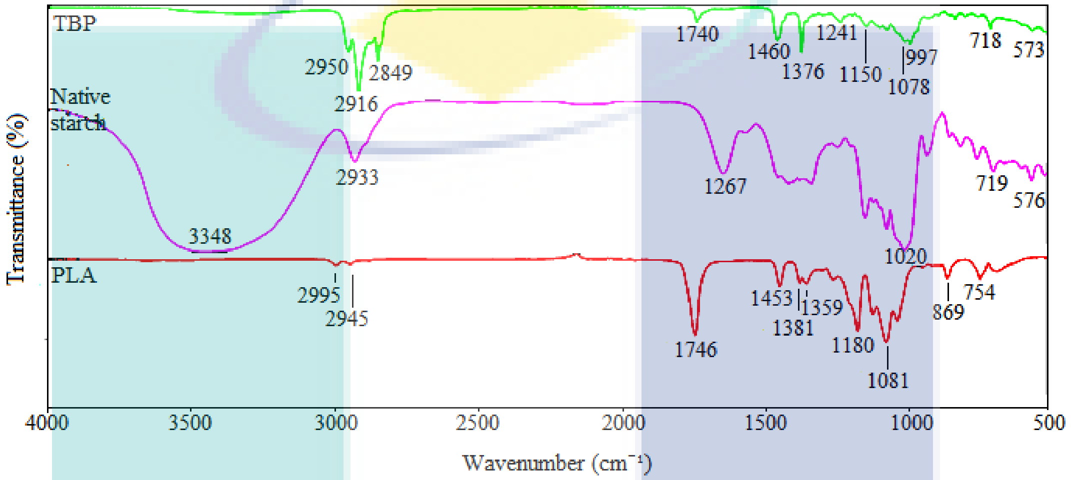

Figure 4.1 Comparison of FTIR spectra between TBP and native starch

According to Figure 4.1, most of the peaks in TBP spectrum were the combination between native starch and PLA spectrum. The band at 3348 cm^{-1}, which was apparently in the native tapioca starch spectrum, was associated with the hydrogen bonded hydroxyl group (O-H) from the complex vibrational stretching, relating to free, inter, and intra molecular bound hydroxyl groups (Jumaidin et al., 2017a, 2017b; Peng & She, 2014). However, the peak at 3348 cm^{-1} disappeared in the TBP result. This finding showed that the TBP consisted of less moisture as compared to native tapioca starch. On the other hand, the peak at 2849 cm^{-1} in the TBP spectrum, which was associated with C-H stretching vibration from CH_2 or CH_3, was suspected from the additive in TBP. The findings reveal that the potential candidate for additives originated from polypropylene-based materials according to comparative results from the FTIR library, which showed 59.98% similarity with polypropylene.

4.2.2 Chemical Composition of Pineapple Leaf Fiber (PALF)

The test results of the chemical composition contained in a single PALF presented that the fibers had four main components, namely moisture, cellulose, hemicellulose and lignin. The test results indicated that the percentage of moisture, cellulose, hemicellulose and lignin in the PALF were 9.6 ± 0.1%, 53.4 ± 0.3%, 31.9 ± 0.3% and 23.0 ± 1.9%, respectively. According to the present study, the cellulose content of 53.4% showed lower value as compared to the previous findings which is between 68% to 73%, as shown in Figure 4.2 (Jawaid & Khalil, 2011; Khalil et al., 2007; Nanthaya & Taweechai, 2014; Siregar, 2011).

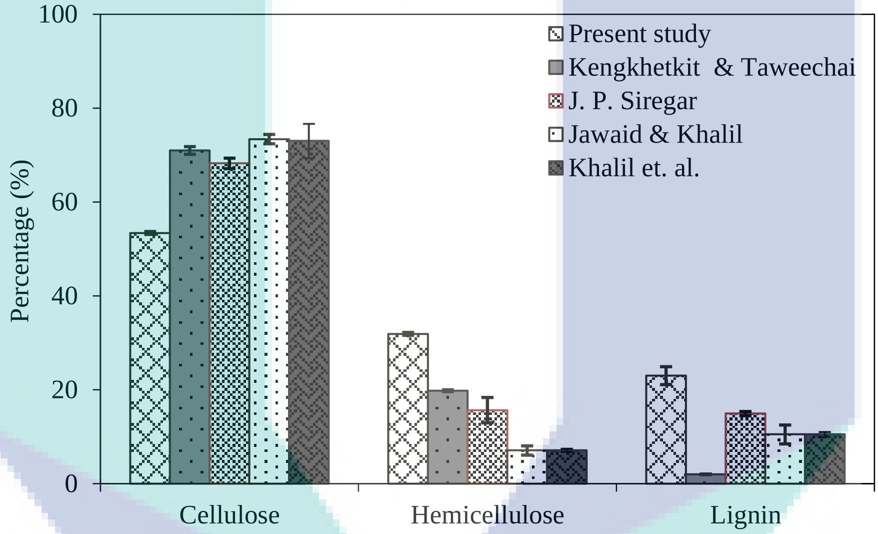

Figure 4.2 Comparison of PALF chemical composition

According to the present study, cellulose content showed lower value as compared to the previous findings, as shown in Figure 4.2. As discussed in the literature review, cellulose was the main structural component of PALF, as it provided strength and stability to the cell walls and the fiber as a whole. Nonetheless, the results of hemicellulose and lignin obtained in the present study were found to be higher than the findings of previous research. Hemicellulose contributes to fiber stiffness and lignin is a highly cross-linked molecular complex with amorphous structure and acts as the binder agent between individual fiber cells and between the fibrils which form the cell wall (Mohanty et al., 2000a). However, higher content of hemicellulose and lignin possesses several disadvantages which cause higher moisture sorption and biodegradation. The differences in chemical composition may have a significant effect on the mechanical properties of a single fiber and performance of PALF as a reinforcement agent for TBP. This phenomenon occurred because the chemical composition of PALF varied, depending on the species and age of fibers, the process used to obtain the fibers and location of the pineapple plant (Liu et al., 2005; Nanthaya & Taweechai, 2014)

4.2.3 Thermal-Physical and Mechanical Properties of Pineapple Leaf Fiber (PALF)

The PALF thermal properties are shown through the TGA results in Figure 4.3. There were two significant weight loss phases of the PALF thermal behavior. The first phase of weight loss of 9.42% occurred during the initial stage of thermal processing as the temperature increased from 26°C to 100°C. The first stage represented moisture evaporation process, in which the maximum point was 80°C (Azwa et al., 2013; George et al., 1996a; George et al., 1996b; Siregar et al., 2011). The second phase of weight loss of 65.8% corresponded to fiber degradation, which was the decomposition of lignin structure that commenced at 200°C and became the limitation in PALF processing temperature. These findings were consistent with the study by Li et al. which recommended less than 200℃ as the natural fiber maximum processing temperature (Liu et al., 2009b).

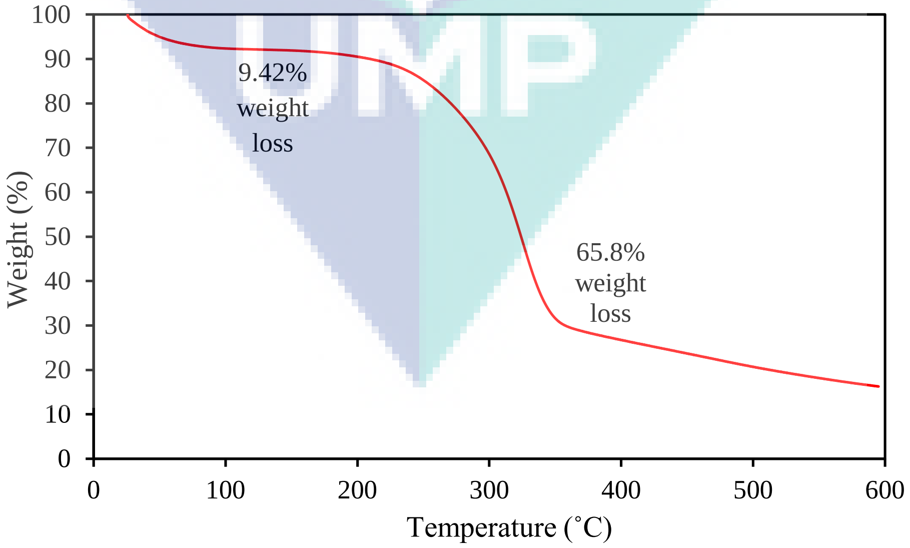

Figure 4.3 Thermogravimetric (TG) curve for PALF

On the other hand, different processes of fiber extraction produce different ranges of fiber diameters. Shown in Figure 4.4 is the distribution of fiber diameter used for the single fiber tensile analysis. The finding illustrated that scrapping technique produced fibers with diameter in the range of 0.05 mm to 0.250 mm. However, most of the PALF extracted by scraping method had diameter between 0.10 mm to 0.15 mm.

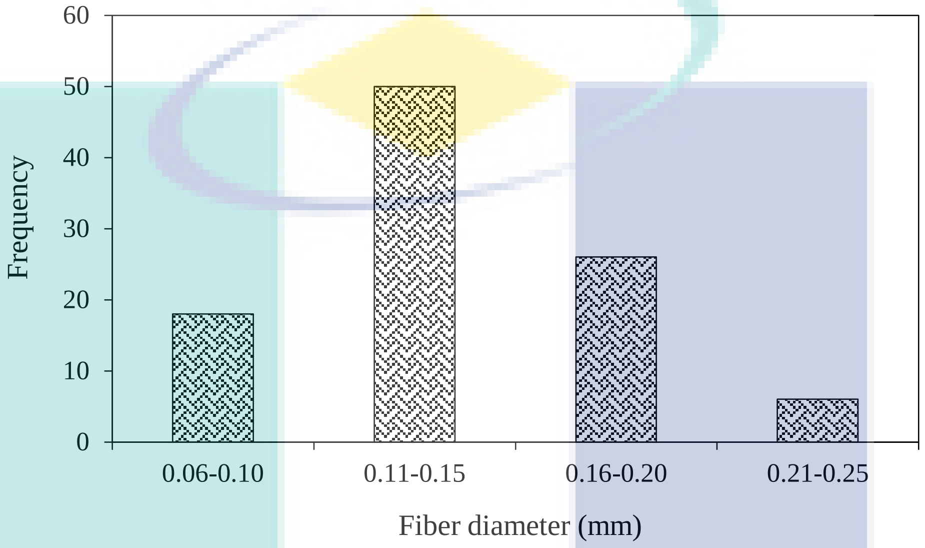

Figure 4.4 Distribution of PALF diameter for single fiber tensile test

Figure 4.5 and Figure 4.6 show the distribution of PALF tensile strength and modulus, respectively. The obtained results indicated that the tensile strength of a single PALF was in the range of 51 MPa and 500 MPa and that of the modulus was between 5.1 GPa and 90 GPa. However, the majority of the tensile strength and modulus were between 100 MPa to 300 MPa and 10 MPa to 30 GPa, respectively. The tensile strength and modulus of the single PALF obtained from the present study and other similar works from literature were compared, as shown in Figure 4.7 (Jawaid & Khalil, 2011; Mohanty et al., 2000b; Nanthaya & Taweechai, 2014; Neto et al., 2015; Neto et al., 2013).

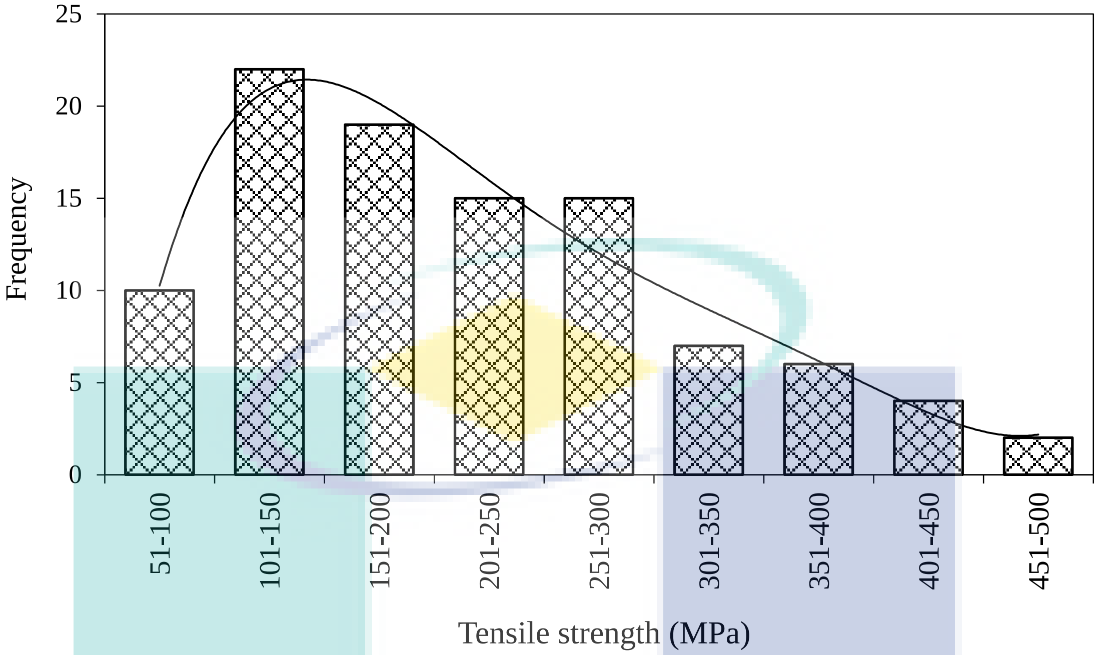

Figure 4.5 Distribution of single PALF tensile strength result

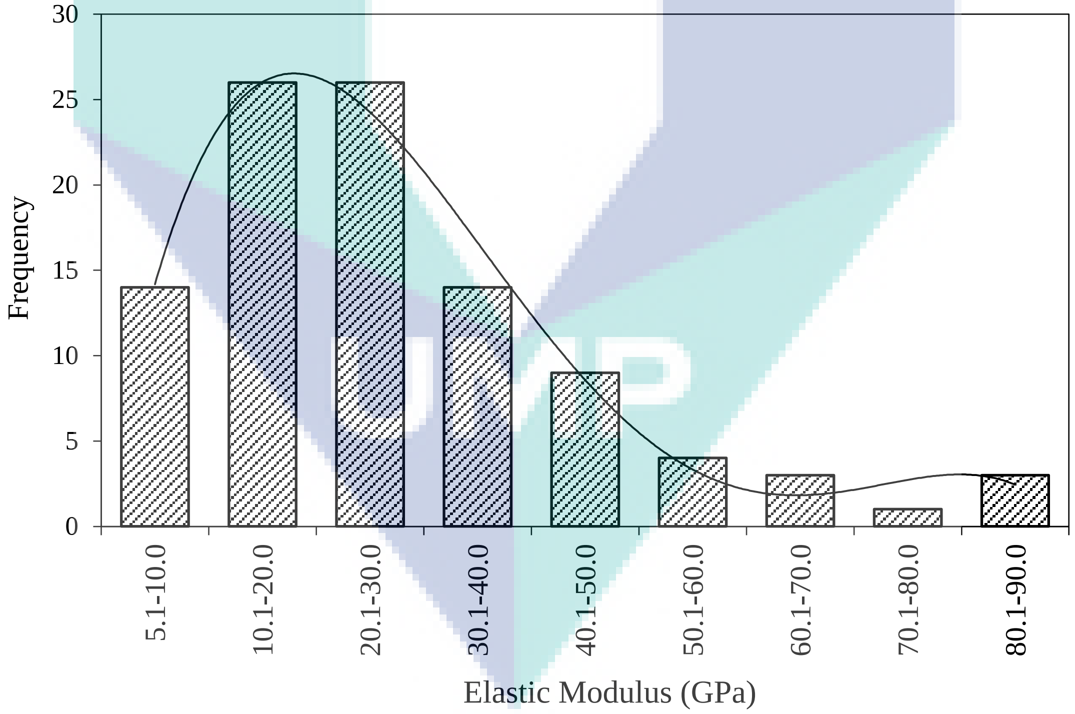

Figure 4.6 Distribution of single PALF tensile modulus result

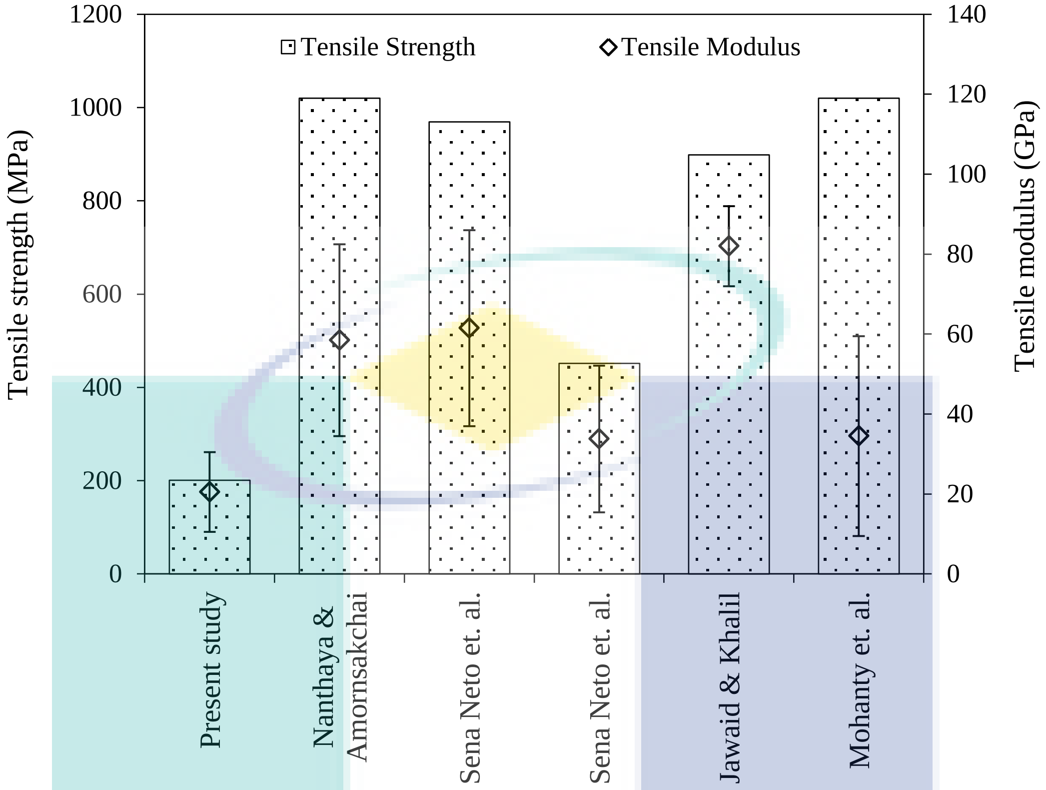

Figure 4.7 Comparison of single PALF tensile strength

According to Figure 4.7, the comparison revealed that single fiber tensile properties found in this research were low as compared to previous results. This might be due to the variation in cellulose contents between the studies. Normally, tensile strength and modulus of single fiber increase as cellulose content and cell length increase as mentioned by the previous studies (Azwa et al., 2013; John & Thomas, 2008; Methacanon et al., 2010). Therefore, this phenomenon influenced the single fiber mechanical properties' results.

4.3 The Determination of Tapioca Biopolymer (TBP) Optimum Processing Temperature

4.3.1 Thermal Properties Analysis

The thermal processing of TBP involves multiple chemical and physical reactions, such as water evaporation, granule expansion, glass transition, melting, and decomposition. The TGA results shown in Figure 4.8 presented three weight loss phases of the TBP thermal processing.

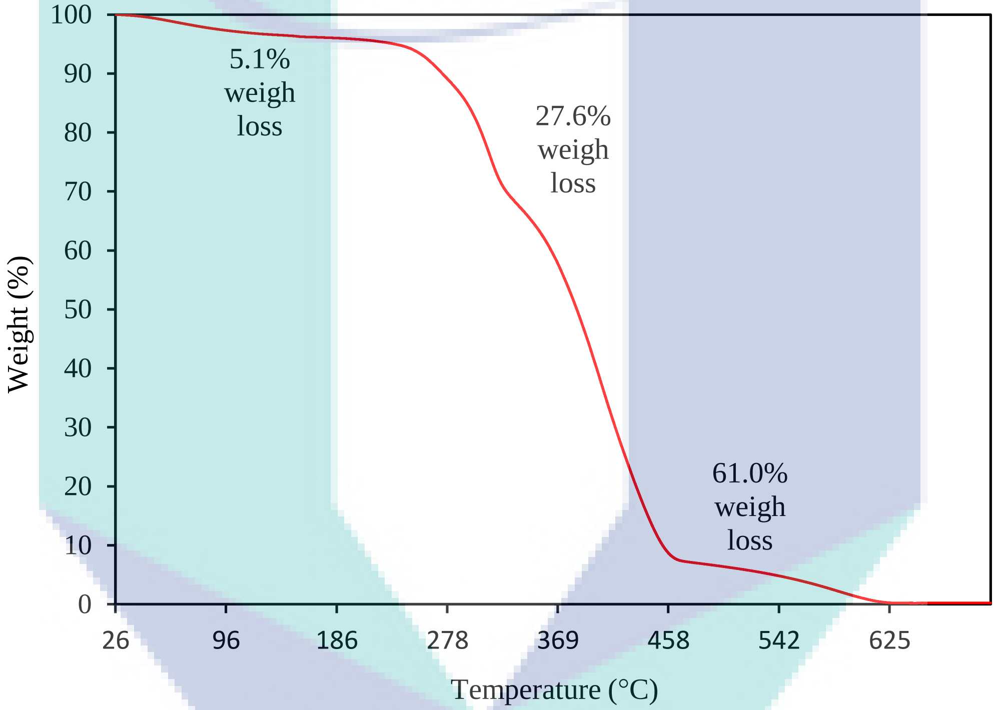

Figure 4.8 Thermogravimetric (TG) curve for tapioca biopolymer

The first phase of weight loss occurred during the initial stage of thermal processing as the temperature increased from 26°C to 100°C. The first stage represented water through the evaporation process, in which the maximum point was 80°C (George et al., 1996a; Nanthaya & Taweechai, 2014; Siregar et al., 2011). At this temperature, the granular structure of TBP remained stable, with the constituent molecules held together in spherules by hydrogen bonds or Van der Waals forces, and was referred to as the water evaporation stage (Liu et al., 2009a). The second and third phase of weight loss corresponded to the thermal decomposition of the main components in cassava biopolymer, which commenced at 185°C and 300°C, respectively. The 185°C and

300°C were suspected to represent the thermal decomposition of starch and PLA, respectively. However, the temperature of 185°C was set as the upper boundary for optimum processing temperature study.

The supplements from the DSC result were necessary to analyze the glass transition and melting temperature because the TGA results only expressed the water evaporation stage and decomposition temperature of TBP. Figure 4.9a shows the DSC result of the TBP. As a comparison, the DSC results of PLA and native starch are presented in Figure 4.9b and Figure 4.9c, respectively. According to Figure 4.9a, the glass transition (T_g) of TBP commenced at 51°C. At this temperature, the crystalline structures in the starch granules started to destruct (Lelievre, 1974; Liu et al., 2009a).

Interestingly, Figure 4.9a presents two melting points of 129°C and 165°C, which are the present melting points for the two main components in TBP. The 129°C is suspected to associate with starch melting temperature. At this temperature, all amylopectin double helices became detached, after more significant swelling and dissolution of crystallites (Lim et al., 2000; Liu et al., 2009a). Moreover, the 165°C was associated with the melting temperature for PLA.

The T_g and T_m for TBP were lower as compared to the net PLA, which are presented in Figure 4.9b. The finding was consistent with the previous research, where the T_g and T_m of PLA, polypropylene and liquid natural rubber blends, also had lower values as compared to the net PLA (Bijarimi et al., 2012). However, the melting point of 129°C was a little bit higher as compared to the native starch melting point, as presented in Figure 4.9c. This phenomenon was expected because of the influence of additive in TBP. According to the TGA and DSC results, the processing temperature for TBP was summarized to be between 165°C to 185°C.

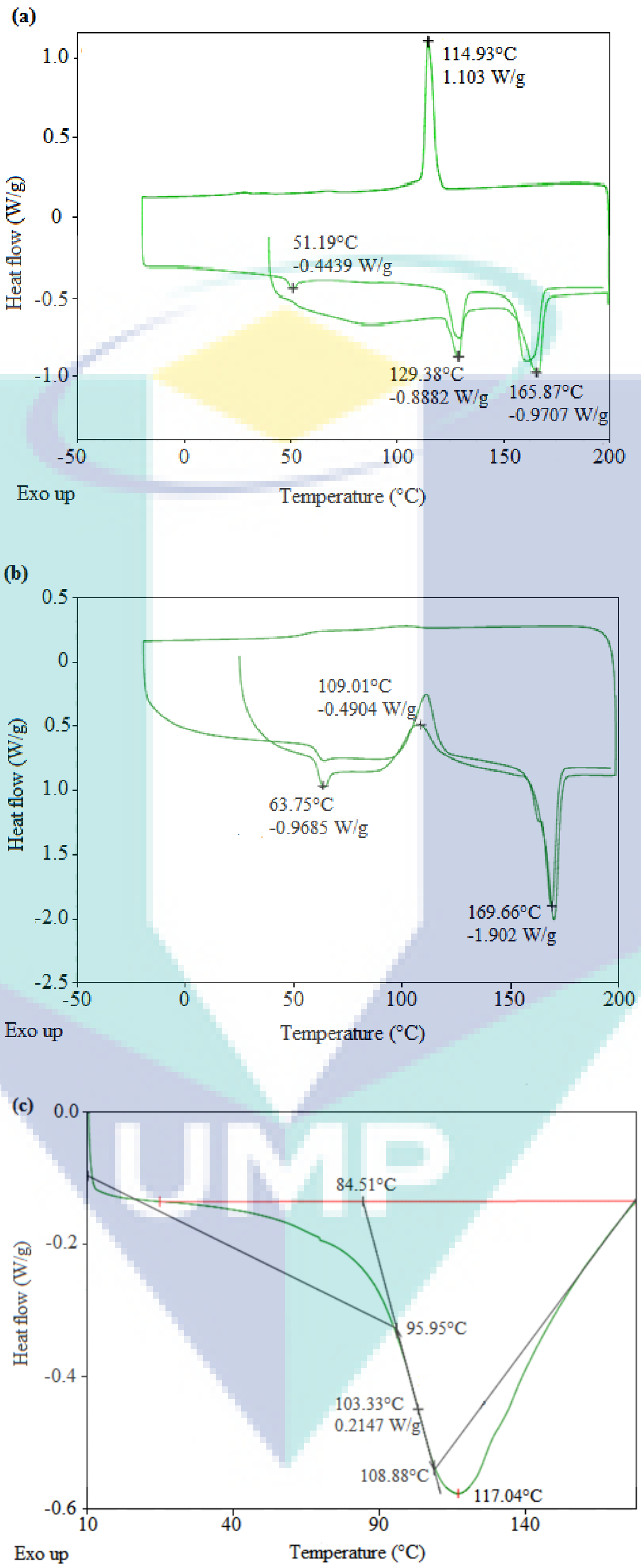

Figure 4.9 DSC result for (a) TBP, (b) PLA, (c) native starch

In addition, Table 4.1 presents the comparison of TBP weight during drying. The optimum drying duration for TBP can be deduced for 4 h. It is due to the six samples of different initial weights (Sample 1, S1; Sample 2, S2; Sample 3, S3; Sample 4, S4; Sample 5, S5 and Sample 6, S6), which showed a constant weight value after 4 h of drying. Moreover, Figure 4.10 exhibits samples of the final test specimens produced by using different processing temperatures. The sample at 185°C could still be provided by using hot-press molding and machined by a CNC machine, but visually, it looked burnt and had a charred smell. These conditions proved the thermal properties analysis that 185°C was the decomposition temperature. As a comparison, Figure 4.11 shows the processing temperature range of TBP and selected petroleum-based polymer, which are PC, PP, PVC, HDPE, LDPE, HIPS and Nylon 6.6 (Callister Jr & Rethwisch, 2012; Gong et al., 2004; Levchik et al., 1999; Luyt et al., 2006; Siregar et al., 2011; Wahrmund et al., 1978).

Table 4.1 Comparison of sample weight during drying process

	Weight (g)	**Weight after drying process (g)**							
		1 hour	**2 hour**	**3 hour**	**4 hour**	**5 hour**	**6 hour**	**7 hour**	**8 hour**
S1	50.50	49.88	49.80	49.78	49.77	49.77	49.76	49.76	49.77
S2	59.40	58.99	58.95	58.94	58.93	58.93	58.92	58.93	58.93
S3	65.15	64.35	63.75	63.65	63.62	63.63	63.62	63.62	63.63
S4	185.31	184.35	183.77	183.55	183.54	183.54	183.55	183.54	183.54
S5	200.84	199.54	198.92	198.37	198.19	198.18	198.17	198.18	198.17
S6	441.1	437.48	436.46	436.40	436.20	435.98	436.10	436.12	436.10

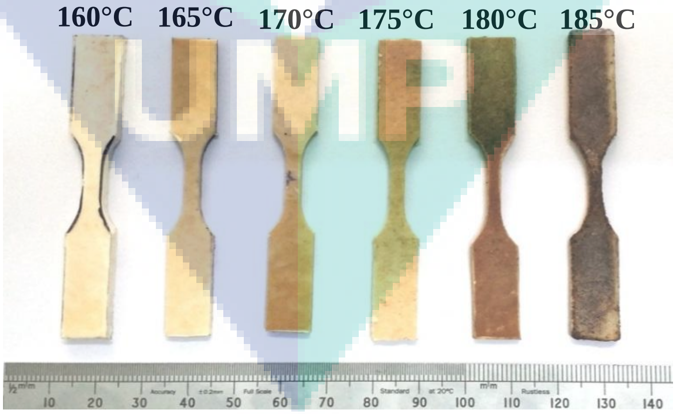

Figure 4.10 TBP final test specimens produced at different processing temperature

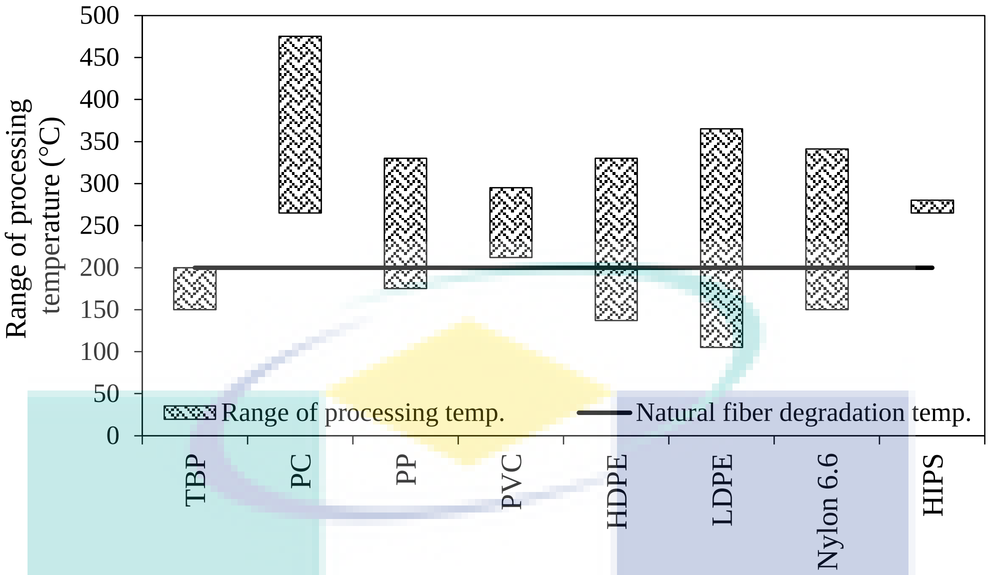

Figure 4.11 Comparison of processing temperature range between TBP and selected petroleum-based polymer

The finding presented that TBP relatively had a lower range of processing temperature as compared to the majority of petroleum-based polymers. However, this small range of processing temperatures was still adequate for TBP to be an alternative to the matrix in the development of bio-composites. Presently, the incompatibility between the processing temperatures of the petroleum-based matrix and natural fiber degradation temperature is one of significant barriers in bio-composites development (Alam et al., 2008; Jamiluddin et al., 2016; Ku et al., 2011). Therefore, the finding in thermal behavior of TBP made the combination of TBP and natural fiber potentially significant in the development of biodegradable composites.

4.3.2 Tensile Properties Analysis

Figure 4.12 shows the stress-strain curve of tensile properties for TBP sample with 160°C processing temperature. The tensile strength results present the value from 9.52 to 11.95 MPa. Meanwhile, the tensile modulus presents the results between 0.25 to 0.36 GPa. The standard deviation for tensile strength and modulus result is 0.92 and 0.04 respectively which indicate consistent output due to the below than 1.

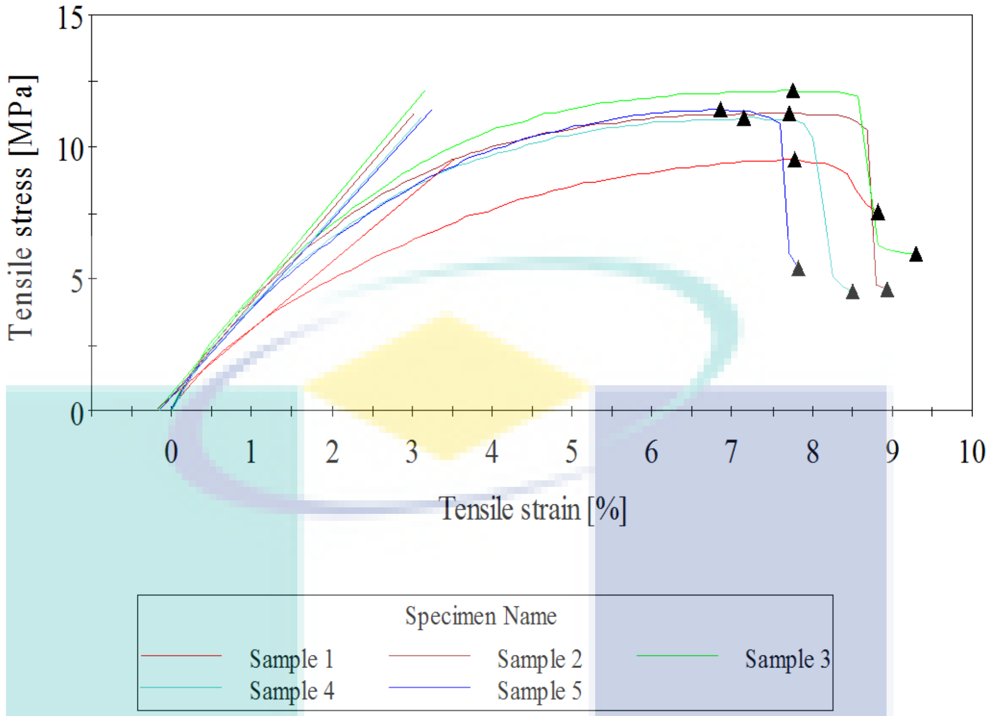

Figure 4.12 The stress-strain curve of tensile properties for TBP sample with 160°C processing temperature

In addition, Figure 4.13 present the comparison results of tensile properties with a mean value displayed according to the different processing temperatures. According to Figure 4.13, the sample at 165°C and sample at 170°C were among the highest mean tensile strength values of 12.94 MPa and 12.67 MPa, respectively. In contrast, the difference in the elastic modulus results between the different processing temperatures was not too noticeable with the highest and lowest mean results at 0.37 GPa and 0.33 GPa, respectively. Moreover, in the maximum strain results also presented no significant difference with the highest and lowest mean results at 9.50% and 8.26%, respectively, as shown in Figure 4.14. Referring to the aforementioned results, the processing temperatures appeared to influence more on tensile strength results as compared to the results of other tensile properties.

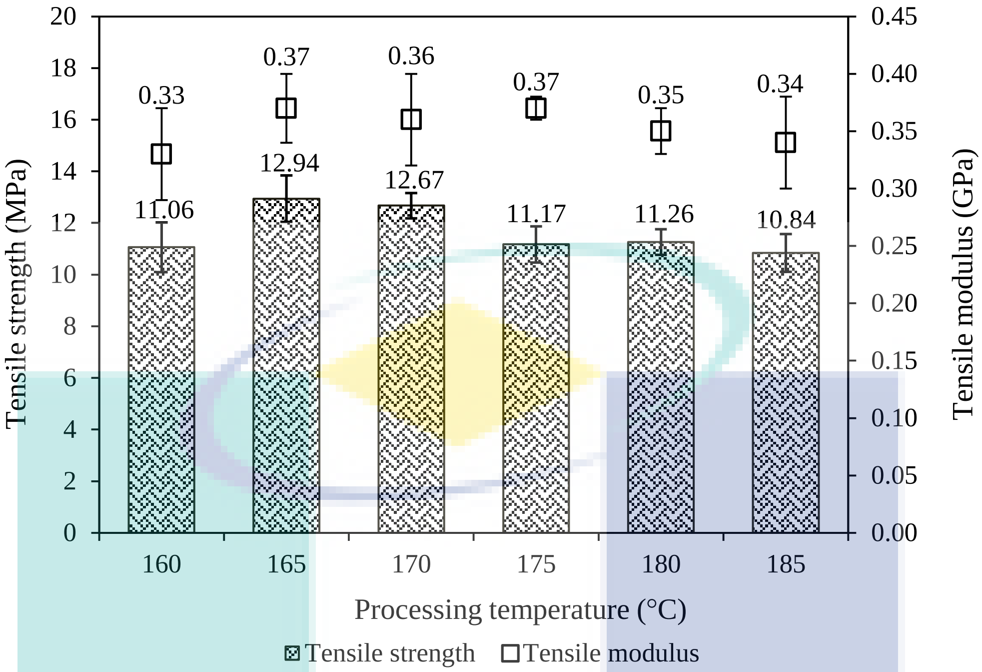

Figure 4.13 Comparison of tensile properties for TBP against different processing temperature

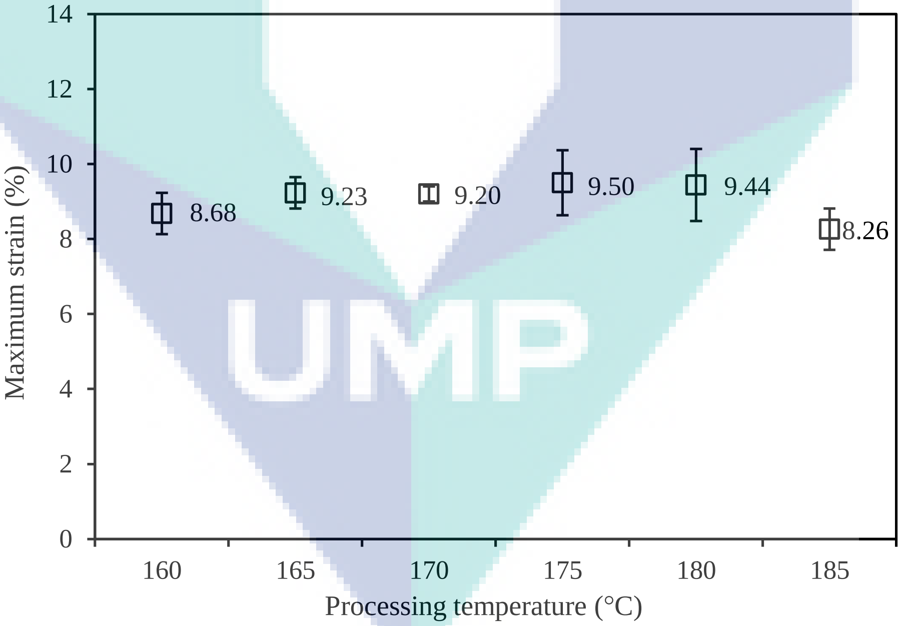

Figure 4.14 Comparison of maximum strain for TBP samples against different processing temperature

4.3.3 Variance Analysis

The analysis of variance (ANOVA) showed that the *p*-value for comparison of tensile strength between 165°C and 170°C was 0.5640, which was higher than 0.05. This result indicated that there was no significant difference between these two temperatures in influencing the tensile strength of TBP.

Moreover, Table 4.2 shows the *p*-value of tensile strength comparison between the samples of 165°C and 170°C processing temperatures with other processing temperatures. The analysis revealed an exciting finding where the processing temperature of 165°C and 170°C showed the apparent significant effect on tensile strength, in which all *p*-values were below than 0.05. These findings reinforced the assumption that temperatures at 165°C and 170°C was the optimum processing temperatures for TBP to produce maximum tensile strength.

Table 4.2 Comparison of *p*-values between processing temperature of 165 °C and 170 °C with other processing temperatures

	160°C	**175°C**	**180°C**	**185°C**
165°C	0.0110*	0.0081*	0.0064*	0.0036*
170°C	0.0085*	0.0044*	0.0022*	0.0017*

* Significant

4.3.4 Morphology Analysis

The SEM photograph of tensile fracture sample is shown in Figure 4.15. According to Figure 4.15, relatively, the co-continuous structure could be seen, except for the sample at 160°C. The sample of 160°C showed the largest phase size among other samples. This finding was as expected because TBP was not completely melted at that temperature, even after it passed the glass transition temperature. This phenomenon caused the fractured sample to have a discontinuous structure in the fracture area. It is widely recognized that a large domain size would usually results in poor mechanical properties (Su et al., 2010).

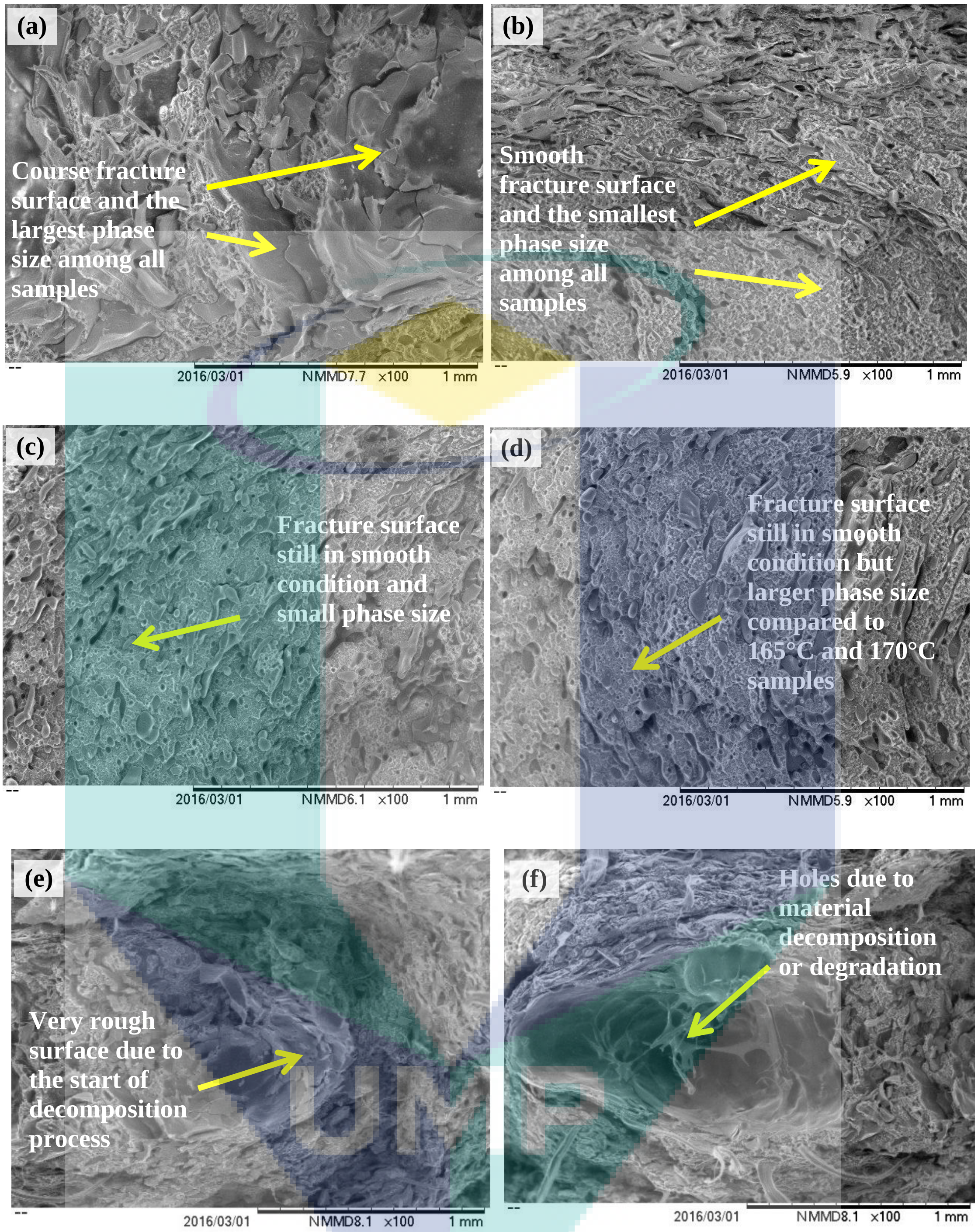

Figure 4.15 SEM image of samples fracture surface for (a) 160°C; (b) 165°C; (c) 170°C; (d) 175°C; (e) 180°C; and (f) 185°C processing temperature

On the other hand, a co-continuous structure can be seen on the fracture area of samples at 165°C, 170°C, 175°C and 180°C. However, it was clear that phase sizes of 165°C, 170°C, 175°C and 180°C increased substantially with the increase in molding temperature (Su et al., 2010). Sample at 165°C presented the finest and smooth fracture surface among all samples. This finding is in agreement with the tensile properties outcome, where sample at 165°C presented the highest mean of tensile strength result as compared to other samples.

In contrast, sample at 185°C fracture surface produced the roughest surface with several obvious holes. It was due to the material that started to decompose at this temperature. Degradation was related to mass loss due to the destruction of the van der Waals forces or hydrogen bonds (Liu et al., 2009a). The previous finding also found that the material showed surface erosion and some cavernous and narrow holes can be observed in the degraded material (Molitoris et al., 1996). The holes due to material decomposition were thought to be the primary factor for crack propagation. This phenomenon provided a significant evidence of low tensile strength result produced by the 185°C sample.

Therefore, it can be concluded that the processing temperature significantly influenced the phase morphology and tensile properties of TBP samples. The present finding, in regard to the relation between processing-properties-structure, was consistent with the past study where a higher processing temperature will produce a larger phase size and influence the mechanical properties (Broutman & McGarry, 1965; Gilbert & Hybart, 1972; Steller & Meissner, 1998; Su et al., 2010).

4.4 Effect of the Different Fiber Lengths on Tensile Properties of Short PALF-TBP Composite

4.4.1 Distribution of Fiber Length

Shown in Figure 4.16 is the distribution of different fiber lengths after crushing and sieving. The overall output for crushing process was less than 2.00 mm of fiber length. However, in order to study the influence of different fiber lengths on tensile properties, the crushed fibers were separated into three groups, which were at most 0.50 mm, 0.51 mm to 1.00 mm, and 1.01 mm to 2.00 mm. The sieved result presented that fiber length that ranged from 1.01 mm to 2.00 mm take the lion share with 55% of the total output. Meanwhile, the output results for fiber length at most 0.50 mm and 0.51 mm to 1.00 mm were 15% and 30%, respectively. It is apparent that the conventional crushing process by using plastic crusher is capable of producing short fibers with length of less than 2.00 mm.

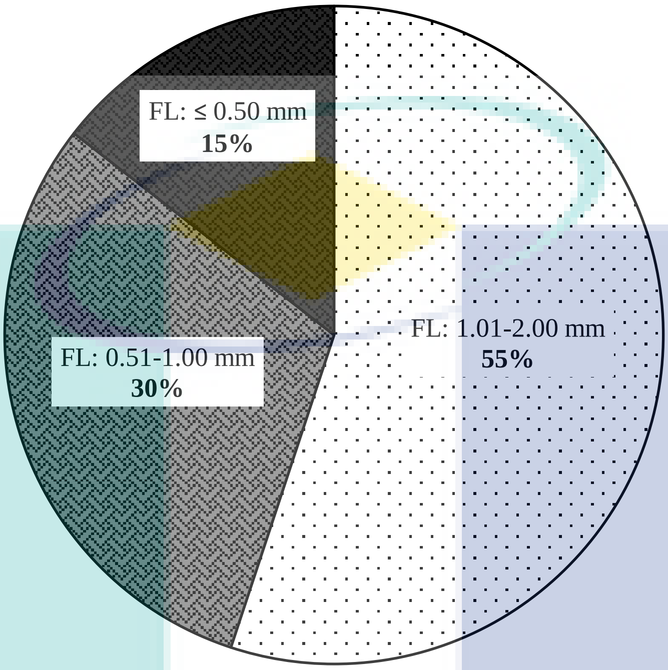

Figure 4.16 Distribution of fiber length (FL) after the crushing and sieving processes

4.4.2 FTIR Analysis

Figure 4.17 presents the FTIR spectra for virgin TBP, PALF and PALF-TBP composites. Referring to the TBP spectrum, the peaks at approximately 2900 cm^{-1} and 1740 cm^{-1} represented the C-H stretching vibration from CH_2 or CH_3 and the stretching vibration of the carbonyl groups (C=O), respectively. The peaks at around 1460 cm^{-1} and 1376 cm^{-1} were assigned to the O-H bonding and methyl (CH_3) bending, respectively (Jumaidin et al., 2017b). The characteristics of the anhydro-glucose ring C-O stretch were associated with the peak at approximately 1078 cm^{-1}. This band was also associated with the C-O-C group stretching from the glucose in starch, and the bands at 718 cm^{-1} to 573 cm^{-1} were assigned to the cassava skeletal (C–C–O) modes (Mutungi et al., 2012). The band at 3300 cm^{-1}, which appeared in the PALF spectrum, was associated with the hydrogen bonded hydroxyl group (O-H) from the complex vibrational stretching, which was related to free, inter, and intra molecular bound hydroxyl groups (Peng & She, 2014). Meanwhile, the peak at 2918 cm^{-1} was associated to the C-H stretching vibration from CH_2 or CH_3. This band was related to the hemicellulose and cellulose components in PALF. The peaks at 1244 cm^{-1} and 1370 cm^{-1} referred to the carbonyl and -CH_2 deformations vibration, respectively. Another broad peak at 1031 cm^{-1} was associated with the C-H group vibration in cellulose and C-H vibration of lignin (Jumaidin et al., 2017a).

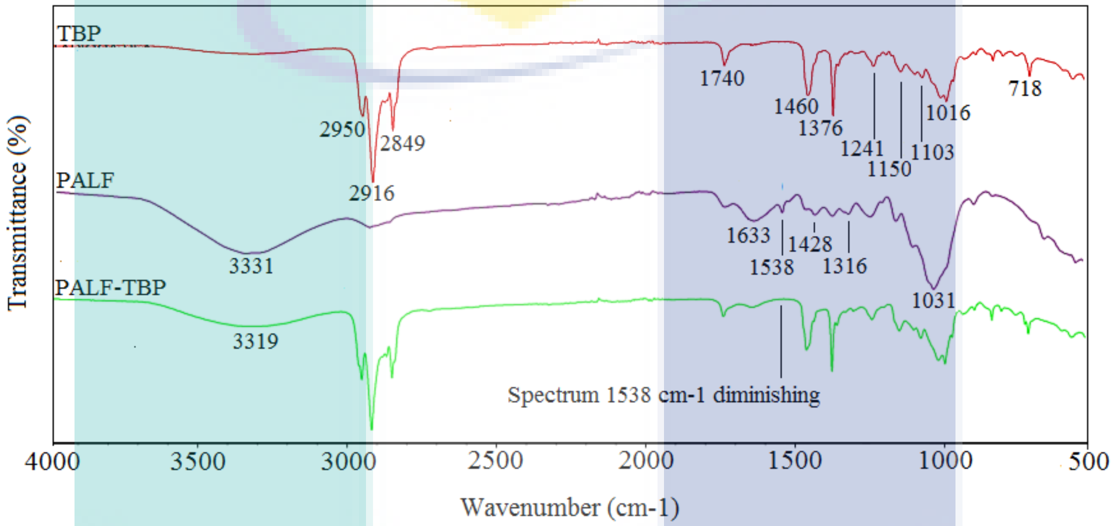

Figure 4.17 Comparison of FTIR spectra between TBP, PALF and PALF-TBP composites

The interaction between the individual components in PALF-TBP composites can be established by recognizing the band position shifting of the spectra. The bands at 3331 cm^{-1} were gradually reallocated to a lower wavenumber, following the compounding between PALF and TBP. This shift indicated the enhancement of intermolecular hydrogen in the PALF-TBP composites. This phenomenon might be attributed to the same hydrophilic behaviour of TBP and PALF. This finding was consistent with the previous FTIR analysis of coconut fiber and tapioca starch bio-composites (Lomelí-Ramírez et al., 2014b) In addition, the characteristic peak of carbonyl at 1538 cm^{-1} diminished, as shown in Figure 4.17. The findings suggested a possible carbonyl interaction between PALF and TBP. This finding was consistent with the previous FTIR analysis of alkali treated that gave fiber reinforced HDPE (Valadez-Gonzalez et al., 1999).

4.4.3 Tensile Properties Analysis

The combination of TBP and short PALF had positive effects on the increase in tensile strength and tensile modulus of the final composite product. Figure 4.18 shows the comparison of tensile properties between virgin TBP and PALF-TBP composites with different fiber lengths (≤ 0.50 mm, 0.51 mm to 1.00 mm, and 1.01 mm to 2.00 mm).

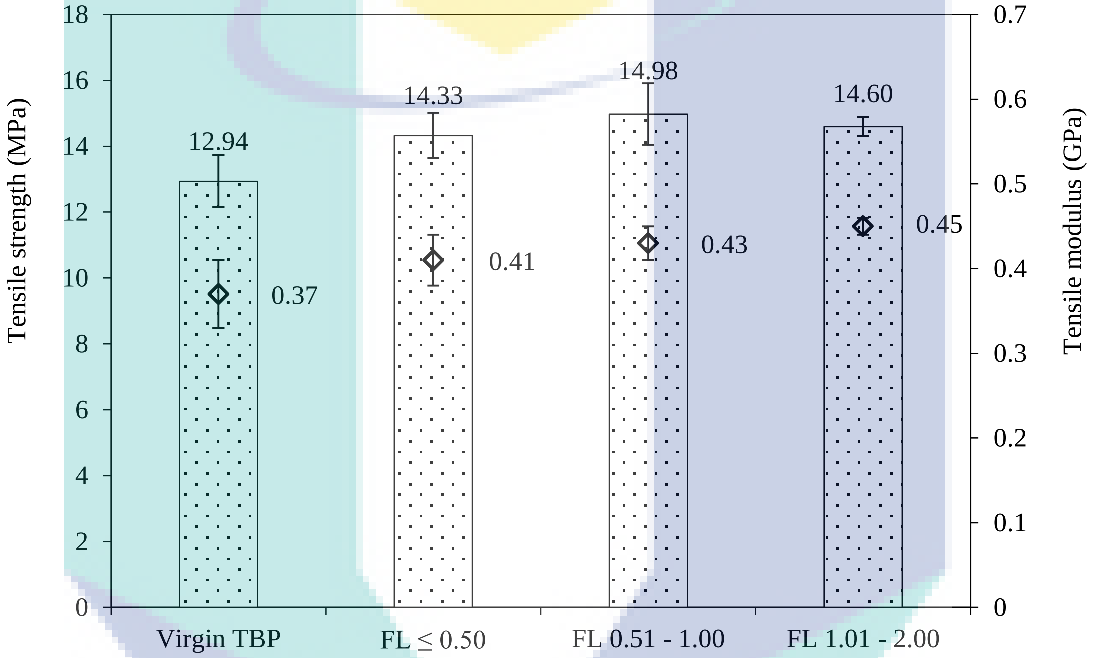

Figure 4.18 Effect of different fiber length (FL)

The composite samples showed good increments as compared to the virgin TBP, with a 10.7% to 15.8% increment for tensile strength and 10.8% to 16.2% for tensile modulus. However, the effects of different lengths of fibers on the tensile properties are visually not significantly different. The difference in tensile strength and modulus results between these three different fiber lengths were 0.1% to 4.5% and 2.4% to 4.9%, respectively. Therefore, more comprehensive analysis needs to be done to determine the effect of different fiber lengths on tensile properties of PALF-TBP composites.

4.4.4 Variance Analysis

The *p*-values for comparison of tensile strength results between virgin TBP and PALF-TBP composite samples (≤ 0.50 mm, 0.51-1.00 mm and 1.01-2.00 mm) were 0.0039, 0.0008, and 0.0018, respectively. Moreover, a *p*-value of 0.0000 was presented in the comparison of modulus result between virgin TBP and all composite samples. These findings showed significant PALF improvements in enhancing the tensile properties of TBP. However, the analysis on tensile strength and modulus between three different fiber lengths presented contradictory findings, where the *p*-value for tensile strength and modulus was higher than 0.05, as presented in Table 4.3 and Table 4.4, respectively. Therefore, the findings revealed that PALF had a positive contribution to PALF-TBP composites. However, the influence of different fiber lengths of up to 2.00 mm produced no significant effect on tensile properties.

Table 4.3 The *p*-values for tensile strength comparison

Fiber length	**≤ 0.50 mm**	**0.51 to 1.00 mm**	**1.01 to 2.00 mm**
≤ 0.50 mm		0.0740	0.9223
0.51 to 1.00 mm			0.0993
1.01 to 2.00 mm			

* Significant

Table 4.4 The *p*-values for tensile modulus comparison

Fiber length	**≤ 0.50 mm**	**0.51 to 1.00 mm**	**1.01 to 2.00 mm**
≤ 0.50 mm		0.1373	0.2594
0.51 to 1.00 mm			0.3501
1.01 to 2.00 mm			

* Significant

This finding is consistent with previous research of PALF-HDPE and PALF-HIPS composites, where different fiber lengths of 0.50 mm, 1.00 mm, and 2.00 mm present no significant differences in tensile strength and tensile modulus results, as shown in Figure 4.19 (Aji et al., 2011; Siregar, 2011).

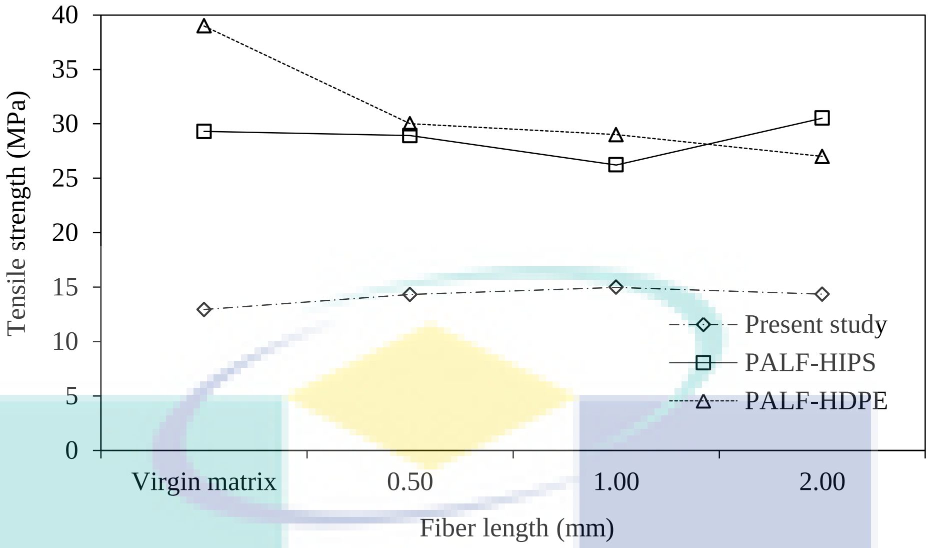

Figure 4.19 Comparison of single PALF tensile strength

The combination of PALF and TBP produce positive impact and better enhancement with 11% to 16% increment of tensile strength result as compared to PALF-HDPE and PALF-HIPS composites which produced -31 to -23% and -11 to 4% enhancements in tensile strength, respectively. These findings provided evidence that PALF and TBP had better compatibility as compared to the petroleum-based polymer. It is expected due to the similar hydrophilic character between PALF and TBP.

4.4.5 Morphology Analysis

The SEM images presented in Figure 4.20 showed the tensile fracture of PALF-TBP composite samples. It is apparent that better compatibility of PALF and TBP can be observed as compared to previous PALF reinforced petroleum-based polymer composites. Previous researchers found that fiber pull-out was the primary failure behavior for PALF reinforced petroleum-based polymer (Aji et al., 2011; Siregar, 2011). However, the fiber failure in all PALF-TBP samples was a combination of fiber pull out and fiber breakage. Also, there was no gap between PALF and TBP even under 1000 magnification.

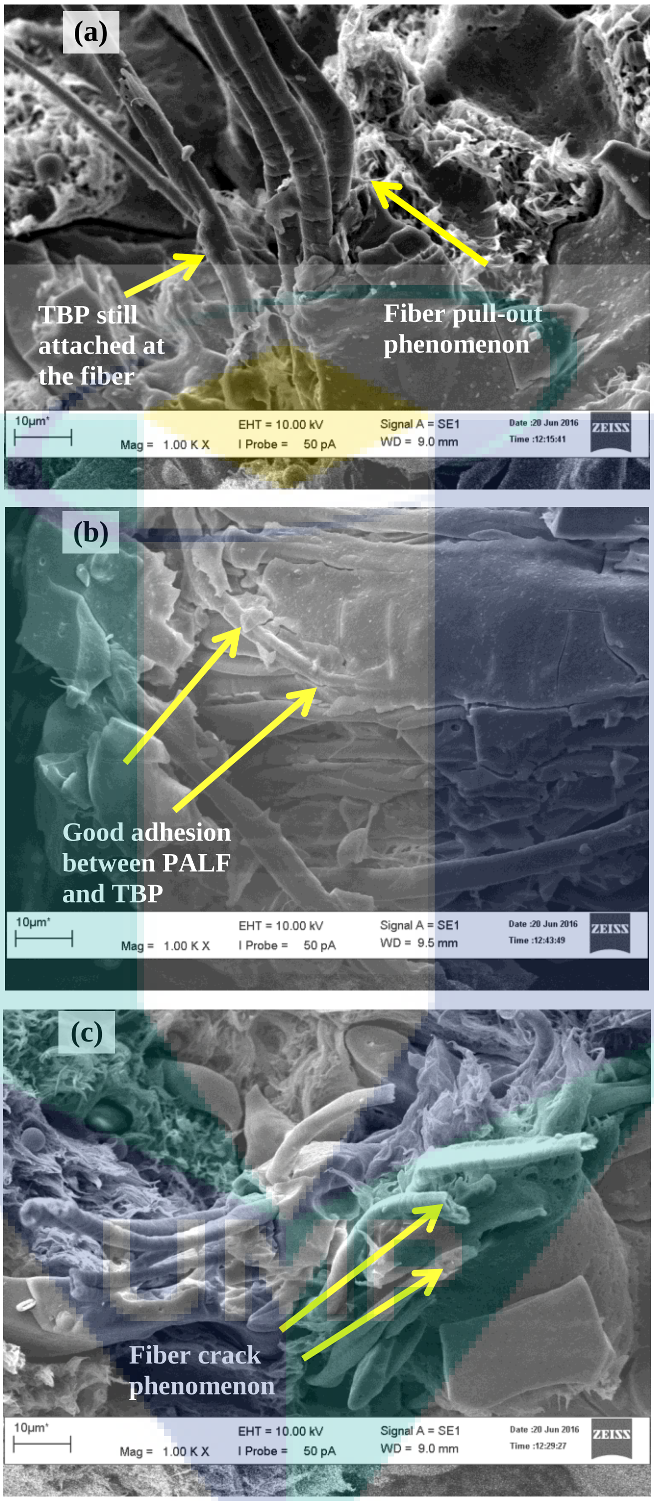

Figure 4.20 Scanning electron micrograph of tensile fracture of PALF-TBP composite samples with different fiber length (FL), a) FL ≤ 0.05 mm, b) FL 0.51 to 1.00 mm, and c) FL 1.01 to 2.00 mm

The morphology analysis illustrated that PALF and TBP were highly compatible, which was indicated through the excellent fiber wetting by the matrix and fiber failure behavior at the fracture surface. Again, this phenomenon was attributing to a similar hydrophilic character between PALF and TBP. As a result of the tensile fracture, the fiber crack phenomenon of PALF indicated the stress-transfer efficiently from the matrix to fiber. This phenomenon produces fiber as an efficient reinforcement in the composites. The present finding corresponded to the significant enhancement percentage in tensile strength result as compared to PALF reinforced petroleum-based polymer, as discussed earlier. However, the similar failure between all PALF-TBP samples reinforced the finding that different fiber lengths of up to 2.00 mm present no significant difference on tensile properties.

4.5 Evaluation of Different Fiber Loadings on the Mechanical Properties of PALF-TBP Composites

4.5.1 Effect of Fiber Loading on Tensile Properties

The current study also measured the mechanical properties of PALF-TBP composites at various PALF percentages to determine the optimum fiber content in generating maximum mechanical properties. Figure 4.21 present the stress-strain curve of tensile properties for PALF-TBP composite samples with 20% fiber loading.

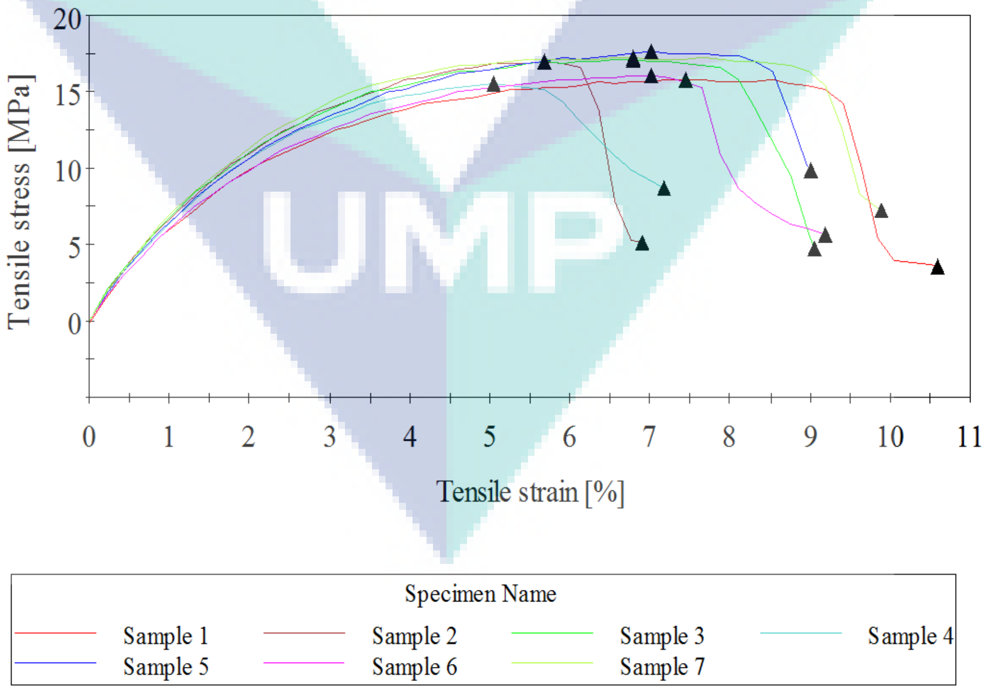

Figure 4.21 Effect of fiber loading on flexural properties of PALF-TBP composites

According to Figure 4.21, the tensile strength value was varied from 15.49 to 17.25 MPa with 16.60 MPa as a mean value. Meanwhile, the results for tensile modulus and maximum tensile strain were varied from 0.66 to 0.75 GPa and 6.90 to 10.60% respectively. In addition, Table 4.5 illustrates the effect of PALF reinforced TBP composites with different fiber contents on tensile properties. The tensile strength of the composite increased with the increase of PALF percentage by up to 30% of fiber loadings. However, a decrease of 14.1% was detected in tensile strength when the fiber content further increased from 30% to 40%. The PALF30sample presented the highest enhancement in tensile strength, at 42.0%, as compared to virgin TBP. In the tensile test, the applied stress transmitted from the matrix to the fibers across the interface. Hence, the interfacial adhesion between fiber and matrix played a significant role in crack propagation (Ku et al., 2011; Liu et al., 2005). At higher fiber loading, the reduction in the matrices percentage caused the interfacial adhesion between the fibers and matrix to become weak. In addition, the fibers with higher fiber percentage tended to aggregate in the composite (Shalwan & Yousif, 2013). This phenomenon led to low tensile strength results in the composites.

Table 4.5 The tensile properties of PALF-TBP composites at different fiber loading

Sample	**Tensile strength (MPa)**	**Tensile modulus (GPa)**	**Maximum strain (%)**
	Mean ± SD	**Mean ± SD**	**Mean ± SD**
Virgin TBP	12.94 ± 0.90	0.37 ± 0.03	9.23 ± 0.42
PALF10	14.35 ± 0.53	0.42 ± 0.02	8.94 ± 0.34
PALF20	16.60 ± 0.82	0.73 ±0.03	8.83 ± 1.35
PALF30	18.37 ± 0.78	0.98 ± 0.07	6.84 ± 0.96
PALF40	15.78 ± 0.76	1.03 ± 0.10	5.73 ± 0.59

* SD – Standard deviation

The tensile modulus results showed an increase in fiber loading by up to 40%. According to Table 4.5, virgin TBP showed a tensile modulus of 0.37 GPa. An increment of 178.4% in tensile modulus was discovered as the fiber content was increased by up to 40%. During the tensile condition, partially separated micro-spaces were created. These obstructed the stress propagation between the PALF and TBP as a matrix; thus, the degree of obstruction increased, which resulted in stiffness increase (Alam et al., 2008; Lomelí-Ramírez et al., 2014b; Pickering et al., 2016). The result in the present study was consistent with the findings of previous studies in which the tensile strength showed a decrease after the optimum fiber loading and the tensile modulus showed compliance with the percentage of fiber (Liu et al., 2005; Threepopnatkul et al., 2009). Furthermore, the maximum strain of the PALF-TBP composite decreased consistently with the increase of fiber composition. The value of maximum strain decreased by almost 38% from 9.23% for virgin TBP matrix when PALF fiber content was increased to 40%. This phenomenon was attributed to the addition of fiber into the polymer matrix, which reduced the matrix mobility. As a result, tensile modulus increased and maximum strain decreased for the composites due to the increase in fiber loading.

4.5.2 Effect of Fiber Loading of Flexural Properties

Like tensile strength, the flexural strength of the composites increased considerably with the addition of PALF. As the fiber content was increased by up to 40%, the flexural strength and modulus increased by up to 81.1% and 366.67%, respectively. Figure 4.22 shows the influence of different fiber loadings on flexural properties of PALF-TBP composites. The above finding is consistent with the previous finding of PALF-PP composites and hybrid PALF, and kenaf reinforced HDPE composite where the flexural strength increased by the increase of fiber percentage of up to 40% (Aji et al., 2011; Nanthaya & Taweechai, 2014).

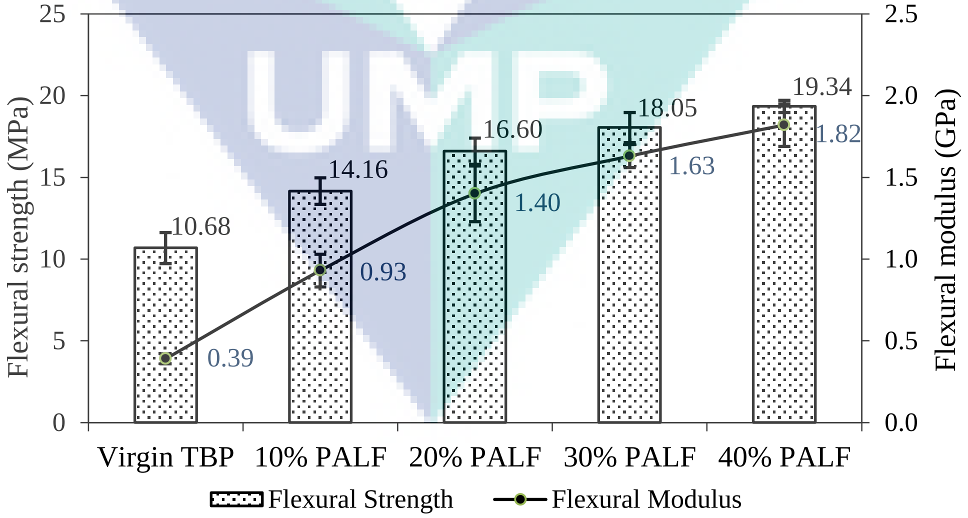

Figure 4.22 Effect of fiber loading on flexural properties of PALF-TBP composites

The tensile and flexural strength results for 30% and higher fiber loadings showed a different trend. Theoretically, flexural behavior involves the combination of the tensile and compressive condition of the composite sample. At the point of loading, the top surface of the specimen is placed in a state of compression, while the bottom surface is in tension. As discussed earlier, interface adhesion between fiber and matrix plays a significant role in crack propagation during tensile condition. However, in compression condition, the applied stress is easily transmitted from the matrix to the fibers across the interface. Furthermore, a higher amount of the fibers will create higher compressive strength. Figure 4.23 presents crack propagation of the composite sample under flexural test, and it shows that the crack starts at the bottom surface of the sample, which is reflected under tensile condition.

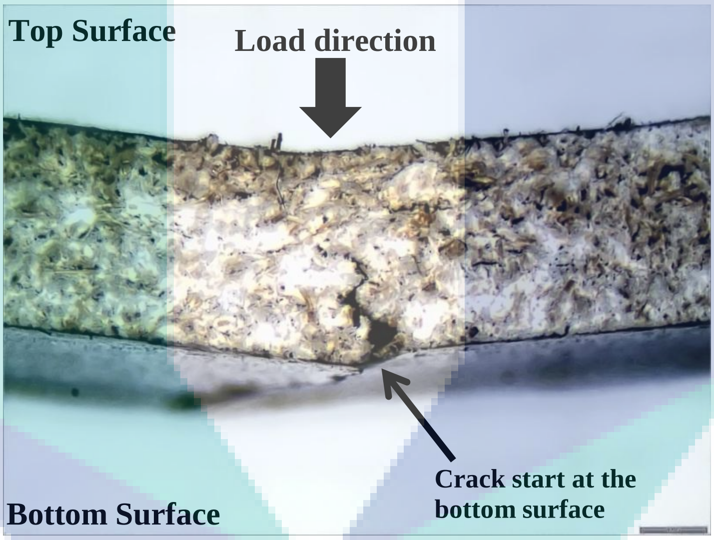

Figure 4.23 Side view of composites sample after flexural test

This phenomenon indicates the agreement with the above discussion. Therefore, the conclusion for increased pattern for flexural strength even over 30% of fiber loading is due to the combination of compressive strength, which caused the result to still increase and adherence to rules of the mixture of up to 40% of fiber composition. However, this phenomenon still depends on interface optimization.

4.5.3 Effect of Fiber Loading of Impact Properties

There was a consistent increase in the impact strength as shown in Figure 4.24. Impact strength of 18.1 kJ/m² was observed for PALF40sample, which was nearly 20.1% higher than the virgin TBP matrix. This was because the utilization of PALF had increased the amount of energy required for pulling it out. The impact strength results in this research were consistent with the findings of previous studies in which the impact strength showed enhancement with the fiber percentage of up to 60% for short basalt fiber reinforced polyester (Amuthakkannan et al., 2013). Also, rice husk-PE and ramie-PLA composites showed impact strength enhancement with increasing fiber content of up to 30% (Rahman et al., 2010; Tao et al., 2009).

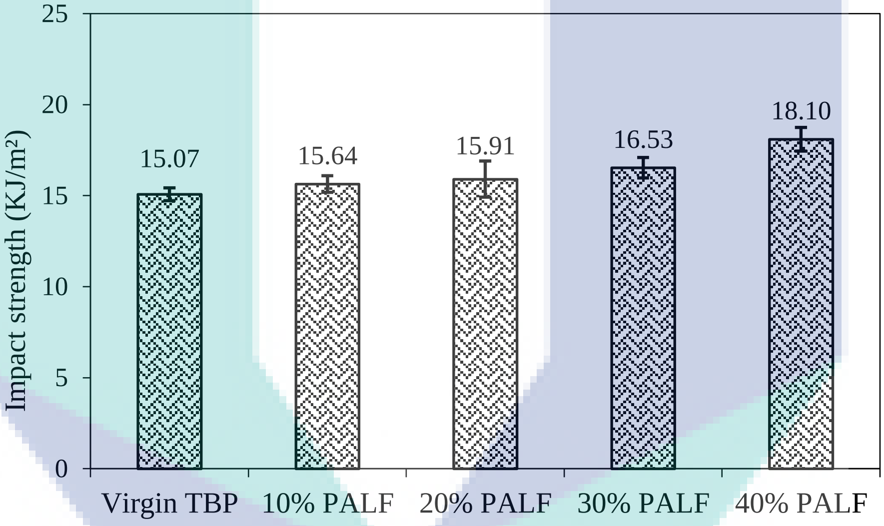

Figure 4.24 Effect of fiber composition on impact strength of PALF-TBP composites

In addition, Figure 4.25 compares the tensile and flexural strength between virgin TBP, 30% of PALF reinforced TBP composite, and the most common conventional polymers used in automotive sectors, which are PET, PP, LDPE, HDPE and HIPS as mention in the literature study. Meanwhile, Figure 4.26 illustrates the comparison of impact strength between virgin TBP, 30% of PALF-TBP composites and LDPE, HDPE, PET, PP and HIPS (Ahmad et al., 2008; Hashemi, 2011; Panyasart et al., 2014; Rana et al., 1998; Siregar et al., 2010; Threepopnatkul et al., 2009; Yang et al., 2007).

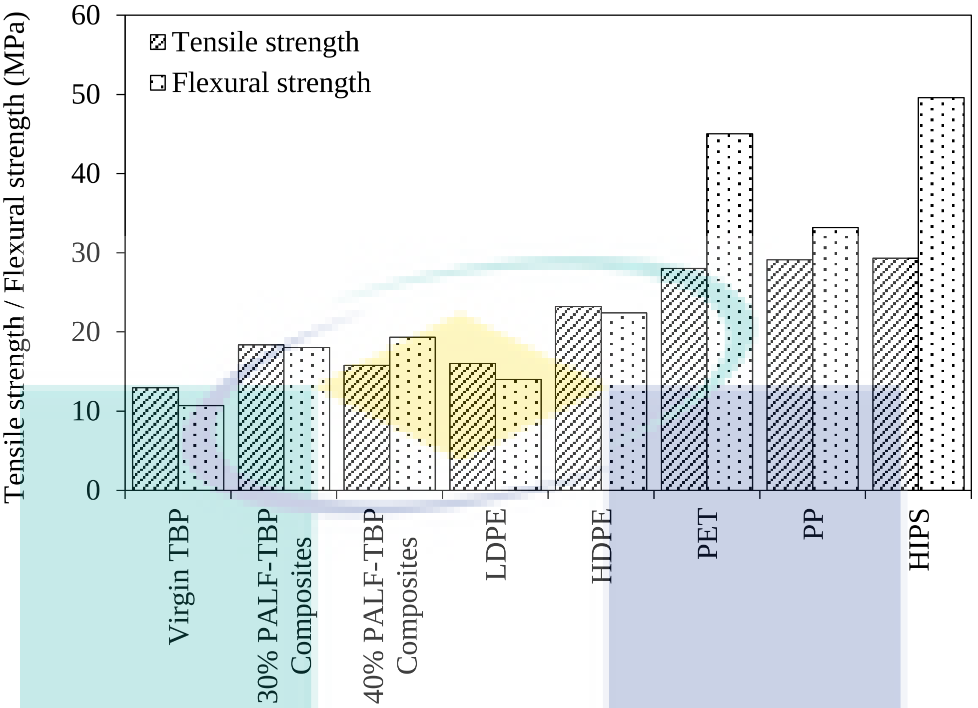

Figure 4.25 Comparison of tensile and flexural strength between TBP, PALF-TBP composites, and selected petroleum-based polymers

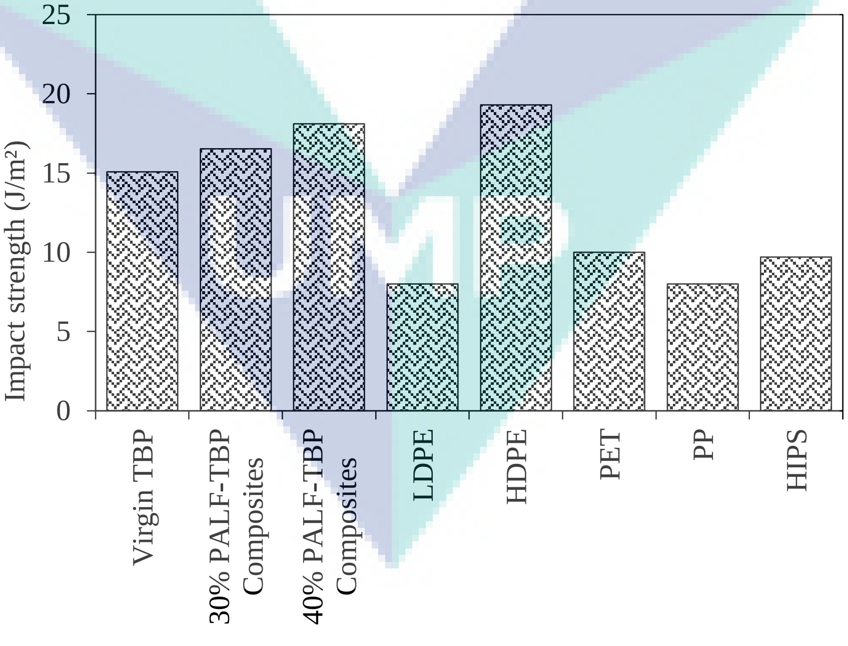

Figure 4.26 Comparison of impact strength between TBP, PALF-TBP composites, and selected petroleum-based polymers

According to the Figure 4.25, virgin TBP presents the lowest tensile and flexural strength values as compared to the common conventional polymers that were used in automotive sectors. The combination of PALF and TBP with 30% fiber loading increased both tensile and flexural properties, and thus was better than the LDPE properties. However, the combination of 40% PALF only capable of producing higher flexural strength result but tensile strength value present slightly lower result compared with LDPE. Therefore, 30% of fiber loading is a reasonable combination between PALF and TBP in producing competitive tensile and flexural properties.

On the other hand, Figure 4.26 presented the comparison of impact strength between virgin TBP, PALF-TBP composites and selected conventional polymers. Interestingly, virgin TBP has higher impact strength value compared with most of the typical conventional polymers. Therefore, the present finding showed that PALF-TBP composite had tremendous potential in the development of entirely biodegradable composites. Moreover, TBP and PALF-TBP presented higher impact strengths as compared to most of the common conventional polymers that were used in the automotive sectors. Therefore, the improvement on the tensile and flexural properties of PALF-TBP composite in the future is expected capable to make it an alternative to petroleum-based polymers for engineering applications, especially in the automotive sector.

4.5.4 Variance Analysis

Visual observation on the mechanical properties' result of PALF-TBP composite showed that the sample containing 40% of fiber loading generated maximum flexural strength, impact strength, and tensile modulus. However, sample PALF30, which contained 30% of fiber loading, was shown to produce the maximum value in its resulting tensile strength. As discussed earlier, the applied stress was transmitted from the matrix to the fibers across the interface in the tensile condition. Hence, the interface adhesion between fiber and matrix played a significant role in crack propagation. As compared with compression condition, the applied stress is easily transmitted from the matrix to the fibers across the interface The selection of optimum fiber content according to the tensile performance was essential in producing good results for the overall mechanical properties. Analysis of variance (ANOVA) was carried out in order to understand the significance of fiber loading in influencing the tensile properties. The *p*-value comparison for tensile strength and tensile modulus between the samples contain 30% of PALF and other samples are presented in Table 4.6 and Table 4.7, respectively.

Table 4.6 The *p*-value comparison of tensile strength between 30% of PALF-TBP composites and other samples

	Virgin TBP	**10% PALF**	**20% PALF**	**40% PALF**
30% PALF	0.00000*	0.00000*	0.00139*	0.00004*

* Significant

Table 4.7 The *p*-value comparison of tensile modulus between 30% of PALF-TBP composites and other samples

	Virgin TBP	**10% PALF**	**20% PALF**	**40% PALF**
30% PALF	0.00000*	0.00000*	0.00001*	0.33511

* Significant

The findings indicated that 30% fiber content presented a significant effect on reinforcement for maximum tensile strength results as compared to other samples. However, the variance analysis of tensile modulus results between PALF30 and PALF40 was 0.3351. The results presented no significant difference between both samples even though sample PALF40 visually presented the highest mean values; thus, the 30% of fiber percentage was selected as the optimum loading for PALF-TBP composites in generating the maximum mechanical properties.

4.5.5 Morphology Analysis

The SEM images presented in Figure 4.27 showed that the tensile fracture of PALF-TBP composite samples with different fiber loading. Fiber pull-out is the primary cause of failure for PALF reinforced petroleum-based polymers (Aji et al., 2011; Siregar, 2011). However, the fiber failure in PALF-TBP was a combination of fiber pull out and fiber breakage. Also, TBP was still attached at the fully pulled out fiber, and there was no gap between PALF and TBP even under 1000 magnification. The morphology analysis illustrated that PALF and TBP were highly compatible, which was indicated through the excellent fiber wetting by the matrix and fiber failure behavior at the fracture surface. Again, this phenomenon might be attributed to a similar hydrophilic character between PALF and TBP. Because of the tensile fracture, the fiber crack phenomenon of PALF indicated that the stress was transferred efficiently from the matrix to fiber. This phenomenon produces fiber as an efficient reinforcement in the composites. This corresponded to the significant percentage of enhancement in tensile strength results, as discussed earlier.

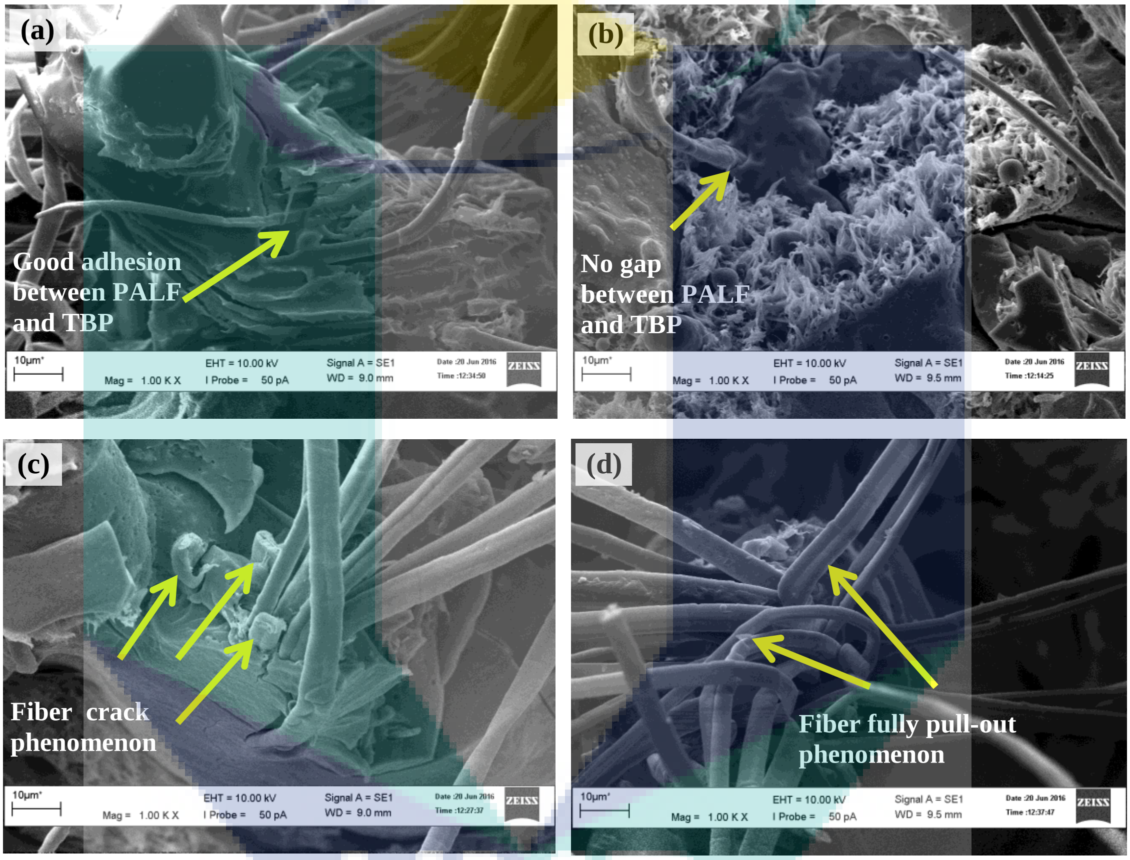

Figure 4.27 Scanning eletron micrograph of tensile fracture of PALF-TBP composite samples with different fiber loading: a) 10%, b) 20%, c) 30% and d) 40%

However, the full fiber pull-out phenomenon was observed in the PALF40 fractured sample containing 40% fiber percentage. As discussed in the literature study, reducing matrix content has resulted in weak interfacial adhesion between fiber and matrix. Moreover, the fibers with higher fiber content tended to aggregate in the composite and thereby weakened the interfacial adhesion between the fiber and the matrix (Shalwan & Yousif, 2013). Therefore, these findings reinforce the results of low tensile strength produced by PALF40 sample against other samples.

4.6 Influence of Selected Treatment on Tensile Properties of Short PALF Reinforced TBP Composites

4.6.1 Selection of Coupling Agent Concentration for PALF-TBP Composites

Figure 4.28 illustrates the tensile properties of PALF-TBP composites against the different concentrations of MAPP compatibilizer. The use of MAPP showed a parallel increase in tensile strength and modulus with an increase in MAPP concentrations of up to 7%. An increment of 21.12% and 44.44% in tensile strength and tensile modulus, respectively, was discovered as the MAPP content increased up to 7%. The finding was consistent with the previous study of short jute fibers reinforced PP, which presented the increments of tensile strength and modulus with the increase of MAPP concentration of up to 4%. Again, according to literature study, a further increase in the concentration of compatibilizer had a virtually little effect. In addition, the maximum suitable percentage for coupling agent is not more than 7% due to environmental friendly and cost issue. According to the previous finding, the effectiveness of coupling agents was associated with the incorporation and incompatibility between the coupling agents and composites matrix. Yang et al. suggested that MAPP appeared to be less effective when PE matrix polymer was used in the composites and vice versa (Yang et al., 2007).

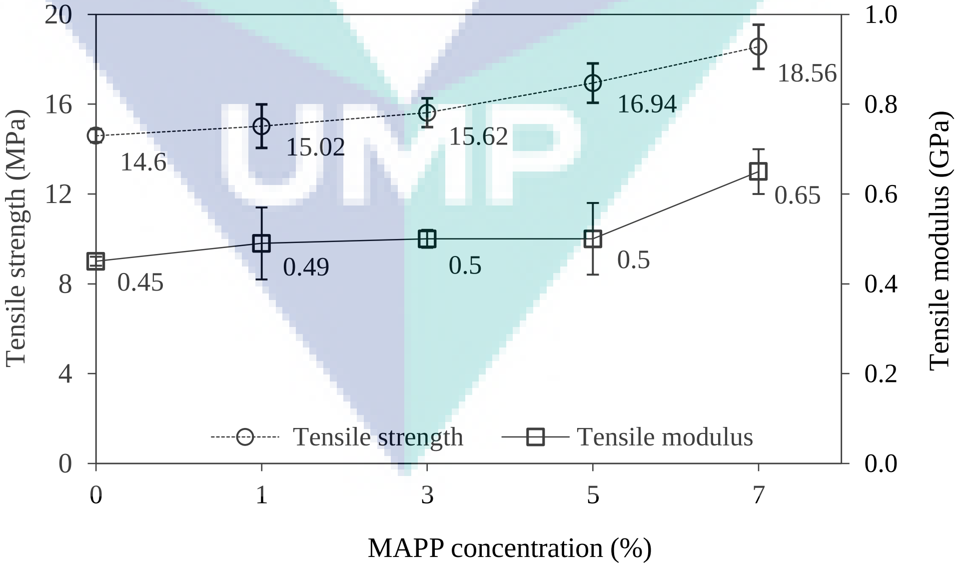

Figure 4.28 Effect of different concentration of MAPP

Contrary to the effect of MAPP, the use of MAPE showed an increase in tensile strength and modulus by up to 3% of concentration only, as shown in Figure 4.29. A decrease by 8.26% and 21.22% was detected in tensile strength and tensile modulus, respectively, as the MAPE content was further increased from 3% to 5%. Nonetheless, all results obtained exceeded the tensile strength of pure TBP, i.e., 14.60 MPa. A similar finding was also observed in MAPE treated with jute reinforced high-density polyethylene composites. A decrease in tensile strength was seen when the MAPE concentrations increased from 1% to 2% (Mohanty et al., 2006). The reduction in tensile properties' result was due to the plasticizing effect from the MAPE, which has a lower molecular weight as compared to TBP. The plasticizing effect eventually lowers the rigidity of the composite; thus, decreasing the tensile strength and modulus (Khalid et al., 2006; Mohanty et al., 2004). Gassan and Bledzki also reported a similar finding for jute and flax fibers reinforced PP composites due to the migration of excess MAPE around the fibers, causing self-entanglement among themselves rather than the polymer matrix, resulting in slippage of the fibers within the matrix (Gassan & Bledzki, 1997).

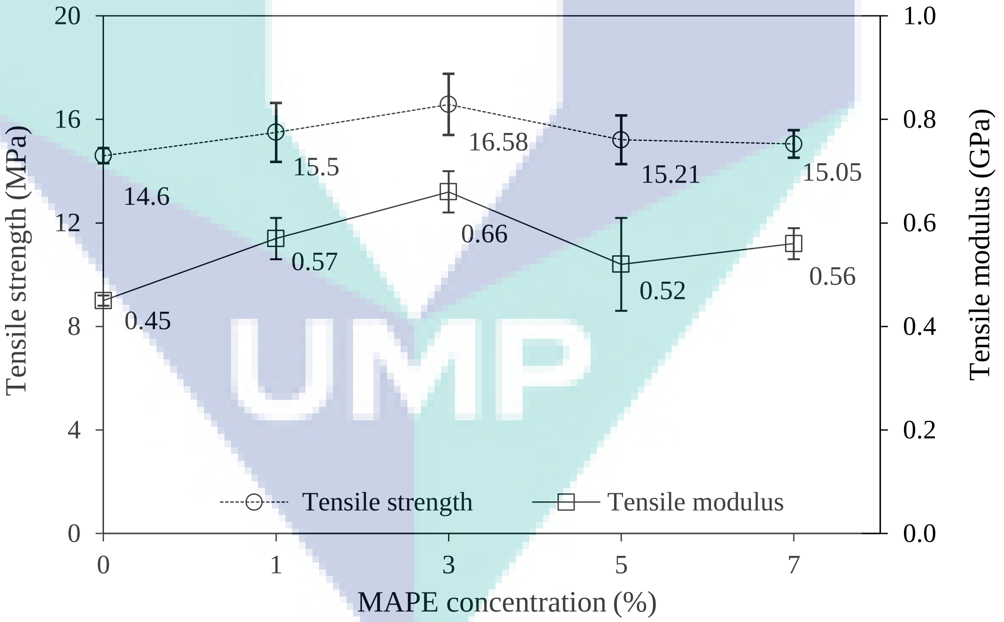

Figure 4.29 Effect of different concentration of MAPE

According to Figure 4.28 and Figure 4.29, 7% of MAPP content and 3% of MAPE content were selected in sample preparation for PALF-TBP-MAPP and PALF-TBP-MAPE samples. Then the sample was used for evaluation on the effect of different treatments, which were alkali treatment, MAPP utilization and MAPE utilization, on tensile properties of PALF-TBP composites.

4.6.2 Effect of Different Treatments on Tensile Properties of PALF-TBP Composites

Figure 4.30 present the stress-strain curve of tensile properties for 30% of PALF-TBP composite samples with MAPP utilization. Tensile strength result was varied from 21.38 to 23.69 MPa with mean value of 22.70 MPa. Meanwhile, tensile modulus and maximum tensile strain present the value varied from 1.04 to 1.22 GPa and 4.19 to 5.30% respectively.

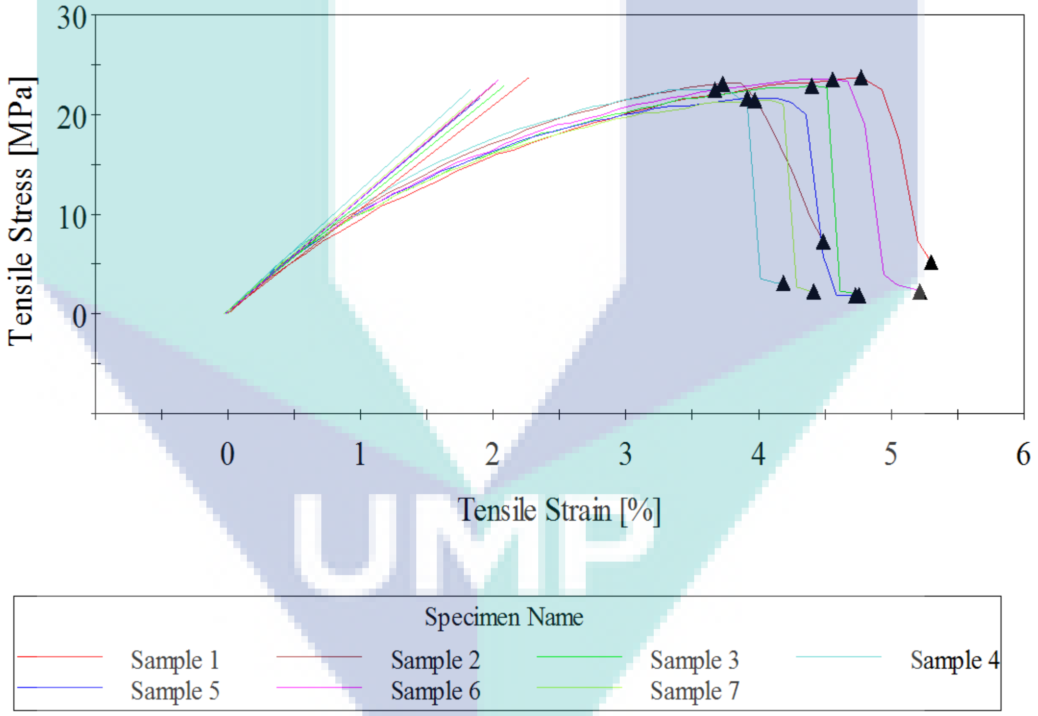

Figure 4.30 Effect of different treatment on tensile strength result

On the other hand, tensile strength and tensile modulus results are presented in Figure 4.31 and Figure 4.32, respectively, indicating the comparison of untreated PALF-TBP composites and different treatments of PALF-TBP composites. Relatively, all types of alkali treatments, which were 7% MAPP and 3% MAPE, had enhanced the tensile properties.

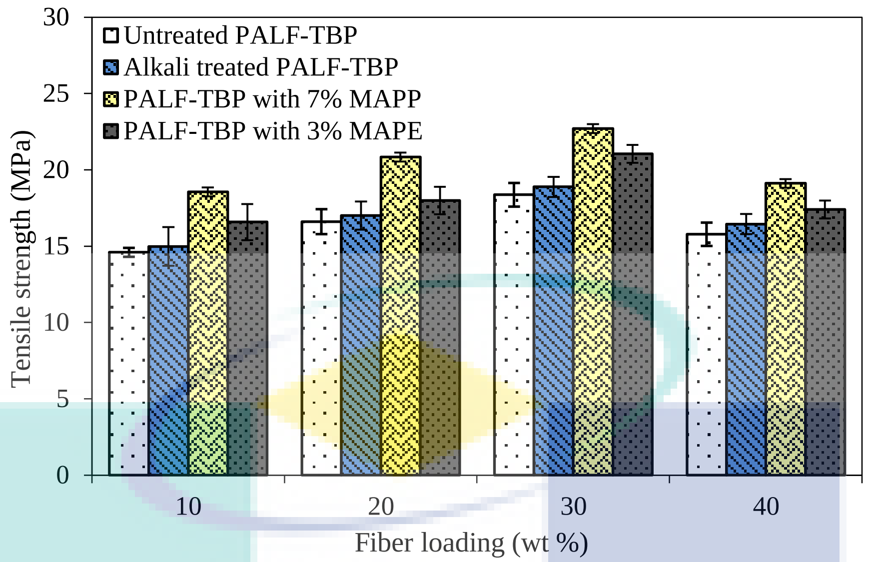

Figure 4.31 Effect of different treatment on tensile strength result

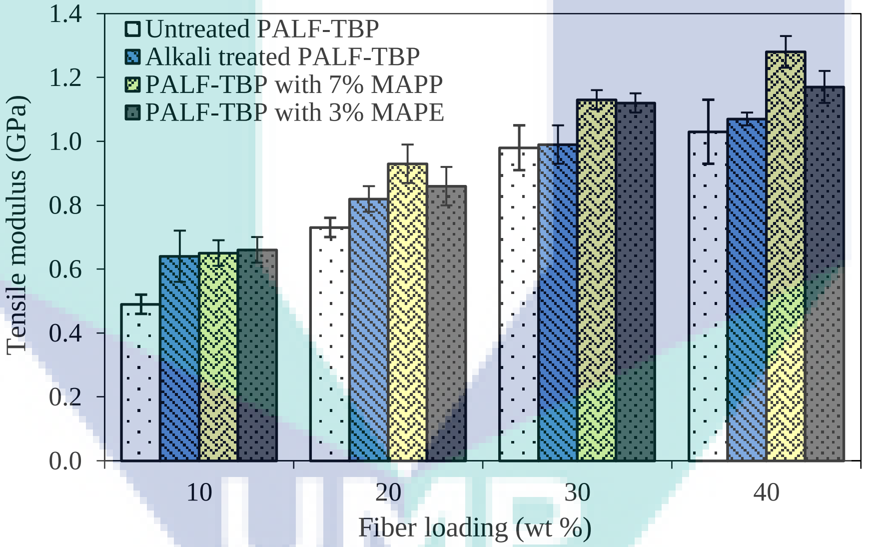

Figure 4.32 Effect of different treatment on tensile modulus result

According to Figure 4.31, the tensile strength of the composites containing MAPP was superior to that of the composites containing MAPE and alkali treated PALF-TBP. Samples of 10%, 20%, 30% and 40% fibers content with MAPP presented an increment in tensile strength of 27.1%, 25.5%, 23.6% and 21.1%, respectively. Moreover, tensile modulus result also presented significant increments, which were 35.7%, 27.4%, 15.3% and 24.3%, respectively. The maleic anhydride groups of MAPP covalently linked with the hydroxyl groups of the fibers, thereby increasing its wettability and dispersion within the matrix. Furthermore, the nonpolar part (PP) of

MAPP became compatible with the virgin TBP, lowering the surface energies of the fibers, thereby, increasing its wettability and dispersion within the TBP matrix (Mohanty et al., 2006).

On the other hand, 10%, 20%, 30% and 40% of PALF-TBP samples with MAPE treatments showed tensile strength increments of 13.6%, 8.3%, 14.58% and 10.3%, respectively. As compared to the MAPP compatibilized composite, the MAPE presented a lower result for tensile strength. These findings contradicted with the experiments of Yang et al., who suggested that MAPE was more effective than MAPP in rice husk flour reinforced HDPE and wood flour-HDPE composites (Yang et al., 2007). Again, as discussed earlier, the effectiveness of coupling agents depended on the suitability of matrix used in composites development, where MAPP appeared less effective when PE polymer was used as a matrix in composites and vice versa. In this work, the tensile strength of the MAPP compatibilized composite was found to be more effective than MAPE.

Among the three different treatments, alkali treatment appeared to be less effective in enhancing the tensile strength values. Alkali treatment only increased the tensile strength of 10%, 20%, 30% and 40% PALF-TBP composites of 2.6%, 0.12% and 2.78% and 4.2%, respectively. Moreover, tensile modulus was enhanced by 28.09%, 9.59% and 1.02% and 3.9%, respectively. These findings were consistent with the previous study of PALF reinforced natural rubber, where the enhancement in tensile strength and tensile modulus were only 6% to 10% and 3% to 12% , respectively (Panyasart et al., 2014). Another finding which agreed quite well with the present study was acacia sawdust reinforced with recycled polyethylene terephthalate (PET), where the effect of alkali treatment presented a non-significant improvement in tensile strength result (Ahmad et al., 2008). The primary factor for this phenomenon was the agglomeration of the filler particles which generated stress concentration points in the composite sample. This phenomenon had caused weakness in the mechanical properties of composites.

The present study summarized that MAPP treatment was superior in enhancing the tensile properties of PALF-TBP composites. However, 40% of PALF-TBP composites with MAPP still showed the same pattern with untreated PALF-TBP composites. Even MAPP was capable of enhancing the interfacial adhesion between fiber and matrix, but 40% of PALF-TBP with MAPP still presented a lower tensile strength result as compared to 30% of PALF sample. Therefore, the findings from this study were crucial in determining the role played by optimum fiber loading to produce a high tensile strength. As such, the combination between optimum fiber loading and selected treatments was regarded as the key role in contributing to high tensile strength of PALF-TBP composites. Concerning the elastic modulus, a different phenomenon was observed where tensile modulus increased with the addition of fiber composition of up to 40%. This can be explained due to the fact that the degree of obstruction mainly increased with the increase in fiber composition, which in turn increased the stiffness, as shown by the previous works (Kang et al., 2011; Lomelí-Ramírez et al., 2014b; Prachayawarakorn et al., 2013; Ranganathan et al., 2016).

Figure 4.33 presents the comparison of tensile strength result between 30% PALF-TBP with MAPP and the most common conventional polymers that reused in the automotive sector, which are LDPE, HDPE, PET, PP, HIPS and ABS as mentioned in the literature study (Ahmad et al., 2008; Hashemi, 2011; Panyasart et al., 2014; Rana et al., 1998; Siregar et al., 2010; Threepopnatkul et al., 2009; Yang et al., 2007).

This comparison is useful to evaluate the potential of PALF-TBP composites as an alternative to petroleum-based polymer for future engineering applications, especially for the automotive sector. PALF-TBP with MAPP showed a higher result as compared to LDPE and at par with HDPE. Therefore, the improvement of PALF-TBP composites, such as utilization of PALF with higher tensile strength and improvement in manufacturing process, is expected to produce a higher tensile strength result of composites in the future. These findings provided evidence that the combination of PALF-TBP and selected treatments like MAPP coupling agents has a great potential for the future development of biodegradable and renewable polymer.

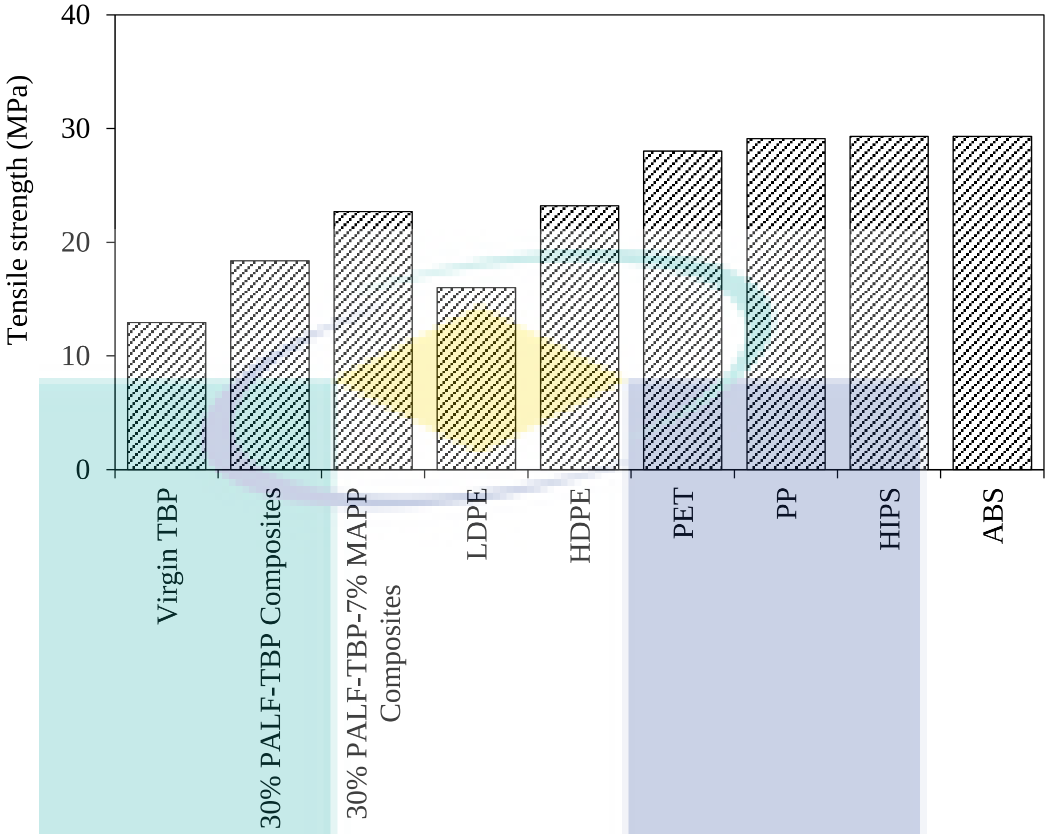

Figure 4.33 Comparison of tensile strength result

4.6.3 Variance Analysis

Visual observation on the tensile properties result of PALF-TBP composites with different treatments showed the sample containing MAPP coupling agent generating maximum tensile strength. As discussed earlier, nonpolar part (PP) of MAPP became compatible with the virgin TBP, and lowered the surface energies of the fibers, thereby increasing its wettability and dispersion within the matrix. Therefore, as verification for the selection of MAPP as the most effective treatment as compared to MAPE and alkali treatment, the analysis of variance (ANOVA) was conducted. Table 4.8 present the *p*-value comparison for tensile strength between the MAPP treatment and other treatments which were untreated, alkali treatment and MAPE coupling agent. The comparison was conducted between samples of 30% fiber comparison because the sample with 30% generated maximum tensile strength result.

Table 4.8 The *p*-value comparison of tensile strength between 30% of PALF-TBP composites and other samples

	Untreated	**Alkali treatment**	**MAPE**
MAPP	0.00000*	0.00000*	0.00135*

* Significant

According to Table 4.8, the analysis of variance verifies that the MAPP coupling agent had a significant effect in producing higher tensile strength result as compared to other treatments. In addition to MAPP effectiveness analysis, Table 4.9 presents the *p*-value comparison between PALF-TBP composite with MAPP utilization sample and untreated sample at different fiber loading. According to the Table 4.9, all *p*-value show the result are 0.00000 which is indicate that the MAPP utilization has a significant capability in enhancement the tensile strength of untreated PALF-TBP composites for all type of fiber loading.

Table 4.9 The *p*-value comparison of tensile strength PALF-TBP-MAPP composites and untreated PAL-TBP samples

	MAPP			
Fiber loading	**10%**	**20%**	**30%**	**40%**
Untreated	0.00000*	0.00000*	0.00000*	0.00000*

* Significant

Moreover, the PALF-TBP composite with MAPP utilization at different loading also compared with virgin TBP in verifying the significance of MAPP utilization. Again, all *p*-value show 0.00000 results which verify that the MAPP utilization has a significant effect on enhance the tensile strength of PALF-TBP composite compared to virgin TBP.

Table 4.10 The *p*-value comparison of tensile strength between PALF-TBP composites with MAPP utilization and virgin TBP samples

	10% PALF-TBP with MAPP	**20% PALF-TBP with MAPP**	**30% PALF-TBP with MAPP**	**40% PALF-TBP with MAPP**
Virgin TBP	0.00000*	0.00000*	0.00000*	0.00000*

* Significant

4.6.4 Fiber Surface and Fracture Morphology

SEM provides an excellent technique for the examination of surface morphology of fibers and fracture surface of fiber composites. The morphology of composites after alkali treatment was examined. Figure 4.34a shows the SEM micrograph of an untreated PALF. Untreated PALF contains impurities, wax and fatty substances. There were significant differences in the fiber morphologies after alkali treatment as compared to the untreated ones. Corresponding with previous findings, utilization of alkali treatment leads to fiber fibrillation, which breaks down the fiber bundles into smaller fibers (Figure 4.34b). Fibrillations lead to an increase in surface area by decreasing the fiber diameter, and consequently enhance the effectiveness of interfacial adhesion between fiber and matrix. This phenomenon is expected due to the dissolution and leaching of fatty acids, hemicellulose and soluble lignin, which cause the fiber surface to become rough. This phenomenon had enhanced the mechanical anchoring between PALF and TBP.

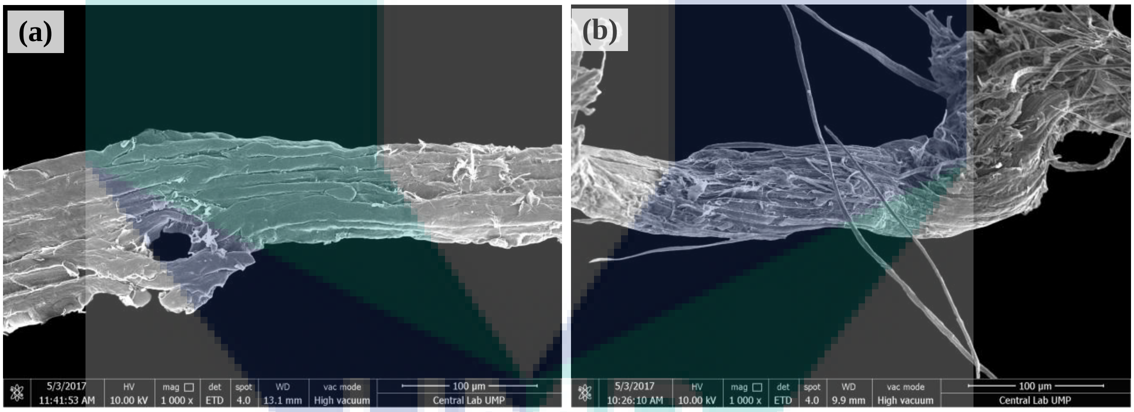

Figure 4.34 Comparison of fiber surface topography between (a) untreated PALF, and (b) treated PALF

SEM analysis was also used as a direct observation on the surface area of failure composites, and particularly to examine the interface between fiber and matrix. The SEM images presented in Figure 4.35 shows the comparison of PALF-TBP interface under 1000 magnification between untreated and different treatments of PALF-TBP samples. Figure 4.35a presents the interfacial bonding between untreated PALF fibers and the TBP matrix were not good, as shown by the gaps between them and the pull-out fibers from the matrix. This phenomenon might be attributed to the low adhesion between the fiber surfaces and TBP resin. Therefore, the tensile strength of this composite was low as compared to the treated sample. The alkali treatment and coupling agent utilization can eliminate impurities and wax from the fiber surface, enhancing the adhesion with the matrix. After the treatment, interfacial bonding between the PALF and TBP was markedly better than in the untreated PALF-TBP composite, and the mechanical properties were improved. Figure 4.35b, Figure 4.35c and Figure 4.35d show that there was no gap between the fiber and matrix, even with observation was made under higher magnification as compared to previous research. The MAPP coupling agent-treated PALF-TBP composite demonstrated a maximum tensile strength due to the interfacial bonding that occurred in the structure. It was due to the fiber crack behavior and fiber breakage into smaller diameter fibrils on the fracture surface, which represented an effective stress transfer between TBP and PALF. Similar behavior was also reported in the study of the chemical treatment effects and coupling agents on roselle fiber-reinforced vinyl ester composites (Nadlene et al., 2016).

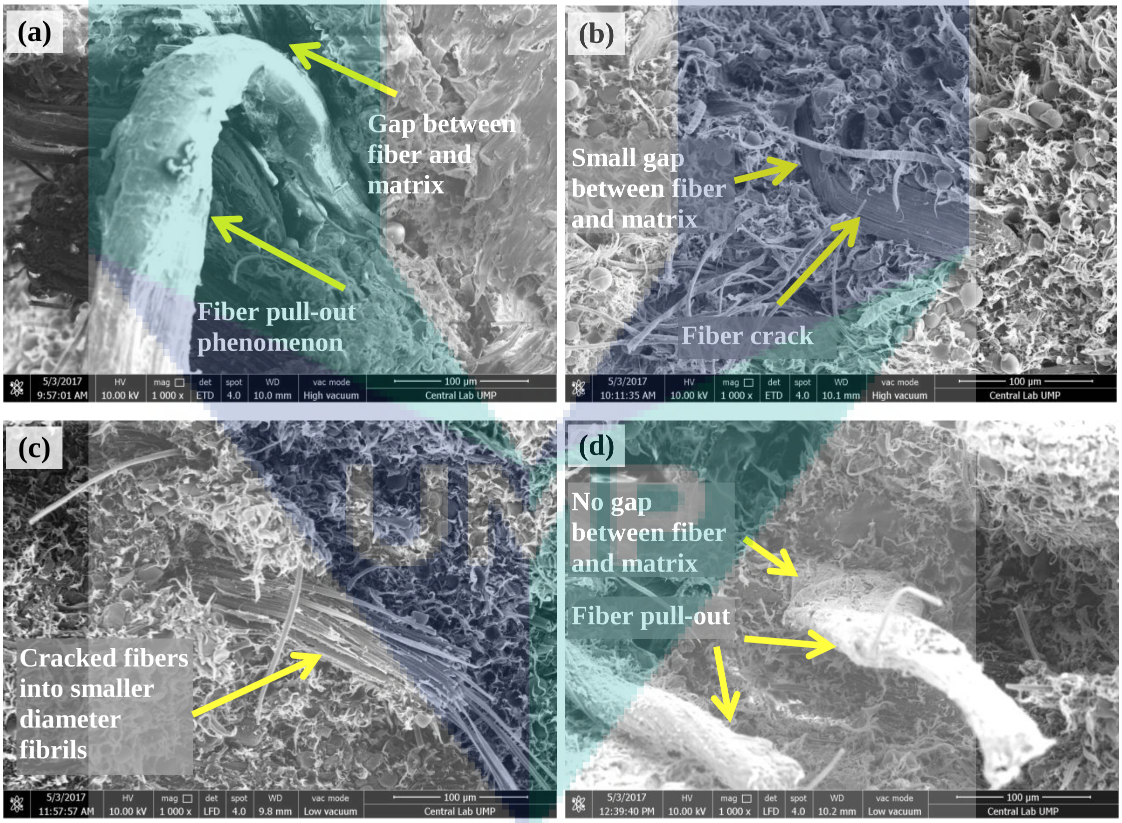

Figure 4.35 Scanning electron micrographs of PALF-TBP composites subjected to different treatments (a) untreated, (b) alkali treatment, (c) 7% MAPP, (d) 3% MAPE

Further analysis on the fracture surface of alkali treatment samples found an exciting finding, which expected a significant factor in causing inconsistent tensile properties for alkali treatment PALF-TBP composites. The side effect produced by fibrillation of short PALF was agglomeration. Figure 4.36a presents the agglomeration area at sample fracture surface and Figure 4.36b focuses on the agglomeration area.

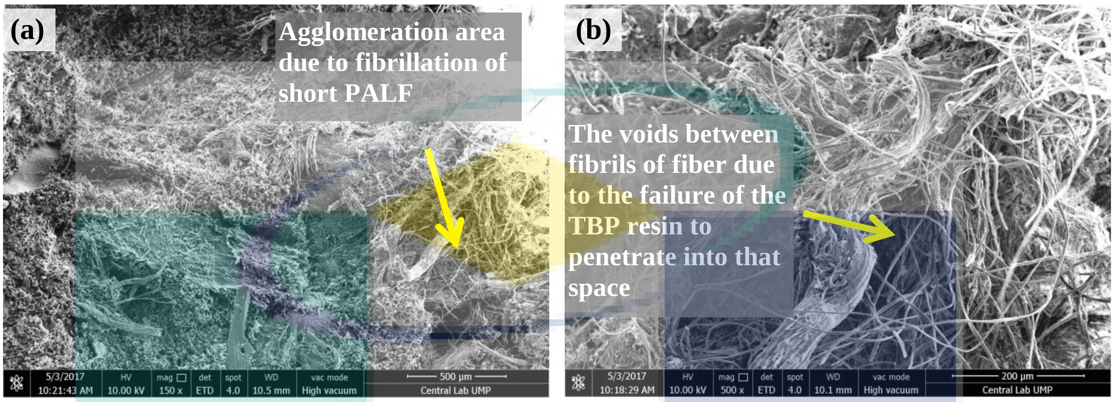

Figure 4.36 Scanning electron micrographs of alkali treatment sample (a) fracture surface, and (b) agglomeration area

The void can be seen clearly between the fibrils of fiber due to the failure of the TBP matrix to penetrate that space. This void was thought to be the primary factor for crack propagation. Moreover, the agglomeration area increased with the increase in fiber percentage. These findings provided an answer to the factor of alkali treatment which appeared less effective in enhancing the tensile strength result. A similar outcome was observed in alkali treatment on acacia sawdust-PET composites and alkali treatment on jute fabrics-polyester amide composites (Mohanty et al., 2000a).

4.6.5 FTIR Analysis

FTIR is essential to observe the functional groups in composite materials. Moreover, the interaction between individual components in the composite materials can be established by recognizing the spectra band position shift or the emergence of new peaks in the FTIR spectra. Figure 4.37 presents the FTIR spectra for untreated PALF-TBP, alkali treatment PALF-TBP, PALF-TBP with MAPP and PALF-TBP with MAPE composites.

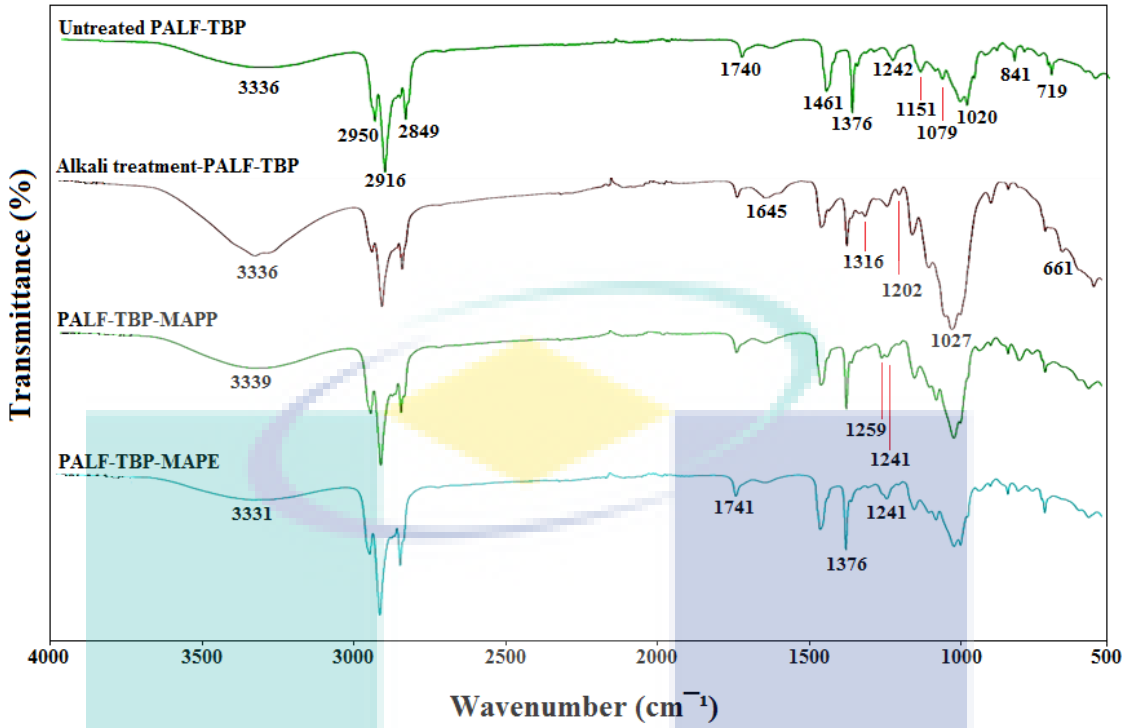

Figure 4.37 Comparison of FTIR results between untreated and treated PALF-TBP composites

The characteristic of the O-H group in the region of 3331 cm^{-1} to 3339 cm^{-1} was visible to all variants. The band was associated with the hydrogen-bonded hydroxyl group (O-H) from the complex vibrational stretching, which was related to free, inter and intra molecular bound hydroxyl groups (Jumaidin et al., 2017a). Moreover, the untreated PALF-TBP showed the presence of band 3336 cm^{-1} for O-H stretching, 2916 cm^{-1} for –CH stretching and 1461cm^{-1} for –CH deformation in lignin. On the other hand, alkali treatment could have reduced the hydrogen bonding by removing the hydroxyl group through the reaction of sodium hydroxide. As a result, the O-H concentration of the treated fiber was demonstrated by the increased intensity of peaks between 1000 cm^{-1} -1600 cm^{-1}.

Other than that, it can be observed from the figure that the bands at 1740 cm^{-1}, which were associated with the symmetric C=O stretching function of maleic anhydride in the MAPP, increased in intensity for PALF-TBP-MAPP. It is worth to note that the MAPP treated PALF-TBP exhibited new peaks at 1259 cm^{-1} and 661 cm^{-1}, which associated with C=O stretching, suggesting the esterification reaction between the hydroxyl and anhydride of MAPP. In all cases, the broad absorption peak between 3331

cm^{-1} to 3339 cm^{-1} was obvious, as commonly observed. Nevertheless, the peak of the hydroxyl group was reduced in the presence of MAPP and MAPE; thereby, suggesting esterification could have taken place. The addition of coupling agents MAPP and MAPE in the PALF-TBP had lowered the hydroxyl group due to the reaction with maleic anhydride. It is well-known that the use of MAPP improves the compatibility of natural fiber, such as PALF and matrix interface. In addition, the maleic anhydride increased the polarity, thus promoting the adhesion in the PALF. This phenomenon could be responsible for the significant increase in tensile strength value, as observed in the PALF-TBP-MAPP variant.

4.7 Summary

The combination of PALF and TBP as renewable and biodegradable material appears to be a perfect balance between the ecology and economic perspectives. The finding indicated that the PALF-TBP composites had tremendous potential as an alternative for the petroleum-based polymer. The development of PALF-TBP composites makes significant contributions as a solution for the current environmental issue and adverse impact produced by non-biodegradable waste from the conventional polymer. The short PALF-TBP composites were suggested to be fabricated through internal mixing-compression molding with 165°C to 170°C processing temperature according to the TBP optimum processing temperature study. The optimum fiber loading in producing maximum mechanical properties was found to be at 30% of PALF content. The enhancements of 30% of PALF-TBP in tensile, flexural and impact strength were 41.96%, 69% and 10%, respectively, as compared to the virgin TBP. However, further increase of fiber composition was a drive to decrease the tensile properties, and the entirely fiber pull-out phenomenon was observed in the microscopy analysis. Also, the different fiber length of up to 2.00 mm did not significantly provide any difference in influencing the tensile properties of composites. Investigation on the effect of the selected treatment on tensile properties found that MAPP coupling agent with 7% concentration was superior in enhancing the tensile properties as compared to alkali treatment and MAPE. The enhancement in tensile strength produced by MAPP utilization was 23.6% as compared to untreated PALF-TBP composites and 75.4% as compared to virgin TBP. The findings presented that PALF-TBP with MAPP showed a higher result as compared to LDPE and at par with HDPE. Moreover, the improvement of PALF-TBP composites in the future, is expected to produce a higher tensile strength result of composites and become competitive with PET, PP, HIPS and ABS in the automotive sector.

CHAPTER 5

CONCLUSION

5.1 Introduction

The present study demonstrated the prospects of PALF and TBP combination as a renewable and biodegradables composite material. The development of PALF-TBP was provided through internal mixing and compression molding with different processing temperatures, fiber lengths, fiber compositions and treatments. The conclusions are described in the following section before ending with recommendations for future work.

5.2 Conclusions

The novel contributions from this study are summarized as follows:

i. The research finding presented that the optimum processing temperature for TBP is between 165°C to 170°C in producing maximum tensile properties result.

ii. The combination of short PALF and TBP with different fiber lengths up to 2.00 mm showed the same capability in enhancing the mechanical properties of TBP biopolymer.

iii. The finding revealed that 30% fiber loading is the optimum fiber percentage for PALF-TBP composites in producing maximum mechanical properties.

iv. Among the three different treatments, PALF-TBP composites with MAPP coupling agent were superior in enhancing the tensile properties of PALF-TBP composites with 50% of enhancement.

Therefore, the best combination for the development of short PALF reinforced TBP composite was produced by a hot press process with a processing temperature of 165°C to 170°C, comprising 30% fiber loading with fiber length up to 2.00 mm and 7% MAPP coupling agent.

5.3 Recommendations for Future Work

Certain investigations with PALF-TBP composites that can be done in the future are listed as follows:

i. The utilization of different species of PALF which have higher mechanical properties may be conducted to determine better enhancement for the performance of PALF-TBP composites.

ii. Since the present study deals with PALF with single extraction method, which is manual scrapping method, experiment by using PALF with a different extraction method can be studied.

iii. The present study only deals with three different treatments, which are alkali treatment, MAPP and MAPE; thus, other modification methods or treatments can be done, such as irradiation beam.

iv. Further investigations can be done on the PALF-TBP composites as a structural part of car structure application and other engineering applications.

REFERENCES

Addivant. (2018). POLYBOND® 3200 polymer modifier. Retrieved from https://www.addivant.com/ accessed on 18/07/2018

Ahmad, F., Choi, H. S., & Park, M. K. (2015). A review: natural fiber composites selection in view of mechanical, light weight, and economic properties. *Macromolecular materials and Engineering, 300*(1), 10-24.

Ahmad, I., Mosadeghzad, Z., Daik, R., & Ramli, A. (2008). The effect of alkali treatment and filler size on the properties of sawdust/UPR composites based on recycled PET wastes. *Journal of Applied Polymer Science, 109*(6), 3651-3658.

Aji, I. S., Zainudin, E. S., Khalina, A., Sapuan, S., & Khairul, M. (2011). Studying the effect of fiber size and fiber loading on the mechanical properties of hybridized kenaf/PALF-reinforced HDPE composite. *Journal of Reinforced Plastics and Composites, 30*(6), 546-553.

Al-Oqla, F. M., Sapuan, S., Ishak, M., & Nuraini, A. (2016). A decision-making model for selecting the most appropriate natural fiber–Polypropylene-based composites for automotive applications. *Journal of Composite Materials, 50*(4), 543-556.

Alam, M. M., Ahmed, T., Haque, M. M., Gafur, M., & Kabir, A. H. (2008). Mechanical properties of natural fiber containing polymer composites. *Polymer-Plastics Technology and Engineering, 48*(1), 110-113.

Ali, B. A., Sapuan, S., Zainudin, E., & Othman, M. (2015). Implementation of the expert decision system for environmental assessment in composite materials selection for automotive components. *Journal of Cleaner Production, 107*, 557-567.

Allen, T. T. (2006). *Introduction to engineering statistics and six sigma: statistical quality control and design of experiments and systems*: Springer Science & Business Media.

Amuthakkannan, P., Manikandan, V., Jappes, J. W., & Uthayakumar, M. (2013). Effect of fibre length and fibre content on mechanical properties of short basalt fibre reinforced polymer matrix composites. *Materials Physics and Mechanics, 16*, 107-117.

Arib, R., Sapuan, S., Ahmad, M., Paridah, M., & Zaman, H. K. (2006). Mechanical properties of pineapple leaf fibre reinforced polypropylene composites. *Materials & Design, 27*(5), 391-396.

Arkema. (2018). Orevac® resins. Retrieved from https://www.arkema.com accessed on 18/07/2018

Asim, M., Jawaid, M., Abdan, K., & Ishak, M. R. (2016). Effect of Alkali and Silane Treatments on Mechanical and Fibre-matrix Bond Strength of Kenaf and Pineapple Leaf Fibres. *Journal of Bionic Engineering, 13*(3), 426-435.

ASTM. (1994). ASTM D5488-94de1 Standard Terminology of Environmental Labeling of Packaging Materials and Packages (Withdrawn 2002). West Conshohocken, PA: ASTM International.

ASTM. (2002). ASTM D790-02 Standard Test Method for Flexural Properties of Unreinforced and Reinforced Plastics and Electrical Insulating Materials. West Conshohocken, PA: ASTM International.

ASTM. (2003a). ASTM C1557-03 Standard Test Method for Tensile Strength and Young's Modulus of Fibers. West Conshohocken, PA: ASTM International.

ASTM. (2003b). ASTM D 638-03 Standard Test Method for Tensile Properties of Plastics. West Conshohocken, PA: ASTM International.

ASTM. (2003c). ASTM D 3418-03 Standard Test Method for Transition Temperatures of Polymers By Differential Scanning Calorimet. West Conshohocken, PA: ASTM International.

ASTM. (2003d). ASTM D 6370-99 (Reapproved 2003) Standard Test Method for Rubber-Compositional Analysis by Thermogravimetry (TGA). West Conshohocken, PA: ASTM International.

ASTM. (2010). ASTM D256-10 Standard Test Method for Determining the Izod Pendulum Impact Resistance of Plastics. West Conshohocken, PA: American Society for Testing and Material.

Avérous, L. (2004). Biodegradable multiphase systems based on plasticized starch: a review. *Journal of Macromolecular Science, Part C: Polymer Reviews, 44*(3), 231-274.

Azwa, Z., Yousif, B., Manalo, A., & Karunasena, W. (2013). A review on the degradability of polymeric composites based on natural fibres. *Materials & Design, 47*, 424-442.

Bachtiar, D., Sapuan, S., & Hamdan, M. (2008). The effect of alkaline treatment on tensile properties of sugar palm fibre reinforced epoxy composites. *Materials & Design, 29*(7), 1285-1290.

Balan, A. K., Parambil, S. M., Vakyath, S., Velayudhan, J. T., Naduparambath, S., & Etathil, P. (2017). Coconut shell powder reinforced thermoplastic polyurethane/natural rubber blend-composites: effect of silane coupling agents on the mechanical and thermal properties of the composites. *Journal of materials science, 52*(11), 6712-6725.

Beg, M., & Pickering, K. (2008). Mechanical performance of Kraft fibre reinforced polypropylene composites: Influence of fibre length, fibre beating and hygrothermal ageing. *Composites Part A: Applied Science and Manufacturing, 39*(11), 1748-1755.

Bijarimi, M., Piah, M., Sahrim, A., & Rozaidi, R. (2012). Mechanical, thermal and morphological properties of PLA/PP melt blends.

Binoj, J., Raj, R. E., Sreenivasan, V., & Thusnavis, G. R. (2016). Morphological, physical, mechanical, chemical and thermal characterization of sustainable Indian areca fruit husk fibers (Areca catechu L.) as potential alternate for hazardous synthetic fibers. *Journal of Bionic Engineering, 13*(1), 156-165.

Bioplastics, E. (2017). Bioplastic materials. Retrieved from https://www.european-bioplastics.org accessed on 10/04/2018

Bledzki, A. K., & Faruk, O. (2004). Wood fiber reinforced polypropylene composites: Compression and injection molding process. *Polymer-Plastics Technology and Engineering, 43*(3), 871-888.

Broutman, L., & McGarry, F. (1965). Fracture surface work measurements on glassy polymers by a cleavage technique. I. Effects of temperature. *Journal of Applied Polymer Science, 9*(2), 589-608.

Callister Jr, W. D., & Rethwisch, D. G. (2012). *Fundamentals of materials science and engineering: an integrated approach*: John Wiley & Sons.

Cao, Y., Shibata, S., & Fukumoto, I. (2006). Mechanical properties of biodegradable composites reinforced with bagasse fibre before and after alkali treatments. *Composites Part A: Applied Science and Manufacturing, 37*(3), 423-429.

Chaudhuri, S., Chakraborty, R., & Bhattacharya, P. (2013). Optimization of biodegradation of natural fiber (Chorchorus capsularis): HDPE composite using response surface methodology. *Iranian Polymer Journal, 22*(11), 865-875.

Cherian, B. M., Leão, A. L., de Souza, S. F., Costa, L. M. M., de Olyveira, G. M., Kottaisamy, M., . . . Thomas, S. (2011). Cellulose nanocomposites with nanofibres isolated from pineapple leaf fibers for medical applications. *Carbohydrate polymers, 86*(4), 1790-1798.

Chew Chong Bew, L. M. S., Ong Beng Sim. (1998). *Statistik*. Kuala Lumpur, Malaysia: Penerbit Fajar Bakti Sdn Bhd.

Chiao, C., Chiao, T., & Lubin, G. (1982). Handbook of Composites. *by G. Lubin, Van Nostrand Reinhold, New York.*

Devi, L. U., Bhagawan, S., & Thomas, S. (1997). Mechanical properties of pineapple leaf fiber-reinforced polyester composites. *Journal of Applied Polymer Science, 64*(9), 1739-1748.

Dhakal, H., Zhang, Z., & Richardson, M. (2007). Effect of water absorption on the mechanical properties of hemp fibre reinforced unsaturated polyester composites. *Composites Science and Technology, 67*(7), 1674-1683.

Du, Y., Wu, T., Yan, N., Kortschot, M. T., & Farnood, R. (2014). Fabrication and characterization of fully biodegradable natural fiber-reinforced poly (lactic acid) composites. *Composites Part B: Engineering, 56*, 717-723.

Duval, A., Bourmaud, A., Augier, L., & Baley, C. (2011). Influence of the sampling area of the stem on the mechanical properties of hemp fibers. *Materials Letters, 65*(4), 797-800.

Edhirej, A., Sapuan, S., Jawaid, M., & Zahari, N. I. (2017a). Cassava/sugar palm fiber reinforced cassava starch hybrid composites: Physical, thermal and structural properties. *International Journal of Biological Macromolecules, 101*, 75-83.

Edhirej, A., Sapuan, S., Jawaid, M., & Zahari, N. I. (2017b). Preparation and characterization of cassava bagasse reinforced thermoplastic cassava starch. *Fibers and Polymers, 18*(1), 162-171.

El-Sabbagh, A. (2014). Effect of coupling agent on natural fibre in natural fibre/polypropylene composites on mechanical and thermal behaviour. *Composites Part B: Engineering, 57*, 126-135.

El-Shekeil, Y., Sapuan, S., Abdan, K., & Zainudin, E. (2012). Influence of fiber content on the mechanical and thermal properties of Kenaf fiber reinforced thermoplastic polyurethane composites. *Materials & Design, 40*, 299-303.

Fairuz, A., Sapuan, S., Zainudin, E., & Jaafar, C. (2015). The effect of gelation and curing temperatures on mechanical properties of pultruded kenaf fibre reinforced vinyl ester composites. *Fibers and Polymers, 16*(12), 2645-2651.

Fuqua, M., & Ulven, C. (2008). Characterization of polypropylene/corn fiber composites with maleic anhydride grafted polypropylene. *Journal of Biobased Materials and Bioenergy, 2*(3), 258-263.

Garlotta, D. (2001). A Literature Review of Poly(Lactic Acis). *Journal of Polymers and the Environmet, 9*(2), 22.

Gassan, J., & Bledzki, A. K. (1997). The influence of fiber-surface treatment on the mechanical properties of jute-polypropylene composites. *Composites Part A: Applied Science and Manufacturing, 28*(12), 1001-1005.

Gay, D., Hoa, S., & Tsai, S. (2007). Ply Properties. *Composite Materials: Design and Applications*.

George, J., Bhagawan, S., & Thomas, S. (1996a). Thermogravimetric and dynamic mechanical thermal analysis of pineapple fibre reinforced polyethylene composites. *Journal of thermal analysis, 47*(4), 1121-1140.

George, J., Janardhan, R., Anand, J., Bhagawan, S., & Thomas, S. (1996b). Melt rheological behaviour of short pineapple fibre reinforced low density polyethylene composites. *Polymer, 37*(24), 5421-5431.

Gilbert, M., & Hybart, F. (1972). Effect of chemical structure on crystallization rates and melting of polymers: Part 1. Aromatic polyesters. *Polymer, 13*(7), 327-332.

Gong, F., Feng, M., Zhao, C., Zhang, S., & Yang, M. (2004). Thermal properties of poly (vinyl chloride)/montmorillonite nanocomposites. *Polymer Degradation and stability, 84*(2), 289-294.

Gruber, P., & O'Brien, M. (2005). Polylactides “Natureworks® PLA”. *Biopolymers Online*.

Hamdan, M., Siregar, J., Bachtiar, D., Rejab, M., Samykano, M., Agung, E., . . . Jaafar, J. (2017). *Effect of alkaline treatment on mechanical properties of woven ramie reinforced thermoset composite.* Paper presented at the IOP Conference Series: Materials Science and Engineering.

Haque, M. M., Hasan, M., Islam, M. S., & Ali, M. E. (2009). Physico-mechanical properties of chemically treated palm and coir fiber reinforced polypropylene composites. *Bioresource Technology, 100*(20), 4903-4906.

Hargitai, H., Rácz, I., & Anandjiwala, R. D. (2008). Development of hemp fiber reinforced polypropylene composites. *Journal of Thermoplastic Composite Materials, 21*(2), 165-174.

Hashemi, W. F. S. a. J. (2011). *Foundation of Materials Science and Engineering* (Fifth SI Edition ed.). Singapore: McGraw-Hill Companies Inc.

Hidayat, P. (2008). Teknologi pemanfaatan serat daun nanas sebagai alternatif bahan baku tekstil. *Jurnal Teknologi Industri, 13*(2), 31-35.

Holbery, J., & Houston, D. (2006). Natural-fiber-reinforced polymer composites in automotive applications. *Jom, 58*(11), 80-86.

Hu, R., & Lim, J.-K. (2007). Fabrication and mechanical properties of completely biodegradable hemp fiber reinforced polylactic acid composites. *Journal of Composite Materials, 41*(13), 1655-1669.

Huda, M. S., Drzal, L. T., Mohanty, A. K., & Misra, M. (2008). Effect of chemical modifications of the pineapple leaf fiber surfaces on the interfacial and mechanical properties of laminated biocomposites. *Composite Interfaces, 15*(2-3), 169-191.

Ibrahim, N. A., Hadithon, K. A., & Abdan, K. (2010). Effect of fiber treatment on mechanical properties of kenaf fiber-ecoflex composites. *Journal of Reinforced Plastics and Composites, 29*(14), 2192-2198.

ICBP. (2017). Technical Data Sheet: ICBP Bio Resin. Retrieved from www.icbp.com.my accessed on 14/12/2017

Jacob, M., Thomas, S., & Varughese, K. T. (2004). Mechanical properties of sisal/oil palm hybrid fiber reinforced natural rubber composites. *Composites Science and Technology, 64*(7), 955-965.

Jamiluddin, J., Siregar, J. P., Sulaiman, A., Jalal, K. A. A., & Tezara, C. (2016). Study on Properties of Tapioca Resin Polymer. *International Journal of Automotive and Mechanical Engineering (IJAME), 13*(1), 3178-3189. doi:http://dx.doi.org/10.15282/ijame.13.1.2016.5.0265

Jawaid, M., & Khalil, H. A. (2011). Cellulosic/synthetic fibre reinforced polymer hybrid composites: A review. *Carbohydrate polymers, 86*(1), 1-18.

John, M. J., & Anandjiwala, R. D. (2008). Recent developments in chemical modification and characterization of natural fiber-reinforced composites. *Polymer composites, 29*(2), 187-207.

John, M. J., & Thomas, S. (2008). Biofibres and biocomposites. *Carbohydrate polymers, 71*(3), 343-364.

Joseph, P., Joseph, K., & Thomas, S. (1999). Effect of processing variables on the mechanical properties of sisal-fiber-reinforced polypropylene composites. *Composites Science and Technology, 59*(11), 1625-1640.

Jumaidin, R., Sapuan, S., Jawaid, M., Ishak, M., & Sahari, J. (2016). Characteristics of thermoplastic sugar palm Starch/Agar blend: Thermal, tensile, and physical properties. *International Journal of Biological Macromolecules, 89,* 575-581.

Jumaidin, R., Sapuan, S. M., Jawaid, M., Ishak, M. R., & Sahari, J. (2017a). Effect of seaweed on mechanical, thermal, and biodegradation properties of thermoplastic sugar palm starch/agar composites. *International Journal of Biological Macromolecules, 99,* 265-273.

Jumaidin, R., Sapuan, S. M., Jawaid, M., Ishak, M. R., & Sahari, J. (2017b). Thermal, mechanical, and physical properties of seaweed/sugar palm fibre reinforced thermoplastic sugar palm Starch/Agar hybrid composites. *International Journal of Biological Macromolecules, 97*, 606-615.

Kalapakdee, A., & Amornsakchai, T. (2014). Mechanical properties of preferentially aligned short pineapple leaf fiber reinforced thermoplastic elastomer: Effects of fiber content and matrix orientation. *Polymer testing, 37*, 36-44.

Kalpakjian, S., & Schmid, S. R. (2014). *Manufacturing engineering and technology*: Pearson Upper Saddle River, NJ, USA.

Kang, O. L., Ramli, N., Said, M., Ahmad, M., Yasir, S. M., & Ariff, A. (2011). Kappaphycus alvarezii waste biomass: A potential biosorbent for chromium ions removal. *Journal of Environmental Sciences, 23*(6), 918-922.

Karmarkar, A., Chauhan, S., Modak, J. M., & Chanda, M. (2007). Mechanical properties of wood–fiber reinforced polypropylene composites: Effect of a novel compatibilizer with isocyanate functional group. *Composites Part A: Applied Science and Manufacturing, 38*(2), 227-233.

Kengkhetkit, N., & Amornsakchai, T. (2012). Utilisation of pineapple leaf waste for plastic reinforcement: 1. A novel extraction method for short pineapple leaf fiber. *Industrial Crops and Products, 40*, 55-61. doi:10.1016/j.indcrop.2012.02.037

Khalid, M., Ali, S., Abdullah, L., Ratnam, C., & Choong, S. T. (2006). Effect of MAPP as coupling agent on the mechanical properties of palm fiber empty fruit bunch and cellulose polypropylene biocomposites. *International Journal of Engineering and Technology, 3*(1), 79-84.

Khalil, H. S. A., Alwani, M. S., & Omar, A. K. M. (2007). Chemical composition, anatomy, lignin distribution, and cell wall structure of Malaysian plant waste fibers. *BioResources, 1*(2), 220-232.

Khondker, O. A., Ishiaku, U. S., Nakai, A., & Hamada, H. (2005). Fabrication mechanical properties of unidirectional jute/PP composites using jute yarns by film stacking method. *Journal of Polymers and the Environment, 13*(2), 115-126.

Kim, H.-S., Kim, S., Kim, H.-J., & Yang, H.-S. (2006). Thermal properties of bio-flour-filled polyolefin composites with different compatibilizing agent type and content. *Thermochimica Acta, 451*(1), 181-188.

Kim, J.-H., Shim, B. S., Kim, H. S., Lee, Y.-J., Min, S.-K., Jang, D., . . . Kim, J. (2015). Review of nanocellulose for sustainable future materials. *International Journal of Precision Engineering and Manufacturing-Green Technology, 2*(2), 197-213.

Ku, H., Wang, H., Pattarachaiyakoop, N., & Trada, M. (2011). A review on the tensile properties of natural fiber reinforced polymer composites. *Composites Part B: Engineering, 42*(4), 856-873.

Lee, B.-H., Kim, H.-J., & Yu, W.-R. (2009). Fabrication of long and discontinuous natural fiber reinforced polypropylene biocomposites and their mechanical properties. *Fibers and Polymers, 10*(1), 83-90.

Lee, M. S., Seo, H. Y., & Kang, C. G. (2016). Comparative study on mechanical properties of CR340/CFRP composites through three point bending test by using theoretical and experimental methods. *International Journal of Precision Engineering and Manufacturing-Green Technology, 3*(4), 359-365.

Lelievre, J. (1974). Starch gelatinization. *Journal of Applied Polymer Science, 18*(1), 293-296.

Levchik, S. V., Weil, E. D., & Lewin, M. (1999). Thermal decomposition of aliphatic nylons. *Polymer International, 48*(7), 532-557.

Li, X., Tabil, L., Panigrahi, S., & Crerar, W. (2006). *The influence of fiber content on properties of injection molded flax fiber-HDPE biocomposites.* Paper presented at the 2006 ASAE Annual Meeting.

Lim, M. H., Wu, H., & Reid, D. S. (2000). The effect of starch gelatinization and solute concentrations on Tg′ of starch model system. *Journal of the Science of Food and Agriculture, 80*(12), 1757-1762.

Liu, H., Xie, F., Yu, L., Chen, L., & Li, L. (2009a). Thermal processing of starch-based polymers. *Progress in polymer science, 34*(12), 1348-1368.

Liu, L., Yu, J., Cheng, L., & Qu, W. (2009b). Mechanical properties of poly (butylene succinate)(PBS) biocomposites reinforced with surface modified jute fibre. *Composites Part A: Applied Science and Manufacturing, 40*(5), 669-674.

Liu, W., Drzal, L. T., Mohanty, A. K., & Misra, M. (2007). Influence of processing methods and fiber length on physical properties of kenaf fiber reinforced soy based biocomposites. *Composites Part B: Engineering, 38*(3), 352-359.

Liu, W., Misra, M., Askeland, P., Drzal, L. T., & Mohanty, A. K. (2005). 'Green'composites from soy based plastic and pineapple leaf fiber: fabrication and properties evaluation. *Polymer, 46*(8), 2710-2721.

Loh, Y., Sujan, D., Rahman, M., & Das, C. (2013). Sugarcane bagasse—The future composite material: A literature review. *Resources, Conservation and Recycling, 75*, 14-22.

Lomelí-Ramírez, M. G., Barrios-Guzmán, A. J., García-Enriquez, S., de Jesús Rivera-Prado, J., & Manríquez-González, R. (2014a). Chemical and mechanical evaluation of bio-composites based on thermoplastic starch and wood particles prepared by thermal compression. *BioResources, 9*(2), 2960-2974.

Lomelí-Ramírez, M. G., Kestur, S. G., Manríquez-González, R., Iwakiri, S., de Muniz, G. B., & Flores-Sahagun, T. S. (2014b). Bio-composites of cassava starch-green coconut fiber: Part II—Structure and properties. *Carbohydrate polymers, 102*, 576-583.

Lopattananon, N., Panawarangkul, K., Sahakaro, K., & Ellis, B. (2006). Performance of pineapple leaf fiber–natural rubber composites: the effect of fiber surface treatments. *Journal of Applied Polymer Science, 102*(2), 1974-1984.

Lu, D., Xiao, C., & Xu, S. (2009). Starch-based completely biodegradable polymer materials. *Express polymer letters, 3*(6), 366-375.

Luyt, A., Molefi, J., & Krump, H. (2006). Thermal, mechanical and electrical properties of copper powder filled low-density and linear low-density polyethylene composites. *Polymer Degradation and stability, 91*(7), 1629-1636.

Ma, X., Yu, J., & Kennedy, J. F. (2005). Studies on the properties of natural fibers-reinforced thermoplastic starch composites. *Carbohydrate polymers, 62*(1), 19-24.

Malkapuram, R., Kumar, V., & Negi, Y. S. (2009). Recent development in natural fiber reinforced polypropylene composites. *Journal of Reinforced Plastics and Composites, 28*(10).

Mallick, P. K. (2007). *Fiber-reinforced composites: materials, manufacturing, and design*: CRC press.

Manaila, E., Stelescu, M. D., & Doroftei, F. (2015). Polymeric composites based on natural rubber and hemp fibers. *Iranian Polymer Journal, 24*(2), 135-148.

Marques, A., Reis, R., & Hunt, J. (2002). The biocompatibility of novel starch-based polymers and composites: in vitro studies. *Biomaterials, 23*(6), 1471-1478.

Martin, O., & Averous, L. (2001). Poly (lactic acid): plasticization and properties of biodegradable multiphase systems. *Polymer, 42*(14), 6209-6219.

Matthies, P., & Seydl, W. F. (1986). History and development of nylon 6 (pp. 39): Springer.

Medina, L., Schledjewski, R., & Schlarb, A. K. (2009). Process related mechanical properties of press molded natural fiber reinforced polymers. *Composites Science and Technology, 69*(9), 1404-1411.

Methacanon, P., Weerawatsophon, U., Sumransin, N., Prahsarn, C., & Bergado, D. (2010). Properties and potential application of the selected natural fibers as limited life geotextiles. *Carbohydrate polymers, 82*(4), 1090-1096.

Mohanty, A., Khan, M., & Hinrichsen, G. (2000a). Influence of chemical surface modification on the properties of biodegradable jute fabrics—polyester amide composites. *Composites Part A: Applied Science and Manufacturing, 31*(2), 143-150.

Mohanty, A., Misra, M., & Drzal, L. (2002). Sustainable Bio-Composites from Renewable Resources: Opportunities and Challenges in the Green Materials World. *Journal of Polymers and the Environment, 10*(1), 19-26. doi:10.1023/a:1021013921916

Mohanty, A., Misra, M., & Hinrichsen, G. (2000b). Biofibres, biodegradable polymers and biocomposites: an overview. *Macromolecular materials and Engineering, 276*(1), 1-24.

Mohanty, S., Nayak, S., Verma, S., & Tripathy, S. (2004). Effect of MAPP as a coupling agent on the performance of jute–PP composites. *Journal of Reinforced Plastics and Composites, 23*(6), 625-637.

Mohanty, S., & Nayak, S. K. (2006). Interfacial, dynamic mechanical, and thermal fiber reinforced behavior of MAPE treated sisal fiber reinforced HDPE composites. *Journal of Applied Polymer Science, 102*(4), 3306-3315.

Mohanty, S., Verma, S. K., & Nayak, S. K. (2006). Dynamic mechanical and thermal properties of MAPE treated jute/HDPE composites. *Composites Science and Technology, 66*(3), 538-547.

Molitoris, H., Moss, S., De Koning, G., & Jendrossek, D. (1996). Scanning electron microscopy of polyhydroxyalkanoate degradation by bacteria. *Applied microbiology and biotechnology, 46*(5), 570-579.

Mutungi, C., Passauer, L., Onyango, C., Jaros, D., & Rohm, H. (2012). Debranched cassava starch crystallinity determination by Raman spectroscopy: Correlation of features in Raman spectra with X-ray diffraction and 13 C CP/MAS NMR spectroscopy. *Carbohydrate polymers, 87*(1), 598-606.

Nadlene, R., Sapuan, S., Jawaid, M., Ishak, M., & Yusriah, L. (2016). The effects of chemical treatment on the structural and thermal, physical, and mechanical and morphological properties of roselle fiber-reinforced vinyl ester composites. *Polymer composites*.

Nanthaya, K., & Taweechai, A. (2014). A new approach to ‘‘Greening’’ plastic composites using pineapple leaf waste for performance and cost effectiveness. *Materials and Design, 55* 292–299.

Ned J. Chou, S. P. K., Ravi Saraf and Ho-Ming Tong. (2010). *Characterization of Polymers* (C. R. B. a. C. A. E. Jr. Ed. Series Edition ed.). New York, USA.: Momentum Press.

Neto, A. R. S., Araujo, M. A., Barboza, R. M., Fonseca, A. S., Tonoli, G. H., Souza, F. V., . . . Marconcini, J. M. (2015). Comparative study of 12 pineapple leaf fiber varieties for use as mechanical reinforcement in polymer composites. *Industrial Crops and Products, 64*, 68-78.

Neto, A. R. S., Araujo, M. A., Souza, F. V., Mattoso, L. H., & Marconcini, J. M. (2013). Characterization and comparative evaluation of thermal, structural, chemical, mechanical and morphological properties of six pineapple leaf fiber varieties for use in composites. *Industrial Crops and Products, 43*, 529-537.

Nopparut, A., & Amornsakchai, T. (2016). Influence of pineapple leaf fiber and it's surface treatment on molecular orientation in, and mechanical properties of, injection molded nylon composites. *Polymer testing, 52*, 141-149.

Otsuki, H., & Funahashi, H. (1959). Synthesis of Polyamide by Ozonolysis of Oleic Acid: ACS Publications.

Paglicawan, M. A., Kim, B. S., Basilia, B. A., Emolaga, C. S., Marasigan, D. D., & Maglalang, P. E. C. (2014). Plasma-treated abaca fabric/unsaturated polyester composite fabricated by vacuum-assisted resin transfer molding. *International Journal of Precision Engineering and Manufacturing-Green Technology, 1*(3), 241-246.

Palumbo, M., Avellaneda, J., & Lacasta, A. (2015). Availability of crop by-products in Spain: New raw materials for natural thermal insulation. *Resources, Conservation and Recycling, 99*, 1-6.

Panyasart, K., Chaiyut, N., Amornsakchai, T., & Santawitee, O. (2014). Effect of surface treatment on the properties of pineapple leaf fibers reinforced polyamide 6 composites. *Energy Procedia, 56*, 406-413.

Park, J.-M., Quang, S. T., Hwang, B.-S., & DeVries, K. L. (2006). Interfacial evaluation of modified Jute and Hemp fibers/polypropylene (PP)-maleic anhydride polypropylene copolymers (PP-MAPP) composites using micromechanical technique and nondestructive acoustic emission. *Composites Science and Technology, 66*(15), 2686-2699.

Paul, A., Joseph, K., & Thomas, S. (1997). Effect of surface treatments on the electrical properties of low-density polyethylene composites reinforced with short sisal fibers. *Composites Science and Technology, 57*(1), 67-79.

Paul, N. (1980). Some methods for the utilisation of waste from fibre crops and fibre wastes from other crops. *Agricultural Wastes, 2*(4), 313-318.

Peng, P., & She, D. (2014). Isolation, structural characterization, and potential applications of hemicelluloses from bamboo: A review. *Carbohydrate polymers, 112*, 701-720.

Pervaiz, M., & Sain, M. M. (2003). Carbon storage potential in natural fiber composites. *Resources, Conservation and Recycling, 39*(4), 325-340.

Pickering, K. L., Efendy, M. A., & Le, T. M. (2016). A review of recent developments in natural fibre composites and their mechanical performance. *Composites Part A: Applied Science and Manufacturing, 83*, 98-112.

Piggott, M. (2002). *Load bearing fibre composites*: Springer Science & Business Media.

Pötschke, P., & Paul, D. (2003). Formation of co-continuous structures in melt-mixed immiscible polymer blends. *Journal of Macromolecular Science, Part C: Polymer Reviews, 43*(1), 87-141.

Prachayawarakorn, J., Chaiwatyothin, S., Mueangta, S., & Hanchana, A. (2013). Effect of jute and kapok fibers on properties of thermoplastic cassava starch composites. *Materials & Design, 47*, 309-315.

Prasad, N., Agarwal, V. K., & Sinha, S. (2016). Banana fiber reinforced low-density polyethylene composites: effect of chemical treatment and compatibilizer addition. *Iranian Polymer Journal, 25*(3), 229-241.

Rahman, M. R., Islam, M. N., Huque, M. M., Hamdan, S., & Ahmed, A. S. (2010). Effect of chemical treatment on rice husk (RH) reinforced polyethylene (PE) composites. *BioResources, 5*(2), 854-869.

Rajesh, M., & Pitchaimani, J. (2017). Mechanical Properties of Natural Fiber Braided Yarn Woven Composite: Comparison with Conventional Yarn Woven Composite. *Journal of Bionic Engineering, 14*(1), 141-150.

Rana, A., Mandal, A., & Bandyopadhyay, S. (2003). Short jute fiber reinforced polypropylene composites: effect of compatibiliser, impact modifier and fiber loading. *Composites Science and Technology, 63*(6), 801-806.

Rana, A., Mandal, A., Mitra, B., Jacobson, R., Rowell, R., & Banerjee, A. (1998). Short jute fiber-reinforced polypropylene composites: effect of compatibilizer. *Journal of Applied Polymer Science, 69*(2), 329-338.

Ranganathan, N., Oksman, K., Nayak, S. K., & Sain, M. (2016). Structure property relation of hybrid biocomposites based on jute, viscose and polypropylene: The effect of the fibre content and the length on the fracture toughness and the fatigue properties. *Composites Part A: Applied Science and Manufacturing, 83*, 169-175.

Rashid, B., Leman, Z., Jawaid, M., Ghazali, M. J., & Ishak, M. R. (2016). The mechanical performance of sugar palm fibres (ijuk) reinforced phenolic composites. *International Journal of Precision Engineering and Manufacturing, 17*(8), 1001-1008.

Rong, M. Z., Zhang, M. Q., Liu, Y., Yang, G. C., & Zeng, H. M. (2001). The effect of fiber treatment on the mechanical properties of unidirectional sisal-reinforced epoxy composites. *Composites Science and Technology, 61*(10), 1437-1447.

Rout, J., Misra, M., Tripathy, S., Nayak, S., & Mohanty, A. (2001). The influence of fibre treatment on the performance of coir-polyester composites. *Composites Science and Technology, 61*(9), 1303-1310.

Sanyang, M., Sapuan, S., Jawaid, M., Ishak, M., & Sahari, J. (2016). Recent developments in sugar palm (Arenga pinnata) based biocomposites and their potential industrial applications: A review. *Renewable and Sustainable Energy Reviews, 54*, 533-549.

Sapuan, S., & Maleque, M. (2005). Design and fabrication of natural woven fabric reinforced epoxy composite for household telephone stand. *Materials & Design, 26*(1), 65-71.

Sapuan, S., Mohamed, A., Siregar, J. P., & Ishak, M. (2011). Pineapple Leaf Fibers and PALF-Reinforced Polymer Composites *Cellulose Fibers: Bio-and Nano-Polymer Composites* (pp. 325-343): Springer.

Sastra, H., Siregar, J., Sapuan, S., & Hamdan, M. (2006). Tensile properties of Arenga pinnata fiber-reinforced epoxy composites. *Polymer-Plastics Technology and Engineering, 45*(1), 149-155.

Seavey, K. C., Khare, N. P., Liu, Y., Williams, T. N., & Chen, C.-C. (2003). A new phase-equilibrium model for simulating industrial nylon-6 production trains. *Industrial & engineering chemistry research, 42*(17), 3900-3913.

Sena Neto, A. R., Araujo, M. A. M., Souza, F. V. D., Mattoso, L. H. C., & Marconcini, J. M. (2013). Characterization and comparative evaluation of thermal, structural, chemical, mechanical and morphological properties of six pineapple leaf fiber varieties for use in composites. *Industrial Crops and Products, 43*, 529-537. doi:10.1016/j.indcrop.2012.08.001

Shah, A. U. M., Sultan, M. T. H., Cardona, F., Jawaid, M., Talib, A. R. A., & Yidris, N. (2017). Thermal Analysis of Bamboo Fibre and Its Composites. *BioResources, 12*(2), 2394-2406.

Shalwan, A., & Yousif, B. (2013). In State of Art: Mechanical and tribological behaviour of polymeric composites based on natural fibres. *Materials and Design, 48*, 14-24.

Shibata, S., Cao, Y., & Fukumoto, I. (2005). Press forming of short natural fiber-reinforced biodegradable resin: Effects of fiber volume and length on flexural properties. *Polymer testing, 24*(8), 1005-1011.

Shih, Y.-F., Chang, W.-C., Liu, W.-C., Lee, C.-C., Kuan, C.-S., & Yu, Y.-H. (2014). Pineapple leaf/recycled disposable chopstick hybrid fiber-reinforced biodegradable composites. *Journal of the Taiwan Institute of Chemical Engineers, 45*(4), 2039-2046.

Siracusa, V., Rocculi, P., Romani, S., & Dalla Rosa, M. (2008). Biodegradable polymers for food packaging: a review. *Trends in Food Science & Technology, 19*(12), 634-643.

Siregar, J. P. (2011). Effect of Selected Treatment on Properties of Pineapple Leaf Fibre Reinforced High Impact Polystyrene Composites. *Thesis, Doctor of Philosophy*(Universiti Putra Malaysia).

Siregar, J. P., Sapuan, S., Rahman, M., & Zaman, H. (2010). The effect of alkali treatment on the mechanical properties of short pineapple leaf fibre (PALF) reinforced high impact polystyrene (HIPS) composites. *J. of Food, Agriculture & Environment, 8*(2), 1103-1108.

Siregar, J. P., Sapuan, S., Rahman, M. Z. A., & Dahlan, K. Z. H. M. (2011). Thermogravimetric Analysis (TGA) and Differential Scanning Calometric (DSC) Analysis of Pineapple Leaf Fibre (PALF) Reinforced High Impact Polystyrene (HIPS) Composites. *Pertanika Jour-nal of Science and Technology, 19*(1), 161-170.

Siti Zanariah Satari, C. Z. L., Farahanim Misni, Norhafizah Moslim, Noryanti Muhammad, Roslinazairimah Zakaria and Siti Roslindar Yaziz. (2015). *Applied Statistic Module*. Malaysia: Universiti Malaysia Pahang.

Smith, W. F., & Hashemi, J. (2011). *Foundations of materials science and engineering*: McGraw-Hill.

Steller, R., & Meissner, W. (1998). Structure and properties of degradable polyolefin-starch blends. *Polymer Degradation and stability, 60*(2-3), 471-480.

Stocchi, A., Lauke, B., Vázquez, A., & Bernal, C. (2007). A novel fiber treatment applied to woven jute fabric/vinylester laminates. *Composites Part A: Applied Science and Manufacturing, 38*(5), 1337-1343.

Štrumberger, N., Gospočić, A., & Bartulić, Č. (2005). Polymeric materials in automobiles. *PROMET-Traffic & Transportation, 17*(3), 149-160.

Su, R., Wang, K., Zhang, Q., Chen, F., & Fu, Q. (2010). Effect of melt temperature on the phase morphology, thermal behavior and mechanical properties of injection-molded PP/LLDPE blends. *Chinese Journal of Polymer Science, 28*(2), 249-255.

Sun, Q., Zhao, X., Wang, D., Dong, J., She, D., & Peng, P. (2018). Preparation and characterization of nanocrystalline cellulose/Eucommia ulmoides gum nanocomposite film. *Carbohydrate polymers, 181*, 825-832.

Szeteiová, K. (2010). Automotive materials plastics in automotive markets today. *Institute of Production Technologies, Machine Technologies and Materials, Faculty of Material Science and Technology in Trnava, Slovak University of Technology Bratislava*.

Takagi, H., & Ichihara, Y. (2004). Effect of fiber length on mechanical properties of" green" composites using a starch-based resin and short bamboo fibers. *JSME International Journal Series A, 47*(4), 551-555.

Tao, Y., Yan, L., & Jie, R. (2009). Preparation and properties of short natural fiber reinforced poly (lactic acid) composites. *Transactions of Nonferrous Metals Society of China, 19*, s651-s655.

TAPPI. (1997). TAPPI T264 cm-97. Preparation of Wood for Chemical Analysis. Atlanta, GA: TAPPI Press.

TAPPI. (1999). TAPPI T203 cm-99, Alpha-, Beta-, and Gamma-Cellulose in Pulp. Atlanta, GA: TAPPI Press.

TAPPI. (2002). TAPPI T222 om-02, Acid-Insoluble Lignin in Wood and Pulp. Atlanta, GA: TAPPI Press.

Threepopnatkul, P., Kaerkitcha, N., & Athipongarporn, N. (2009). Effect of surface treatment on performance of pineapple leaf fiber–polycarbonate composites. *Composites Part B: Engineering, 40*(7), 628-632.

Tian, X., Wang, B., Wang, B., Li, J., & Chen, K. (2017). Structural Characterization of Lignin Isolated from Wheat-Straw during the Alkali Cooking Process. *BioResources, 12*(2), 2407-2420.

Tong, J. Y., Royan, N. R. R., Ng, Y. C., Ab Ghani, M. H., & Ahmad, S. (2014). Study of the mechanical and morphology properties of recycled HDPE composite using rice husk filler. *Advances in Materials Science and Engineering, 2014*.

Tungjitpornkull, S., & Sombatsompop, N. (2009). Processing technique and fiber orientation angle affecting the mechanical properties of E-glass fiber reinforced wood/PVC composites. *journal of materials processing technology, 209*(6), 3079-3088.

Väisänen, T., Das, O., & Tomppo, L. (2017). A review on new bio-based constituents for natural fiber-polymer composites. *Journal of Cleaner Production, 149*, 582-596.

Valadez-Gonzalez, A., Cervantes-Uc, J., Olayo, R., & Herrera-Franco, P. (1999). Effect of fiber surface treatment on the fiber–matrix bond strength of natural fiber reinforced composites. *Composites Part B: Engineering, 30*(3), 309-320.

Valášek, P., D'Amato, R., Müller, M., & Ruggiero, A. (2018). Musa textilis Cellulose Fibres in Biocomposites–An Investigation of Mechanical Properties and Microstructure. *BioResources, 13*(2), 3177-3194.

Valášek, P., Ruggiero, A., & Müller, M. (2017). Experimental description of strength and tribological characteristic of EFB oil palm fibres/epoxy composites with technologically undemanding preparation. *Composites Part B: Engineering, 122*, 79-88.

Vink, E. T., Rabago, K. R., Glassner, D. A., & Gruber, P. R. (2003). Applications of life cycle assessment to NatureWorks™ polylactide (PLA) production. *Polymer Degradation and stability, 80*(3), 403-419.

Wahrmund, D., Paul, D., & Barlow, J. (1978). Polyester–polycarbonate blends. I. Poly (butylene terephthalate). *Journal of Applied Polymer Science, 22*(8), 2155-2164.

Westman, M., Laddha, S., Fifield, L., Kalentzis, T., & Simmons, K. (2010). Natural Fiber Composites: A Review. *U.S. Department of Energy under Contract DE-AC05-76LD01830, PNNL-19220*.

Wise, L. E., Murphy, M., & D'Addieco, A. A. (1946). Paper Trade J., 122, No. 2, 35 (1946). *Tech. Assoc. Papers, 29*, 210.

Xia, X., Shi, X., Liu, W., Zhao, H., Li, H., & Zhang, Y. (2017). Effect of flax fiber content on polylactic acid (PLA) crystallization in PLA/flax fiber composites. *Iranian Polymer Journal, 26*(9), 693-702.

Xu, Y., & Wu, P. (2007). A study of water dehydration in nylon 6 as a function of temperature using two-dimensional (2D) correlation near-infrared (NIR) analysis. *Journal of molecular structure, 833*(1), 145-149.

Yang, H.-S., Wolcott, M. P., Kim, H.-S., Kim, S., & Kim, H.-J. (2007). Effect of different compatibilizing agents on the mechanical properties of lignocellulosic material filled polyethylene bio-composites. *Composite Structures, 79*(3), 369-375.

Yang, K., & El-Haik, B. S. (2003). *Design for six sigma*: McGraw-Hill New York.

Yousif, B., Shalwan, A., Chin, C., & Ming, K. (2012). Flexural properties of treated and untreated kenaf/epoxy composites. *Materials & Design, 40*, 378-385.

Yu, T., Ren, J., Li, S., Yuan, H., & Li, Y. (2010). Effect of fiber surface-treatments on the properties of poly (lactic acid)/ramie composites. *Composites Part A: Applied Science and Manufacturing, 41*(4), 499-505.

Yun, I. S., Hwang, S. W., Shim, J. K., & Seo, K. H. (2016). A study on the thermal and mechanical properties of poly (butylene succinate)/thermoplastic starch binary blends. *International Journal of Precision Engineering and Manufacturing-Green Technology, 3*(3), 289-296.

Zampaloni, M., Pourboghrat, F., Yankovich, S., Rodgers, B., Moore, J., Drzal, L., . . . Misra, M. (2007). Kenaf natural fiber reinforced polypropylene composites: a discussion on manufacturing problems and solutions. *Composites Part A: Applied Science and Manufacturing, 38*(6), 1569-1580.

Zhong, J., Li, H., Yu, J., & Tan, T. (2011). Effects of natural fiber surface modification on mechanical properties of poly (lactic acid)(PLA)/sweet sorghum fiber composites. *Polymer-Plastics Technology and Engineering, 50*(15), 1583-1589.

APPENDIX A1
TENSILE TEST OF VIRGIN TBP (160°C)

For tensile properties analysis of different processing temperature of TBP.

13/1/2016 10:39:52 AM

FACULTY OF MECHANICAL ENGINEERING
UNIVERSITI MALAYSIA PAHANG

TAPIOCA BIOPOLYMER TENSILE TEST RESULT

Tensile Test Based on ASTM D638-03
Crosshead Speed 1mm/min
Temperature : 24.9°C
Humidity : 55%

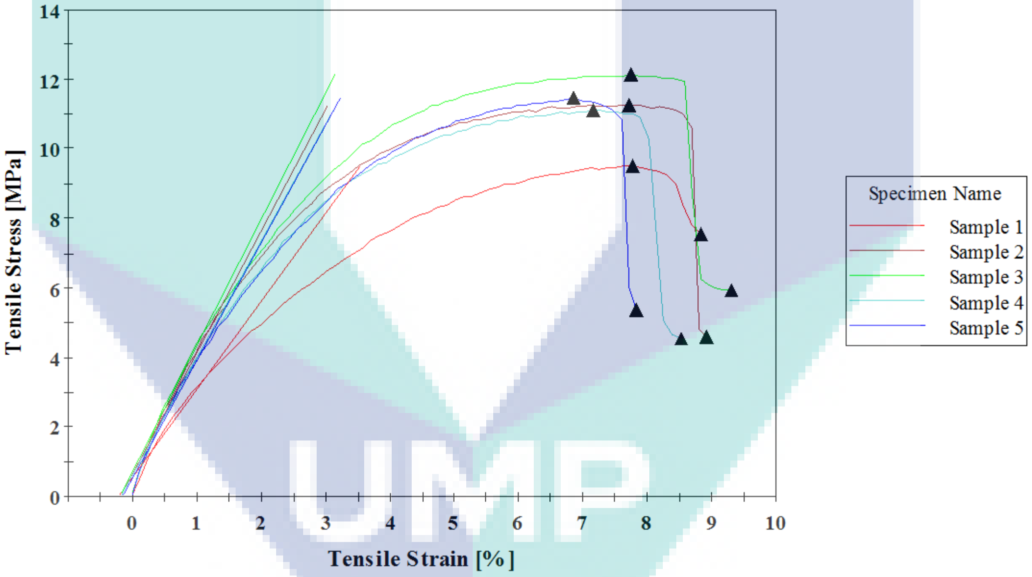

Specimen label	Length [mm]	Thickness [mm]	Width [mm]	Modulus [GPa]	Tensile strength [MPa]	Maximum strain [%]	Time at break [min]
Sample 1	9.75	3.08	3.56	0.25	9.52	8.82	1.1
Sample 2	9.82	3.08	3.58	0.35	11.25	8.93	1.2
Sample 3	9.88	3.06	3.59	0.36	11.95	9.30	1.3
Sample 4	9.72	3.06	3.57	0.34	11.11	8.51	1.2
Sample 5	9.82	3.09	3.58	0.34	11.45	7.83	1.1
Mean	**9.80**	**3.07**	**3.58**	**0.33**	**11.06**	**8.68**	**1.2**
Std dev	**0.06**	**0.01**	**0.01**	**0.04**	**0.92**	**0.55**	**0.09**

Page 1 of 1

APPENDIX A2
TENSILE TEST OF VIRGIN TBP (165°C)

For tensile properties analysis of different processing temperature of TBP.

13/1/2016 11:02:51 AM

FACULTY OF MECHANICAL ENGINEERING
UNIVERSITI MALAYSIA PAHANG

TAPIOCA BIOPOLYMER TENSILE TEST RESULT

Tensile Test Based on ASTM D638-03
Crosshead Speed 1mm/min
Temperature : 24.9°C
Humidity : 55%

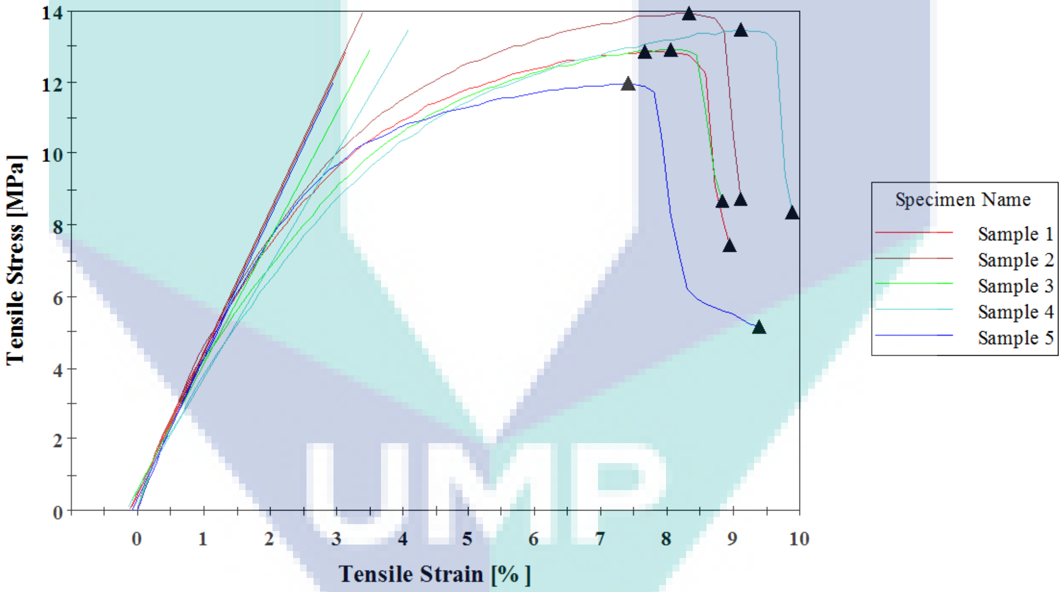

Specimen label	Length [mm]	Thickness [mm]	Width [mm]	Modulus [GPa]	Tensile strength [MPa]	Maximum strain [%]	Time at break [min]
Sample 1	9.60	3.08	3.68	0.39	12.86	8.95	1.1
Sample 2	9.62	3.09	3.56	0.39	13.94	9.11	1.2
Sample 3	9.64	3.08	3.66	0.35	12.91	8.83	1.1
Sample 4	9.62	3.07	3.68	0.32	13.47	9.88	1.2
Sample 5	9.66	3.07	3.53	0.39	11.55	9.38	1.2
Mean	**9.63**	**3.08**	**3.62**	**0.37**	**12.94**	**9.23**	**1.2**
Std dev	**0.02**	**0.01**	**0.07**	**0.03**	**0.90**	**0.42**	**0.05**

APPENDIX A3
TENSILE TEST OF VIRGIN TBP (170°C)

For tensile properties analysis of different processing temperature of TBP.

13/1/2016 11:26:27 AM

FACULTY OF MECHANICAL ENGINEERING
UNIVERSITI MALAYSIA PAHANG

TAPIOCA BIOPOLYMER TENSILE TEST RESULT

Tensile Test Based on ASTM D638-03
Crosshead Speed 1mm/min
Temperature : 24.9°C
Humidity : 55%

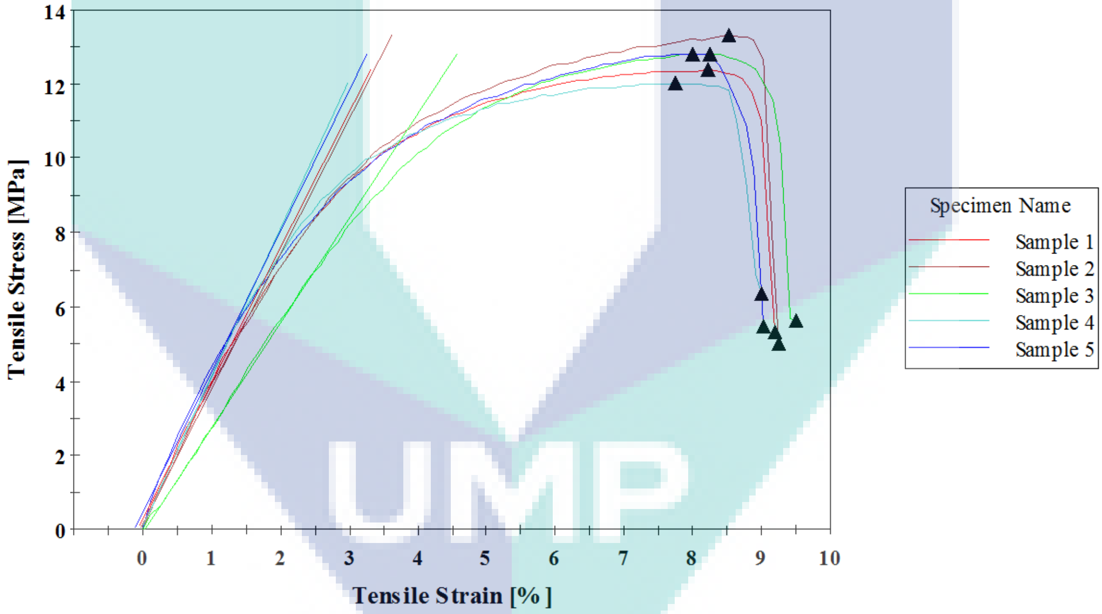

Specimen label	Length [mm]	Thickness [mm]	Width [mm]	Modulus [GPa]	Tensile strength [MPa]	Maximum strain [%]	Time at break [min]
Sample 1	9.98	3.05	3.68	0.36	12.38	9.20	1.2
Sample 2	9.92	3.06	3.68	0.36	13.32	9.25	1.2
Sample 3	9.92	3.05	3.68	0.28	12.82	9.50	1.2
Sample 4	9.92	3.05	3.67	0.40	12.01	9.01	1.2
Sample 5	9.92	3.08	3.67	0.38	12.82	9.03	1.2
Mean	**9.92**	**3.06**	**3.68**	**0.36**	**12.67**	**9.20**	**1.2**
Std dev	**0.03**	**0.01**	**0.01**	**0.04**	**0.49**	**0.20**	**0.03**

Page 1 of 1

APPENDIX A4
TENSILE TEST OF VRIGIN TBP (175°C)

For tensile properties analysis of different processing temperature of TBP.

13/1/2016 11:46:47 AM

FACULTY OF MECHANICAL ENGINEERING
UNIVERSITI MALAYSIA PAHANG

TAPIOCA BIOPOLYMER TENSILE TEST RESULT

Tensile Test Based on ASTM D638-03
Crosshead Speed 1mm/min
Temperature : 24.9°C
Humidity : 55%

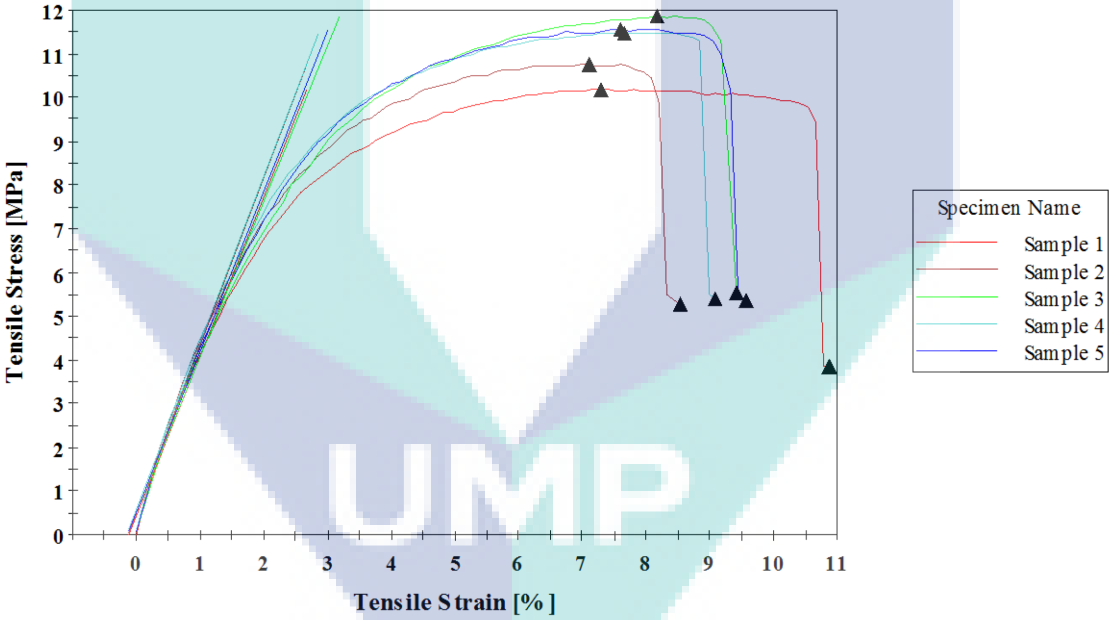

Specimen label	Length [mm]	Thickness [mm]	Width [mm]	Modulus [GPa]	Tensile strength [MPa]	Maximum strain [%]	Time at break [min]
Sample 1	9.62	3.09	3.68	0.36	10.16	10.87	1.4
Sample 2	9.60	3.08	3.68	0.38	10.74	8.53	1.2
Sample 3	9.61	3.09	3.67	0.36	11.86	9.43	1.1
Sample 4	9.62	3.09	3.65	0.38	11.49	9.08	1.1
Sample 5	9.62	3.05	3.65	0.37	11.58	9.57	1.1
Mean	**9.61**	**3.08**	**3.67**	**0.37**	**11.17**	**9.50**	**1.2**
Std dev	**0.01**	**0.02**	**0.02**	**0.01**	**0.70**	**0.87**	**0.12**

APPENDIX A5
TENSILE TEST OF VIRGIN TBP (180°C)

For tensile properties analysis of different processing temperature of TBP.

13/1/2016 12:06:44 PM

FACULTY OF MECHANICAL ENGINEERING
UNIVERSITI MALAYSIA PAHANG

TAPIOCA BIOPOLYMER TENSILE TEST RESULT

Tensile Test Based on ASTM D638-03
Crosshead Speed 1mm/min
Temperature : 24.9°C
Humidity : 55%

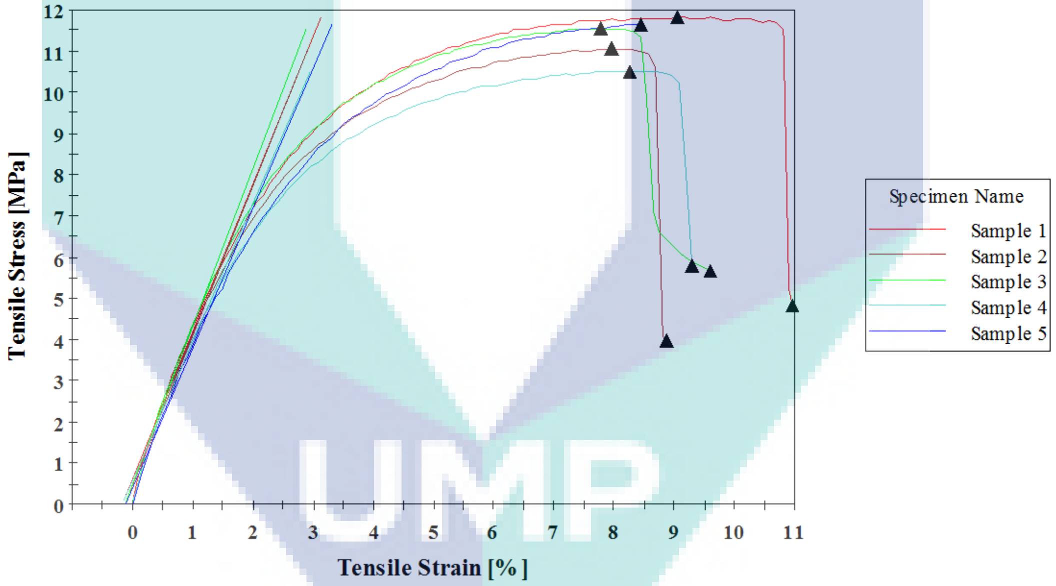

Specimen label	Length [mm]	Thickness [mm]	Width [mm]	Modulus [GPa]	Tensile strength [MPa]	Maximum strain [%]	Time at break [min]
Sample 1	9.28	3.10	3.68	0.36	11.75	10.97	1.7
Sample 2	9.62	3.09	3.67	0.36	11.06	8.89	1.2
Sample 3	9.22	3.10	3.67	0.38	11.33	9.61	1.5
Sample 4	9.24	3.09	3.68	0.34	10.51	9.29	1.3
Sample 5	9.62	3.08	3.67	0.34	11.67	8.43	1.2
Mean	**9.40**	**3.10**	**3.67**	**0.35**	**11.26**	**9.44**	**1.4**
Std dev	**0.21**	**0.01**	**0.01**	**0.02**	**0.50**	**0.96**	**0.19**

Page 1 of 1

APPENDIX A6
TENSILE TEST OF VIRGIN TBP (185°C)

For tensile properties analysis of different processing temperature of TBP.

.

13/1/2016 12:26:14 PM

FACULTY OF MECHANICAL ENGINEERING
UNIVERSITI MALAYSIA PAHANG

TAPIOCA BIOPOLYMER TENSILE TEST RESULT

Tensile Test Based on ASTM D638-03
Crosshead Speed 1mm/min
Temperature : 24.9°C
Humidity : 55%

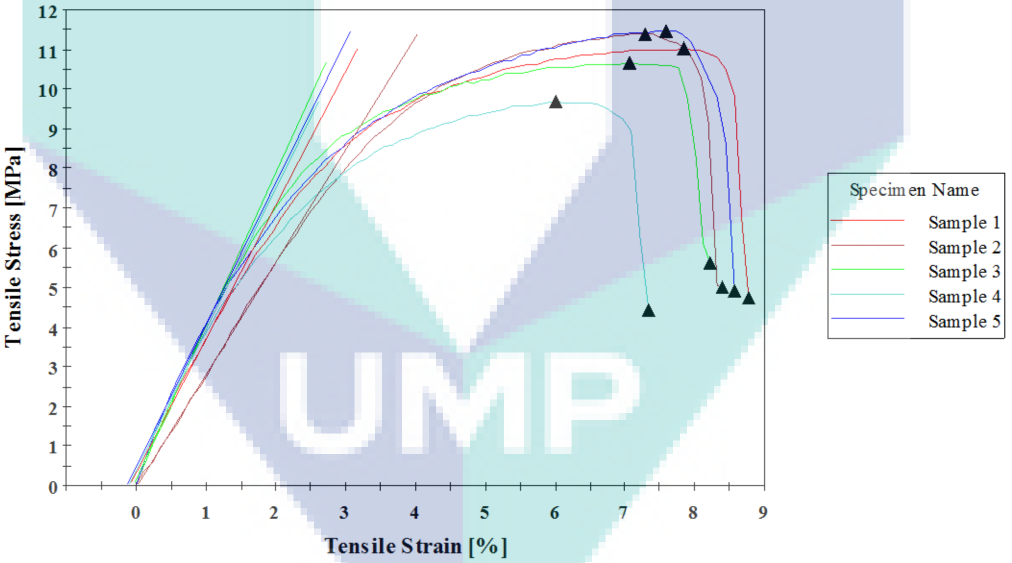

Specimen label	Length [mm]	Thickness [mm]	Width [mm]	Modulus [GPa]	Tensile strength [MPa]	Maximum strain [%]	Time at break [min]
Sample 1	9.65	3.59	3.08	0.34	11.02	8.76	1.2
Sample 2	9.65	3.60	3.08	0.28	11.38	8.40	1.2
Sample 3	9.65	3.61	3.07	0.39	10.66	8.22	1.2
Sample 4	9.63	3.59	3.07	0.35	9.68	7.34	1.0
Sample 5	9.64	3.60	3.08	0.36	11.48	8.56	1.2
Mean	**9.64**	**3.60**	**3.08**	**0.34**	**10.84**	**8.26**	**1.2**
Std dev	**0.01**	**0.01**	**0.01**	**0.04**	**0.73**	**0.55**	**0.09**

Page 1 of 1

APPENDIX B1
TENSILE TEST OF LESS THAN 0.50 MM FIBER LENGTH

For tensile properties analysis of different fiber length of PALF.

14/4/2016 12:26:14 PM

FACULTY OF MECHANICAL ENGINEERING
UNIVERSITI MALAYSIA PAHANG

10% PALF REINFORCED TBP TENSILE TEST

Tensile Test Based on ASTM D638-03
Crosshead Speed 1mm/min
Temperature : 24.9°C
Humidity : 55%

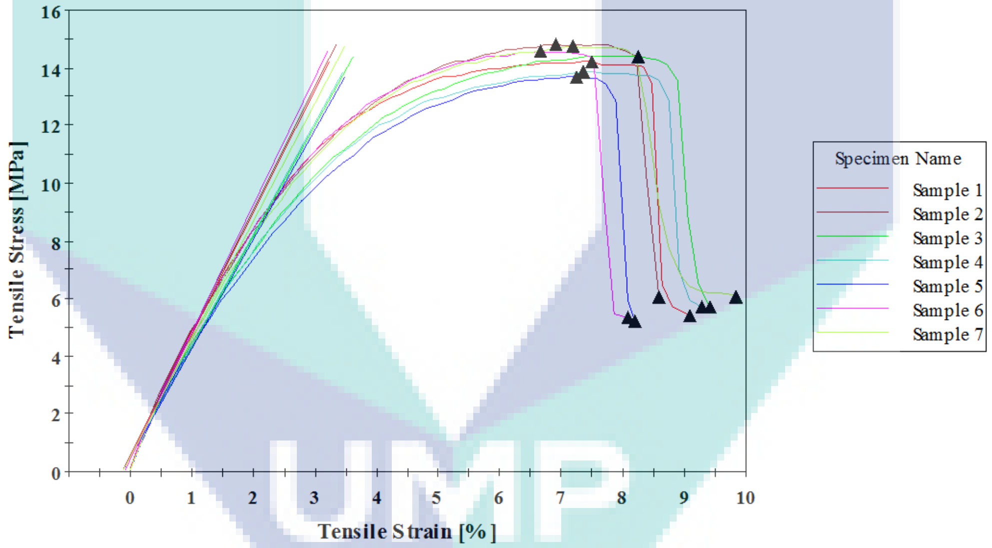

Specimen label	**Length [mm]**	**Thickness [mm]**	**Width [mm]**	**Modulus [GPa]**	**Tensile strength [MPa]**	**Maximum strain [%]**	**Time at break [min]**
Sample 1	9.61	3.08	3.57	0.42	14.22	9.09	0.8
Sample 2	9.63	3.09	3.58	0.42	14.82	8.58	1.1
Sample 3	9.63	3.10	3.58	0.38	14.42	9.41	0.8
Sample 4	9.62	3.09	3.58	0.39	13.84	9.26	0.8
Sample 5	9.61	3.08	3.57	0.38	13.67	8.20	0.8
Sample 6	9.61	3.10	3.58	0.44	14.58	8.07	0.8
Sample 7	9.62	3.09	3.57	0.41	14.73	9.82	0.7
Mean	**7.62**	**3.09**	**3.58**	**0.41**	**14.33**	**8.92**	**0.8**
Std dev	**0.01**	**0.01**	**0.01**	**0.02**	**0.44**	**0.65**	**0.11**

Page 1 of 1

APPENDIX B2
TENSILE TEST OF 0.51 TO 1.00 MM FIBER LENGTH

For tensile properties analysis of different fiber length of PALF.

14/4/2016 4:48:13 PM

FACULTY OF MECHANICAL ENGINEERING
UNIVERSITI MALAYSIA PAHANG

10% PALF REINFORCED TBP TENSILE TEST

Tensile Test Based on ASTM D638-03
Crosshead Speed 1mm/min
Temperature : 24.9°C
Humidity : 55%

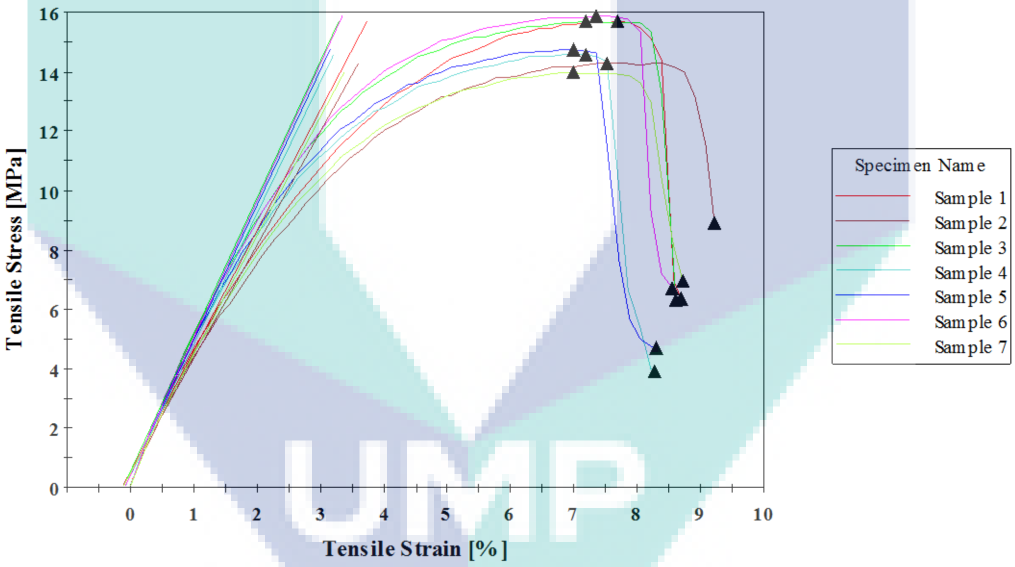

Specimen label	Length [mm]	Thickness [mm]	Width [mm]	Modulus [GPa]	Tensile strength [MPa]	Maximum strain [%]	Time at break [min]
Sample 1	9.86	3.10	3.58	0.41	15.70	8.69	1.2
Sample 2	9.87	3.09	3.57	0.38	14.28	9.22	1.0
Sample 3	9.86	3.08	3.58	0.46	15.69	8.62	1.1
Sample 4	9.86	3.09	3.57	0.44	14.59	8.28	1.0
Sample 5	9.87	3.08	3.57	0.46	14.77	8.29	1.4
Sample 6	9.95	3.09	3.58	0.46	15.89	8.55	1.0
Sample 7	9.97	3.10	3.56	0.40	13.96	8.73	0.9
Mean	**9.89**	**3.09**	**3.57**	**0.43**	**14.98**	**8.63**	**1.1**
Std dev	**0.05**	**0.01**	**0.01**	**0.03**	**0.77**	**0.32**	**0.16**

Page 1 of 1

APPENDIX B3
TENSILE TEST OF 1.01 TO 2.00 MM FIBER LENGTH

For tensile properties analysis of different fiber length of PALF and different fiber composition (10%).

14/4/2016 5:18:03 PM

FACULTY OF MECHANICAL ENGINEERING
UNIVERSITI MALAYSIA PAHANG

10% PALF REINFORCED TBP TENSILE TEST

Tensile Test Based on ASTM D638-03
Crosshead Speed 1mm/min
Temperature : 24.9°C
Humidity : 55%

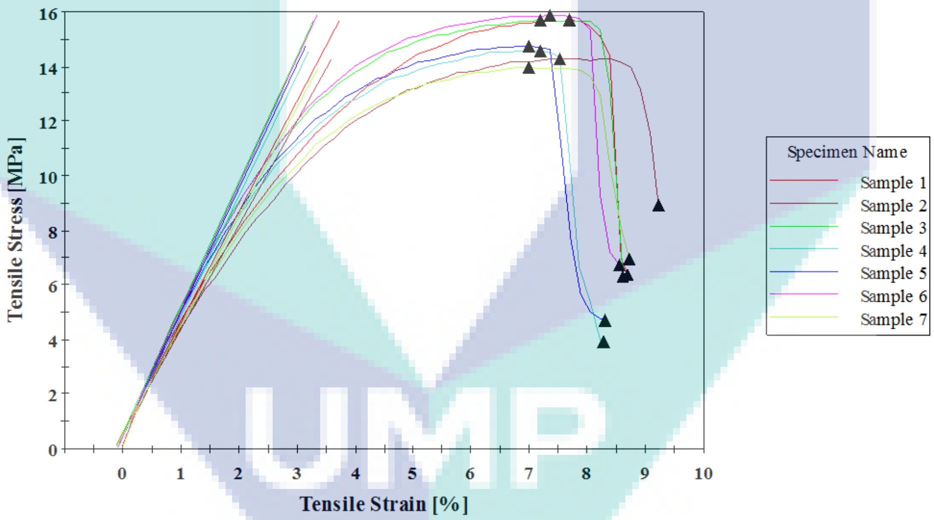

Specimen label	Length [mm]	Thickness [mm]	Width [mm]	Modulus [GPa]	Tensile strength [MPa]	Maximum strain [%]	Time at break [min]
Sample 1	9.88	3.10	3.58	0.43	15.01	9.00	1.2
Sample 2	9.87	3.09	3.57	0.42	13.99	9.51	1.0
Sample 3	9.87	3.09	3.56	0.40	14.89	9.01	1.1
Sample 4	9.89	3.09	3.58	0.43	13.76	8.51	1.0
Sample 5	9.88	3.10	3.57	0.41	14.61	8.52	1.4
Sample 6	9.87	3.11	3.57	0.41	14.47	8.99	1.0
Sample 7	9.87	3.10	3.58	0.42	13.73	9.03	0.9
Mean	**9.88**	**3.10**	**3.57**	**0.42**	**14.35**	**8.94**	**1.1**
Std dev	**0.01**	**0.01**	**0.01**	**0.01**	**0.53**	**0.34**	**0.16**

Page 1 of 1

APPENDIX C1
TENSILE TEST OF 20% FIBER COMPOSITION

For tensile properties analysis of different fiber composition.

10/30/2016 3:47:46 PM

FACULTY OF MECHANICAL ENGINEERING
UNIVERSITI MALAYSIA PAHANG

TENSILE TEST RESULT OF 20% FIBER COMPOSITION

Tensile Test Based on ASTM D638-03
Crosshead Speed 1mm/min
Temperature : 24.9°C
Humidity : 55%

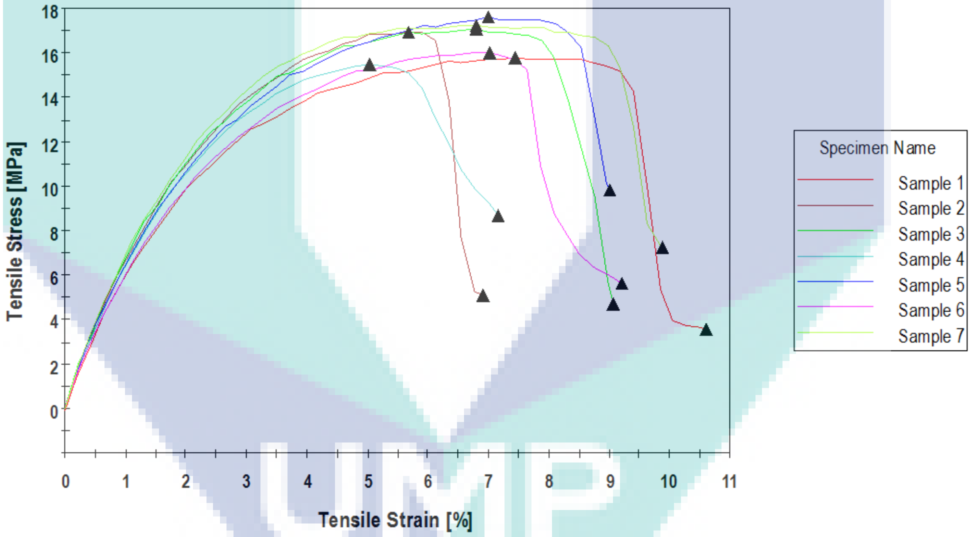

Specimen label	Length [mm]	Thickness [mm]	Width [mm]	Modulus [GPa]	Tensile strength [MPa]	Maximum strain [%]	Time at break [min]
Sample 1	9.80	3.09	3.52	0.70	15.81	10.60	0.8
Sample 2	9.81	3.11	3.52	0.74	16.96	6.90	0.5
Sample 3	9.81	3.10	3.51	0.75	17.10	9.06	0.7
Sample 4	9.83	3.09	3.51	0.73	15.49	7.18	0.5
Sample 5	9.81	3.09	3.53	0.75	17.60	9.00	0.7
Sample 6	9.80	3.08	3.53	0.66	16.01	9.20	0.7
Sample 7	9.80	3.08	3.50	0.76	17.25	9.88	0.8
Mean	**9.81**	**3.09**	**3.52**	**0.73**	**16.60**	**8.83**	**0.7**
Std dev	**0.01**	**0.01**	**0.01**	**0.03**	**0.82**	**1.35**	**0.10**

Page 1 of 1

APPENDIX C2
TENSILE TEST OF 30% FIBER COMPOSITION

For tensile analysis of different fiber composition.

FACULTY OF MECHANICAL ENGINEERING
UNIVERSITI MALAYSIA PAHANG

TENSILE TEST RESULT OF 30% FIBER COMPOSITION

Tensile Test Based on ASTM D638-03
Crosshead Speed 1mm/min
Temperature : 24.9°C
Humidity : 55%

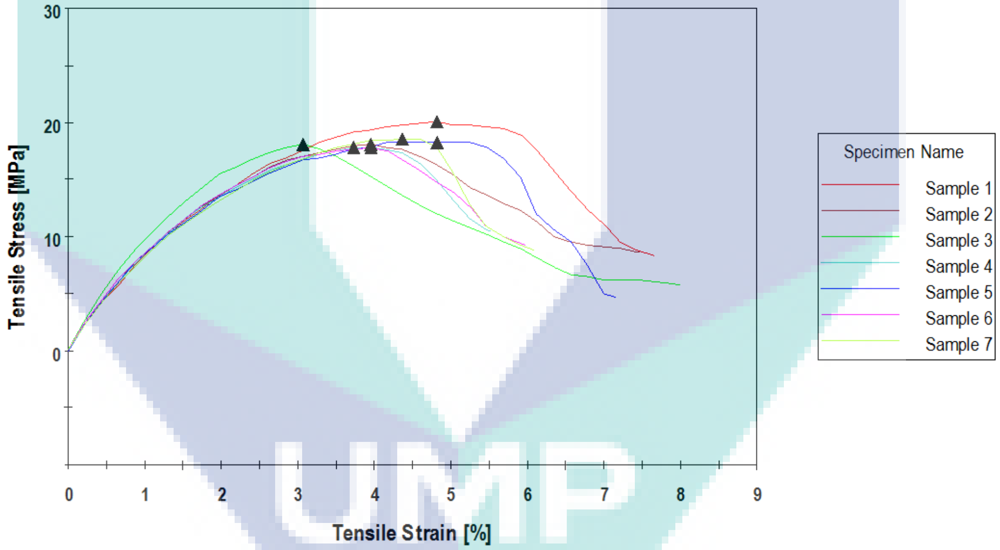

Specimen label	Length [mm]	Thickness [mm]	Width [mm]	Modulus [GPa]	Tensile Strength [MPa]	Maximum Strain [%]	Time at Break [min]
Sample 1	9.84	3.11	3.55	0.92	20.05	7.65	0.6
Sample 2	9.83	3.12	3.53	0.97	18.12	7.47	0.6
Sample 3	9.83	3.15	3.54	1.11	18.03	8.00	0.6
Sample 4	9.83	3.1	3.55	1.00	17.80	5.53	0.4
Sample 5	9.85	3.15	3.54	0.98	18.27	7.15	0.5
Sample 6	9.85	3.15	3.53	0.98	17.80	5.98	0.5
Sample 7	9.84	3.12	3.53	0.92	18.52	6.08	0.5
Mean	**9.84**	**3.13**	**3.54**	**0.98**	**18.37**	**6.84**	**0.5**
Std dev	**0.01**	**0.02**	**0.01**	**0.07**	**0.78**	**0.96**	**0.07**

APPENDIX C3
TENSILE TEST OF 40% FIBER COMPOSITION

For tensile analysis of different fiber composition.

10/30/2016 6:32:47 PM

Universiti Malaysia PAHANG
Engineering • Technology • Creativity

FACULTY OF MECHANICAL ENGINEERING
UNIVERSITI MALAYSIA PAHANG

TENSILE TEST RESULT OF 40% FIBER COMPOSITION

Tensile Test Based on ASTM D638-03
Crosshead Speed 1mm/min
Temperature : 24.9°C
Humidity : 55%

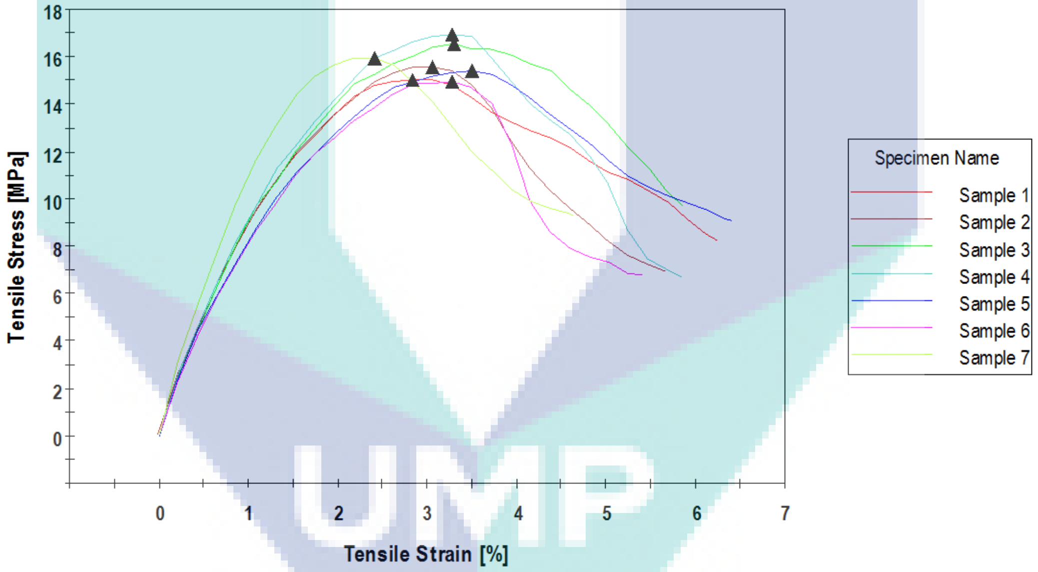

Specimen label	Length [mm]	Thickness [mm]	Width [mm]	Modulus [GPa]	Tensile strength [MPa]	Maximum strain [%]	Time at break [min]
Sample 1	9.80	3.01	3.58	1.05	15.05	6.25	0.5
Sample 2	9.81	3.02	3.59	1.00	15.56	5.67	0.4
Sample 3	9.78	3.02	3.59	1.00	16.58	5.87	0.4
Sample 4	9.78	3.01	3.59	1.01	16.96	5.85	0.4
Sample 5	9.78	3.01	3.58	0.98	15.37	6.41	0.5
Sample 6	9.80	3.03	3.57	0.92	14.98	5.40	0.4
Sample 7	9.79	3.02	3.58	1.23	15.97	4.63	0.4
Mean	**9.79**	**3.02**	**3.58**	**1.03**	**15.78**	**5.73**	**0.4**
Std dev	**0.01**	**0.01**	**0.01**	**0.10**	**0.76**	**0.59**	**0.04**

Page 1 of 1

APPENDIX D1
FLEXURAL TEST OF VIRGIN TBP

For flexural properties analysis of different fiber composition.

3/15/2017 1:27:06 PM

FACULTY OF MECHANICAL ENGINEERING
UNIVERSITI MALAYSIA PAHANG

FLEXURAL TEST OF VIRGIN TAPIOCA BIOPOLYMER

Flexural Test Based on ASTM D790-03
Crosshead Speed 1.28 mm/min
Support Span 48.0 mm
Temperature : 24.9°C
Humidity : 55%

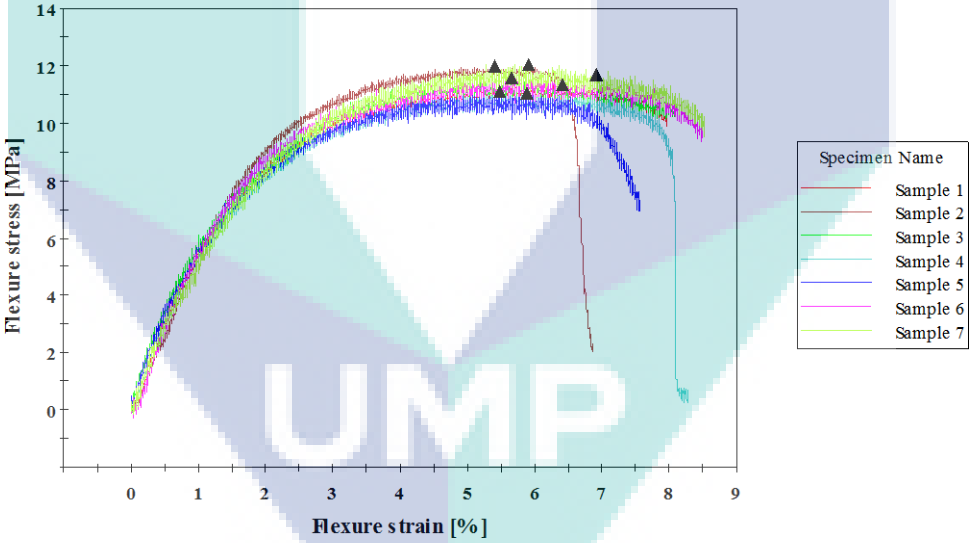

Specimen label	Thickness [mm]	Width [mm]	Flexural modulus [GPa]	Maximum stress [MPa]
Sample 1	3.00	12.70	0.55	11.37
Sample 2	2.99	12.70	0.56	11.99
Sample 3	3.00	12.71	0.56	11.58
Sample 4	3.00	12.69	0.56	11.11
Sample 5	3.01	12.70	0.55	11.05
Sample 6	2.99	12.68	0.56	11.71
Sample 7	3.00	12.70	0.56	12.07
Mean	**3.00**	**10.13**	**0.56**	**11.56**
Std dev	**0.01**	**0.01**	**0.004**	**0.40**

APPENDIX D2
FLEXURAL TEST OF 10% FIBER COMPOSITION

For flexural properties analysis of different fiber composition.

3/20/2017 10:07:25 PM

FACULTY OF MECHANICAL ENGINEERING
UNIVERSITI MALAYSIA PAHANG

FLEXURAL TEST OF 10% PALF-TBP COMPOSITES

Flexural Test Based on ASTM D790-03
Crosshead Speed 1.28 mm/min
Support Span 48.0 mm
Temperature : 24.9°C
Humidity : 55%

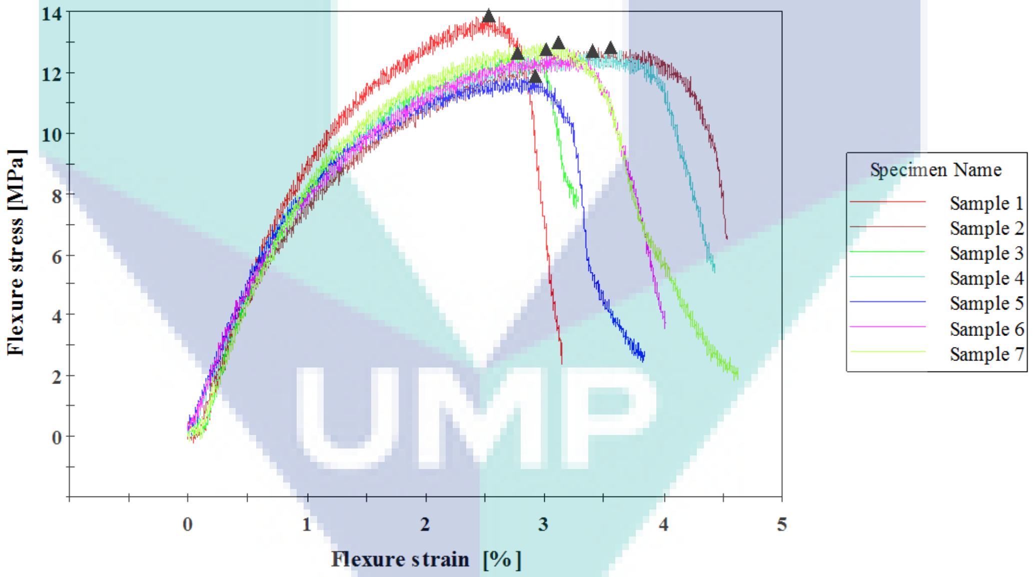

Specimen label	Thickness [mm]	Width [mm]	Flexural modulus [GPa]	Maximum stress [MPa]
Sample 1	3.00	12.70	0.99	13.88
Sample 2	3.01	12.71	0.98	12.83
Sample 3	3.00	12.72	0.99	12.62
Sample 4	3.00	12.69	0.99	12.73
Sample 5	3.01	12.70	0.98	11.90
Sample 6	3.01	12.71	0.98	12.78
Sample 7	3.01	12.69	1.00	13.01
Mean	**3.00**	**12.70**	**0.99**	**12.82**
Std dev	**0.01**	**0.01**	**0.01**	**0.58**

Page 1 of 1

APPENDIX D3
FLEXURAL TEST OF 20% FIBER COMPOSITION

For flexural properties analysis of different fiber composition.

3/20/2017 10:30:10 PM

FACULTY OF MECHANICAL ENGINEERING
UNIVERSITI MALAYSIA PAHANG

FLEXURAL TEST OF 20% PALF-TBP COMPOSITES

Flexural Test Based on ASTM D790-03
Crosshead Speed 1.28 mm/min
Support Span 48.0 mm
Temperature : 24.9°C
Humidity : 55%

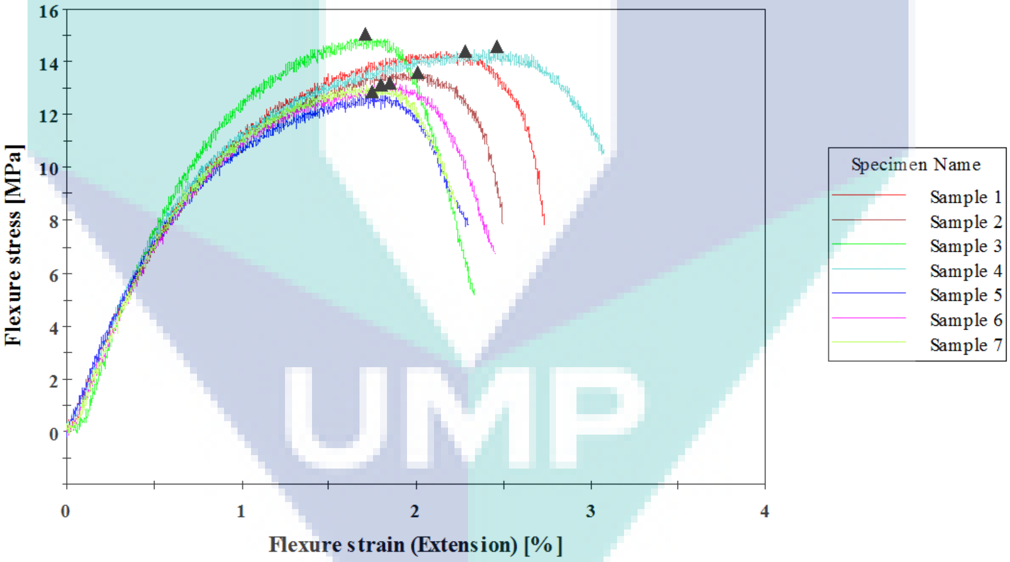

Specimen label	Thickness [mm]	Width [mm]	Flexural modulus [MPa]	Maximum stress [MPa]
Sample 1	3.00	12.73	1.60	14.43
Sample 2	2.98	12.73	1.59	13.63
Sample 3	3.01	12.72	1.59	15.09
Sample 4	3.03	12.69	1.59	14.60
Sample 5	2.85	12.70	1.60	12.85
Sample 6	3.00	12.73	1.59	13.20
Sample 7	2.95	12.75	1.59	13.16
Mean	**2.97**	**12.72**	**1.59**	**13.85**
Std dev	**0.06**	**0.02**	**0.004**	**0.85**

Page 1 of 1

APPENDIX D4
FLEXURAL TEST OF 30% FIBER COMPOSITION

For flexural properties analysis of different fiber composition.

3/20/2017 10:45:09 PM

FACULTY OF MECHANICAL ENGINEERING
UNIVERSITI MALAYSIA PAHANG

FLEXURAL TEST OF 30% PALF-TBP COMPOSITES

Flexural Test Based on ASTM D790-03
Crosshead Speed 1.28 mm/min
Support Span 48.0 mm
Temperature : 24.9°C
Humidity : 55%

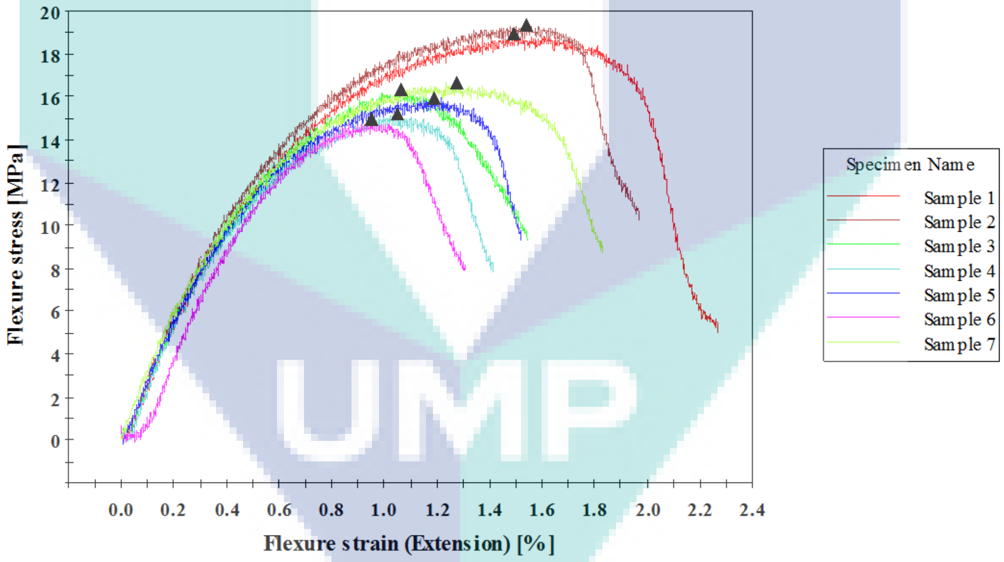

Specimen label	Thickness [mm]	Width [mm]	Flexural modulus [MPa]	Maximum stress [MPa]
Sample 1	2.90	12.75	2.90	18.95
Sample 2	2.90	12.75	2.90	19.34
Sample 3	2.95	12.74	2.90	16.39
Sample 4	2.90	12.71	2.89	15.20
Sample 5	2.95	12.73	2.89	15.95
Sample 6	2.95	12.72	2.87	14.99
Sample 7	2.90	12.74	2.90	16.67
Mean	**2.92**	**12.73**	**2.90**	**16.79**
Std dev	**0.03**	**0.02**	**0.01**	**1.72**

APPENDIX D5

FLEXURAL TEST OF 40% FIBER COMPOSITION

For flexural properties analysis of different fiber composition.

3/20/2017 10:54:58 PM

FACULTY OF MECHANICAL ENGINEERING
UNIVERSITI MALAYSIA PAHANG

FLEXURAL TEST OF 40% PALF-TBP COMPOSITES

Flexural Test Based on ASTM D790-03
Crosshead Speed 1.28 mm/min
Support Span 48.0 mm
Temperature : 24.9°C
Humidity : 55%

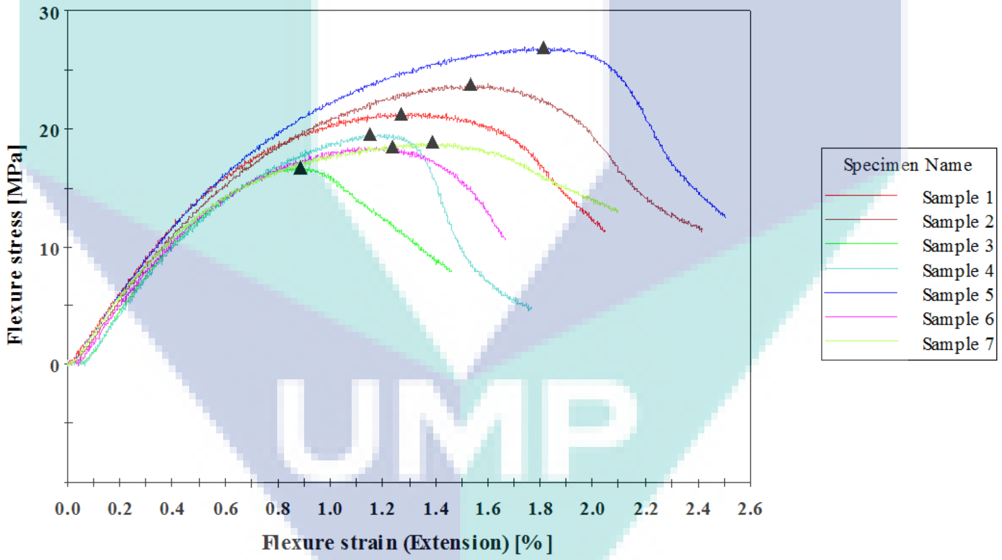

Specimen label	Thickness [mm]	Width [mm]	Flexural modulus [MPa]	Maximum stress [MPa]
Sample 1	3.10	12.70	3.14	21.36
Sample 2	3.09	12.75	3.14	23.75
Sample 3	3.07	12.74	3.15	16.72
Sample 4	3.10	12.70	3.15	19.58
Sample 5	3.08	12.75	3.15	26.93
Sample 6	3.08	12.73	3.14	18.54
Sample 7	3.10	12.71	3.15	18.89
Mean	**3.09**	**12.73**	**3.15**	**20.82**
Std dev	**0.01**	**0.02**	**0.01**	**3.50**

Page 1 of 1

APPENDIX E1
IMPACT TEST RESULT

3/25/2017 9:22:37 AM

FACULTY OF MECHANICAL ENGINEERING
UNIVERSITI MALAYSIA PAHANG

Impact Test Based on ASTM D256
Machine used : Zwick B 5113.300 impact test machine
Temperature : 23.5°C
Humidity : 55%

Sample : Virgin TBP

Sample	Specimen Dimension		Impact Test Result	
	Width (mm)	Thickness (m)	Energy abrosp (J)	Impact strength (kJ/m²)
Sample 1	0.0095	0.0032	0.464	15.34
Sample 2	0.0092	0.0032	0.458	15.61
Sample 3	0.0093	0.0032	0.447	15.00
Sample 4	0.0098	0.0032	0.460	14.74
Sample 5	0.0091	0.0032	0.446	15.32
Sample 6	0.0096	0.0032	0.458	14.85
Sample 7	0.0097	0.0032	0.452	14.61
Sample 8	0.0096	0.0032	0.452	14.76
Sample 9	0.0095	0.0032	0.453	14.95
Sample 10	0.0090	0.0032	0.448	15.54
Mean				**15.07**
Standard Deviation				**0.35**

Sample : 10% PALF-TBP Composites

Sample	Specimen Dimension		Impact Test Result	
	Width (mm)	Thickness (mm)	Energy abrosp (J)	Impact strength (kJ/m²)
Sample 1	0.0096	0.0032	0.464	15.07
Sample 2	0.0093	0.0032	0.463	15.54
Sample 3	0.0093	0.0032	0.465	15.59
Sample 4	0.0094	0.0032	0.464	15.36
Sample 5	0.0088	0.0032	0.461	16.43
Sample 6	0.0092	0.0032	0.461	15.63

Sample 7	0.0088	0.0032	0.462	16.44
Sample 8	0.0091	0.0032	0.459	15.78
Sample 9	0.0094	0.0032	0.461	15.26
Sample 10	0.0095	0.0032	0.465	15.33
Mean				**15.64**
Standard Deviation				**0.46**

APPENDIX E2
IMPACT TEST RESULT

3/25/2017 10:15:57 AM

FACULTY OF MECHANICAL ENGINEERING
UNIVERSITI MALAYSIA PAHANG

Impact Test Based on ASTM D256
Machine used : Zwick B 5113.300 impact test machine
Temperature : 23.5°C
Humidity : 55%

Sample : 20% PALF-TBP Composites

Sample	Specimen Dimension		Impact Test Result	
	Width (mm)	Thickness (m)	Energy abrosp (J)	Impact strength (kJ/m²)
Sample 1	0.0091	0.0032	0.473	16.30
Sample 2	0.0097	0.0032	0.471	15.22
Sample 3	0.0098	0.0032	0.477	15.26
Sample 4	0.0093	0.0032	0.473	15.83
Sample 5	0.0096	0.0032	0.478	15.50
Sample 6	0.0094	0.0032	0.477	15.79
Sample 7	0.0100	0.0032	0.476	14.93
Sample 8	0.0080	0.0032	0.471	18.44
Sample 9	0.0097	0.0032	0.485	15.66
Sample 10	0.0092	0.0032	0.477	16.22
Mean				**15.91**
Standard Deviation				**0.99**

Sample : 30% PALF-TBP Composites

Sample	Specimen Dimension		Impact Test Result	
	Width (mm)	Thickness (mm)	Energy abrosp (J)	Impact strength (kJ/m²)
Sample 1	0.0094	0.0032	0.485	16.21
Sample 2	0.0094	0.0032	0.496	16.44
Sample 3	0.0085	0.0032	0.471	17.36
Sample 4	0.0086	0.0032	0.48	17.36
Sample 5	0.0089	0.0032	0.482	17.00
Sample 6	0.0097	0.0032	0.486	15.72

Sample 7	0.0094	0.0032	0.494	16.35
Sample 8	0.0091	0.0032	0.484	16.57
Sample 9	0.0093	0.0032	0.489	16.40
Sample 10	0.0094	0.0032	0.481	15.92
Mean				**16.53**
Standard Deviation				**0.56**

APPENDIX E3
IMPACT TEST RESULT

3/25/2017 11:05:17 AM

FACULTY OF MECHANICAL ENGINEERING
UNIVERSITI MALAYSIA PAHANG

Impact Test Based on ASTM D256
Machine used : Zwick B 5113.300 impact test machine
Temperature : 23.5°C
Humidity : 55%

Sample : 40% PALF-TBP Composites

Sample	**Specimen dimension**		**Impact test result**	
	Width (mm)	**Thickness (m)**	**Energy abrosp (J)**	**Impact strength (kJ/m²)**
Sample 1	0.0089	0.0032	0.540	18.96
Sample 2	0.0089	0.0032	0.518	18.23
Sample 3	0.0095	0.0032	0.521	17.17
Sample 4	0.0093	0.0032	0.547	18.34
Sample 5	0.0089	0.0032	0.518	18.13
Sample 6	0.0091	0.0032	0.528	18.23
Sample 7	0.0094	0.0032	0.523	17.48
Sample 8	0.0091	0.0032	0.525	18.03
Sample 9	0.0088	0.0032	0.537	19.11
Sample 10	0.0097	0.0032	0.535	17.27
Mean				**18.10**
Standard deviation				**0.65**

APPENDIX F1
TENSILE TEST OF 1% MAPE CONCENTRATION

For tensile properties analysis of different coupling agent concentrations.

3/15/2017 10:23:39 AM

FACULTY OF MECHANICAL ENGINEERING
UNIVERSITI MALAYSIA PAHANG

10% PALF-TBP COMPOSITES WITH 1% MAPE TENSILE TEST RESULT

Tensile Test Based on ASTM D638-03
Crosshead Speed 1mm/min
Temperature : 24.9°C
Humidity : 55%

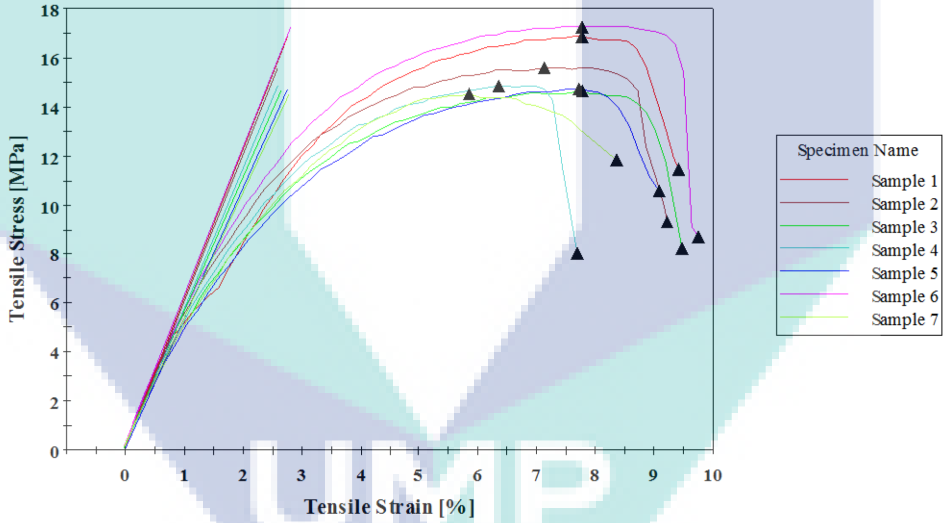

Specimen label	Length [mm]	Thickness [mm]	Width [mm]	Modulus [GPa]	Tensile strength [MPa]	Maximum strain [%]	Time at break [min]
Sample 1	9.84	3.02	3.55	0.61	16.85	9.41	1.0
Sample 2	9.83	3.00	3.54	0.60	15.62	9.23	1.0
Sample 3	9.85	3.00	3.53	0.55	14.62	9.48	1.0
Sample 4	9.85	3.01	3.53	0.57	14.89	7.70	0.8
Sample 5	9.85	3.01	3.54	0.53	14.75	9.09	0.9
Sample 6	9.85	3.00	3.55	0.61	17.29	9.75	1.0
Sample 7	9.83	3.03	3.55	0.51	14.50	8.36	0.9
Mean	**9.84**	**3.01**	**3.54**	**0.57**	**15.50**	**9.00**	**0.9**
Std dev	**0.01**	**0.01**	**0.01**	**0.04**	**1.14**	**0.72**	**0.08**

Page 1 of 1

APPENDIX F2
TENSILE TEST OF 3% MAPE CONCENTRATION

For tensile properties analysis of different coupling agent concentrations and analysis of different treatment effect on tensile properties of PALF-TBP composites.

3/15/2017 11:38:21 AM

FACULTY OF MECHANICAL ENGINEERING
UNIVERSITI MALAYSIA PAHANG

10% PALF-TBP COMPOSITES WITH 3% MAPE TENSILE TEST RESULT

Tensile Test Based on ASTM D638-03
Crosshead Speed 1mm/min
Temperature : 24.9°C
Humidity : 55%

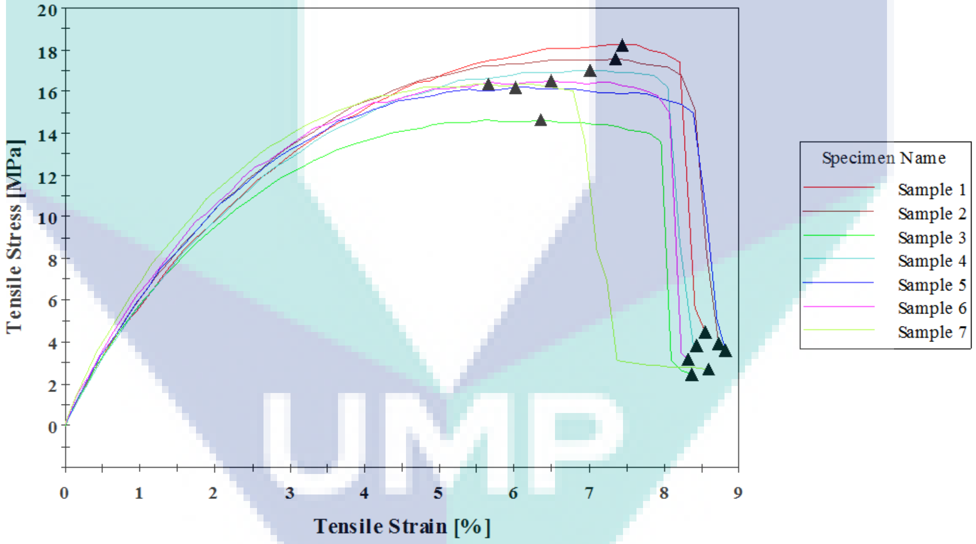

Specimen label	Length [mm]	Thickness [mm]	Width [mm]	Modulus [GPa]	Tensile strength [MPa]	Maximum strain [%]	Time at break [min]
Sample 1	9.88	3.12	3.51	0.63	18.25	8.55	0.7
Sample 2	9.88	3.10	3.50	0.65	17.53	8.74	0.8
Sample 3	9.89	3.10	3.50	0.65	14.61	8.37	1.0
Sample 4	9.88	3.11	3.51	0.63	17.04	8.44	0.8
Sample 5	9.89	3.11	3.51	0.67	16.19	8.81	0.9
Sample 6	9.87	3.09	3.52	0.68	16.50	8.32	0.9
Sample 7	9.88	3.09	3.52	0.74	15.93	8.60	1.0
Mean	**9.88**	**3.10**	**3.51**	**0.66**	**16.58**	**8.55**	**0.9**
Std dev	**0.01**	**0.01**	**0.01**	**0.04**	**1.18**	**0.18**	**0.09**

Page 1 of 1

APPENDIX F3
TENSILE TEST OF 5% MAPE CONCENTRATION

For tensile properties analysis of different coupling agent concentrations.

FACULTY OF MECHANICAL ENGINEERING
UNIVERSITI MALAYSIA PAHANG

10% PALF-TBP COMPOSITES WITH 5% MAPE TENSILE TEST RESULT

Tensile Test Based on ASTM D638-03
Crosshead Speed 1mm/min
Temperature : 24.9°C
Humidity : 55%

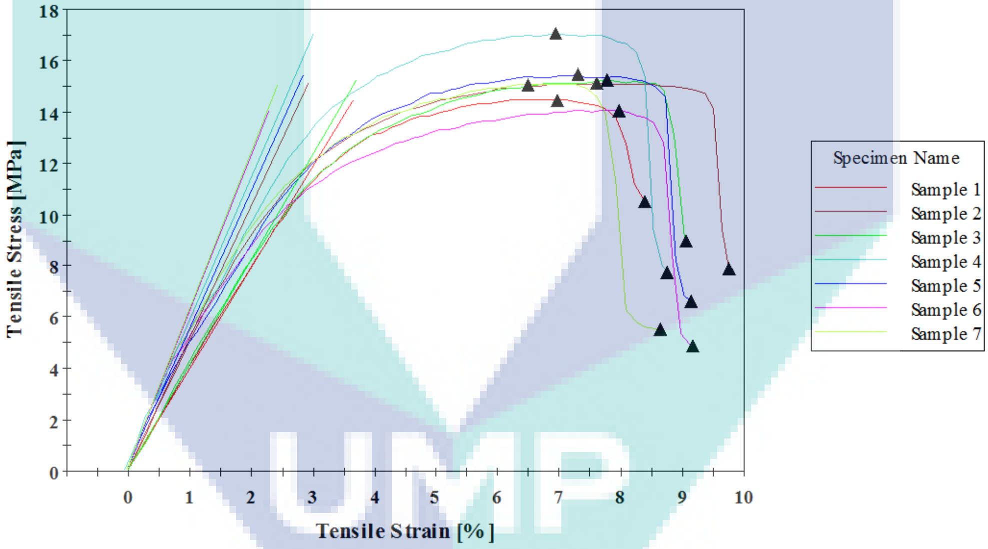

Specimen label	Length [mm]	Thickness [mm]	Width [mm]	Modulus [GPa]	Tensile strength [MPa]	Maximum strain [%]	Time at break [min]
Sample 1	9.88	3.12	3.51	0.39	14.48	8.38	0.9
Sample 2	9.88	3.10	3.50	0.51	15.11	9.76	1.0
Sample 3	9.89	3.10	3.50	0.41	15.23	9.05	1.0
Sample 4	9.88	3.11	3.51	0.56	17.04	8.76	1.0
Sample 5	9.89	3.11	3.51	0.54	15.42	9.13	1.0
Sample 6	9.87	3.09	3.52	0.61	14.07	9.16	1.1
Sample 7	9.88	3.09	3.52	0.61	15.09	8.64	0.9
Mean	**9.88**	**3.10**	**3.51**	**0.52**	**15.21**	**8.98**	**1.0**
Std dev	**0.01**	**0.01**	**0.01**	**0.09**	**0.94**	**0.44**	**0.06**

APPENDIX F4
TENSILE TEST OF 7% MAPE CONCENTRATION

For tensile properties analysis of different coupling agent concentrations.

3/15/2017 11:56:09 AM

FACULTY OF MECHANICAL ENGINEERING
UNIVERSITI MALAYSIA PAHANG

10% PALF-TBP COMPOSITES WITH 7% MAPE TENSILE TEST RESULT

Tensile Test Based on ASTM D638-03
Crosshead Speed 1mm/min
Temperature : 24.9°C
Humidity : 55%

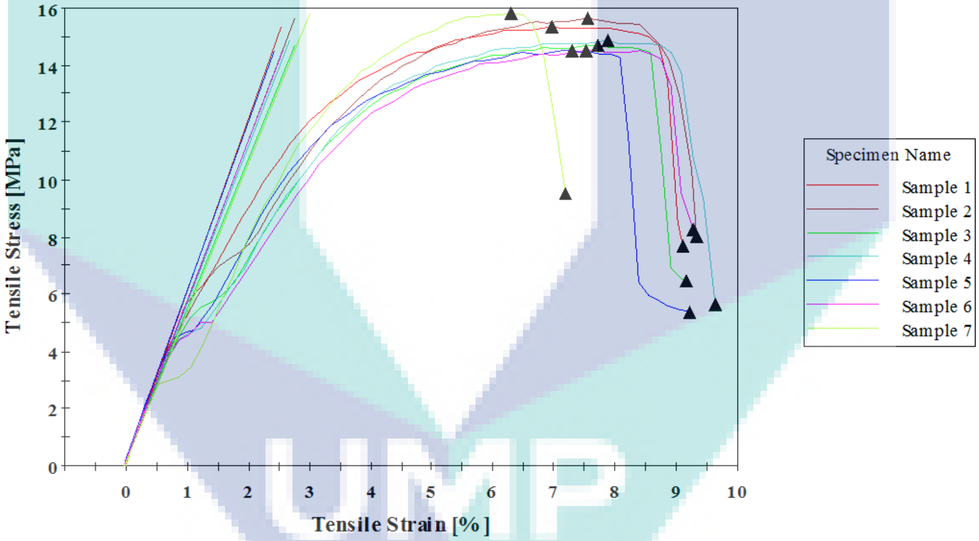

Specimen label	Length [mm]	Thickness [mm]	Width [mm]	Modulus [GPa]	Tensile strength [MPa]	Maximum strain [%]	Time at break [min]
Sample 1	9.98	3.22	3.56	0.60	15.36	9.12	1.0
Sample 2	9.98	3.20	3.57	0.56	15.62	9.33	0.9
Sample 3	9.99	3.21	3.59	0.53	14.72	9.15	0.9
Sample 4	9.98	3.21	3.58	0.55	14.84	9.63	0.9
Sample 5	9.97	3.21	3.58	0.59	14.52	9.23	1.0
Sample 6	9.97	3.19	3.57	0.56	14.53	9.28	0.9
Sample 7	9.97	3.19	3.59	0.52	15.80	7.19	0.7
Mean	**9.98**	**3.20**	**3.58**	**0.56**	**15.05**	**8.99**	**0.9**
Std dev	**0.01**	**0.01**	**0.01**	**0.03**	**0.53**	**0.81**	**0.10**

Page 1 of 1

APPENDIX G1
TENSILE TEST OF 1% MAPP CONCENTRATION

For tensile properties analysis of different coupling agent concentrations.

4/12/2017 12:18:30 PM

FACULTY OF MECHANICAL ENGINEERING
UNIVERSITI MALAYSIA PAHANG

10% PALF-TBP COMPOSITES WITH 1% MAPP TENSILE TEST RESULT

Tensile Test Based on ASTM D638-03
Crosshead Speed 1mm/min
Temperature : 24.9°C
Humidity : 55%

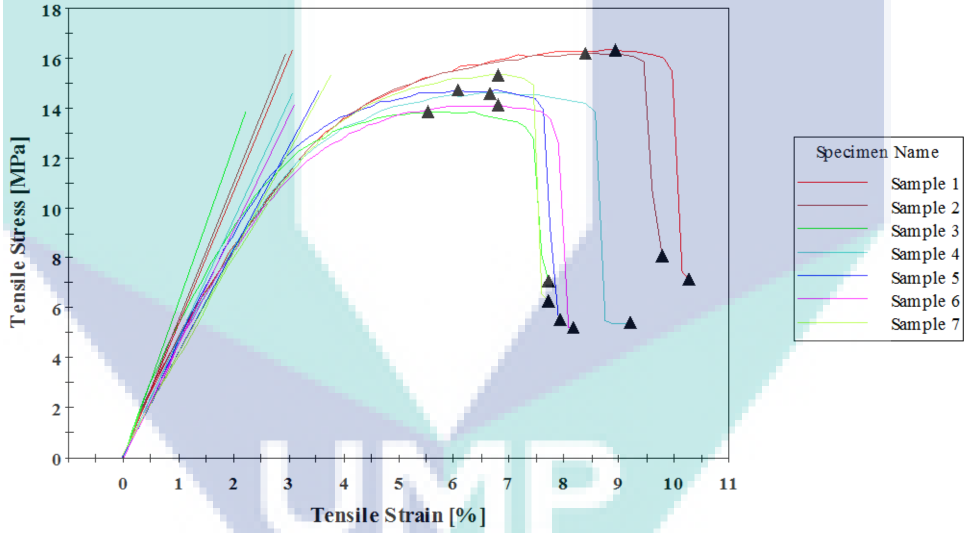

Specimen label	Length [mm]	Thickness [mm]	Width [mm]	Modulus [GPa]	Tensile strength [MPa]	Maximum strain [%]	Time at break [min]
Sample 1	9.63	3.11	3.43	0.53	16.34	10.28	1.0
Sample 2	9.63	3.11	3.46	0.55	16.20	9.78	0.9
Sample 3	9.64	3.11	3.42	0.63	13.87	7.71	0.8
Sample 4	9.64	3.12	3.43	0.47	14.60	9.22	0.9
Sample 5	9.65	3.11	3.46	0.41	14.72	7.93	0.9
Sample 6	9.65	3.13	3.46	0.46	14.09	8.18	0.9
Sample 7	9.63	3.14	3.45	0.40	15.34	7.71	0.8
Mean	**9.64**	**3.12**	**3.44**	**0.49**	**15.02**	**8.69**	**0.9**
Std dev	**0.01**	**0.01**	**0.02**	**0.08**	**0.97**	**1.06**	**0.07**

Page 1 of 1

APPENDIX G2
TENSILE TEST OF 3% MAPP CONCENTRATION

For tensile properties analysis of different coupling agent concentrations.

4/12/2017 12:31:36 PM

FACULTY OF MECHANICAL ENGINEERING
UNIVERSITI MALAYSIA PAHANG

10% PALF-TBP COMPOSITES WITH 3% MAPP TENSILE TEST RESULT

Tensile Test Based on ASTM D638-03
Crosshead Speed 1mm/min
Temperature : 24.9°C
Humidity : 55%

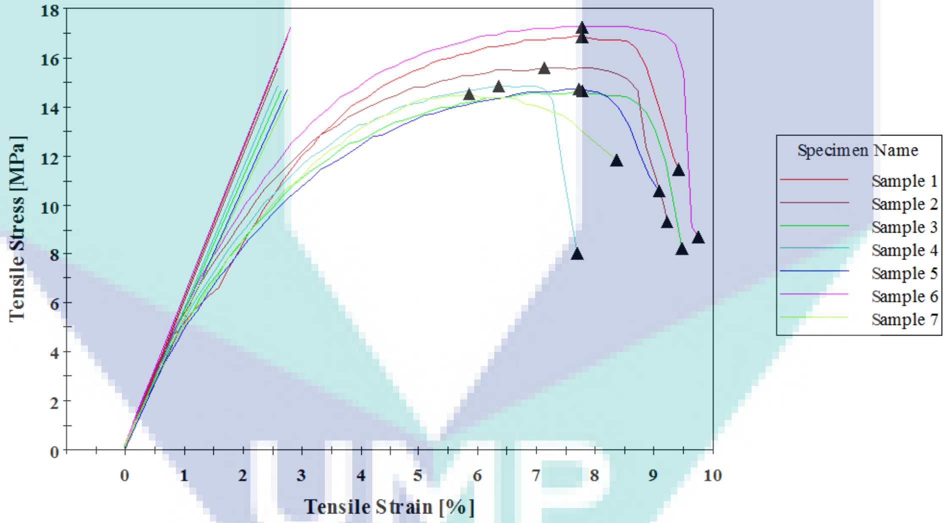

Specimen label	Length [mm]	Thickness [mm]	Width [mm]	Modulus [GPa]	Tensile strength [MPa]	Maximum strain [%]	Time at break [min]
Sample 1	9.99	3.11	3.63	0.52	15.25	6.00	0.6
Sample 2	9.93	3.10	3.62	0.50	15.63	6.16	0.7
Sample 3	9.98	3.09	3.62	0.47	16.99	7.80	0.7
Sample 4	9.98	3.11	3.63	0.50	15.52	6.12	0.6
Sample 5	9.93	3.11	3.61	0.50	15.62	5.87	0.7
Sample 6	9.93	3.09	3.63	0.49	15.08	7.98	0.8
Sample 7	9.93	3.09	3.63	0.52	15.24	9.80	1.0
Mean	**9.95**	**3.10**	**3.62**	**0.50**	**15.62**	**7.11**	**0.7**
Std dev	**0.03**	**0.01**	**0.01**	**0.02**	**0.64**	**1.48**	**0.15**

Page 1 of 1

APPENDIX G3
TENSILE TEST OF 5% MAPP CONCENTRATION

For tensile properties analysis of different coupling agent concentrations.

4/12/2017 12:53:56 PM

Universiti Malaysia PAHANG
Engineering • Technology • Creativity

FACULTY OF MECHANICAL ENGINEERING
UNIVERSITI MALAYSIA PAHANG

10% PALF-TBP COMPOSITES WITH 5% MAPP TENSILE TEST RESULT

Tensile Test Based on ASTM D638-03
Crosshead Speed 1mm/min
Temperature : 24.9°C
Humidity : 55%

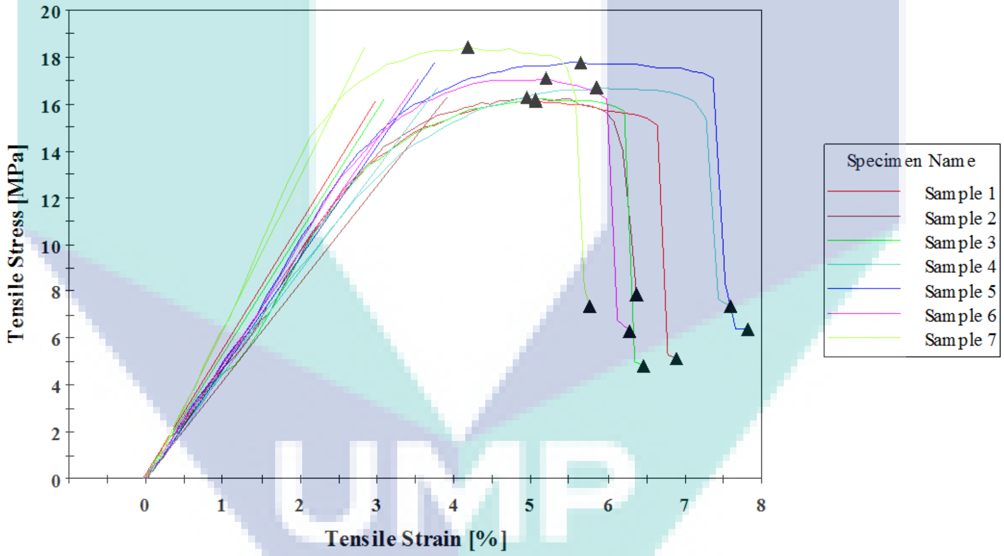

Specimen label	Length [mm]	Thickness [mm]	Width [mm]	Modulus [GPa]	Tensile strength [MPa]	Maximum strain [%]	Time at break [min]
Sample 1	9.66	3.02	3.35	0.54	16.13	6.89	0.8
Sample 2	9.63	3.01	3.32	0.42	16.26	6.37	0.9
Sample 3	9.65	3.03	3.33	0.52	16.22	6.47	0.7
Sample 4	9.65	3.01	3.33	0.44	16.70	7.59	0.8
Sample 5	9.64	3.01	3.34	0.48	17.80	7.82	0.9
Sample 6	9.64	3.00	3.36	0.48	17.07	6.29	0.8
Sample 7	9.66	3.04	3.35	0.66	18.42	5.76	0.9
Mean	**9.65**	**3.02**	**3.53**	**0.50**	**16.94**	**6.74**	**0.8**
Std dev	**0.01**	**0.01**	**0.01**	**0.08**	**0.88**	**0.74**	**0.07**

Page 1 of 1

APPENDIX G4
TENSILE TEST OF 7% MAPP CONCENTRATION

For tensile properties analysis of different coupling agent concentrations and analysis of different treatment effect on tensile properties of PALF-TBP composites.

4/12/2017 3:58:02 PM

Universiti Malaysia PAHANG
Engineering • Technology • Creativity

FACULTY OF MECHANICAL ENGINEERING
UNIVERSITI MALAYSIA PAHANG

10% PALF-TBP COMPOSITES WITH 7% MAPE TENSILE TEST RESULT

Tensile Test Based on ASTM D638-03
Crosshead Speed 1mm/min
Temperature : 24.9°C
Humidity : 55%

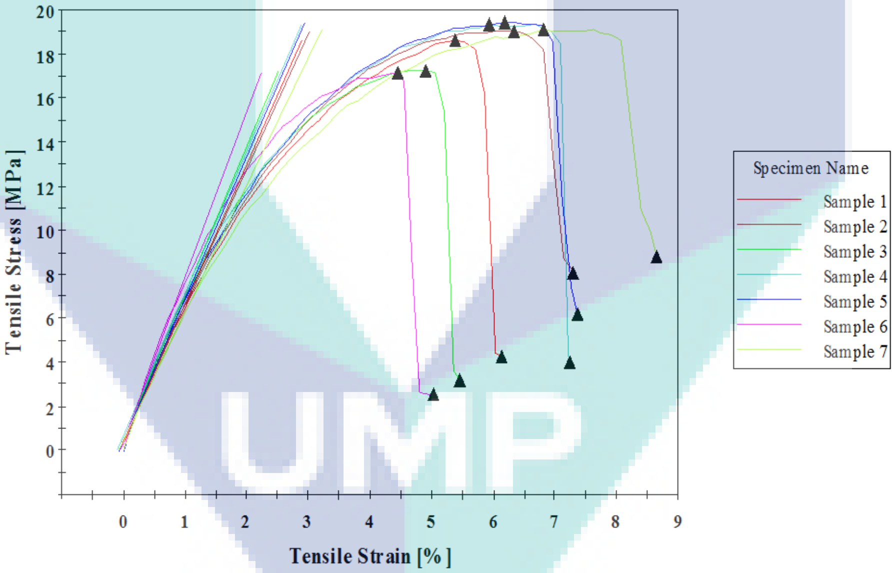

Specimen label	Length [mm]	Thickness [mm]	Width [mm]	Modulus [GPa]	Tensile strength [MPa]	Maximum strain [%]	Time at break [min]
Sample 1	9.54	3.05	3.32	0.63	18.59	6.13	0.6
Sample 2	9.55	3.04	3.35	0.61	19.06	7.30	0.8
Sample 3	9.55	3.04	3.32	0.67	17.23	5.47	0.6
Sample 4	9.52	3.06	3.32	0.65	19.36	7.25	0.8
Sample 5	9.52	3.06	3.31	0.64	19.45	7.37	0.8
Sample 6	9.52	3.04	3.36	0.75	17.15	5.02	0.7
Sample 7	9.51	3.06	3.36	0.58	19.08	8.65	0.9
Mean	**9.53**	**3.05**	**3.33**	**0.65**	**18.56**	**6.74**	**0.7**
Std dev	**0.02**	**0.01**	**0.02**	**0.05**	**0.98**	**1.26**	**0.10**

Page 1 of 1

APPENDIX H1
TENSILE TEST OF ALKALI TREATMENT (10% PALF)

For tensile properties analysis of different treatment on PALF-TBP composites.

5/24/2017 4:39:58 PM

FACULTY OF MECHANICAL ENGINEERING
UNIVERSITI MALAYSIA PAHANG

TENSILE TEST RESULT OF 10% PALF-TBP COMPOSITES WITH ALKALI TREATMENT

Tensile Test Based on ASTM D638-03
Crosshead Speed 1mm/min
Temperature : 24.9°C
Humidity : 55%

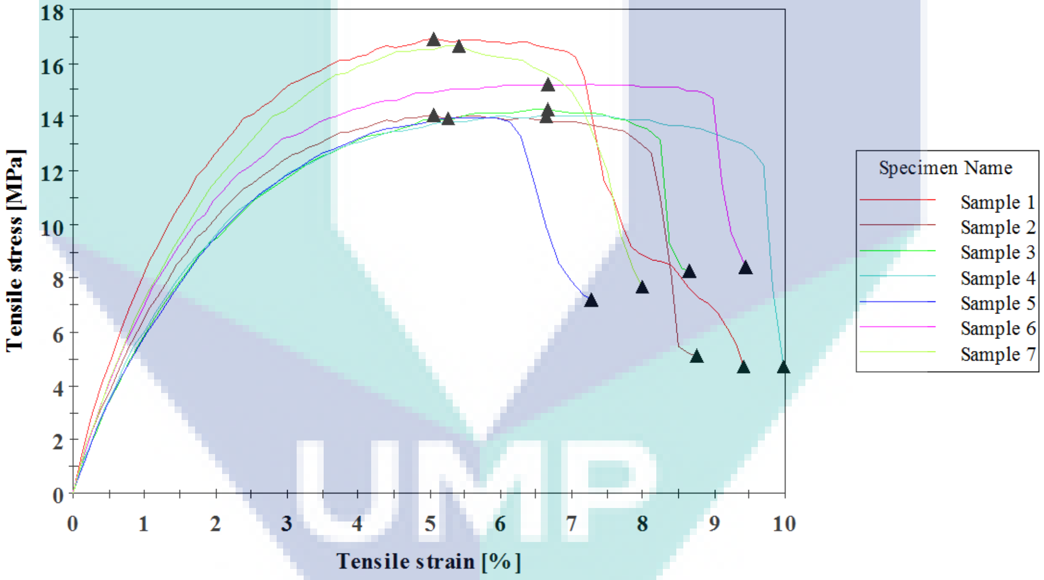

Specimen label	Length [mm]	Thickness [mm]	Width [mm]	Modulus [GPa]	Tensile strength [MPa]	Maximum strain [%]	Time at break [min]
Sample 1	9.20	3.16	3.01	0.78	16.83	9.417	1.2
Sample 2	9.21	3.15	3.07	0.62	13.97	8.742	1.1
Sample 3	9.21	3.13	3.02	0.58	14.28	8.655	0.9
Sample 4	9.25	3.15	3.02	0.59	13.98	9.969	1.2
Sample 5	9.24	3.16	3.05	0.57	13.99	7.265	0.7
Sample 6	9.24	3.15	3.06	0.67	15.15	9.432	1.3
Sample 7	9.20	3.13	3.06	0.69	16.64	7.997	0.8
Mean	**9.22**	**3.15**	**3.04**	**0.64**	**14.98**	**8.783**	**1.0**
Std dev	**0.02**	**0.01**	**0.02**	**0.08**	**1.27**	**0.93**	**0.22**

Page 1 of 1

APPENDIX H2
TENSILE TEST OF ALKALI TREATMENT (20% PALF)

For tensile properties analysis of different treatment on PALF-TBP composites.

5/24/2017 5:27:41 PM

FACULTY OF MECHANICAL ENGINEERING
UNIVERSITI MALAYSIA PAHANG

TENSILE TEST RESULT OF 20% PALF-TBP COMPOSITES WITH ALKALI TREATMENT

Tensile Test Based on ASTM D638-03
Crosshead Speed 1mm/min
Temperature : 24.9°C
Humidity : 55%

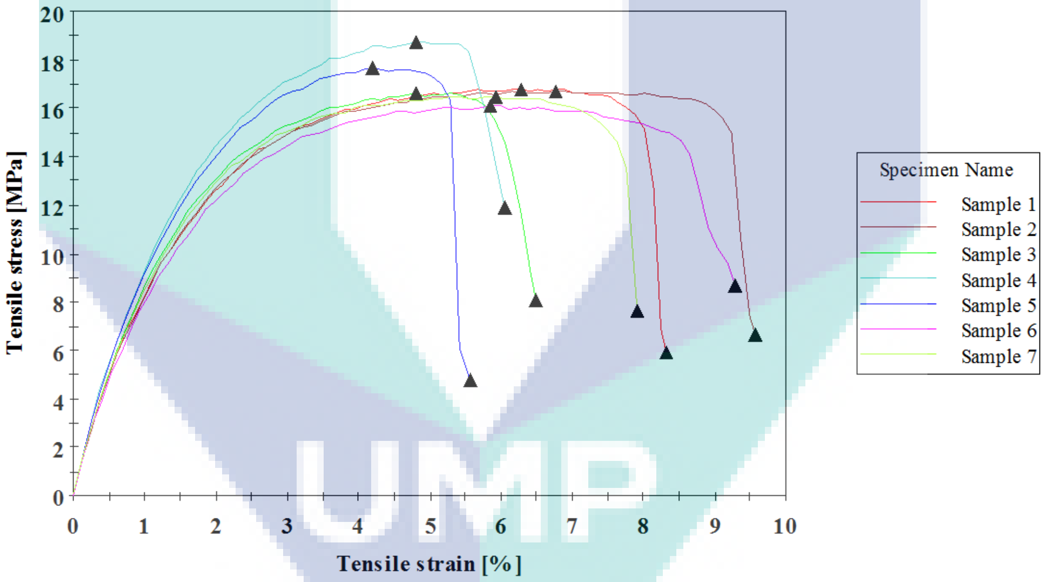

Specimen label	Length [mm]	Thickness [mm]	Width [mm]	Modulus [GPa]	Tensile strength [MPa]	Maximum strain [%]	Time at break [min]
Sample 1	9.55	3.36	3.21	0.81	16.81	8.325	1.1
Sample 2	9.54	3.35	3.27	0.80	16.65	9.557	1.3
Sample 3	9.53	3.31	3.22	0.82	16.61	6.488	0.9
Sample 4	9.55	3.31	3.22	0.89	18.76	6.052	0.8
Sample 5	9.55	3.32	3.22	0.86	17.66	5.577	0.8
Sample 6	9.55	3.35	3.26	0.75	16.01	9.285	1.2
Sample 7	9.53	3.35	3.25	0.81	16.49	7.920	1.1
Mean	**9.22**	**3.15**	**3.04**	**0.82**	**17.00**	**7.600**	**1.0**
Std dev	**0.01**	**0.02**	**0.02**	**0.04**	**0.92**	**1.58**	**0.20**

Page 1 of 1

APPENDIX H3
TENSILE TEST OF ALKALI TREATMENT (30% PALF)

For tensile properties analysis of different treatment on PALF-TBP composites.

Universiti
Malaysia
PAHANG
Engineering • Technology • Creativity

FACULTY OF MECHANICAL ENGINEERING
UNIVERSITI MALAYSIA PAHANG

TENSILE TEST RESULT OF 30% PALF-TBP COMPOSITES WITH ALKALI TREATMENT

Tensile Test Based on ASTM D638-03
Crosshead Speed 1mm/min
Temperature : 24.9°C
Humidity : 55%

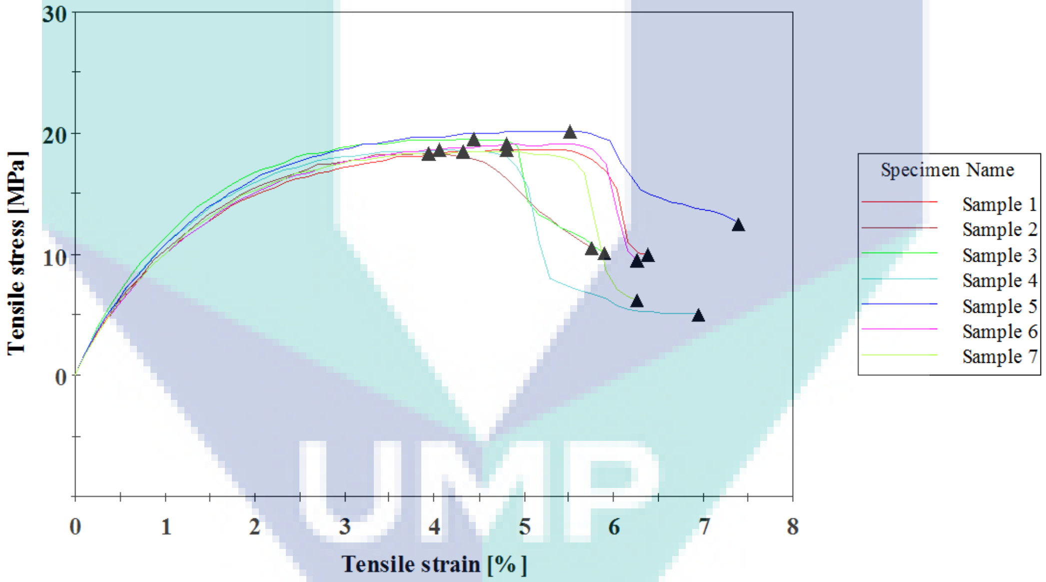

Specimen label	Length [mm]	Thickness [mm]	Width [mm]	Modulus [GPa]	Tensile strength [MPa]	Maximum strain [%]	Time at break [min]
Sample 1	9.25	3.00	3.41	0.94	18.68	6.375	0.9
Sample 2	9.22	3.01	3.45	0.97	18.32	5.763	0.8
Sample 3	9.22	3.00	3.45	1.11	19.56	5.897	0.8
Sample 4	9.21	3.00	3.44	1.00	18.15	6.951	0.9
Sample 5	9.26	3.01	3.40	1.01	19.94	7.394	1.1
Sample 6	9.27	3.02	3.41	0.93	19.03	6.267	0.8
Sample 7	9.26	3.02	3.41	0.97	18.50	6.256	0.8
Mean	**9.24**	**3.01**	**3.42**	**0.99**	**18.88**	**6.415**	**0.9**
Std dev	**0.02**	**0.01**	**0.02**	**0.06**	**0.66**	**0.58**	**0.10**

APPENDIX H4
TENSILE TEST OF ALKALI TREATMENT (40% PALF)

For tensile properties analysis of different treatment on PALF-TBP cmposites.

5/24/2017 5:59:21 PM

Universiti Malaysia PAHANG
Engineering • Technology • Creativity

FACULTY OF MECHANICAL ENGINEERING
UNIVERSITI MALAYSIA PAHANG

TENSILE TEST RESULT OF 40% PALF-TBP COMPOSITES WITH ALKALI TREATMENT

Tensile Test Based on ASTM D638-03
Crosshead Speed 1mm/min
Temperature : 24.9°C
Humidity : 55%

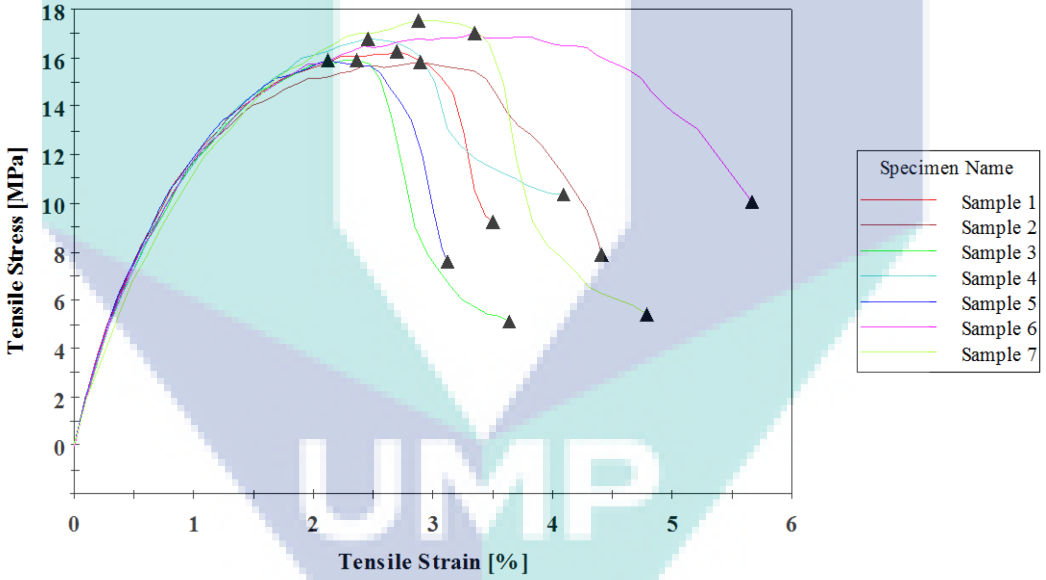

Specimen label	Length [mm]	Thickness [mm]	Width [mm]	Modulus [GPa]	Tensile strength [MPa]	Maximum strain [%]	Time at break [min]
Sample 1	9.01	3.18	3.11	1.07	16.25	3.50	0.6
Sample 2	9.01	3.19	3.12	1.07	15.83	4.42	0.8
Sample 3	9.00	3.20	3.12	1.06	15.88	3.63	0.6
Sample 4	9.09	3.21	3.12	1.08	16.81	4.10	0.6
Sample 5	9.08	3.10	2.99	1.08	15.91	3.13	0.6
Sample 6	9.08	3.10	3.00	1.07	16.82	5.66	1.0
Sample 7	9.09	3.09	2.98	1.06	17.59	4.79	0.7
Mean	**9.05**	**3.15**	**3.06**	**1.07**	**16.44**	**4.17**	**0.7**
Std dev	**0.04**	**0.05**	**0.07**	**0.01**	**0.66**	**0.87**	**0.15**

Page 1 of 1

APPENDIX I1
TENSILE TEST OF MAPP SAMPLE (20% PALF)

For tensile properties analysis of different treatment on PALF-TBP composites.

5/25/2017 4:31:14 PM

FACULTY OF MECHANICAL ENGINEERING
UNIVERSITI MALAYSIA PAHANG

TENSILE TEST RESULT OF 20% PALF-TBP COMPOSITES WITH MAPP COUPLING AGENT

Tensile Test Based on ASTM D638-03
Crosshead Speed 1mm/min
Temperature : 24.9°C
Humidity : 55%

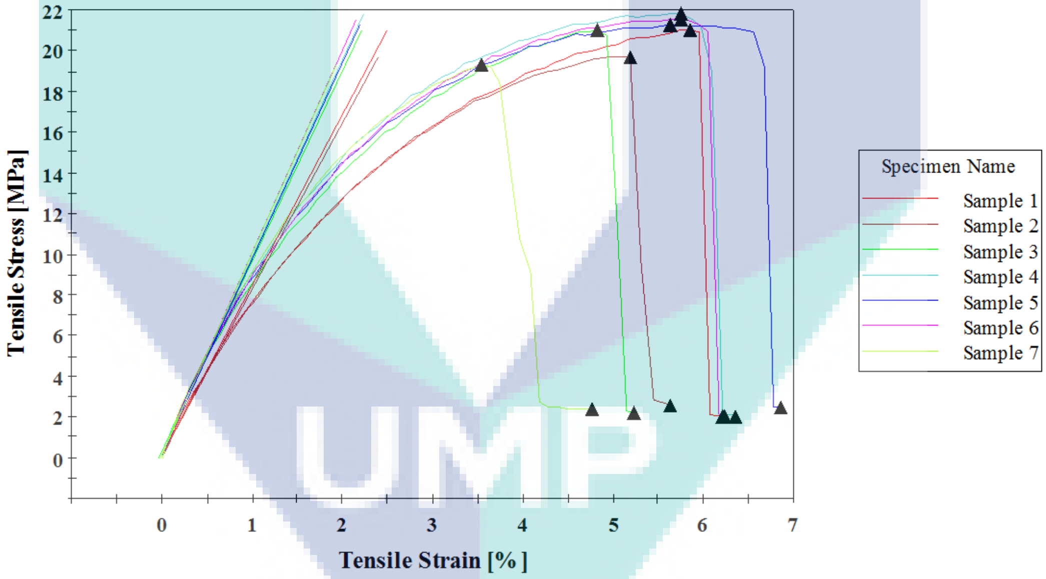

Specimen label	Length [mm]	Thickness [mm]	Width [mm]	Modulus [GPa]	Tensile strength [MPa]	Maximum strain [%]	Time at break [min]
Sample 1	9.55	3.17	3.22	0.84	21.04	6.23	0.9
Sample 2	9.55	3.18	3.23	0.81	19.72	5.63	0.7
Sample 3	9.54	3.17	3.22	0.93	21.01	5.24	0.8
Sample 4	9.54	3.19	3.22	0.97	21.79	6.36	0.9
Sample 5	9.50	2.98	3.23	0.96	21.27	6.86	1.1
Sample 6	9.51	2.98	3.25	0.99	21.58	6.21	1.0
Sample 7	9.50	2.99	3.25	0.99	19.36	4.78	0.7
Mean	**9.53**	**3.09**	**3.23**	**0.93**	**20.83**	**5.90**	**0.9**
Std dev	**0.02**	**0.10**	**0.01**	**0.07**	**0.93**	**0.72**	**0.14**

Page 1 of 1

APPENDIX I2
TENSILE TEST OF MAPP SAMPLE (30% PALF)

For tensile properties analysis of different treatment on PALF-TBP composites.

5/25/2017 5:11:21 PM

Universiti
Malaysia
PAHANG
Engineering • Technology • Creativity

FACULTY OF MECHANICAL ENGINEERING
UNIVERSITI MALAYSIA PAHANG

TENSILE TEST RESULT OF 30% PALF-TBP COMPOSITES WITH MAPP COUPLING AGENT

Tensile Test Based on ASTM D638-03
Crosshead Speed 1mm/min
Temperature : 24.9°C
Humidity : 55%

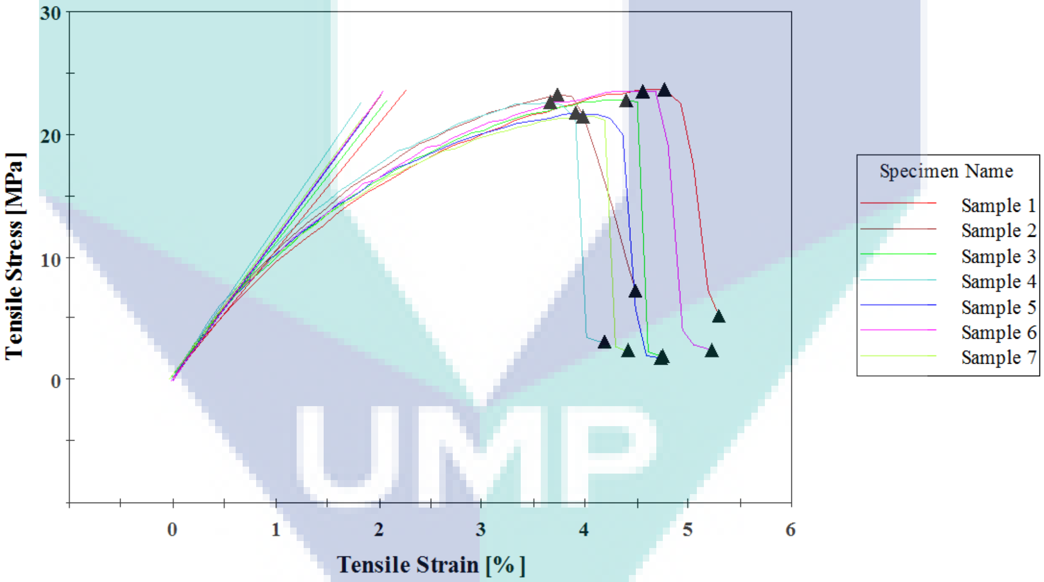

Specimen label	Length [mm]	Thickness [mm]	Width [mm]	Modulus [GPa]	Tensile strength [MPa]	Maximum strain [%]	Time at break [min]
Sample 1	9.53	3.20	3.15	1.04	23.69	5.30	0.6
Sample 2	9.53	3.19	3.15	1.14	23.21	4.49	0.6
Sample 3	9.55	3.19	3.14	1.08	22.82	4.76	0.7
Sample 4	9.55	3.20	3.14	1.22	22.56	4.19	0.6
Sample 5	9.53	2.91	3.13	1.13	21.72	4.73	0.7
Sample 6	9.53	2.99	3.13	1.14	23.54	5.22	0.7
Sample 7	9.54	2.99	3.14	1.14	21.38	4.42	0.7
Mean	**9.54**	**3.10**	**3.14**	**1.13**	**22.70**	**4.73**	**0.7**
Std dev	**0.01**	**0.13**	**0.01**	**0.06**	**0.88**	**0.41**	**0.07**

Page 1 of 1

APPENDIX I3
TENSILE TEST OF MAPP SAMPLE (40% PALF)

For tensile properties analysis of different treatment on PALF-TBP composites.

5/25/2017 5:39:42 PM

FACULTY OF MECHANICAL ENGINEERING
UNIVERSITI MALAYSIA PAHANG

TENSILE TEST RESULT OF 40% PALF-TBP COMPOSITES WITH MAPP COUPLING AGENT

Tensile Test Based on ASTM D638-03
Crosshead Speed 1mm/min
Temperature : 24.9°C
Humidity : 55%

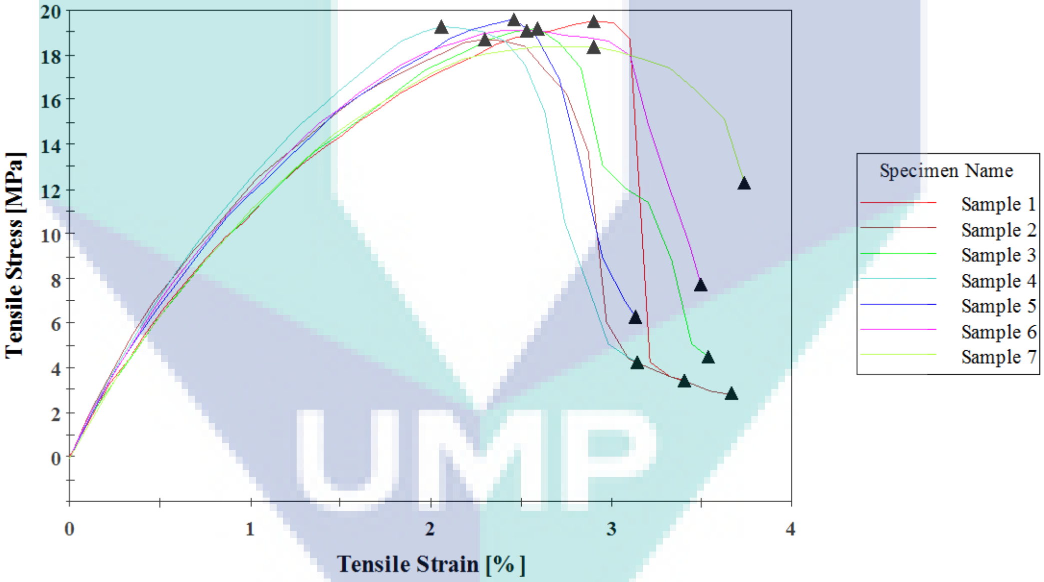

Specimen label	Length [mm]	Thickness [mm]	Width [mm]	Modulus [GPa]	Tensile strength [MPa]	Maximum strain [%]	Time at break [min]
Sample 1	9.45	3.30	3.15	1.20	19.53	3.40	0.5
Sample 2	9.46	3.30	3.14	1.38	18.72	3.67	0.5
Sample 3	9.46	3.28	3.14	1.19	19.16	3.54	0.5
Sample 4	9.46	3.28	3.16	1.36	19.23	3.14	0.5
Sample 5	9.45	3.10	3.15	1.30	19.58	3.14	0.4
Sample 6	9.44	3.10	3.15	1.32	19.13	3.50	0.5
Sample 7	9.45	3.11	3.15	1.24	18.39	3.74	0.4
Mean	**9.45**	**3.21**	**3.15**	**1.28**	**19.11**	**3.45**	**0.5**
Std dev	**0.01**	**0.10**	**0.01**	**0.08**	**0.43**	**0.24**	**0.04**

Page 1 of 1

APPENDIX J1
TENSILE TEST OF MAPE SAMPLE (20% PALF)

For tensile properties analysis of different treatment on PALF-TBP composites.

5/26/2017 9:45:21 AM

FACULTY OF MECHANICAL ENGINEERING
UNIVERSITI MALAYSIA PAHANG

TENSILE TEST RESULT OF 20% PALF-TBP COMPOSITES WITH MAPE COUPLING AGENT

Tensile Test Based on ASTM D638-03
Crosshead Speed 1mm/min
Temperature : 24.9°C
Humidity : 55%

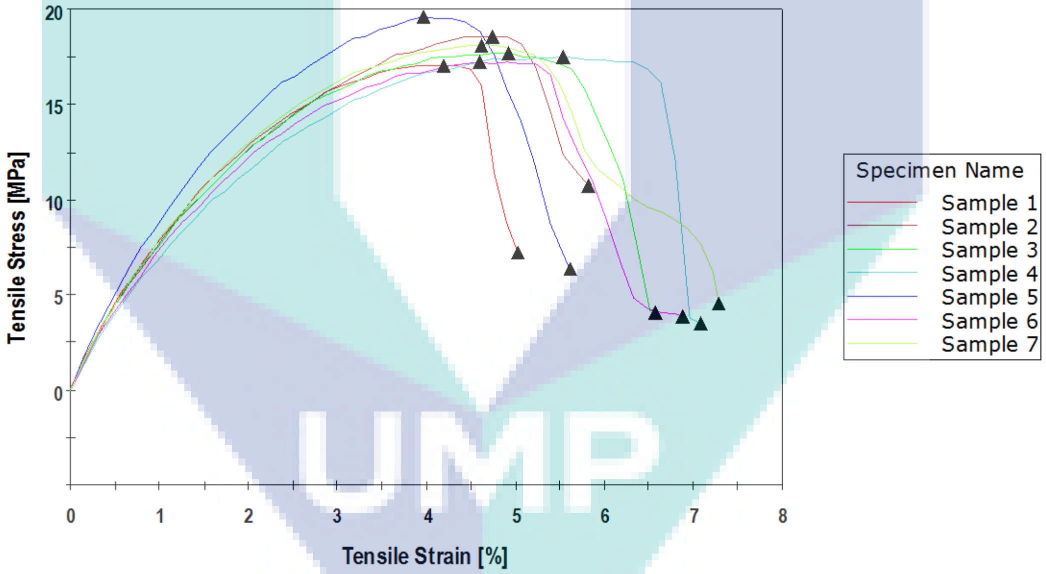

Specimen label	Length [mm]	Thickness [mm]	Width [mm]	Modulus [GPa]	Tensile strength [MPa]	Maximum strain [%]	Time at break [min]
Sample 1	9.55	3.10	3.22	0.88	17.09	5.02	0.6
Sample 2	9.54	3.11	3.20	0.86	18.59	5.83	0.6
Sample 3	9.55	3.12	3.22	0.86	17.69	6.57	0.8
Sample 4	9.55	3.10	3.21	0.77	17.52	7.08	0.7
Sample 5	9.54	3.10	3.21	0.97	19.66	5.61	0.6
Sample 6	9.53	3.10	3.22	0.82	17.22	6.87	0.7
Sample 7	9.55	3.09	3.22	0.85	18.13	7.29	0.8
Mean	**9.54**	**3.10**	**3.21**	**0.86**	**17.98**	**6.32**	**0.7**
Std dev	**0.01**	**0.01**	**0.01**	**0.06**	**0.90**	**0.85**	**0.10**

Page 1 of 1

APPENDIX J2
TENSILE TEST OF MAPE SAMPLE (30% PALF)

For tensile properties analysis of different treatment on PALF-TBP composites.

5/26/2017 10:24:37 AM

FACULTY OF MECHANICAL ENGINEERING
UNIVERSITI MALAYSIA PAHANG

TENSILE TEST RESULT OF 30% PALF-TBP COMPOSITES WITH MAPE COUPLING AGENT

Tensile Test Based on ASTM D638-03
Crosshead Speed 1mm/min
Temperature : 24.9°C
Humidity : 55%

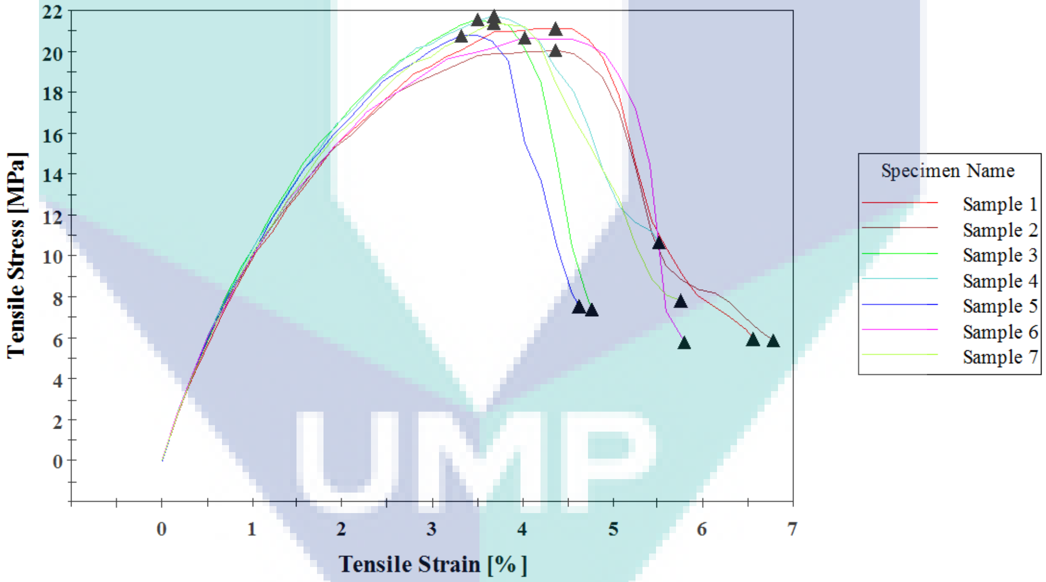

Specimen label	Length [mm]	Thickness [mm]	Width [mm]	Modulus [GPa]	Tensile strength [MPa]	Maximum strain [%]	Time at break [min]
Sample 1	9.50	3.33	3.20	1.06	21.11	6.57	0.6
Sample 2	9.50	3.33	3.19	1.13	20.07	6.78	0.6
Sample 3	9.51	3.34	3.21	1.14	21.55	4.76	0.5
Sample 4	9.51	3.33	3.25	1.12	21.74	5.51	0.5
Sample 5	9.50	3.32	3.25	1.14	20.77	4.63	0.4
Sample 6	9.51	3.33	3.26	1.14	20.70	5.80	0.6
Sample 7	9.50	3.34	3.21	1.10	21.39	5.75	0.5
Mean	**9.50**	**3.33**	**3.22**	**1.12**	**21.05**	**5.68**	**0.5**
Std dev	**0.01**	**0.01**	**0.03**	**0.03**	**0.58**	**0.81**	**0.08**

Page 1 of 1

APPENDIX J3
TENSILE TEST OF MAPE SAMPLE (40% PALF)

For tensile properties analysis of different treatment on PALF-TBP composites.

5/26/2017 10:45:23 AM

FACULTY OF MECHANICAL ENGINEERING
UNIVERSITI MALAYSIA PAHANG

TENSILE TEST RESULT OF 40% PALF-TBP COMPOSITES WITH MAPE COUPLING AGENT

Tensile Test Based on ASTM D638-03
Crosshead Speed 1mm/min
Temperature : 24.9°C
Humidity : 55%

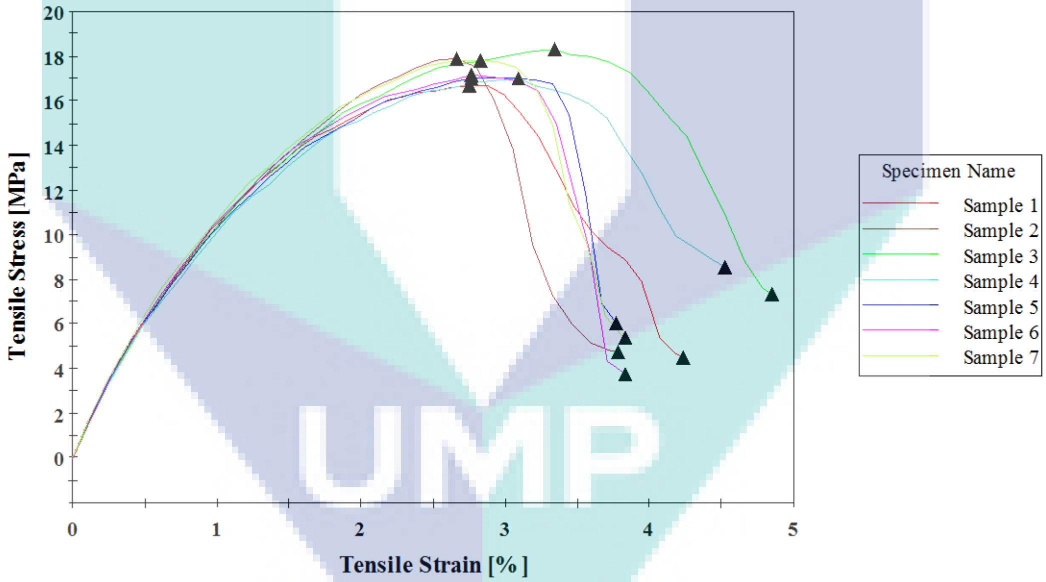

Specimen label	Length [mm]	Thickness [mm]	Width [mm]	Modulus [GPa]	Tensile strength [MPa]	Maximum strain [%]	Time at break [min]
Sample 1	9.45	3.12	3.15	1.16	16.69	4.23	0.6
Sample 2	9.46	3.12	3.14	1.17	17.89	3.78	0.5
Sample 3	9.44	3.13	3.15	1.18	18.27	4.85	0.6
Sample 4	9.44	3.13	3.15	1.14	17.00	4.52	0.6
Sample 5	9.45	3.01	3.15	1.17	17.02	3.76	0.5
Sample 6	9.44	3.00	3.15	1.17	17.14	3.83	0.5
Sample 7	9.44	3.01	3.14	1.21	17.82	3.83	0.5
Mean	**9.45**	**3.07**	**3.15**	**1.17**	**17.40**	**4.11**	**0.6**
Std dev	**0.01**	**0.06**	**0.00**	**0.02**	**0.58**	**0.43**	**0.05**

Page 1 of 1

APPENDIX K
PROCEDURE FOR THE DETERMINATION OF CELLULOSE AND HEMICELLULOSE CONTENT

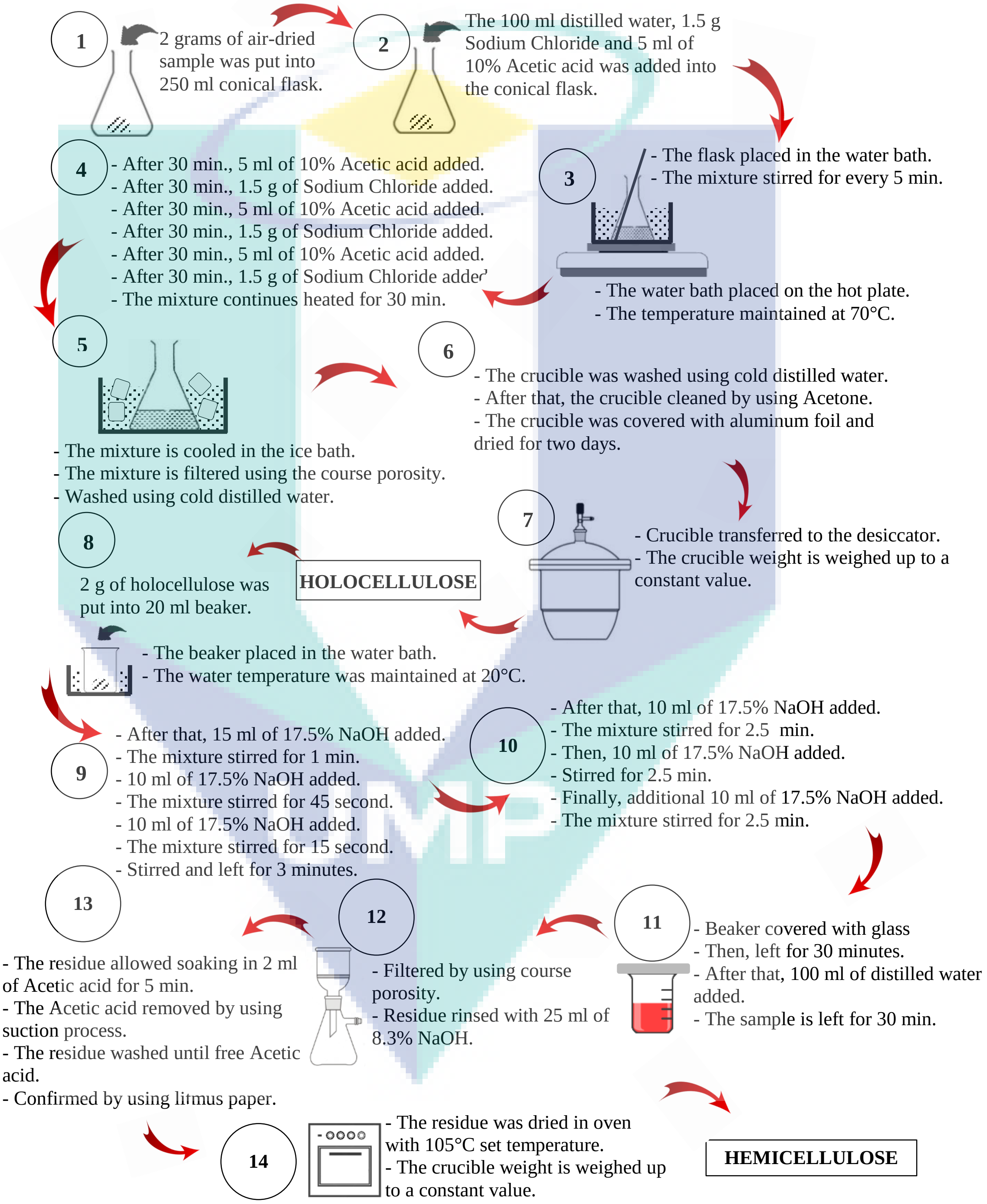

1 2 grams of air-dried sample was put into 250 ml conical flask.

2 The 100 ml distilled water, 1.5 g Sodium Chloride and 5 ml of 10% Acetic acid was added into the conical flask.

3
- The flask placed in the water bath.
- The mixture stirred for every 5 min.
- The water bath placed on the hot plate.
- The temperature maintained at 70°C.

4
- After 30 min., 5 ml of 10% Acetic acid added.
- After 30 min., 1.5 g of Sodium Chloride added.
- After 30 min., 5 ml of 10% Acetic acid added.
- After 30 min., 1.5 g of Sodium Chloride added.
- After 30 min., 5 ml of 10% Acetic acid added.
- After 30 min., 1.5 g of Sodium Chloride added.
- The mixture continues heated for 30 min.

5
- The mixture is cooled in the ice bath.
- The mixture is filtered using the course porosity.
- Washed using cold distilled water.

6
- The crucible was washed using cold distilled water.
- After that, the crucible cleaned by using Acetone.
- The crucible was covered with aluminum foil and dried for two days.

7
- Crucible transferred to the desiccator.
- The crucible weight is weighed up to a constant value.

HOLOCELLULOSE

8 2 g of holocellulose was put into 20 ml beaker.
- The beaker placed in the water bath.
- The water temperature was maintained at 20°C.

9
- After that, 15 ml of 17.5% NaOH added.
- The mixture stirred for 1 min.
- 10 ml of 17.5% NaOH added.
- The mixture stirred for 45 second.
- 10 ml of 17.5% NaOH added.
- The mixture stirred for 15 second.
- Stirred and left for 3 minutes.

10
- After that, 10 ml of 17.5% NaOH added.
- The mixture stirred for 2.5 min.
- Then, 10 ml of 17.5% NaOH added.
- Stirred for 2.5 min.
- Finally, additional 10 ml of 17.5% NaOH added.
- The mixture stirred for 2.5 min.

11
- Beaker covered with glass
- Then, left for 30 minutes.
- After that, 100 ml of distilled water added.
- The sample is left for 30 min.

12
- Filtered by using course porosity.
- Residue rinsed with 25 ml of 8.3% NaOH.

13
- The residue allowed soaking in 2 ml of Acetic acid for 5 min.
- The Acetic acid removed by using suction process.
- The residue washed until free Acetic acid.
- Confirmed by using litmus paper.

14
- The residue was dried in oven with 105°C set temperature.
- The crucible weight is weighed up to a constant value.

HEMICELLULOSE

APPENDIX L
FOURIER TRANSFORM INFRARED SPECTROSCOPY (FTIR) TEST RESULT FOR TAPIOCA BIOPOLYMER (TBP) CHARACTERIZATION

FACULTY OF CHEMICAL ENGINEERING AND NATURAL RESOURCES
UNIVERSITI MALAYSIA PAHANG

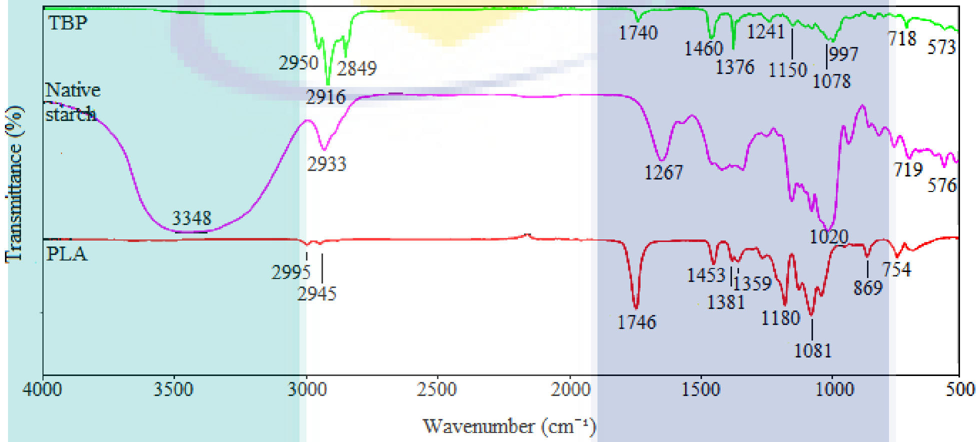

DETAILS FUNCTIONAL GROUP FOR TBP

No.	Tapioca Resin Wave Number, cm^{-1}	Functional Group	Type of Vibration
1	2950.60	CH_2/CH_3	Stretch
2	2916.37	CH_2/CH_3	Stretch
3	2849.84	CH_2/CH_3	Stretch
4	1740.47	C=O	Stretch
5	1460.36	O-H	Stretch
6	1376.47	CH_3	Bending
7	1241.95	C-N	Stretch
8	1150.35	C-O	Stretch
9	1103.10	C-N	Stretch
10	1078.03	C-O	Stretch
11	1016.32	C-O	Stretch
12	997.52	=C-H	Bending
13	718.85	=C-H	Bending
14	573.25	C-Br	Stretch

MATCHING

No.	Title	Composites (%)	Folder
1	Aliphatic polyester	49.40	HR Nicolet Sampler Library
2	Mono and diglycride	20.89	HR Nicolet Sampler Library
3	Prolypropelene	19.50	HR Nicolet Sampler Library
4	3-Metil-2Buten-1-OL	10.21	HR Aldrich Phosphorous & Sulfur Compounds

LIST OF PUBLICATIONS

The list of publication that is acknowledged as follows:

ISI Indexed Journals:

1. **J. Jamiluddin**, J. P. Siregar, M. H. M. Hamdan, C. Tezara and S. M. Sapuan, 2018. Characterisation of cassava biopolymers and the determination of their optimum processing temperatures. *Plastics rubber and composites. 47(10), pp. 447-457*. **Published Q3 (IF: 0.848)**

2. **Jamiluddin Jaafar,** Januar Parlaungan Siregar, Ahmed Nurye Oumer, Mohammad Hazim Mohamad Hamdan, Cionita Tezara and Mohd Sapuan Salit, 2018. Experimental investigation on performance of short pineapple leaf fiber reinforced tapioca biopolymer composites. *BioResources, 13(3), pp. 6341-6355.* **Published Q2 (IF: 1.202)**

3. **Jamiluddin Jaafar,** Januar Parlaungan Siregar, Mohd Bijarimi Mat Piah, Cionita Tezara, Sharmiza Adnan and Teuku Rihayat, 2018. Influence of selected treatment on tensile properties of short pineapple leaf fiber reinforced tapioca resin biopolymer composites. *Journal of Polymers and the Environment, 26(11), pp. 4271-4281*. **Published Q2 (IF: 1.971)**

4. Januar Parlaungan Siregar, **Jamiluddin Jaafar,** Tezara Cionita, Choo Chee Jie, Dandi Bachtiar, Mohd Ruzaimi Mat Rejab and Yuli Panca Asmara, 2018. The effect of maleic anhydride polyethylene on mechanical properties of pineapple leaf fibre reinforced polylactic acid composites. *International Journal of Precision Engineering and Manufacturing – Green Technology. 6(1), pp. 101–112.* **Published Q1 (IF: 3.774)**

5. **Jamiluddin Jaafar,** Januar Parlaungan Siregar, Salwani Mohd Salleh, Mohd Hazim Mohd Hamdan, Cionita Tezara and Teuku Rihayat, 2018. Important considerations in manufacturing of natural fiber composites: A review. *International Journal of Precision Engineering and Manufacturing – Green Technology.* **Revision Under Review Q1 (IF: 3.774)**

SCOPUS Indexed Journals:

1. **J. Jamiluddin**, J. P. Siregar, A. Sulaiman, K. A. A. Jalal and C. Tezara, 2016. Study on properties of tapioca resin polymer. *International Journal of Automotive and Mechanical Engineering, 13(1), pp. 3178-3189.* **Published.**

List of Conference Proceedings:

1. **J. Jamiluddin**, J. P. Siregar, A. Sulaiman, K. A. A. Jalal and C. Tezara. Study on properties of tapioca resin polymer. International Conference of Mechanical Engineering Research, 2015, 18 – 19 August, Zenith Hotel, Kuantan, Pahang, Malaysia.